Department of Chemical Engineering

Imperial College London

Novel Processes for Extraction and Fractionation of Fatty Acids from Microbial Cell Mass

By

Andreia Manuela Martins Miranda

A thesis submitted in partial fulfilment of the requirements for the degree of Doctor of Philosophy in Chemical Engineering

May 2014

The copyright of this thesis rests with the author and is made available under a Creative Commons Attribution-Non Commercial-No Derivatives licence. Researchers are free to copy, distribute or transmit the thesis on the condition that they attribute it, that they do not use it for commercial purposes and that they do not alter, transform or build upon it. For any reuse or distribution, researchers must make clear to others the licence terms of this work.

Abstract

In this thesis a novel integrated process for extraction and fractionation of long chain polyunsaturated fatty acids (LC-PUFA), particularly the high-value docosahexaenoic acid (DHA), from wet microbial cell mass was investigated. The research was focused in two main aspects: (i) selection of enzymes for stepwise hydrolysis of triacylglycerols present the cell mass, and (ii) evaluation of a biphasic membrane contactor system, comprising an asymmetric membrane, for extraction of released fatty acids.

The kinetics of hydrolysis of triacylglycerols to diacylglycerols, monoacylglycerols and free fatty acids for specific and non-specific lipases was characterised. It was demonstrated that the enzymatic hydrolysis of triacylglycerols can be effectively performed directly in the cell mass suspension, i.e. without previous isolation of the lipid fraction. New analytical methods were developed for the analyses of acylglycerols and fatty acids by LC-ESI-MS. The access to the concentration profiles of tri-, di-, and monoacylglycerols throughout the reaction enabled a better evaluation of the performance of enzymes tested in terms of kinetics and selectivity. An effective selective hydrolysis can be attained by employing specific and non-specific lipases in the enzymatic hydrolysis of triacylglycerols. Based on the results obtained, optimum combinations of enzymes for process applications can be proposed.

Asymmetric polyimide membranes were prepared and tested for the separation of fatty acids in the biphasic membrane contactor system. It was found that the type of polymer, the membrane molecular weight cut-off, and the composition of the aqueous phase all had considerable effect on mass transfer across the membrane. Significantly higher mass transfer coefficients of long-chain fatty acids than previously reported were achieved. The solute transport mechanism through asymmetric polyimide porous membranes in the biphasic

system was also explored. However, the membrane mass transfer coefficients calculated based on the solute transport model proposed, did not explain experimental observations well.

The feasibility of the proposed integrated process for sequential enzymatic hydrolysis of triacylglycerols and simultaneous separation of released fatty acids was demonstrated. As expected, the presence of an emulsion in the aqueous phase limited the mass transfer through the membrane. However, promising results were observed, and mass transfer rates may be improved by further optimisation of the operating conditions. It is then concluded that the objective of the present work was accomplished as a partial fractionation of the main fatty acids was obtained.

Declaration

I declare that the work presented in this thesis is my own, and the work of others is appropriately acknowledged.

Andreia M. M. Miranda
May 2014

Acknowledgments

The work presented in this thesis was part of a collaboration project between Imperial College London, DUE MILJØ AS (Oslo, Norway), SINTEF-Materials and Chemistry (Trondheim, Norway), and Evonik-Membrane Extraction Technology, Ltd.

First of all, I wish to thank my academic supervisor Professor Andrew Livingston, PRI advisor, Inga M. Aasen, and Eddy Torp, for their guidance and infinite support. I also want to thank Dr. Ines Baptista for assistance during my stays at Imperial College, and also Dr. Andrea Meniconi, Dr. Andrew Boam and Dr. Ludmila Peeva, from whom I received some valuable advice during some more difficult times. Thanks to all my colleagues at Imperial College and SINTEF for making the time in the lab even more enjoyable, and for not complaining too much about the 'fishy' smell of my samples.

I also wish to acknowledge the 6th Framework Programme of the European Commission Marie Curie Initiative for funding this work (contract number: MRTN-CT-2006-036053-InSolEx), as well as the Research Council of Norway and DUE MILJØ AS.

Um obrigada muito especial à Lígia e ao Ottar, pois foi graças a eles que eu embarquei nesta aventura, e por me terem acompanhado ao longo destes anos. Muito, muito obrigada também à Família Perfeito que me 'adoptou' desde o meu primeiro dia em Trondheim.

E claro, para os meus pais, Manuel e Fátima, e manas, Raquel e Sara, o maior obrigada do mundo, pelo amor e apoio infinitos que sempre se fez sentir apesar da distância.

И накрая, но не на последно място, един милион благодарение на Руслан за това, че винаги, когато има чувство на неудовлетвореност пое, за водене ме насърчава да продължи, и ме кара да се чувствам специална ...

Thank you! Takk! Благодаря! Obrigada!

Publications and Patents arising from the work presented in this thesis

Patents:

Process for extracting fatty acids from aqueous biomass in a membrane contactor module

Patent No.	US 8,455,669, NO 329,999, EP 2,440,670 (allowed)
Applicant(s)	DUE MILJØ AS
Inventor(s)	Andreia M. M. Miranda, Eddy G. Torp, Inga M. Aasen, Andrew G. Livingston
Priority date	10-06-2009
Publication date	04-06-2013

Polyimide membrane

Patent Appl. No.	WO 2010/142979 (A1)
Applicant(s)	Evonik-Membrane Extraction Technology Ltd
Inventor(s)	Andrew T. Boam, Andreia M. M. Miranda, Andrew G. Livingston
Priority date	10-06-2009
Publication date	16-12-2010

Publications:

Enzymatic Hydrolysis of Lipids in a Lipid containing Marine Biomass for Production of Fatty Acids
Authors: A. M. M. Miranda, K. Zahlsen, I. M. Aasen and A. G. Livingston
To be submitted to Enzyme and Microbial Technology.

Fractionation of Fatty Acids in a Biphasic System using Asymmetric Polyimide Membranes
Authors: A. M. M. Miranda, I. M. Aasen and A. G. Livingston
To be submitted to Membranes.

Table of Contents

List of Figures **12**
List of Tables **16**
Abbreviations **18**
Nomenclature **20**

Chapter 1 - Introduction **21**
1.1. Overview and Scope of Thesis 21
1.2. Background and Literature Review 23
1.2.1. Lipids, PUFAs and DHA – Definition, sources and applications 23
1.2.2. Extraction, fractionation and purification methods 25
1.2.3. Membrane filtration technology for oil refining 35
1.2.4. Product stability 37
1.3. Thesis Aims and Research Strategy 38
1.4. Structure of the Thesis 42

Chapter 2 - Production, Characterisation and Concentration of the Microbial Cell Mass
2.1. Summary 44
2.2. Background and Literature Review 45
2.2.1. Microorganisms for production of PUFAs 45
2.2.2. Analytical methods for characterisation of microbial cell mass lipid content 50
2.2.3. Concentration of the microbial cell mass 52
2.2.4. Objectives 55
2.3. Materials and Methods 55
2.3.1. Production of cell mass by fermentation 55
2.3.2. Analytical methods 58
2.3.3. Cross flow microfiltration system 60
2.4. Results and Discussion 63
2.4.1. Characterisation of the microbial cell mass lipid fraction 63
2.4.1.1. Total lipids 63
2.4.1.2. Lipid class composition 64
2.4.1.3. Profile of total fatty acids 65
2.4.1.4. Positional distribution of fatty acids in the triacylglycerols 66
2.4.2. Cross flow microfiltration for concentration of the cell mass 67
2.5. Conclusions 69

Chapter 3 - Hydrolysis of Triacylglycerols in a Lipid containing Microbial Cell Mass for Production of Fatty Acids 71
3.1. Summary 71
3.2. Background and Literature Review 72
3.2.1. Hydrolysis of lipids as part of a wet microbial cell mass 72
3.2.2. Lipase specificity and influence of fatty acid structure in the enzymatic hydrolysis of triacylglycerols 74
3.2.3. Kinetics and challenges related to lipases in general and microbial cell mass 77
3.2.4. Analytical methods for quantification of acylglycerols and free fatty acids 78
3.2.5. Objectives and process hypotheses 79
3.3. Materials and Methods 81
3.3.1. Cell mass and enzymes 81
3.3.2. Chemical hydrolysis of lipids as part of the microbial cell mass suspension 82
3.3.3. Enzymatic hydrolysis of triacylglycerols as part of the microbial cell mass suspension 82
3.3.4. Pre-treatment of the microbial cell mass before triacylglycerol hydrolysis 84
3.3.5. Analytical methods – LC-ESI-MS 84
3.4. Results and Discussion 85
3.4.1. Chemical hydrolysis of lipids as part of the microbial cell mass 85
3.4.2. Enzymatic hydrolysis of triacylglycerols as part of the microbial cell mass suspension 88
3.4.2.1. Evaluation of operating conditions affecting enzymatic hydrolysis rates 88
3.4.2.2. Evaluation of lipases selectivity 91
3.4.2.3. Quantification of mono, di and triacylglycerols throughout enzymatic hydrolysis 92
3.4.2.4. Influence of pre-treatment of the cell mass in the hydrolysis of triacylglycerols . 103
3.4.2.5. Strategy and selection of enzymes for stepwise enzymatic hydrolysis of triacylglycerols and simultaneous separation of released fatty acids 111
3.5. Conclusions 113

Chapter 4 - Kinetic Model for the Stepwise Enzymatic Hydrolysis of Triacylglycerols in O/W Emulsions – Multiple Substrates and Products 115
4.1. Summary 115
4.2. Background and Literature Review 116
4.2.1. Existing models for the evaluation of enzyme kinetics 116
4.2.2. New challenges in the enzyme kinetic studies – multiple substrates and products . 117
4.2.3. Objectives and model hypotheses 118

4.3. Materials and Methods 119
4.3.1. Oil, chemicals and enzymes 119
4.3.2. Preparation of the O/W emulsions 119
4.3.3. Determination of interfacial area of O/W emulsions 119
4.3.4. Enzymatic hydrolysis of microbial oil in an O/W emulsion 120
4.3.5. Analytical methods 120
4.4. Mathematical Model and Simulation 122
4.4.1. Mechanism of the process 122
4.4.2. Development of the reaction rate equations 125
4.5. Results and Discussion 134
4.5.1. Evaluation of emulsion stability and calculation of the interfacial area 134
4.5.2. Application of the model 136
4.6. Conclusions 139

Chapter 5 - Transport of Fatty Acids through Asymmetric Polyimide Membranes in a Biphasic Membrane Contactor System 140
5.1. Summary 140
5.2. Background and Literature Review 141
5.2.1. Biphasic membrane contactor systems in the extraction of solutes from complex mixtures 141
5.2.2. Transport phenomena through membranes 144
5.2.3. Objectives and process hypotheses 146
5.3. Materials and Methods 147
5.3.1. Cell mass and chemicals 147
5.3.2. Preparation of fatty acid rich solution – chemical hydrolysis 147
5.3.3. Asymmetric membranes preparation 148
5.3.4. Asymmetric membranes characterisation 148
5.3.5. Measurement of organic/aqueous partition coefficients 149
5.3.6. Mass transfer experiments – Membrane contactor design 149
5.3.7. Analytical methods 151
5.4. Mathematical Analysis 151
5.4.1. Solute transport through porous membranes in a biphasic system 152
5.4.2. Calculation of the experimental overall mass transfer coefficient, OMTC – Kaq 156
5.4.3. Estimation of individual liquid-film mass transfer coefficients – k_{aq} *and* k_{org} 158
5.5. Results and Discussion 159
5.5.1. Organic/aqueous partition coefficients – $m_{org/aq}$ 159
5.5.2. Membranes flux, rejection and MWCO curves 160

5.5.3. Evaluation of the performance of different polyimide membranes for the separation of fatty acids in the biphasic system 163

5.5.4. Characterisation of solute transport through porous membranes in the biphasic system 174

5.5.4.1. Estimation of membrane porosity based on solute rejection using the Bowen and Welfoot model 175

5.5.4.2. Estimation of individual mass transfer coefficients 182

5.6. Conclusions 183

Chapter 6 - Fractionation of Fatty Acids in a Biphasic Membrane Contactor System using Asymmetric Polyimide Membranes 186

6.1. Summary 186

6.2. Background and Literature Review 187

6.2.1. Membrane bioreactors for simultaneous production and separation of a desired product 187

6.2.2. Biphasic membrane contactor systems for fractionation of fatty acids 190

6.2.3. Objectives and process hypotheses 191

6.3. Materials and Methods 192

6.3.1. Cell mass, chemicals and membranes 192

6.3.2. Preparation of the fatty acid rich solution – enzymatic hydrolysis 193

6.3.3. Mass transfer experiments – Membrane contactor design 194

6.3.4. Analytical methods 196

6.4. Results and Discussion 196

6.4.1. Influence of the presence of emulsion in the simultaneous enzymatic hydrolysis and separation of fatty acids 197

6.4.2. Fractionation achieved by carrying out simultaneous hydrolysis and separation of fatty acids in the biphasic membrane contactor system 199

6.5. Feasibility and applicability of the developed process at industrial scale 205

6.5.1. Preliminary economic analysis of the integrated process 206

6.6. Conclusions 208

Chapter 7 - Final Conclusions and Future Perspectives 210

Appendix 217

References 219

List of Figures

Figure 1.1: Chemical structure of docosahexaenoic acid - DHA - $C_{22}H_{32}O_2$..... 25

Figure 1.2: Typical process stages followed to extract and purify DHA from a fermentation broth, the conventional methods used for each stage, and which of these stages will be covered by the proposed novel integrated process. 39

Figure 1.3: Schematic diagram of the integrated process (T1 - bioreactor for cultivation of the microbial cell mass and further enzymatic hydrolysis of lipid content; M2 - cross-flow membrane filtration system for continuous cell harvesting; M1 - membrane biphasic system for product extraction; T2 - product recovery tank). 40

Figure 2.1: Thraustochytrids of the *Aurantiochytrium* sp. strain T66 in liquid medium (image adapted with permission from Anita N. Jakobsen PhD Thesis, NTNU, 2008). 49

Figure 2.2. Fatty acids composition of two thraustochytrid strains isolated at SINTEF-Materials and Chemistry, Norway. 50

Figure 2.3: Diagram of the rented cross-flow minipilot (Orelis, Novasep, Applexion, France)... 61

Figure 2.4: Total lipid content and dry weight of the microbial cell mass during the pilot scale fermentation (150 L) for strain T29..... 63

Figure 2.5: Illustration of a lipid body. 64

Figure 2.6: Enlarged carbonyl region (172.0-173.4 ppm) of a 600 MHz ^{13}C-NMR spectrum obtained for the thraustochytrids oil in casu, showing positional distribution of DHA, SFA and MUFA in the triacylglycerol fraction. 67

Figure 2.7: Variations of permeance with time for the membrane KERMBMM1 (100 nm cut-off) at different transmembrane pressures (Pin-Pout (bar); initial broth concentration ~45 g L^{-1}; T=25ºC, v=5 m s-1; pH~7). 68

Figure 2.8: Variations in permeance with cell concentration for two microfiltration membranes (KERMBMM1 - 100 nm and KERMBMM2 - 200 nm) operating at the same transmembrane pressure (Pin=0.8 bar - Pout =0.6 bar). (T=25ºC, v=5 m s-1; pH~7). 69

Figure 3.1: Schematic representation of base catalysed hydrolysis of triacylglycerols. 73

Figure 3.2: Schematic representation of different possible scenarios of enzymatic hydrolysis of a triacylglycerol comprising a saturated (SFA) or monounsaturated (MUFA) fatty acid in sn-1,3 positions, and one polyunsaturated fatty acid (PUFA) in sn-2 position, while using a non-specific lipase. 74

Figure 3.3: Illustration of three different triacylglycerol molecules: A - Tridocosahexaenoin – glycerol+three DHA molecules; B - Trioleoyl – glycerol+three OLA molecules; C - Tripalmitin – glycerol+three PLA molecules. Ester bonds linking the fatty acid to the glycerol molecule are marked in green; red arrows illustrate the access 'point' of the lipases (chemical structures adapted from www.chemicalbook.com). 76

Figure 3.4: Amounts of main fatty acids extracted at different pH-values, after chemical hydrolysis of microbial cell mass lipid content (150 g L^{-1}, 1 hour, 60°C; PLA-palmitic acid; OLA-oleic acid; DHA docosahexaenoic acid). 86

Figure 3.5: Total fatty acids released by enzymatic hydrolysis of the microbial cell mass lipid fraction for different reaction times and three different enzyme concentrations, for two of the four enzymes under study: A – Lipozyme TL 100L (LPZ); B – *Candida rugosa* (CR)..... 90

Figure 3.6: Yields of the main fatty acids obtained after enzymatic hydrolysis of the triacylglycerol fraction of the wet cell mass after 24 hours reaction for the four enzymes in this

study (CR – *Candida rugosa*; MJ – *Mucor javanicus*; LPZ – Lipozyme TL 100L; PS - *Pseudomonas sp*). Cell mass concentration of 50 g L^{-1}; enzyme concentration of 100 kU L^{-1} of cell mass suspension. 92

Fig 3.7a: Composition profile of selected TAGs during enzymatic hydrolysis of the lipid fraction of the microbial cell mass suspension for each of the enzymes considered in this study, namely Lipozyme TL 100L (LPZ), *Candida rugosa* (CR), and *Mucor javanicus* (MJ). (Tests carried out with a cell mass concentration of 50 g L^{-1}, and an enzyme concentration of 100 kU L^{-1}). 95

Fig 3.7b: Composition profile of selected TAGs during enzymatic hydrolysis of the lipid fraction of the microbial cell mass suspension for each of the enzymes considered in this study, namely Lipozyme TL 100L (LPZ), *Candida rugosa* (CR), and *Mucor javanicus* (MJ). (Tests carried out with a cell mass concentration of 50 g L^{-1}, and an enzyme concentration of 100 kU L^{-1}). 96

Figure 3.8: Composition profile of selected DAGs during enzymatic hydrolysis of the lipid fraction of the microbial cell mass suspension for each of the enzymes considered in this study, namely Lipozyme TL 100L (LPZ), *Candida rugosa* (CR), and *Mucor javanicus* (MJ). (Tests carried out with a cell mass concentration of 50 g L^{-1}, and an enzyme concentration of 100 kU L^{-1}). 98

Figure 3.9: Composition profile of selected MAGs during enzymatic hydrolysis of the lipid fraction of the microbial cell mass suspension for each of the enzymes in study, namely Lipozyme TL 100L (LPZ), *Candida rugosa* (CR), and *Mucor javanicus* (MJ). (Tests carried out with a cell mass concentration of 50 g L^{-1}, and an enzyme concentration of 100 kU L^{-1}). 100

Figure 3.10: Composition profile of the main fatty acids released during enzymatic hydrolysis of the lipid fraction of the microbial cell mass suspension for each of the enzymes under study, namely Lipozyme TL 100L (LPZ), *Candida rugosa* (CR), and *Mucor javanicus* (MJ). (Tests carried out with a cell mass concentration of 50 g L^{-1}, and an enzyme concentration of 100 kU L^{-1}). 102

Figure 3.11: Composition of selected acylglycerols and free fatty acids in the reaction mixture during enzymatic hydrolysis of the lipid fraction of the microbial cell mass suspension after protease pre-treatment. (TAG-triacylglycerols; DAG-diacylglycerols; MAG-monoacylglycerols; FFA-free fatty acids). 104

Figure 3.12: Composition of selected acylglycerols and free fatty acids in the reaction mixture during enzymatic hydrolysis of the lipid fraction of the microbial cell mass suspension after phospholipase pre-treatment. (TAG-triacylglycerols; DAG-diacylglycerols; MAG-monoacylglycerols; FFA-free fatty acids). 106

Figure 3.13: Illustrative diagram of lipid bodies agglomeration formed as a consequence of hydrolysis of proteins present in the microbial cell mass suspension. 108

Figure 3.14: Illustrative diagram of distribution of lipid bodies in the wet cell mass suspension after hydrolysis of the phospholipid fraction of the microbial cell mass. 109

Figure 3.15: Microscopic images of the fermentation broth (A), and the cell mass suspension during lipid hydrolysis without pre-treatment (B). 110

Figure 3.16: Schematic representation of the stepwise enzymatic hydrolysis of triacylglycerols. 112

Figure 4.1: Schematic representation of the stepwise reactions for the three parallel mechanisms considered (triacylglycerols – TAG1, TAG2, TAG3; diacylglycerols – DAG1, DGA2, DAG3; monoacylglycerols – MAG1, MAG2; saturated and monounsaturated fatty acids – S; polyunsaturated fatty acids – P; glycerol – G; enzyme – E). 122

Figure 4.2: Sub-mechanism TAG1. 123

Figure 4. 3: Sub-mechanism TAG2. 124

Figure 4.4: Sub-mechanism TAG3. 124

Figure 4.5: Concentration profiles of TAG, DAG, and MAG, S and P throughout enzymatic hydrolysis of triacylglycerols in a stable oil:water emulsion as given by the kinetic model developed. 137

Figure 4.6: Profile of triacylglycerols (TAG), diacylglycerols (DAG), monoacylglycerols (MAG) and fatty acids (FFA) composition during enzymatic hydrolysis of microbial oil in an oil-in-water emulsion with lipase *Mucor javanicus* (o/w ratio: 0.0137; enzyme concentration: 100 kU enzyme mL^{-1} emulsion). 138

Figure 5.1: Schematic of biphasic membrane contactor used for extraction of fatty acids. The arrow indicates the direction of solute transport. (T1-bioreactor containing the fatty acid rich suspension; T2-reservoir containing the organic solvent; M1-Membrane Contactor Module; (1) aqueous compartment of the membrane contactor module; (2) asymmetric polyimide membrane; (3) organic compartment of the membrane contactor module). 150

Figure 5.2. Schematic of solute concentrations with interfaces immobilised in a porous hydrophobic asymmetric membrane in a biphasic membrane contactor system. 152

Figure 5.3: Molecular weight cut off curve, MWCO, for Starmem™ 240 membrane (filtration carried out at a constant pressure of 30 bar and with polystyrene oligomers solution (PS, 200-1200 Da, 1 g L^{-1}) in toluene. 161

Figure 5.4: Molecular weight cut off curves, MWCO, for M1, M2 and M3 (filtrations carried out at a constant pressure of 5 bar and with individual polyethylene glycol solutions (1 g L^{-1}, of 3 kDa, 6 kDa, 10 kDa, 12 kDa, 20 kDa and 35 kDa PEG) in toluene. 162

Figure 5.5: Chemical structure of P84 polyimide polymer (BTDA - benzophenone tetracarboxylic acid dianhydride; MDI - 4,4'-methylene-bis(phenylisocyanate); TDI - toluene diisocyanate). 165

Figure 5.6: Chemical structure of Matrimid 5218 (BTDA - benzophenone tetracarboxylic acid dianhydride; DAPI - 4',6-diamidino-2-phenylindole). 165

Figure 5.7: Concentration profile of docosahexaenoic acid (DHA) and palmitic acid (PLA) in the aqueous phase (AQ) and organic phase (ORG) (Exp. A: membrane M1, Vaq=550 mL, Vorg=100 mL; Exp. B: membrane M2, Vaq=550 mL, Vorg=100 mL; Exp. C: membrane M3, Vaq=550 mL, Vorg=200 mL).). 167

Figure 5.8: Concentration profile of docosahexaenoic acid (DHA) and palmitic acid (PLA) in the aqueous and organic phases (Exp. D: membrane M3, Vaq=275 mL, Vorg=200 mL). 169

Figure 5.9: Cumulative mass transfer (right hand side of Eq. 5.13) against time for the calculation of the overall mass transfer coefficient (OMTC, K_{aq}) of DHA from the fatty acids rich solution (aqueous phase) to hexane (organic phase) (Exp. C: membrane M3). 171

Figure 5.10: Overall mass transfer coefficients (OMTC) obtained for DHA and PLA at different aqueous/organic volume ratios. (Exp B: M2, Vaq/Vorg= 5.5; Exp C: M3, Vaq/Vorg= 2.75; Exp D: M3, Vaq/Vorg= 1.325). 172

Figure 5.11: Volumetric productivities and yields of DHA obtained after 22 hours in experiments with Matrimid based membranes. (Exp B: M2, Vaq/Vorg= 5.5; Exp C: M3, Vaq/Vorg= 2.75; Exp D: M3, Vaq/Vorg= 1.325; Exp E: Starmem™ 240, Vaq/Vorg=1.325). 173

Figure 5.11: Starmem™ 240. 181

Figure 5.12: Membrane M3 – Matrimid in DMF. 182

Figure 6.1. Schematic representation of the stepwise enzymatic hydrolysis of triacylglycerols and simultaneous extraction of released fatty acids in a membrane contactor system, comprising an asymmetric polyimide ultrafiltration membrane. (G – Glycerol; SFA – Saturated Fatty Acids: MUFA – Monounsaturated Fatty Acids; DHA – Docosahexaenoic Acid; AQ – Aqueous Phase; ORG – Organic Phase; E1 and E2 – Enzymes). 191

Figure 6.2: Simplified schematic of the stepwise enzymatic hydrolysis and simultaneous membrane separation for fractionation of fatty acids. 195

Figure 6.3. Concentration profiles of DHA and PLA in the organic phase (hexane) during mass transfer experiments while using enzymatic hydrolysis (UF membrane - M3, lipase MJ)..... 198

Figure 6.4: Concentration profiles of DHA and PLA in the organic phase (hexane) and recovery during simultaneous hydrolysis and separation of fatty acids in the biphasic membrane system (UF membrane - M3, 1st Stage – lipase MJ, 2nd Stage – lipase LPZ), after phospholipase pre-treatment. 201

Figure 6.5: DHA fraction of the total fatty acids present in the aqueous (AQ) and organic (ORG) phases initially and at the end of each stage of the simultaneous hydrolysis and separation of fatty acids in the biphasic membrane system (UF membrane - M3), after phospholipase pre-treatment. 202

Figure 6.6: Composition of each stream of the integrated stepwise enzymatic hydrolysis of triacylglycerols directly on the cell mass suspension, and simultaneous separation of released fatty acids based on experimental results (S1-1st stage; S2-2nd stage)..... 204

List of Tables

Table 2.1: Percentage of fatty acids with 14 or more carbon atoms within the lipids of selected marine microorganisms. (H-heterotrophic; P-phototrophic; adapted from Sijtsma et al. [8]) ... 47

Table 2.2: Lipid class and respective extraction mixtures [75]. ... 51

Table 2.3: Growth medium composition. ... 56

Table 2.4: Main characteristics of microfiltration membranes used - Kerasep™ ceramic membranes (KERMBMM1 and KERMBMM2; Orelis, Novasep, Applexion, France). ... 62

Table 2.5: Lipid class composition of extracted microbial oil. ... 65

Table 2.6: Amount of main fatty acids released by direct transesterification of microbial cell mass, and fraction in relation to total fatty acids accounted for. ... 66

Table 3.1: Enzymes applied in the study of hydrolysis, their activity and specificity according to the supplier. One unit (1U) will hydrolyse 1 micromole of fatty acid from a triacylglycerol molecule in one hour at the optimum operating conditions of each lipase. ... 81

Table 3.2: Content of the main fatty acids (FFA) of the cell mass, determined by chemical hydrolysis (150 g L^{-1} cell mass, 0.39 M KOH, 2 hours at 60°C), and direct transesterification (FAME), see section 2.4.1.3. ... 87

Table 3.3: Acylglycerols selected for quantification throughout the enzymatic hydrolysis reaction, corresponding molecular weight and position of the fatty acids in the acylglycerol molecule. ... 93

Table 3.4: Triacylglycerols and free fatty acids composition in the cell mass before lipase addition, as determined with and without pre-treatment of the cell mass. ... 107

Table 4.1: List of most common monoacylglycerols (MAG), diacylglycerols (DAG) and triacylglycerols (TAG) by combinations of main fatty acids present in the oil (DHA, PLA and OLA), and respective molecular weight. (G – glycerol, S – saturated and monounsaturated fatty acis, P – polyunsaturated fatty acids). ... 121

Table 4.2: Sauter diameter (D (3,2)) and total interfacial area calculated for the emulsions tested. ... 135

Table 5.1 Composition of the ultrafiltration membranes prepared for the study of transport of fatty acids in a biphasic system. ... 148

Table 5.2: Partition coefficients (morg/aq) of docosahexaenoic acid (DHA) and palmitic acid (PLA) between hexane (org) and water:ethanol (aq). ... 160

Table 5.3: Flux values for the four membranes tested with toluene and polystyrene oligomers (PS, 200-1200 Da, 1 g L^{-1}) solution in toluene. ... 161

Table 5.4: Membrane, initial concentration of DHA in the aqueous phase ($C_{DHA,i}$), flow rates of aqueous and organic streams, and initial volumes of aqueous ($V_{i,aq}$) and organic ($V_{i,org}$) phases for each of the experiments carried out. ... 164

Table 5.5: Overall mass transfer coefficients - OMTC, Kaq, of docosahexaenoic acid (DHA) and palmitic acid (PLA) from the aqueous fatty acids rich phase (water:ethanol) to the organic phase (hexane) for the four asymmetric polyimide membranes tested in the membrane contactor system. ... 170

Table 5.6: Calculated solute radius used determining the MWCO of Starmem™ 240. ... 177

Table 5.7: Calculated solute radius determining MWCO of M1 and M3. ... 178

Table 5.8: Estimated pore radius of Starmem™ 240 membrane based on the rejection and solute radius of polystyrene oligomers which presented rejections above 60%. 179

Table 5.9: Estimated pore radius of M1 and M3 membranes based on the rejection and solute radius of polyethylene glycol solutions which presented rejections above 60%. 179

Table 5.10: Calculated membrane porosities, ε, for Starmem™ 240 membrane as a function of membrane thickness, flux per pore, number of pores and surface area occupied by pores..... 180

Table 5.11: Calculated membrane porosities, ε, for M1 membrane as a function of membrane thickness, flux per pore, number of pores and surface area occupied by pores. 180

Table 5.12: Calculated membrane porosities, ε, for M3 membrane as a function of membrane thickness, flux per pore, number of pores and surface area occupied by pores. 181

Table 5.13: Estimated individual mass transfer coefficients. 183

Table 6.1: Overall mass transfer coefficients, OMTC/K_{aq}, of DHA and PLA from the aqueous fatty acids rich phase (water/ethanol) to the organic phase (hexane) for Matrimid membrane in DMF (M3). 202

Abbreviations

ALC	Alcalase
AQ	Aqueous phase
ARA	Arachidonic acid
BHT	Butylated hydroxytoluene
BSA	Bovine serum albumin
CCC	Counter-current chromatography
CPC	Centrifugal partition chromatography
CR	Candida rugosa
DAG	Diacylglycerols
DHA	Docosahexaenoic acid
DMF	N,N-Dimethylformamide
DPA	Docosapentaenoic acid
EPA	Eicosapentaenoic acid
ESI	Electrospray ionisation
FAEEs	Fatty acid ethyl esters
FAMEs	Fatty acid methyl esters
FFA	Free fatty acids
GC	Gas chromatography
GG	Guar gum
HPCCC	High performance counter-current chromatography
HPLC	High performance liquid chromatography
HP-TLC	High performance thin layer chromatography
IPA	Isopropanol
LCMS	Liquid chromatography mass spectrometry
LC-PUFA(s)	Long chain polyunsaturated fatty acid (s)
LPZ	Lipozyme TL 100L
ODE	Ordinary differential equation
OLA	Oleic acid
OMTC	Overall mass transfer coefficient
ORG	Organic phase

OSN	Organic solvent nanofiltration
MAG	Monoacylglycerols
MAT	Matrimid
MF	Microfiltration
MJ	Mucor javanicus
MUFA	Monounsaturated fatty acids
MW	Molecular weight
MWCO	Molecular weight cut-off
NF	Nanofiltration
NMR	Nuclear magnetic resonance
NMP	1-methyl-2-pyrrolidinone
PA	Polyamide
PCB	Polychlorinated biphenyls
PI	Polyimide
PEEK	Polyether ether ketone
PEG	Polyethylene glycol
PL	Phospholipids
PLA	Palmitic acid
PP	Polypropylene
PS	Polystyrene
Psp	Pseudomonas sp
PTFE	Polytetrafluroethylene
RV	Reference values
SEM	Scanning Electron Microscopy
SFA	Saturated fatty acids
SFE	Supercritical fluid extraction
TAG	Triacylglycerols
TBHQ	Tertiary butylhydroquinone
TMP	Transmembrane pressure
TT	Triton X100
UF	Ultrafiltration
UIC	Urea inclusion compounds

Nomenclature

A	Interfacial area (m^2)
Am	Membrane area (m^2)
C_E	Concentration of enzyme (kg m^{-3})
$C_{E,0}$	Initial concentration of enzyme (kg m^{-3})
C_i	Concentration of component *i* (mol m^{-3})
C_{aq}	Concentration in the aqueous phase (g L^{-1})
C_{org}	Concentration in the organic phase (g L^{-1})
C_M	Concentration inside the membrane (g L^{-1})
Di,org	Diffusion coefficient of solute *i* in the organic phase (m s^{-1})
k_1 to k_{22}	Rate constants of elementary reactions
K_1 to K_{16}	Kinetic constants (m^4 mol^{-1} kg^{-1})
K_E	Adsorption constant of enzyme (m^3 kg^{-1})
K_i	Adsorption constant of component *i* (m)
q_{Ei}	Concentrations of enzyme component *i* complexes adsorbed at interface (kg m^{-2})
q_{S^*,P^*}	Concentration of acylated form of enzyme complex adsorbed at interface (kg m^{-2})
$q_{E,max}$	Saturated concentration of enzyme adsorbed at interface (kg m^{-2})
$q_{E,total}$	Total concentration of enzyme adsorbed at interface (kg m^{-2})
q_i	Concentrations of component *i* adsorbed at interface (mol m^{-2})
r_i	Reaction rates of component *i* adsorbed at interface (kg m^{-2} h^{-1})
T	Temperature (ºC)
V	Volume of emulsion (m^3)
V_{aq}	Volume of aqueous phase (L)
V_{org}	Volume of organic phase (L)
Δx	Membrane layer thickness (m)

Chapter 1

Introduction

1.1. Overview and Scope of Thesis

Due to the documented beneficial health effects of the omega-3 long chain polyunsaturated fatty acids eicosapentaenoic acid (EPA; C20:5n-3) and docosahexaenoic acid (DHA, C22:6n-3) the demand for these fatty acids are rapidly increasing [1-3]. DHA is very concentrated in some tissues, such as the retina and brain in mammals and vertebrates, and is important to their specific functions [1, 4, 5], and therefore constitutes the highest number of beneficial health claims. Omega-3 long chain polyunsaturated fatty acids (LC-PUFAs) applied as food supplements or pharmaceutical products, should have a high-quality with undamaged fatty acids (e.g. less oxidation, minimum isomerisation) in the form of mono-, di-, or triacylglycerols, or esters of fatty acids with a minimum amount of impurities [6].

The main sources of omega-3 PUFAs, including DHA and EPA, are fatty fish species, such as herring, mackerel, sardine and salmon [4]. Recently, reports of the possible accumulation of toxic pollutants, including heavy metals as mercury compounds, dioxins and polychlorinated biphenyls (PCBs), from the marine environment into fish livers and other fat containing

organs, have added another argument against the use of fish oils in human diets [5]. This makes fish oil processing even more demanding. Some authors recommended that ‘‘oily fish’’ should not be eaten more than once a week [5, 7]. Furthermore, there is the concern that insufficient fish oil will be available in the future to meet the expected growth in world demand for omega-3 oils [4]. Plant oils are relatively cheap and are generally considered to be healthier than animal fats, due to their relatively high amounts of unsaturated fatty acids. However, vegetable oils do not contain the long chain PUFAs (longer than C18) [7].

Enrichment of DHA-content in fish oil is challenging, due to a complex fatty acid profile [7]. The production of DHA as the main LC-PUFA has been reported recently in many species of marine microorganisms. Commercial production has been established based on two groups of marine microbes, the dinoflagellate *Crypthecodiniaceae*, and the protists *Thraustochytriidae* [4, 8].

Despite the large number of publications claiming discovery of new microbial strains and optimisation of growth media, processes for extraction and purification of fatty acids from oil containing microbial cell mass have not been much explored. Methods used for extraction of oils from vegetable and fish oils have been adapted for microbial biomass [9, 10]. Microbial oils are normally extracted from dried cell mass, or cell mass with a residual water content, using organic solvents. By removing the water, formation of emulsions is avoided, which increases the extraction yields, but also carries high costs for the industry.

DHA concentrates can be produced by hydrolysis or alcoholysis of the oil fraction. An enzymatic hydrolysis or alcoholysis catalysed by lipases has the advantage over chemical methods that a selective release of fatty acids may be achieved [11-15]. Saturated (SFA) and

monounsaturated (MUFA) fatty acids are preferably released and can be separated from the remaining oil fraction, leaving an oil rich in PUFAs.

Only a few research groups have focused on exploring new and more effective procedures to separate products from marine microorganisms. Therefore, research for new technologies to improve the extraction, fractionation and purification and consequently the final product quality is needed.

This thesis concerns (i) enzymatic hydrolysis of the lipids of a wet microbial biomass, with characterisation of the kinetics of a range of enzymes for the hydrolysis of the cell mass lipid content, and (ii) development and evaluation of membranes with respect to mass transfer of fatty acids in a biphasic membrane contactor system. By combining these two process steps, the fatty acids released in a controlled manner, can be immediately extracted from the biomass suspension, without isolation of the lipid fraction.

1.2. Background and Literature Review

1.2.1. Lipids, PUFAs and DHA – Definition, sources and applications

Lipids

Lipids are an important component of living cells, together with proteins and carbohydrates, and they are indispensable for the growth and survival of all organisms [8]. They are one of the most important structural components of cell membranes, giving flexibility, fluidity and selective permeability proprieties to cell membranes. They are easily stored in the body and they serve as a source of fuel, playing a crucial role in energy storage. Natural sources of lipids include plants, animals and microorganisms. Lipids are classified according to their solubility in organic solvents; thus, they include several groups of compounds with diverse

chemical and physical characteristics [6]. Lipids can be divided in two main classes: neutral and polar lipids. Neutral lipids include triacylglycerols, sterols, wax esters and hydrocarbons, phospholipids and glycolipids are included among polar lipids. Lipid complexes with other chemical compounds, e.g. the lipoproteins, glycolipids and phospholipids, are also known as compound lipids. Triacylglycerols are usually regarded as energy storage products, whereas phospholipids and glycolipids are structural lipids contained in the cell membranes [9]. The predominant component of most fats and oils are triacylglycerols, which are actually esters of glycerol with three fatty acids. Fatty acids are carboxylic acids with a long hydrocarbon chain (typically from 4 to 28 carbon atoms), which can be saturated (SFA), monounsaturated (MUFA) or polyunsaturated (PUFA), depending on the number of double bonds between the carbon atoms.

Long-Chain Polyunsaturated Fatty Acids – LC-PUFAs

PUFAs are essential components of higher eukaryotes [1]. Long-chain PUFAs are composed of a long hydrocarbon chain, with 18 or more carbon atoms, and a terminal carboxylate group [8]. They are classified in two main groups, the omega-3 (n-3) and omega-6 (n-6) fatty acids. The number designation is determined according to the position of the first double bond, counting from the methyl group. The position of the double bond in the fatty acid strongly affects its properties. Of the omega-6 PUFAs, arachidonic acid (ARA; 20:4n-6) is of particular importance, as it is a major precursor of many prostaglandins and eicosanoids [4]. The omega-3 PUFAs are known for several beneficial functions, including decreasing the incidence of coronary heart disease, stroke, and rheumatoid arthritis [3]. Evidence of the benefits and risks of omega-3 PUFAs for human health was reviewed by Takahata *et al.* [2]. Eicosapentaenoic acid (EPA; 20:5n-3) and docosahexaenoic acid (DHA; 22:6n-3), are two

omega-3 PUFAs that are currently receiving much attention, and are the most studied PUFAs within the omega-3 group.

Docosahexaenoic Acid - DHA

The most unsaturated fatty acid found in significant quantities in nature is docosahexaenoic acid, DHA (Figure 1.1). In recent years, DHA has attracted much attention because of its beneficial effect on human health, as reported by several authors. This fatty acid is known to be especially important for neural development in animals; indeed, DHA together with ARA are the major structural components of the grey matter of the brain and the eye retina and an important component in neural and heart tissue [1]. A deficiency in DHA has been linked to impaired brain and visual development in neonates [7]. Once the physiological role of DHA had been realised, this fatty acid became a candidate for commercial microbial production as no traditional lipid source rich in this long chain-polyunsaturated fatty acid alone was known [7].

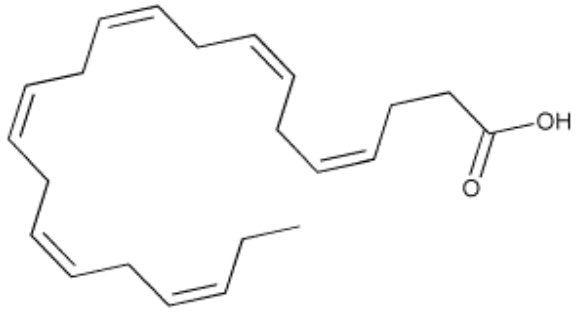


Figure 1.1: Chemical structure of docosahexaenoic acid - DHA - $C_{22}H_{32}O_2$.

1.2.2. Extraction, fractionation and purification methods

For nutritional supplements and pharmaceutical products the DHA-content of the oils often needs to be increased. Normally, the lipid fraction is first extracted from the raw material by a solvent or solvent mixture, and further refined in order to obtain an oil rich in the fatty acid of

interest [9, 10]. In general, extraction and refining methods should be fast, efficient and gentle in order to reduce degradation of the fatty acids. The methods conventionally used for fractionation and purification of fatty acids or fatty acid derived esters are chromatography, distillation, crystallisation, urea complexation, and supercritical extraction. A short description of conventional extraction, hydrolysis and fractionation/purification methods is presented next.

Lipid extraction

Generally, the cultivated cell mass needs to be treated before lipid extraction, in order to achieve a high product yield. This pre-treatment often includes dewatering, or even drying, and homogenisation/cell disruption, mechanical or chemical, for degradation of other compounds that may compromise a successful extraction. The drying is normally included in order to increase yields and reproducibility, as well as to reduce the amount of solvent needed and to avoid problems related to emulsion formation. However, some authors explain that lipids from microorganisms may be extracted in the wet state directly after harvesting [16] (Hoeksema, US Patent No. 6166231; Liddell, US Patent No. 6180376 B1). Direct extraction of fatty acids from wet *Phaeodactylum tricornutum* biomass (after harvesting by centrifugation) with 96% ethanol produced only slightly lower yields (90%) than those obtained from lyophilised biomass (96%) [9]. The presence of water also helps the quantitative extraction of polar lipids and removal of non-lipids [9]. Indeed, while extracting from dried biomass, in some cases the lipid yield may be increased by adding a small amount of water to the extractant. Water causes swelling of the cellular structures rich in polysaccharides, thereby facilitating access of extracting solvents to the lipids.

The need for a mechanical or chemical cell disruption step prior to extraction depends on the nature of the cell wall and how the lipids are associated. The cell wall of microorganisms generally includes polysaccharides, but may also contain lipids (e.g. lipopolysaccharides) and protein. The cell wall of thraustochytrids has not been characterised in detail, but in a study on two different strains, both sugars and protein were identified [17]. In addition to the physical barrier of the cell wall, the lipids may be bound, or associated, to other macromolecules in a way that reduces the extractability. There are three main types of association in which lipids participate: i) hydrophobic or Van der Waals interactions; ii) hydrogen bonding and electrostatic association; iii) covalent association (not frequent). In the first case, the weak hydrophobic interactions can easily be disrupted by non-polar organic solvents. The hydrogen bonds may require the use of polar organic solvents for cell wall disintegration, and stronger electrostatic forces may break with drastic pH changes (acidic or basic region) [9].

Ultrasound at high acoustic intensities is known to disrupt microbial cells in suspension, namely *Thraustochytrium sp.* [18]. The advantage is that these processes can be combined with solvent extraction, but this method is not applicable to large-scale use, because of the associated high costs. For large-scale cell disruption of algae, mechanical shearing in a bead mill appears most suitable. Studies have been carried out on different microalgae, but since algae have very different types of cell walls, the results are not necessarily transferable between different organisms [9]. Disruption by high pressure release has also often been used (Hoeksema, US Patent No. 6166231; Liddell, US Patent No. 6180376) with thraustochytrids biomass. However, these methods may destroy parts of the final product during the disruption process, hence the importance of avoiding their use.

Another possibility for cell lysis under very mild conditions is the use of hydrolysing enzymes, also applicable at industrial scale (Kobzeff, US Patent No. 2006/0099693 A1). In addition enzymes offer selectivity during product release. Enzymes hydrolyse the cell walls, and when sufficient wall has been removed, the internal osmotic pressure bursts the membrane allowing the intracellular components to be released [10]. A specific enzyme for thraustochytrid cell wall disruption is not known yet, since the cell wall has not been characterised. However, short term heating followed by treatment with a protease have demonstrated to increase the extraction yields, as reported by Jakobsen *et al.* [19].

Various solvents or solvent combinations can be applied for extraction of individual lipids, depending on their polarity [9, 10, 20, 21]. In general, non-polar solvents, such as hexane or chloroform, extract the neutral lipids, and polar solvents, such as alcohols, extract the polar lipids. The extraction solvent or solvent mixture should be inexpensive, volatile (for ready removal and reclamation later), free from toxic or reactive impurities (to avoid reaction with the lipids), able to form a two-phase system with water (to remove non-lipids), and be poor extractors of unwanted components (e.g. proteolipids, and other small molecules).

Suitable solvents for acylglycerols extraction include aliphatic hydrocarbons, such as hexane or various petroleum ethers. Other solvents indicated include esters, ethers, ketones, and nitrated and chlorinated hydrocarbons, as long as the solvents are immiscible in water. Hexane has been the organic solvent most commonly used for oil extraction, more specifically the triacylglycerol fraction, both on analytical and industrial scales. It is completely miscible with oil, immiscible with water and it does not give an unpleasant odour to the oil or meal. This organic solvent has demonstrated considerable efficiency not only for extraction of triacylglycerols from microalgae [22, 23], but also the derived fatty acids after

saponification/interesterification of the biomass oil content [24-26]. Chloroform is known to extract hydrocarbons, carotenoids, chlorophyls, sterols, triacylglycerols, wax esters, long chain alcohols, aldehydes and free fatty acids. Acetone is not used so often, but it extracts mono and diacylglycerols, cerebrosides and sulfolipids. However, it is miscible with water and must be protected against absorbing too much water from the incoming material [9].

Alcohol containing solvent mixtures inactivate many of the lipid-degrading phosphatidases and lipases, and also help disruption of lipid-protein complexes and dissolution of the lipids. Methanol is normally included in the extraction mixture for extraction of phospholipids and traces of glycolipids. However, alcohol solvents also extract some cellular contaminants such as sugars, amino acids, salts, hydrophobic proteins and pigments.

Lipid hydrolysis

For isolation of fatty acids such as DHA, the lipid fraction of the microbial cell mass has to be hydrolysed. Hydrolysis is the reaction between water and lipids, including triacylglycerols (TAG), which results in the formation of diacylglycerols (DAG), monoacylglycerols (MAG), free fatty acids (FFA), and glycerol. The water content influences or even determines the rate and extent of hydrolysis. For the lipid hydrolysis, two main alternatives exist: chemical hydrolysis (alkaline or acid) and enzymatic hydrolysis.

The alkaline hydrolysis is commonly used by the oil and fat industry (e.g. Hoeksema, US Patent No. 6166231) and involves saponification with NaOH or KOH (the hydrolysing agent), which can be performed either with or without previous extraction of the lipid fraction from the biomass [16, 27]. However, chemical hydrolysis involves high energy utilisation and yields a product requiring costly purification. Due to the use of temperatures around 60-80°C

for extended periods of time, the oxidation and polymerisation of unsaturated fatty acids are inevitable. Hence, chemical hydrolysis has not been considered practical for the splitting of sensitive triacylglycerols for production of high value polyunsaturated oils.

The application of enzymes for lipid hydrolysis has become more attractive, since enzymatic hydrolysis may create significantly less burden on the environment in terms of energy consumption and waste produced [28, 29]. Enzymatic processes are carried out at mild conditions (temperatures around 30-40ºC and neutral pH), which can help to prevent the fatty acids oxidation. Development and evaluation of enzymatic methods for production of fatty acids and fatty acid-derived esters has been a focus in both academic and industrial circles [6, 9, 26, 28-31].

The rate of the enzymatic reaction is influenced by several factors, namely: the water content; the nature of the enzyme; the concentration and ratios of reactants; the presence of other compounds in the reaction solution; temperature and pH; and the experimental apparatus [9]. The key is to find the right reaction conditions and the appropriate substrate and enzyme combination. Most frequently, enzymatic reactions take place in aqueous solutions, since water participates in all non-covalent interactions. However, enzymatic conversions can also be performed in water-immiscible substrate mixtures, for instance when a non-polar solvent is added for substrate dissolution [32].

Hydrolysis by lipases has been described as a method for enrichment of the long chain PUFA-content in triacylglycerols, by removal of the saturated and monounsaturated medium chain fatty acids, in both vegetable [28, 33-38] and fish oils [9, 30, 39]. This aspect will be explored in more detail in Chapter 3.

Chromatography

Chromatographic separation of fatty acids is widely used in order to obtain individual fatty acids with high purity. Counter-Current Chromatography (CCC) or Centrifugal Partition Chromatography (CPC) has gained much attention in recent years for isolation of polyunsaturated fatty acids. This liquid chromatographic technique does not require a solid support, it uses liquid-liquid partition, and counter-current distribution of solute mixture between two liquid phases to perform separation of complex mixture of chemical substances [6]. Decomposition and denaturation of valuable sample components, often faced with conventional packed chromatographic columns, are virtually non-existent under the mild operating conditions used in CPC. The other advantages of CPC are the low solvent consumption, and the same solvent combination may be used to conduct both normal and reversed-phase elution. The crucial selection of solvent systems for CPC is based on the solubility of the sample, and the difference in partition coefficients of the compounds to be separated. Solvent phase diagrams are also commonly used for selection of adequate solvent systems for CPC. Bousquet *et al.* have tested CPC for separation of EPA and DHA from microbial oil and were able to isolate pure EPA and DHA from this oil with excellent yield [40, 41]. In order to isolate ultra-pure DHA (99%, fine chemical grade), pre-purification of algal oil-FFA was needed by complexing with urea to remove the coeluting C14:0 (myristic acid). CPC is claimed to be a process-scale separation technology, offering distinct advantages over other methods for the separation, isolation, and purification of fatty acids [6]. It is also complementary to HPLC. Although capital investment for a CPC often runs higher than that for HPLC, operating costs are generally an order of magnitude lower. Another advantage is that it is possible to run the separation under a blanket of nitrogen or other inert gas, when working with substances susceptible to oxidation. So far it has demonstrated its

potential for the separation of lipid molecules at the level of a few grams and is expected to develop into production at kilogram levels [6].

Silver nitrate HPLC is a rapid semi-preparative pre-fractionation method for highly unsaturated fatty esters with 3-6 double bonds. It has proven being able to isolate individual fatty acid methyl esters., they can be separated on the basis of number, position, and geometric configuration of double bonds [9]. The method is based on the formation of a reversible charge-transfer complex involving the silver ion and the double bonds. Fatty acids that are poorly resolved by reverse-phase chromatography may be separated on silver nitrate columns, because the number of double bond is the only basis for the separation. In reverse-phase separations, the effect of double bonds is sometimes neutralized by that of the chain length [9]. Teshima *et al.* used a silver nitrate-impregnated silica gel column to separate EPA and DHA from squid liver oil fatty acid methyl esters with a purity of 85–96% EPA and 95–98% DHA and a yield of 39% and 48%, respectively [42]. Dejarlais *et al.* were able to enrich the omega-3 content of commercial omega-3-PUFA concentrates from 76.5% to 99.8% using isocratic elution from a silver resin column [43].

Distillation

Distillation has been used for partial separation of mixtures of fatty acid alkyl esters. This method takes advantage of existing differences in the boiling point and molecular weight of fatty acids under reduced pressure and requires high temperatures of approximately 250ºC. However, fractionation of PUFA-rich oils (e.g., marine oil esters) is difficult because separation of these components becomes less effective with increasing molecular weight [9]. Distillation is often used in combination with other purification techniques.

Crystallisation

It has long been known that the higher saturated fatty acids are much less soluble than their correspondent unsaturated counterparts and may be partially separated from a mixture. Therefore, crystallisation at ordinary zero, and sub-zero temperatures has been a useful method of purifying fatty acids and their derivates [44]. Fractionation by crystallisation using the differences of melting point of fatty acids or triacylglycerols is done in two ways. Dry fractionation, also known as the low-temperature crystallisation, consisting of the enrichment of oil with the more unsaturated triacylglycerols by removing saturated, high melting components at low temperature and does not need the use of organic solvents. The other method is solvent crystallisation, which involves use of organic solvents such as acetone or hexane in order to improve the yield of each fraction [6].

Urea complexation

The applications of urea inclusion compounds (UIC) in separation of fatty acids involve isolation of PUFA and cyclic free fatty acids in the non-inclusion fraction. UIC-based fractionation is very efficient in removing saturated fatty acids as a UIC fraction. The main selectivity for separation of fatty acids via forming UIC includes: (i) increased discrimination against inclusion as the number of double bonds per molecule increases; (ii) preference of molecules of longer chain length; (iii) preference for *trans*- versus *cis*- double bonds with *trans*- monoenes are often preferred over the corresponding saturate, and; (iv) sensitivity for double bond position [6]. Therefore, formation of urea inclusion compounds depends on the degree of unsaturation of the fatty acids involved. Alternatively, this procedure can be carried out using methyl or ethyl esters of fatty acids rather than free fatty acids. There are advantages and drawbacks for each of these options. For example, fatty acids are more soluble in alcohol than their corresponding esters hence they require a much smaller volume of alcohol for

processing. Han *et al.* have tested a series of solvents (ethanol, methanol, water, formamide, and acetonitrile) as wetting agents for urea [45]. The presence of phospholipids, di- and triacylglycerols greatly reduces the amount of UIC formed, and so refining of FFA mixtures prior to UIC-based fractionation is necessary. Methanol and ethanol are preferred solvents for small-scale fractionation, but recently Han *et al.* found that water may offer the best choice of solvent for large-scale operations because of its low cost and lack of toxicity [45]. Many publications have described the application of urea complexation in both analytical and preparative applications. It should also be noted that in urea complexation, the complexed crystals are very stable, and hence, filtration at the very low temperatures used for solvent crystallisation of fatty acids is not required. Use of urea complexation in combination with chromatographic separation allows preparation of fatty acids with a high degree of purity.

Supercritical Fluid Extraction – SFE

Some years ago, the replacement of the conventional solvent by a sub- or supercritical one appeared as an alternative for reduction of contamination of high value compounds [6, 9, 46, 47], for example the extraction of fatty acids from *Schizochytrium sp.* [48]. Supercritical Fluid Extraction (SFE) uses compressed gas as the extraction medium and avoids some of the problems associated with the use of classical separation techniques involving organic solvents. Classically, the separation of the supercritical solvent from the extracted solute is achieved by decompression. This leads to savings of energy or the design of acceptable green processes with carbon dioxide [47]. For edible applications, CO_2 is chosen because it has moderate critical temperature and pressure and is inert, inexpensive, non-flammable, environmentally acceptable, readily available, and safe. Carbon dioxide has critical temperature of 31.1ºC (at ~74 bar), which allows the extractions to be carried out at temperatures below 100ºC [6]. The separation of PUFA by SFE is dependent on the molecular

size of the components involved rather than their degree of unsaturation. Therefore, a prior concentration step is needed to achieve a high concentration of PUFA in the final product. Oils to be used for enriching PUFA by SFE require preparation steps of extraction, hydrolysis, and esterification by conventional methods. Supercritical fluid extraction has been effectively used to refine fish oils and to remove cholesterol, polychlorinated biphenyls (PCB), Vitamin E, and other components. Some published examples concern the extraction of natural pigments such as carotenoids [49] and the fractionation of fish oils [46]. Recently, propane has gained more attention in extraction technology, especially in the nutraceuticals industry. However, more research will be required to determine the extent of its use for separation of PUFA from different oils. Extremely high pressures and high capital costs required might limit the widespread use of this method for industrial-scale production.

From this, it can be concluded that a single method may not be enough to achieve high degrees of purity in most of the cases. Depending on the complexity of the raw material and the desired purity of the final product, more than one fractionation technique may be required.

1.2.3. Membrane filtration technology for oil refining

Membrane technology for separation of water-soluble compounds in aqueous systems is a well-established industrial technology. Use of membranes for separation of hydrophobic compounds is a less developed, but emerging technology, and it has drawn much attention in the last years, particularly using organic solvent nanofiltration (OSN) [45, 50-56]. OSN has shown potential to be an alternative to conventional separation and purification techniques especially high energy consumption technologies such as distillation and crystallisation. This development opens opportunities for the marine-lipid industry to reduce production costs and create new products. In particular those producing high-value concentrates of omega-3 fatty

acids for the nutraceuticals and pharmaceutical industry, with high requirements for purity, may benefit from this emerging technology.

A membrane-assisted solvent extraction process is attractive compared to classical processes, such as dispersion column or mixer–settler. For process applications the membrane modules and systems can be adapted to the special needs of the specific separation process to achieve optimal conditions. Use of special polymers, in the case of polymeric membranes, and suitable manufacturing techniques gives desired performance characteristics [56]. Membrane processes can be scaled up and the possibility of using the same materials and configurations in different sizes from laboratory to process scale reduces the validation effort [10].

Application of membrane technology in the processing of fats and oils has been studied in the areas of lipid refining, separation, decolouring, and decontamination [33, 34, 36, 57]. However, the application of these techniques is so far more commonly found in vegetable oils refining. Several authors have studied different configurations of membrane processes for oil refining, frequently combining simultaneous enzymatic reactions and separation [28, 29, 31, 58, 59]. Molinari *et al.* presented one of the first membrane reactors for fatty acid production [29]. Simultaneous reaction and separation in enzymatic hydrolysis of high oleate sunflower oil using membrane filtration technology was also explored by Gan *et al.* [28, 31]. The lower fluxes and recoveries obtained due to emulsification and accumulation of enzyme in the pressurised side of the membrane were the main limitations of such systems. In most cases, phase demulsification is necessary before product recovery by ultrafiltration or microfiltration of either the oil or the aqueous phase can be achieved.

Micro and ultrafiltration membranes have also demonstrated suitable application on microbial processes at industrial scale. US Patent No. 5378369 [60] describes an effective separation of β-carotene dissolved in an organic phase, passing the latter through a semi-permeable membrane, i.e. made by a material which is hydrophobic (e.g. polysulphones, polypropylene and polyfluorinated hydrocarbons). However, reference to applications of membrane technology for extraction or fractionation of fatty acids directly from a microbial biomass has not been found. This is one of the two main topics of the present thesis, and will be addressed in more detail in Chapters 5 and 6.

1.2.4. Product stability

Non-conjugated methylene groups of PUFAs are very easily attacked by oxygen resulting in hydroperoxides with conjugated double bonds. This reaction can proceed rapidly, depending on the degree of oxidation of the acid. Cosgrove *et al.* have studied the kinetics of some PUFAs oxidation in comparison to monounsaturated fatty acids [61]. They have reported that the degree of oxidation of DHA (C22:6) is over five times greater than that of oleic acid (C18:1). Once PUFA oxidation has started, it may be propagated by a series of autocatalytic reactions, leading to very diverse and, often, little known natural products including aldehydes, acids and other low molecular weight compounds. Polymerisation reactions may also occur [1]. The oxidation rate is accelerated by light, heat, oxygen, moisture and the presence of catalysts such as metal ions. Working in an inert atmosphere (e.g. nitrogen) can minimise the exposure of PUFAs to these oxidation agents during processing. Separation techniques that employ heat should also be avoided.

Lipids, and particularly PUFAs, must be protected against oxidation also during storage. For temporary storage, diluting the oil with a solvent, such as petroleum ether (low oxygen

solubility) or hexane, may greatly reduce the rate of oxidation [62]. Auto-oxidation is proportional to oxygen concentration at low partial pressures; therefore oxygen must be rigorously kept out. Ideally, the oils should be sealed under vacuum with minimum headspace. Low temperature storage is essential. At - 20°C the rate of deterioration is only about $1/16^{th}$ that of at room temperature. Extended good quality storage of several years requires yet lower temperatures of -40°C to -80°C [9].

Antioxidant additives can effectively slow oxidation of PUFAs [63]. Effective antioxidants are tertiary butylhydroquinone (TBHQ), butylated hydroxytoluene (BHT) and octyl gallate. In view of the potential toxicity of these synthetic antioxidants, use of natural ones obtained from the resinous residues of the first phase of pollen digestion by bees, has been suggested [63].

1.3. Thesis Aims and Research Strategy

Production of DHA-rich oils or free DHA from microbial biomass is currently an expensive, multi-step process (see Figure 1.2). Reduction of the number of process steps may reduce the production costs. This applies in particular to the drying of the cell mass, which is very energy demanding. Freeze drying will be too expensive in process scale, and other large scale drying methods consist of air-drying and/or heat and should not be applied for the easily oxidable LC-PUFAs. The development of integrated processes for extraction and fractionation of fatty acids in one single operation has become more attractive, in comparison to a multi-step process. It could help reducing the extractant volumes required, enhancing yields and quality of the final product.

The overall aim of this work was to combine enzymatic hydrolysis of triacylglycerols to fatty acids, and membrane separation of the released fatty acids, with wet biomass as raw material, in order to reduce the number of process steps needed to produce DHA-rich oils or free DHA. The central concept is to carry out the hydrolysis of the cell mass lipid content to free fatty acids directly in the cell mass concentrate, i.e. without previous isolation of the lipid fraction.

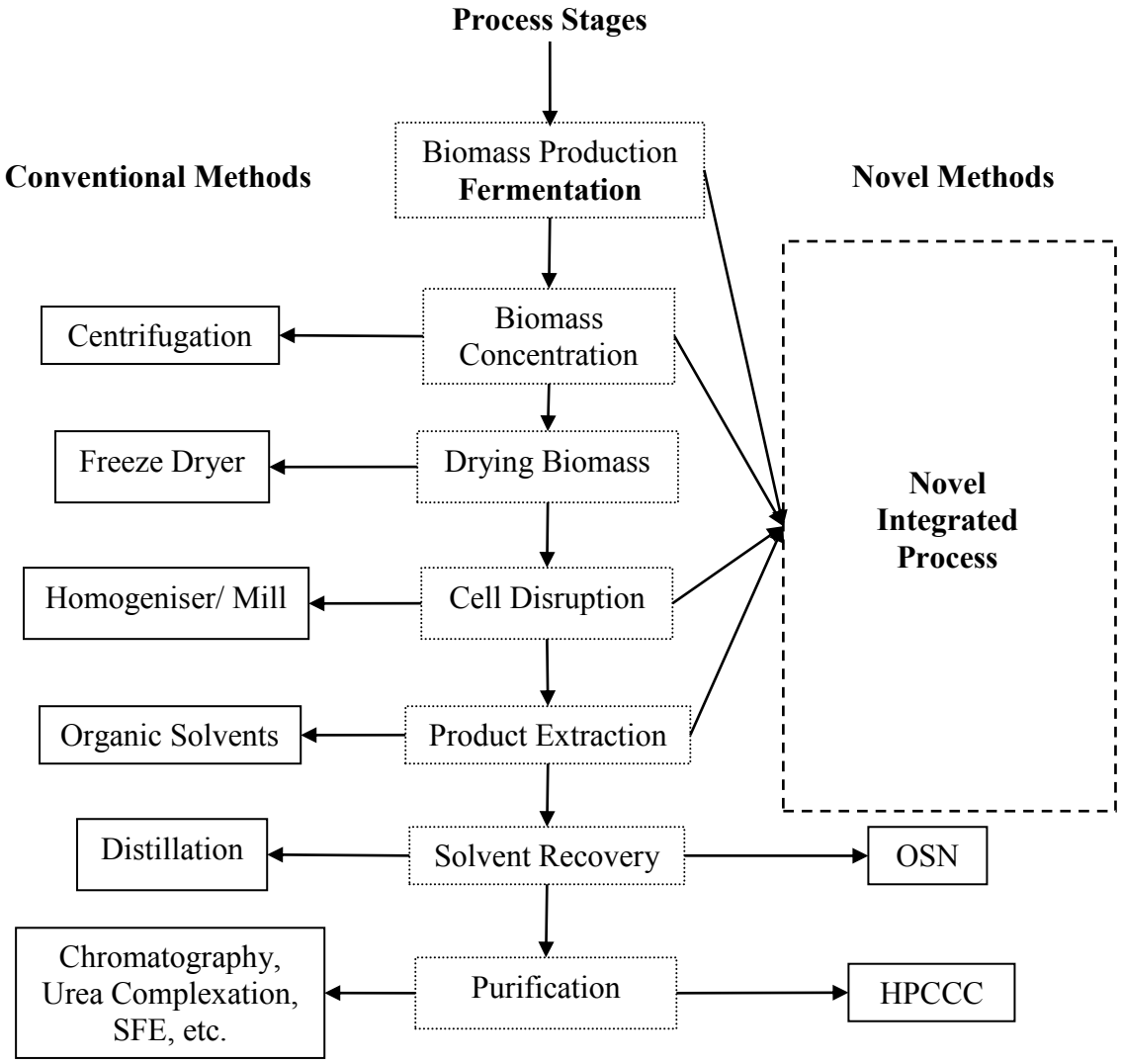


Figure 1.2: Typical process stages followed to extract and purify DHA from a fermentation broth, the conventional methods used for each stage, and which of these stages will be covered by the proposed novel integrated process.

A potential integrated process was designed for extraction and fractionation of DHA from other fatty acids starting with a wet cell mass of thraustochytrids, as illustrated in Figure 1.3.

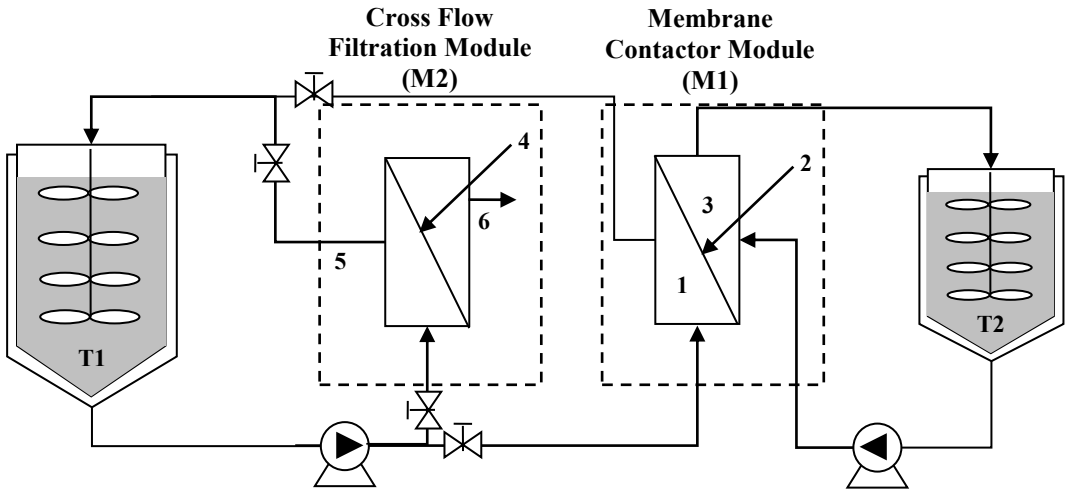


Figure 1.3: Schematic diagram of the integrated process (T1 - bioreactor for cultivation of the microbial cell mass and further enzymatic hydrolysis of lipid content; M2 - cross-flow membrane filtration system for continuous cell harvesting; M1 - membrane biphasic system for product extraction; T2 - product recovery tank).

The novel integrated process consists of: a bioreactor (T1) for cultivation of the microbial cell mass and further enzymatic hydrolysis of lipid content; a cross-flow membrane filtration system (M2) specially designed for continuous cell harvesting; a membrane biphasic system (M1) for product extraction; and a product recovery tank (T2). After cell mass cultivation, the fermentation broth is first circulated from the bioreactor T1 through the cross-flow membrane module M2, generating a waste permeate (6) across the membrane (4), consisting mainly of water and low molecular weight compounds. The retentate (5) is directed back to the bioreactor, where hydrolysis of the cell mass lipid content for production of free fatty acids is performed. After that, the cell mass suspension containing the free fatty acids is circulated to the aqueous compartment (1) of the membrane contactor module M1, extracting the fatty

acids across the membrane (2) to the organic solvent circulating in the organic compartment (3) of the membrane contactor, accumulating in a product recovery tank T2. A solution rich in DHA is the preferred product obtained at the end of the integrated process.

This requires selection of suitable enzymes for selective release of DHA, and membranes with high transport rates for DHA. The main parts of this investigation have been directed at these two topics, with the specific aims:

- Characterise the thraustochytrid cell mass: determine lipid composition, including lipid classes, fatty acid composition and distribution among lipid classes;
- Select enzymes for selective hydrolysis of triacylglycerols, based on their specificity and reaction kinetics;
- Investigate the needs for pre-treatment of the biomass by mechanical or chemical methods, and the influence of the pre-treatment on the enzymatic hydrolysis performance;
- Develop a kinetic model for the enzymatic hydrolysis of triacylglycerols in presence of multiple substrates and products;
- Prepare and characterise membranes with respect to molecular weight cut-off and mass transfer performance;
- Study solute transport through asymmetric polyimide porous membranes in a biphasic membrane contactor system;
- Select membranes and operating conditions for effective separation of fatty acids from a fatty acid rich solution to an organic phase in a biphasic membrane contactor system;
- Demonstrate the integration of selective hydrolysis of triacylglycerols and simultaneous separation of released fatty acids in the biphasic membrane contactor system (proof of concept).

Additionally, it was a part of the work to become familiar with fermentation processes and their optimisation. Parameters including glycerol (feed stock) and nitrogen concentration, oxygen level, stirring, pH and sterile air flow have to be controlled. The understanding of the influence of each parameter on the growth and lipid yields and how to manipulate them for a better performance were addressed.

Further, cross-flow membrane filtration was demonstrated as an efficient method for dewatering of the biomass before hydrolysis. Membranes and process conditions for efficient dewatering of the cultivated cell mass by cross flow microfiltration were evaluated.

In order to determine the hydrolysis kinetics, which is a multi-step reaction from triacylglycerols, via di- and monoacylglycerols to free fatty acids, new analytical methods were required. In the present investigation, qualitative and quantitative analyses of acylglycerols and free fatty acids were conducted preferentially by liquid chromatography coupled with electrospray mass spectrometry (LC-ESI-MS), and not gas chromatography (GC).

1.4. Structure of the Thesis

This thesis is composed of seven chapters:

- Chapter 1 presents the background relevant for the present investigation, the motivation for the present investigation, the main objectives and work strategy.
- Chapter 2 gives insight into the production and characterisation of the raw material used in this investigation. Different methods for pre-treatment of the cell mass are also approached.

- Chapter 3 presents the work carried out for the study of hydrolysis of the cell mass lipid content. Chemical and enzymatic hydrolysis methods were evaluated. New information about the reaction kinetics for a range of enzymes on the biomass lipids is presented.

- A kinetic model for the stepwise enzymatic hydrolysis of triacylglycerols in an oil:water emulsion, considering multiple substrates and products is proposed in Chapter 4.

- The study of solute transport, namely DHA, through integrally skinned asymmetric polyimide membranes in a biphasic membrane contactor system is presented in Chapter 5. Performances of several polymeric membranes for the separation of fatty acids were studied.

- Chapter 6 includes the description of the integrated process designed and corresponding proof of concept, and a short analysis about the feasibility and applicability of the process at industrial scale.

- Main conclusions of the PhD work and suggestions for future work are enumerated in Chapter 7.

Chapters 2-6 each include the background literature search carried out for each subject, enumeration of the specific objectives and hypotheses, the description of materials and methods, results and corresponding discussion, and finally the main conclusions are pointed out, emphasizing which of them motivated further research.

Chapter 2

Production, Characterisation and Concentration of the Microbial Cell Mass

2.1. Summary

In this chapter, an overview on microorganism as a source for production of polyunsaturated fatty acids, such as DHA, is presented. A thraustochytrid species was selected as raw material for this investigation. The fermentation parameters used for the cultivation of the cell mass are described. Next, the lipid content of the cell mass was characterised by well-established analytical methods. Total lipid content was found to be 40-42 wt% of the cell dry weight, of which 85% were triacylglycerols and 14 wt% phospholipids. In respect to fatty acids composition, DHA constituted 42 wt% of total fatty acids, followed by palmitic acid (PLA, 29 wt%) and oleic acid (OLA, 18 wt%). Information regarding the positional distribution of fatty acids in triacylglycerols was obtained. More than 50% of DHA was found to be in sn-2 position, while over 80% of PLA and OLA were distributed between sn-1,3 positions. This information was of great importance for further development of the selective enzymatic hydrolysis of triacylglycerols. Finally, cross-flow microfiltration was tested for concentration of the fermentation broth. Permeances in the range 200-300 L m^{-2} h^{-1} bar^{-1} were obtained for ceramic membranes at low transmembrane pressure and cell concentrations above 100 g L^{-1}

dry weight. The fermentation broth could be concentrated from 50 g L^{-1} to 200 g L^{-1} dry weight.

2.2. Background and Literature Review

2.2.1. Microorganisms for production of PUFAs

It is a general concept that microorganisms can produce, at least in theory, any product that can currently be identified in any living cell. They will produce them faster, more safely (since there is no or little need to spray them with pesticides, herbicides, etc.) than any other system. They are the ultimate controlled living system [7]. Fish oil is still the major source of DHA, but nowadays production using microorganisms has been increasing. Marine microorganisms may contain large quantities of DHA (see Table 2.1), and are considered a potential source of this important fatty acid. Indeed, it is now well known that these microbes are the basis of the food chain among fish, and are responsible for the synthesis of the DHA that appears in fish oil.

Although all living organisms must synthesise a minimum amount of lipid for their membranes and other structural and functional roles, only a relatively small number of identified microorganisms are able to accumulate lipid above about 20% of their cell mass. These are the so called oleaginous species [7]. The oils from microorganisms are referred to as Single Cell Oils (SCO), SCOs have an advantage over the traditional sources for provision of LC-PUFA since they are produced by fermentation, ensuring that the quality and supply can be closely controlled and guaranteed [64]. Also, the growth of microorganisms is very rapid in comparison with agricultural crops and animals; usually fermentation times are 4 to 10 days. As a result, the supply of SCO is accepted in the market, avoiding oversupply or shortage problems that can be an issue with traditional oils [1].

Of crucial importance in the further development of single cell oils processes is understanding how the microorganisms synthesise their fatty acids and how they are able to accumulate large amounts of oil. In some microorganisms, the content of oil can exceed 70% of the biomass [5]. In order to achieve lipid accumulation in a microorganism, it needs to be grown in a medium with excess of carbon substrate and a limiting amount of nitrogen. The cells, as a consequence of this nutrient exhaustion, can no longer grow and multiply, but they do continue to take up the carbon source present in the medium. It is this surplus carbon that then becomes the source for lipid biosynthesis [7].

Optimisation and manipulation of culture conditions to produce the amounts and types of PUFA required for specific applications are attracting extensive research for each strain taken toward commercial production. This is evidenced by a collection of articles and patents published [65-70] (Yokochi *et al.* US Patent No. 6582941, 2003; Barclay US Patent No. 5340594, 1992).

Marine protists and dinoflagellates, such as species of *Thraustochytrium, Schizochytrium* and *Crypthecodinium* are rich sources of DHA, as evidenced in Table 2.1. These microorganisms are heterotrophic, i.e. can grow without light, with organic carbon sources. However, the best current source of EPA appears to be photosynthetic microalgae, of which *Porphyridium cruentum*, *Isochrysis galbana*, *Nannochloropsis oculata*, and *Phaeodactylum tricornutum* are the prime candidates [7]. However, there are some important cultivation aspects of each that could determine the choice.

Table 2.1: Percentage of fatty acids with 14 or more carbon atoms within the lipids of selected marine microorganisms. (H-heterotrophic; P-phototrophic; adapted from Sijtsma et al. [8])

Organism	14:0	16:0	16:1	18:0	18:1	18:2	18:3	18:4	20:4n-6	20:5n-3	22:5n-6	22:6n-3
Thraustochytrium aureum (H)	3	8			16	2	2		3			52
Schizochytrium sp. (H)	4	55		1							6	30
Crypthecodinium cohnii (H)	17	17	1	2	10							44
Amphidinium carterae (H)	8	15	5	3	5	6	17			4	4	2
Isochrysis galbana (P)	12	10	11	1	3	2		11		25		11
Skeletonema costatum (P)	17	17	11		2	1		6		41		7
Amphidinium sp. (P)	5	27		18	17	2	2			8		17
Pavlova lutheri (P)	14	11	10		3			4		12		7

Heterotrophic versus Phototrophic Microalgae Production

Phototrophic microalgae need only CO_2 as carbon source and light as energy source. However, the use of sunlight limits the production to certain areas of the world. Artificial light is energy demanding, expensive, and possible only for high-value products. Even with technologically advanced bioreactors for algal fermentations, maximum cell densities and growth rate attained are low (typically below 5 g L^{-1}), making such processes normally cost-prohibitive for production of industrial products [69-71]. Heterotrophic algae are grown in conventional fermenters, and do not need light as a prerequisite for growth. With heterotrophs, photosynthesis for carbon and energy generation is replaced by the supply of glucose or other utilizable carbon source to the medium [7]. It may only be limited by viscosity and oxygen transfer. Cell densities above 150 g L^{-1} can be achieved and at higher growth rates [19]. The *de novo* synthesis of omega-3 and omega-6 PUFAs by thraustochytrids and other heterotrophic microorganisms may provide an easier and less expensive means of producing PUFA-rich biomass and oils. An increasing number of research groups into microheterotrophic PUFA production has concentrated on the thraustochytrids.

Thraustochytrids

Thraustochytrids, a group of marine unicellular eukaryotic protists, are common marine microheterotrophs, taxonomically aligned with heterokont algae. Several studies have shown that some thraustochytrid strains can be cultured to produce high biomass. During the last 15 years, a large number of thraustochytrid strains have been isolated and characterised with respect to lipid and DHA production [18, 72, 73], and commercial production is established by at least two companies. Actually, the best microbial sources of DHA are strains from the genus *Thraustochytrium* and *Schizochytrium*. They often accumulate more than 50% of their dry weight as lipids, with DHA frequently constituting more than 25% of total of lipids [4, 66,

67]. SINTEF (Trondheim, Norway) has established a collection of approximately 100 isolated strains of thraustochytrids (Figure 2.1) [74]. Selection of production strains was based on productivity, lipid content and fatty acid profile.

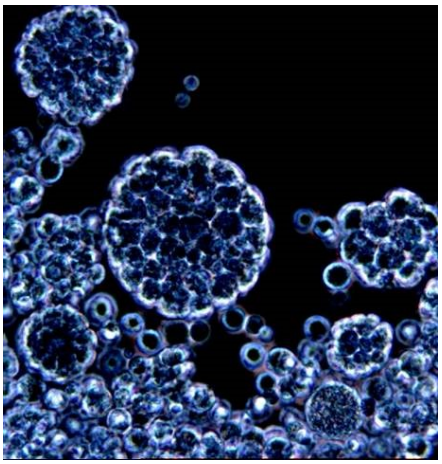


Figure 2.1: Thraustochytrids of the *Aurantiochytrium* sp. strain T66 in liquid medium (image adapted with permission from Anita N. Jakobsen PhD Thesis, NTNU, 2008).

For two strains studied at SINTEF, a cell mass of 80-100 g L^{-1} with 60% total lipids has been achieved for *Aurantiochytrium* sp. strain T66 [19], and 50 g L^{-1} with 45-50% total lipids for strain T29 (SINTEF, unpublished). The fatty acid composition of these two strains is presented in Figure 2.2.

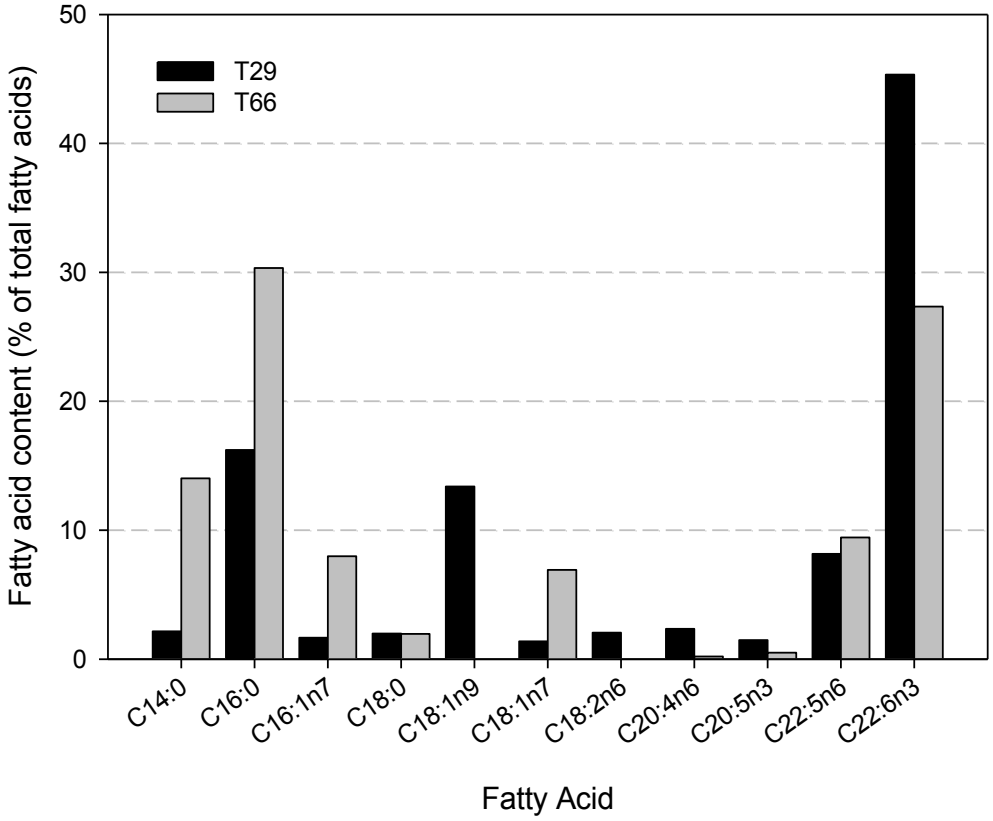


Figure 2.2. Fatty acids composition of two thraustochytrid strains isolated at SINTEF-Materials and Chemistry, Norway.

2.2.2. Analytical methods for characterisation of microbial cell mass lipid content

An efficient lipid extraction system, and the most routinely used procedure for analytical quantification of total lipids is a mixture of chloroform and methanol. In a simplified and improved procedure, Bligh & Dyer used a single-phase extractant, chloroform-methanol-water (1:2:0.8 by volume) for extraction of lipids from fresh tissues [9]. This method is applicable to a variety of materials, including animal or plant tissue, and microorganisms. Burja *et al.* recently evaluated various modifications of the standard Bligh & Dyer method, also combining with different disruption methods, for extraction of fatty acids from a dried biomass of thraustochytrids [18]. For analytical purposes, the thraustochytrid cell mass is normally freeze-dried (lyophilised) before extraction [18, 25]. These authors explain that

freeze-drying breaks up the cells and turns the algal material into a loose, fine powder, often making homogenisation unnecessary.

Total lipid extraction with a low-toxicity solvent mixture, such as hexane-isopropanol (3:2, v/v), followed by a wash of the extract with aqueous sodium sulphate, to remove the non-lipid contaminants, has some advantages over the Bligh & Dyer system [9, 20]. Namely, the extract contains less non-lipid material; interference in processing by proteolipid protein contamination is avoided; the two phases separate rapidly during the washing step; the solvent density is low enough to permit centrifugation of the homogenate as an alternative to filtration; the solvents are cheaper; the solvents can be eliminated by vacuum evaporation to dryness; and the washed extract can be directly applied to a chromatographic column with UV detection [9].

Pinkart *et al.* have developed an analytical method to separate the different lipid classes commonly found in microorganisms [75]. They used aminopropyl solid phase extraction columns to separate the different classes with specific solvents for each class, as listed in Table 2.2.

Table 2.2: Lipid class and respective extraction mixtures [75].

Solvents	Lipid Classes
Chloroform	Neutral Lipids
Methanol:Chloroform	Polar Lipids
n-Hexane	Sterial Esters
n-Hexane:Methylene Chloride:Chloroform	Triacylglycerols
n-Hexane:Ethyl Acetate	Sterols and Diacylglycerols
Methanol:Chloroform	Monoacylglycerols

Lipid classes are commonly analysed by HP-TLC [76]. For characterisation of the fatty acid content of microbial biomasses, several gas chromatographic (GC) separation methods are available for analytical purposes [70], and liquid chromatographic (LC) methods have been applied for preparative and industrial scale separation [77]. Recent developments and drawbacks of these methods relevant for the present investigation are addressed section 3.2.4.

2.2.3. Concentration of the microbial cell mass

Different techniques such as centrifugation, dead-end filtration or cross-flow filtration may be used to concentrate cell mass from fermentation media. The feasibility of the methods will depend on factors such as the cell size, nature of the fermentation broth (e.g. viscosity and density difference) and whether the product is intracellular (in the cell mass) or extracellular (in the broth). The centrifugation often leaves fine solids in the supernatant, necessitating a further clarification step [78]. For dead-end filtration, the operating costs are lower, however, the small size and high deformability of the cells generate very rapid fouling either by forming a deposit on the membrane surface or by clogging pores. After a few minutes of operation, permeation rates become extremely low [79].

An alternative to these approaches, which has been developed over the last years, is cross-flow filtration. Compared with the separation techniques referred to above, cross-flow filtration represents an improvement in the permeation flux, the operating times and costs, scale-up is simple and cell washing is possible in a single process step [10]. Both microfiltration (MF) and ultrafiltration (UF) techniques are suitable for the separation of microorganisms. The choice is normally done according to the cell broth characteristics.

However, this method still presents some problems. Cells and other small size components tend to foul membranes, either by clogging the pores or by adsorbing into the membrane or by forming a compressible layer at the membrane surface, causing low permeation. The influence of tangential feed velocity, transmembrane pressure, starting conditions, cells and medium components concentrations on cross-flow filtration performances have been widely studied. Rossignol *et al.* tested these parameters with eight commercial membranes for the harvesting of two marine microalgae, *Haslea ostrearia* and *Skeletonema costatum*, both widely cultivated in western France [80]. The effects of antifoams, which are normally added during fermentation, on permeation and solute rejection in membrane filtration processes were studied by McGregor *et al.* [81] and Yamagiwa *et al*. [82]. Some authors have also investigated new systems to reduce fouling, such as air injections into the feed, co-current recirculation of permeate as in the bactocatch system [83].

Ceramic membranes have advantages over organic membranes in some industrial operations, not only because of their higher chemical and thermal stability, but also because interactions between cells and inorganic membranes are negligible. Therefore, filtration of fermentation media is best performed with ceramic membranes [78]. For example, Rossi *et al.* focused on the study of the performance of different inorganic membranes (microfiltration and ultrafiltration) for harvesting of a cyanobacterium – *Arthrospira platensis* [84].

The continuous circulation of microorganisms in a cross-flow system induces perturbations and then the damage of fragile cells, which could carry losses of desired product. It is a question requiring special attention, i.e. the shear stress of microbial cell suspensions in tangential flow filtration systems [85]. Choosing a suitable pumping system, may reduce the shear forces. Jaouen *et al.* had the integrity and viability of living cells during the

concentration process as priority on their study [85]. Vandanjon *et al*. investigated the effects of shear on two microalgae species, testing different pumps, intrinsic characteristics and operation conditions [86].

It has been reported that the efficiency of microfiltration for concentration of broths is often improved by increasing the particle size through flocculation [45]. A polymer solution, namely polyethyleneimine, was used as a flocculant by Han *et al*. [45]. However, the introduction of more chemical compounds in the medium makes the further purification even more difficult, in particular when the cell mass is the product.

While a few examples of cross-flow filtration at the pilot-scale and the manufacturing scale have been published, there is still a limited amount of information available regarding practical scale-up issues. Russotti *et al.* [87] developed a pilot-scale microfiltration harvest for the isolation of *Streptomyces griseofuscus* broth (200-400 liters). A two-fold concentration was achieved when using a broth with an initial concentration of suspended solids of ~30% (v/v) before diafiltration. Goklen *et al.* [88] developed an efficient cross-flow filtration process for the commercial-scale isolation (1000 liters) of an extracellular bacterial lipase.

Typical cell mass concentrations for phototrophic algae are 5 g L^{-1} or lower as mentioned before, while the concentrations of heterotrophic PUFA-producers are above 100 g L^{-1}. Concentration of the fermentation broth is therefore a more critical and expensive process step for phototrophic algae than for the heterotrophic, which also is reflected in the number of publications available. No specific information about cross-flow microfiltration of thraustochytrids has been found. Thraustochytrids are relatively large, with cell sizes in the range 10-20 μm, i.e. in the same order as yeast cells and many microalgae. Probably, the

performance and flux while concentrating a fermentation broth of thraustochytrids will be comparable to processes with these organisms. However, how the high oil content and the fragility of the thraustochytrid cells will affect the filtration performance is unknown.

2.2.4. Objectives

The overall aim of the work presented in this chapter was to study the production of the biomass used in this investigation, and to characterise the cell mass composition and the lipid fraction.

The following objectives were defined:

- Familiarisation with the fermentation process for production of the microbial cell mass;
- Determine the total lipid content of the microbial cell mass produced, lipid classes, fatty acid composition, and fatty acid positional distribution in the triacylglycerol molecules, using established analytical methods;
- Establish whether a cross-flow microfiltration system is suitable for concentration of the fermentation broth.

Information collected in this chapter forms the basis for further development of the integrated extraction and fractionation process.

2.3. Materials and Methods

2.3.1. Production of cell mass by fermentation

Microorganisms

Two strains, *Aurantiochytrium sp.* T66 and strain T29 were used [19, 74]. Strain T66 was produced in several batches (9 L) and applied for the cross-flow microfiltration experiments,

while strain T29 was produced in a pilot scale fermentation (150 L) and used for all other experiments throughout this investigation. The strains were stored in 15% glycerol at -80°C. For inoculum preparation, approximately 1 mL of the stock cultures was added to 50 mL growth medium in shake flasks, which were incubated in an orbital shaker at 200 rpm for 2 days (optical density (OD_{660}) between 5 and 10).

Medium and growth conditions

Fermentation was carried out as described by Jakobsen *et al.* [19, 74]. The growth medium (Table 2.3) was based on previously published work which was modified to give higher growth yields [19]. The medium was supplemented with 5.0 mL L^{-1} of an antibiotic solution (ampicillin/streptomycin, 60 g L^{-1}), 1.0 mL L^{-1} of a vitamin solution (0.2 g L^{-1} vitamin B12 (cyanocobalamin), 0.5 g L^{-1} thiamine-HCl, 0.05 g L^{-1} biotin, 0.10 g L^{-1} folic acid, 2.00 g L^{-1} Ca-Panthotenat) plus 1.0 mL L^{-1} trace mineral solution [74].

Table 2.3: Growth medium composition.

Component(1)	**Concentration (g L^{-1})**
Glycerol (87%)	90.0(2)
$MgCl_2.6H_2O$	0.8
Na-Glutamate	20.0
NaCl	14.4
Tris-base	6.1
Na_2SO_4	2.4
$CaCl_2.2H_2O$	0.5
KCl	0.4
Maleic Acid	5.8
*KH_2PO_4	0.5

(1) For strain T29 the medium was supplemented with 2 g L^{-1} yeast extract.

(2) Initial concentration. The concentration was kept around 20 g L^{-1} by addition of glycerol batches during the cultivation period. Total concentration ~150 g L^{-1}.

For biomass cultivation, bioreactors were used (14 and 300 L (from Chemap, Switzerland). They were equipped with a pH-controller, to maintain the pH between 6.8-7.3 (by automatic addition of NaOH and H_2SO_4), and an automatic stirrer speed controller, to keep the dissolved oxygen level above 20% of saturation. Fermentors were autoclaved (including growth medium) and then inoculated with 2% inoculum. The supplementary solutions were added after sterilization. 1 mL L^{-1} of antifoam (Clerol FBA 622, 10% w/w) was added. The normal fermentation period was 7-8 days for strain T29 and 5-6 days for strain T66. Strain T29 was cultivated at 25ºC and T66 at 28ºC.

Cell mass determination

The cell mass concentration and density was monitored during the cultivation period, measuring the broth turbidity (Optical Density – OD – by spectrometry) and cell dry weight (DW, g L^{-1}). For DW determination, a sample (e.g. 10 mL) was harvested by centrifugation (4000 rpm for 10 min) and washed with an isotonic NaCl solution (10%) and dried at ~100ºC for 24hr.

Cell harvesting and storage

T66 cell mass produced in 9 L batches was concentrated by cross-flow microfiltration, see section 2.3.3. T29 cell mass produced in pilot fermentation was harvested by a semi-continuous centrifuge (Sharples). The cell paste was stored at -40°C and used wet or freeze-dried.

2.3.2. Analytical methods

Total lipids

Total lipids were extracted from freeze-dried cell mass with chloroform-methanol-water according to the modified Bligh & Dyer (B&D) method as presented by Jakobsen *et al.* [74]. Some samples were submitted to an enzymatic treatment (protease from *Streptomyces griseus*, in a trisbuffer solution (0.1 M, pH 7.5) at 50ºC for 1 hr) prior to Bligh & Dyer extraction, as described by the same authors.

The total lipid content of the cell mass is calculated by:

$$Total\ lipid = \frac{(weight\ of\ test\ tube\ with\ lipid - weight\ of\ empty\ test\ tube) \times (added\ volume\ of\ chloroform)}{(transferred\ and\ evaporated\ volume\ of\ chloroform)} \qquad \text{(Eq. 2.1)}$$

Once the total lipid value is obtained, the percentage of fat on cells mass is calculated dividing the total lipids value by the weight of the cell mass into the test tube:

$$\%Fat = \frac{Total\ Lipid}{Cell\ mass\ Weight} \times 100 \qquad \text{(Eq. 2.2)}$$

The chloroform extract was used for determination of lipid class composition and analysis of the positional distribution of fatty acids in triacylglycerols.

Lipid class composition

Lipid classes were separated by an Iatroscan thin layer chromatography-flame ionization detector system (TLC-FID) (Iatron Laboratories, Tokyo, Japan). Chromarods SIII (Iatron laboratories, Tokyo Japan) were first scanned twice through the Iatroscan FID immediately

before sample application, in order to remove possible contaminants from the rods. Chloroform solutions of the lipids (1 μL, concentration 20 μg mL^{-1}) were spotted on the Chromarods SIII by the use of a single spotting action and a 10 μL chromatographic syringe. After spotting, the rods were conditioned in a constant humidity chamber for 8 min over a saturated NaCl solution and then transferred immediately to the developing tank. The solvent system consisted of hexane/diethyl ether/formic acid (85:35:0.04).

Fatty acid composition

For a complete characterisation of the fatty acid content and composition, freeze-dried samples of the cell mass were methylated according to the modified direct transesterification method of Metcalfe *et al.* [89], as described by Jakobsen *et al.* [74]. Analyses of fatty acid methyl esters (FAME) were carried out using a PerkinElmer gas chromatograph equipped with an autoinjector (injection volume of 1 μL) operated at 280°C and a flame ionization detector. A fused-silica capillary column, coating CP-wax 52CB, 25 m, 0.25 mm internal diameter, from Varian, was used. The oven was operated at maximum temperature of 250°C for 35 min. Helium was used as the carrier gas. The signals were identified by comparison with known standards (mixture ME 81; Larodan Fine Chemicals, Sweden) and quantified according to the response factor of the internal fatty acid standard (methylated heneicosanoic acid, C21:0; Larodan Fine Chemicals, Sweden) added to the samples before analysis. The peak area corresponding to the known amount of internal standard added was used for quantification of other fatty acids in the sample, from calibration curves prepared by using three distinct mixtures containing different concentrations of the fatty acids to be analysed.

Positional distribution of fatty acids in the triacylglycerols

Distribution of saturated fatty acids (SFA), monounsaturated fatty acids (MUFA) and DHA among sn-2 and sn-1,3 positions in the triacylglycerol fraction of the chloroform extracts from the selected samples of cell mass was determined by ^{13}C-nuclear magnetic resonance (^{13}C-NMR) spectroscopy, as described by Standal *et al.* [90].

2.3.3. Cross flow microfiltration system

Microbial suspension

Fresh fermentation broth was produced in Chemap fermentors (~9 L working volume). Strain T66 was chosen, since it presents faster growth than T29. The fermentation was stopped when a cell mass concentration of about 45-50 g L^{-1} dry weight was achieved. In order to compare membrane filtration performance, all trials were carried out with a cell mass concentration in this range.

Filtration equipment

The diagram presented in Figure 2.3 illustrates the cross-flow microfiltration minipilot rented from Orelis, Novasep, Applexion, France. The fermentation broth was continuously recycled from and to the vessel (1) through the membrane filtration module (3) by a monoscrew pump (2), with a constant speed (as indicated by the supplier: 35 Hz or 5 m/s for ceramic membranes). Permeate was collected in a reservoir placed in an electronic balance, which was connected to a laptop for data acquisition (permeate weight values were saved every 30 seconds). Filtration pressure was adjusted with main/ball/recirculation valve (V3).

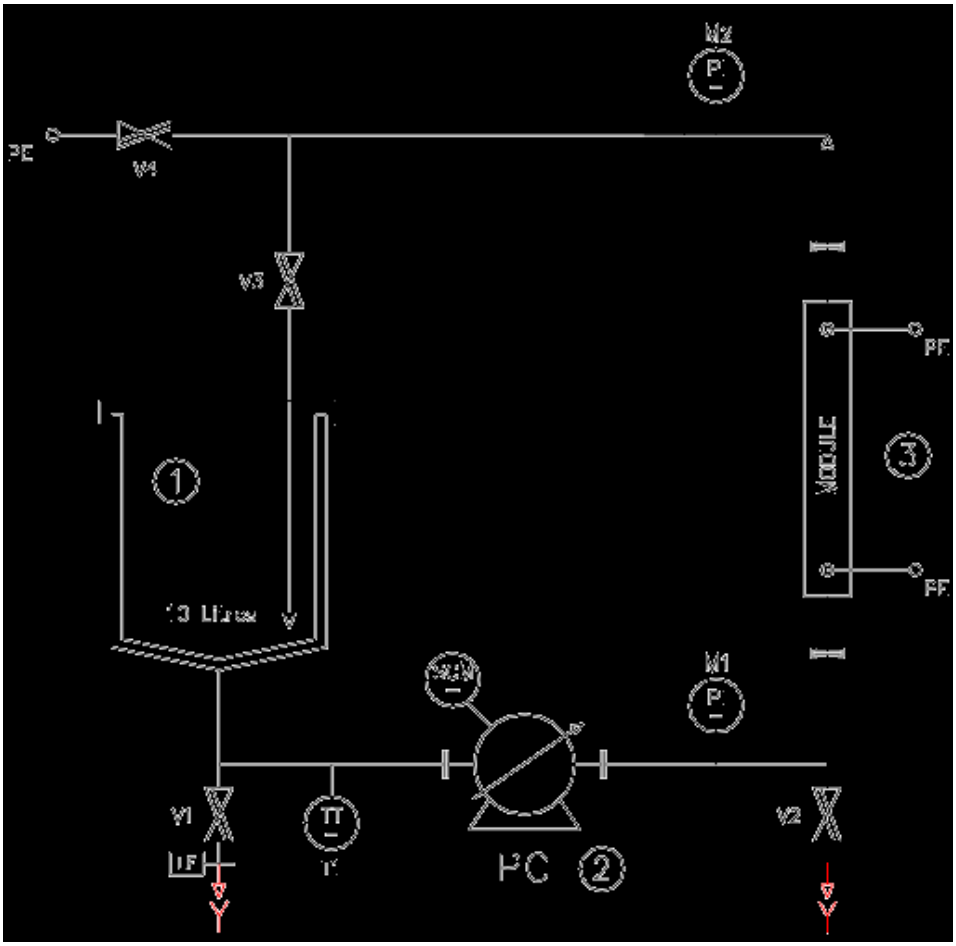


Figure 2.3: Diagram of the rented cross-flow minipilot (Orelis, Novasep, Applexion, France).

Membranes

Two microfiltration Kerasep^{TM} ceramic membranes – KERMBMM1 and KERMBMM2 (also supplied by Orelis, Novasep, Applexion, France) - with cut-offs of 100 nm and 200 nm (as given by the suppliers), respectively, were used in these experiments. The membrane dimensions are given in Table 2.4.

Table 2.4: Main characteristics of microfiltration membranes used - Kerasep™ ceramic membranes (KERMBMM1 and KERMBMM2; Orelis, Novasep, Applexion, France).

External Diameter	10 mm
Internal Diameter	6 mm
Length	400 mm
Membrane Area	0.008 m^2

Analytical techniques

The filtration flux was calculated based on the permeate weight variation, and the concentration factor from the difference between the dry weight of the original fermentation broth and the retentate.

Membrane cleaning procedure

After each experiment, the membrane was rinsed using demineralised water, starting at ambient temperature and progressively heating to ~50ºC, until obtaining a clear rinsed solution. The chemical cleaning started with an alkaline solution of soda (15 g L^{-1} NaOH; pH ~12) recirculating in the system for 1 hr at ~60ºC. After that, the system was again rinsed with demineralised water until neutrality. The acid cleaning was carried out using nitric acid solution (4 mL L^{-1}; pH ~2) at 50ºC, recirculating during 30 min. A demineralised water rinsing was done to restore the neutrality. The sequence was repeated until the regeneration of the membrane. The pure water flux of a membrane after cleaning denotes its cleanness. A solution of Ultrasil 11 (10 g L^{-1}) was used for the alkaline cleaning, instead of NaOH solution, for a more effective cleaning in the cases of persistent fouling.

2.4. Results and Discussion

2.4.1. Characterisation of the microbial cell mass lipid fraction

2.4.1.1. Total lipids

The total lipid content of the cell mass increased during the fermentation period, as depicted in Figure 2.4. Some samples were submitted to protease pre-treatment prior to lipid extraction, and the fat content values obtained for the same sample at different times of the cultivation period were considerably higher in this case.

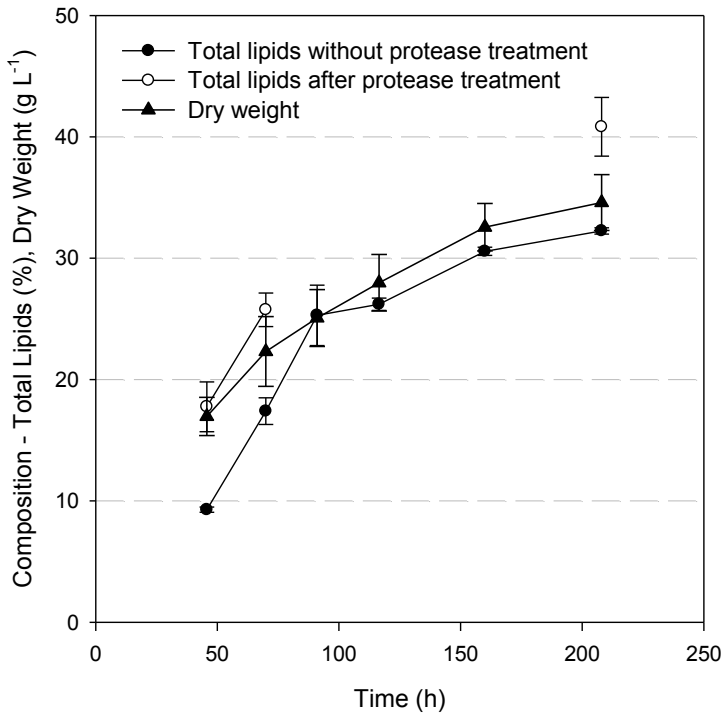


Figure 2.4: Total lipid content and dry weight of the microbial cell mass during the pilot scale fermentation (150 L) for strain T29.

The total lipid content measured in the samples collected at the end of the fermentation period, without the protease treatment prior lipid extraction, were 36% of the cell dry weight, increasing to 42% when protease treatment was performed. This difference confirmed that the lipid extraction when protease treatment was not performed was incomplete. As previously

discussed by Jakobsen *et al.* [19], and reported by other authors [91], the intracellular lipids of thraustochytrid cells are stored in lipid bodies surrounded by a protein layer (as illustrated in Figure 2.5).

Therefore, it was assumed that the complexes formed between lipids and proteins in the cells limited the separation of the lipid fraction. The protease treatment was responsible for the hydrolysis of the proteins surrounding the lipid bodies. Consequently, the subsequent extraction of the lipid fraction was facilitated.

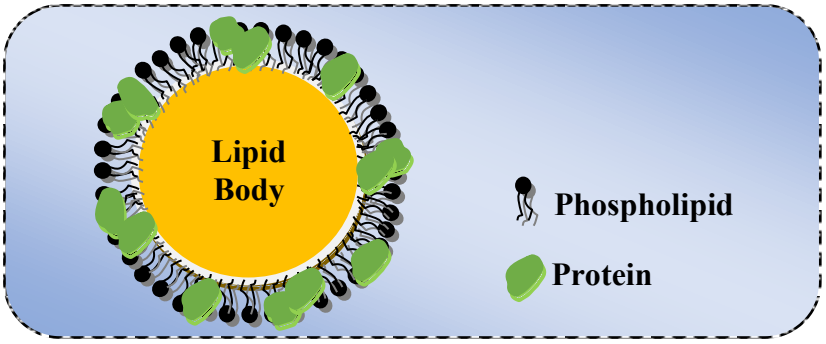


Figure 2.5: Illustration of a lipid body.

This observation is of particular importance when developing an industrial process for extraction and fractionation of high value compounds present in a cell mass, as it is the case of the present investigation, because an incomplete extraction would result in a considerable loss of the product of interest. This will be discussed in more detail later in Chapters 3 and 6.

2.4.1.2. Lipid class composition

As indicated in Table 2.5, HP-TLC analyses revealed that triacylglycerols were the main constituent of the lipid fraction extracted by the modified B&D protocol and after protease treatment (85 wt%), followed by phospholipids (14 wt%). The fatty acid composition of the

two main lipid classes was also determined. In the triacylglycerol fraction, DHA constituted 48 wt%, PLA 20 wt% and OLA 10 wt% of the total fatty acids. In the phospholipid fraction, PLA and OLA were in similar proportions, 27 and 29 wt%, respectively, and DHA corresponded to only 11 wt% of the total fatty acids.

Table 2.5: Lipid class composition of extracted microbial oil.

Lipid class	Composition ($g\ kg^{-1}$ cell mass)	Fraction (wt%)
Triacylglycerols	356.72 ± 0.03	84.89
Phospholipids	58.88 ± 0.24	14.02
Cholesterol	2.56 ± 0.18	0.61
Others	2.02 ± 0.03	0.49

2.4.1.3. Profile of total fatty acids

Table 2.6 shows the amount of each fatty acid methyl ester considered per kilogram of microbial cell mass. Docosahexaenoic acid (DHA, C22:6), palmitic acid (PLA, C16:0) and oleic acid (OLA, C18:1) constituted 90.4 wt% of total fatty acids. The remaining 9.6 wt% were mainly stearic acid (C18:0), arachidonic acid (ARA-C20:4), and docosapentaenoic acid (DPA - C22:5). These values were used as a reference for the results achieved while studying hydrolysis of the cell mass lipid content (Chapter 3).

Table 2.6: Amount of main fatty acids released by direct transesterification of microbial cell mass, and fraction in relation to total fatty acids accounted for.

Fatty Acid (FA)	Composition ($g\ kg^{-1}$ cell mass)	Fraction (wt%)
C14:0	4.0 ± 0.1	1.0
C16:0	118.4 ± 2.7	29.0
C16:1	0.9 ± 0.0	0.2
C18:0	14.1 ± 0.3	3.5
C18:1	76.0 ± 2.2	18.6
C18:2	7.1 ± 0.2	1.7
C20:1	1.4 ± 0.6	0.4
C20:4	11.4 ± 0.2	2.8
C22:6	174.9 ± 4.8	42.8
TOTAL	**408.2 ± 10.2**	**100**

2.4.1.4. Positional distribution of fatty acids in the triacylglycerols

The position of main fatty acids in the triacylglycerol fraction of the cell mass was determined as a basis for selection of enzymes for enzymatic hydrolysis, which is explored in Chapter 3. ^{13}C-NMR analyses showed that approximately 57% of total DHA was in the sn-2 position, as evidenced in the ^{13}C-NMR spectrum for the carbonyl region in Figure 2.6, with the rest distributed between sn-1,3 positions. Peaks at 172.85 and 173.25 correspond to monounsaturated and saturated fatty acids, in sn-2 and sn-1,3 positions, respectively. Therefore, approximately 80% of the SFA and MUFA, in this specific case mostly PLA and OLA, respectively, were located in sn-1,3 positions, and the remaining 20% in sn-2 position.

A significant fraction of the DHA (43%) occurred in the sn-1,3 positions. This is important information for the enzymatic hydrolysis, and differs from fish oils where a higher fraction of the DHA has been found to be in the sn-2 position in average 72% for Atlantic salmon oil,

and 74% for cod liver oil, and for harp seal oil above 80% (Aursand *et al.* [92]; Standal *et al.* [90]). The pattern of fatty acids distribution in triacylglycerol molecules is usually characteristic, and more or less unique for different marine oils, and this information can be used for identifying the source of a given fish oil, as well as to evaluate their quality [90, 92, 93].

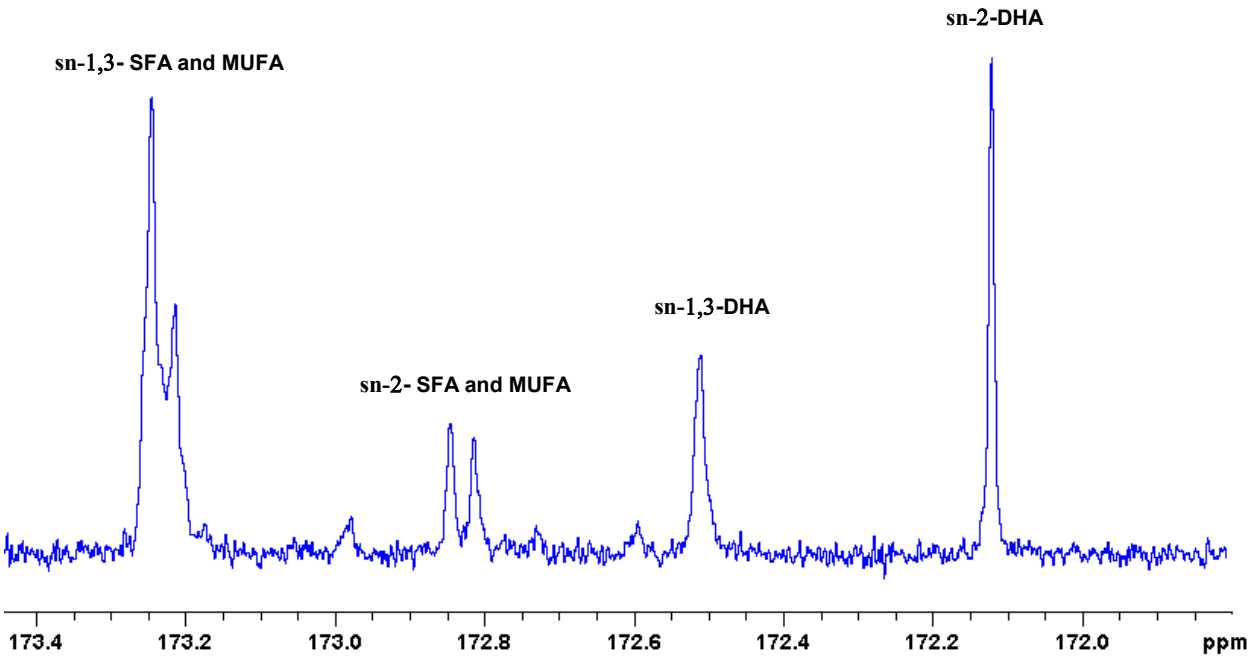


Figure 2.6: Enlarged carbonyl region (172.0-173.4 ppm) of a 600 MHz ^{13}C-NMR spectrum obtained for the thraustochytrids oil in casu, showing positional distribution of DHA, SFA and MUFA in the triacylglycerol fraction.

2.4.2. Cross flow microfiltration for concentration of the cell mass

Cross flow microfiltration was tested for concentration of the cell mass from the fermentation broth, as an alternative to centrifugation. Two ceramic membranes with different pore sizes were compared with respect to permeance at different transmembrane pressures (TMP) and cell concentrations.

A relatively low TMP (0.7 bar) was found to be the optimum when comparing permeate permeance at TMPs in the range 0.5-1.4 bar (Figure 2.7) for filtration with the membrane KERMBMM1 (100 nm nominal cut off). The higher the operating pressure, the more the cells tend to accumulate at the membrane surface, clogging the pores, hence the lower permeance observed. A TMP of 0.7 bar (Pin=0.8 bar; Pout=0.6 bar) was found to be ideal for this system.

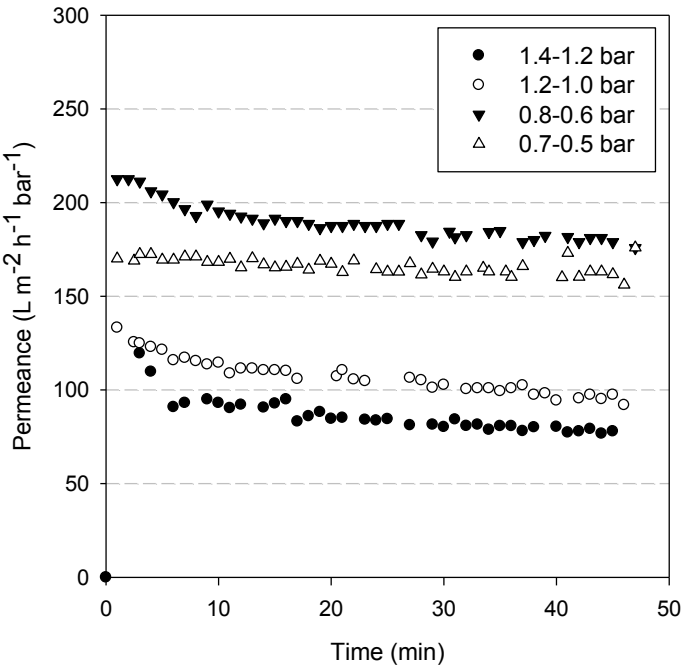


Figure 2.7: Variations of permeance with time for the membrane KERMBMM1 (100 nm cut-off) at different transmembrane pressures (Pin-Pout (bar); initial broth concentration ~45 g L^{-1}; T=25ºC, v=5 m s-1; pH~7).

When comparing the membranes KERMBMM1(100 nm) and KERMBMM2 (200 nm) at the same initial cell concentration and the same transmembrane pressure it is evident that KERMBMM2 had the best performance (Figure 2.8). After 2 hours running time, the final concentration achieved was in average 2-3 times the original concentration (~45 g L^{-1}).

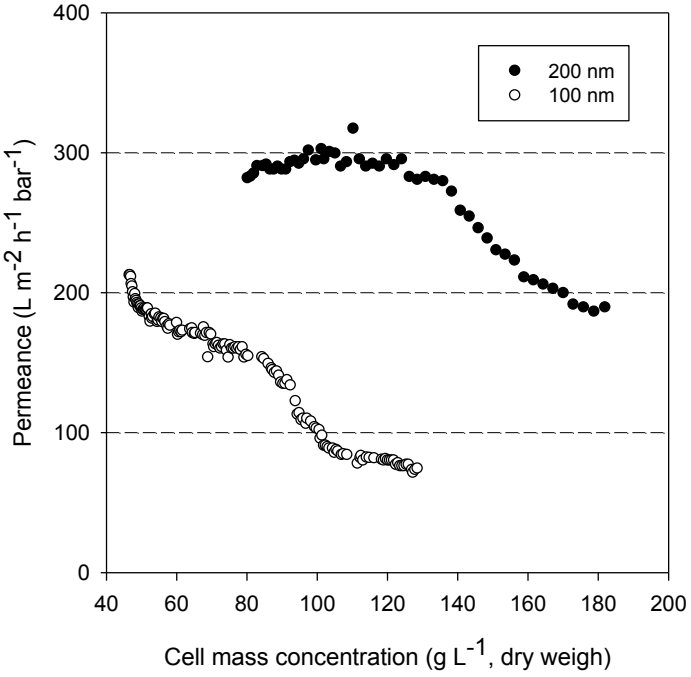


Figure 2.8: Variations in permeance with cell concentration for two microfiltration membranes (KERMBMM1 - 100 nm and KERMBMM2 - 200 nm) operating at the same transmembrane pressure (Pin=0.8 bar - Pout =0.6 bar). (T=25ºC, v=5 m s-1; pH~7).

The results show that cross-flow microfiltration with ceramic membranes is an efficient method for concentration of thraustochytrid cell mass. Any cell mass concentration in the range 50-200 g L^{-1} can be reached, with permeance 200-300 L m^{-2} h^{-2} bar^{-1}. For industrial strains giving cell mass above 100 g L^{-1}, concentration may not be required.

2.5. Conclusions

The lipid extraction yield increased considerably when the cell mass was submitted to a protease pre-treatment prior to extraction, giving a cell mass lipid content around 42 wt% at the end of the fermentation. The protease pre-treatment carried out is responsible for the hydrolysis of the protein content of the cell mass, consequently the following extraction of the

lipid fraction was facilitated. This observation was taken into consideration in the enzymatic hydrolysis experiments.

As expected, triacylglycerols were the largest fraction (~85 wt%), followed by the phospholipids (~14 wt%) of total lipids. The fatty acid content of the cell mass was determined as fatty acid methyl esters (FAMEs). DHA, palmitic and oleic acids constituted 90.4 wt% of total fatty acids. The remaining 9.6 wt% were mainly composed of stearic acid (C18:0), arachidonic acid (C20:4), and docosapentaenoic acid (DPA - C22:5). 57% of total DHA was in sn-2 position of triacylglycerols, as evidenced by the NMR spectrum, and the rest distributed between sn-1,3 positions.

Membrane permeance profiles and final concentrations achieved while testing the cross-flow microfiltration system for fermentation broth concentration were very good, whilst using low transmembrane pressure, which avoided cell damage and minimised membrane fouling. It demonstrated that the water content of the fermentation broth can be adjusted by membrane microfiltration. Any concentration in the range 50-200 g L^{-1} can be reached. Water flux recovery was possible, despite some loss observed after the first experiment.

However, cell mass dewatering was shown to be unnecessary, as will be explained in the next chapter, but the information about the cell mass characteristics was of high importance for the design of the new enzymatic hydrolysis approach.

Chapter 3

Hydrolysis of Triacylglycerols in a Lipid containing Microbial Cell Mass for Production of Fatty Acids

3.1. Summary

In this chapter a new approach to the enzymatic hydrolysis of triacylglycerols in a high lipid containing microbial cell mass is presented. Enzymatic hydrolysis was carried out directly on the wet cell mass, i.e. without previous isolation of the triacylglycerol fraction. The objective was to select the optimum enzyme or enzyme combination for a selective release of the targeted fatty acids, namely docosahexaenoic acid (C22:6-DHA), palmitic acid (C16:0-PLA) and oleic acid (C18:1-OLA). Initially, the performance of a range of lipases for the hydrolysis was evaluated with respect to hydrolysis rates, yields and selectivity. Suitable lipases for the desired selective release of the targeted fatty acids were identified. New analytical methods using LC-ESI-MS were developed for quantification of free fatty acids and individual mono-, di- and triacylglycerols throughout the reaction. The effect of protein and phospholipid hydrolysis as pre-treatments for the microbial cell mass prior to the triacylglycerol hydrolysis were evaluated. The desired enhancement of the initial release rates was not observed, and so it was concluded that the pre-treatment of the cell mass was not an advantage.

3.2. Background and Literature Review

3.2.1. Hydrolysis of lipids as part of a wet microbial cell mass

Today's industrial production of omega-3 LC-PUFA concentrates is based on purchased fish oil. With an oil as a raw material, transesterification (also known as alcoholysis) with e.g. ethanol is the most common process. When starting with a microbial cell mass, with a higher water content, hydrolysis may be more feasible, since two process steps can be omitted, namely water removal and oil extraction.

In the present work, the aim has been to use enzymatic hydrolysis, and to utilize the enzyme specificities to obtain a selective and sequential release of the main fatty acids, as part of a separation process. Chemical hydrolysis of wet biomass was carried out as a reference. However, it is essential to point out that a chemical hydrolysis or transesterification will release fatty acids not only from the triacylglycerols, but also from the phospholipids.

Chemical hydrolysis

The alkaline hydrolysis is commonly used by the oil and fat industry (e.g. Hoeksema, US Patent No. 6166231) and involves saponification with NaOH or KOH (the hydrolysing agent), i.e. formation of the sodium or potassium salts of the fatty acids, as illustrated in Figure 3.1. The process is carried out at elevated temperatures (60-80ºC). The salts of the fatty acids are insoluble, and pH reduction (~pH 1) is required in order to obtain the free fatty acids [9]. Direct saponification during extraction from the biomass is faster and less expensive than separate extraction followed by saponification, but more severe operating conditions are necessary [16, 27]. Acid catalysed hydrolysis with HCl or H_2SO_4 is used for analytical purposes. This method generates the free fatty acids directly, but is even more detrimental to

the fatty acids than the base catalysed hydrolysis. At the high temperature employed, the acid will react with the double bonds of the long-chain PUFAs.

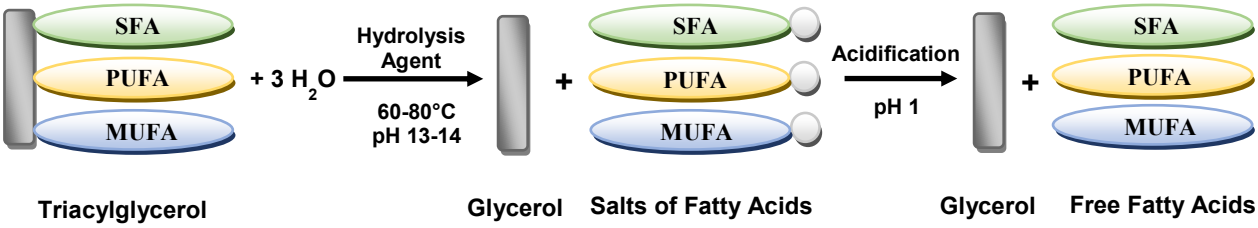


Figure 3.1: Schematic representation of base catalysed hydrolysis of triacylglycerols.

Enzymatic hydrolysis of triacylglycerols

Enzymatic hydrolysis of triacylglycerols (TAG) to free fatty acids (FFA) is a multi-step reaction, which results in the formation of diacylglycerols (DAG) and monoacylglycerols (MAG) as intermediate products, and FFA and glycerol as final products. Different di- and monoacylglycerol are be formed, depending on the fatty acid composition of the triacylglycerols and the lipase used, as illustrated in Figure 3.2.

The rate of the enzymatic reaction is influenced by several factors, namely: the water content; the nature of the enzyme; the concentration and ratios of reactants; the presence of other compounds in the reaction solution; temperature and pH; and the experimental apparatus [9]. The key is to find the right reaction conditions and the appropriate substrate and enzyme combination.

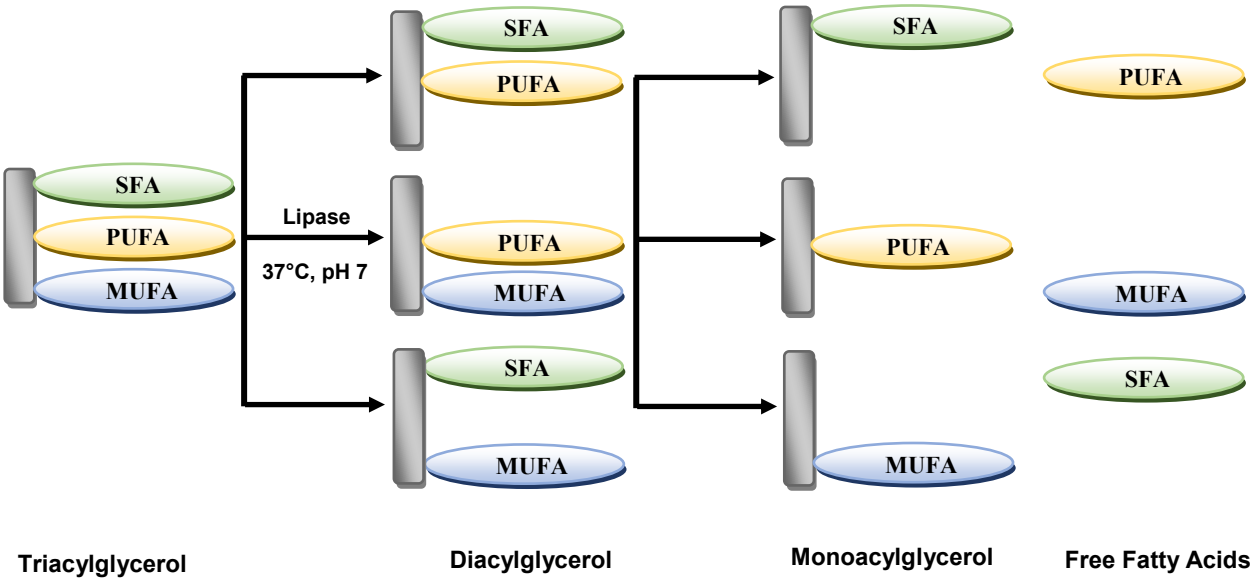


Figure 3.2: Schematic representation of different possible scenarios of enzymatic hydrolysis of a triacylglycerol comprising a saturated (SFA) or monounsaturated (MUFA) fatty acid in sn-1,3 positions, and one polyunsaturated fatty acid (PUFA) in sn-2 position, while using a non-specific lipase.

3.2.2. Lipase specificity and influence of fatty acid structure in the enzymatic hydrolysis of triacylglycerols

An enzymatic hydrolysis by lipases has the advantage over chemical hydrolysis that a selective release of fatty acids may be achieved [11, 13, 30, 94]. Lipases may be position or fatty acid specific. Regarding the positional-specific lipases, they are generally specific either for the fatty acids in sn-1,3 positions of the triacylglycerol molecule or non-specific, i.e. attack all three positions. Okada *et al.* tested a collection of specific and non-specific lipases for production of omega-3 polyunsaturated fatty acids in concentrated oil from sardines [30]. They have found that the use of non-specific enzymes allowed a significant improvement in the concentration of omega-3 PUFAs, over that obtained when using sn-1,3 position specific lipases; it indicated that often the selectivity observed is due to the molecular structure of the fatty acids.

Position specific lipases have been used in exploring the distribution of fatty acids in triacylglycerol molecules, since knowledge of the triacylglycerol structure helps in the selection of the appropriate enzymes for application in oil refining processes involving enzymatic hydrolysis [90].

Hydrolysis by lipases has been described as a method for enrichment of the long chain PUFA-content in triacylglycerols, by removal of the saturated and monounsaturated medium chain fatty acids, in both vegetable [28, 33-38] and fish oils [9, 30, 39]. An enzymatic process seems to be less efficient for hydrolysis of PUFA-glycerol bonds. Several lipases have been found to discriminate between omega-3 PUFA, such as DHA and EPA, and other fatty acids [11, 13, 30, 39, 94]. This can be explained by the limited access of the lipase to the ester bond linking the polyunsaturated fatty acid to the glycerol molecule. The steric hindrance caused by the *cis* carbon-carbon double bonds of polyunsaturated fatty acids leads to the bending of the fatty acid chains, transferring the terminal methyl groups very close to the ester bonds, compromising the access of the lipase, as the molecular structure of tridocosahexaenoin (a triacylglycerol comprising three DHA molecules) presented in Figure 3.3-A illustrates.

On the other hand, saturated fatty acids (SFA, e.g. palmitic acid-PLA) and monounsaturated fatty acids (MUFA, e.g. oleic acid-OLA) are easier to release from a triacylglycerol molecule, because of their nearly linear configuration. The access of the lipase to the ester bonds is not compromised in this case (see by means of an example the configuration of tripalmitin and trioleoyl in Figure 3.3-C and B, respectively). When a triacylglycerol molecule comprises a combination of PUFA, MUFA or SFA, SFA and MUFA would still be preferentially released,

and so the remaining acylglycerol molecules will be enriched in polyunsaturated fatty acids, such as DHA and EPA.

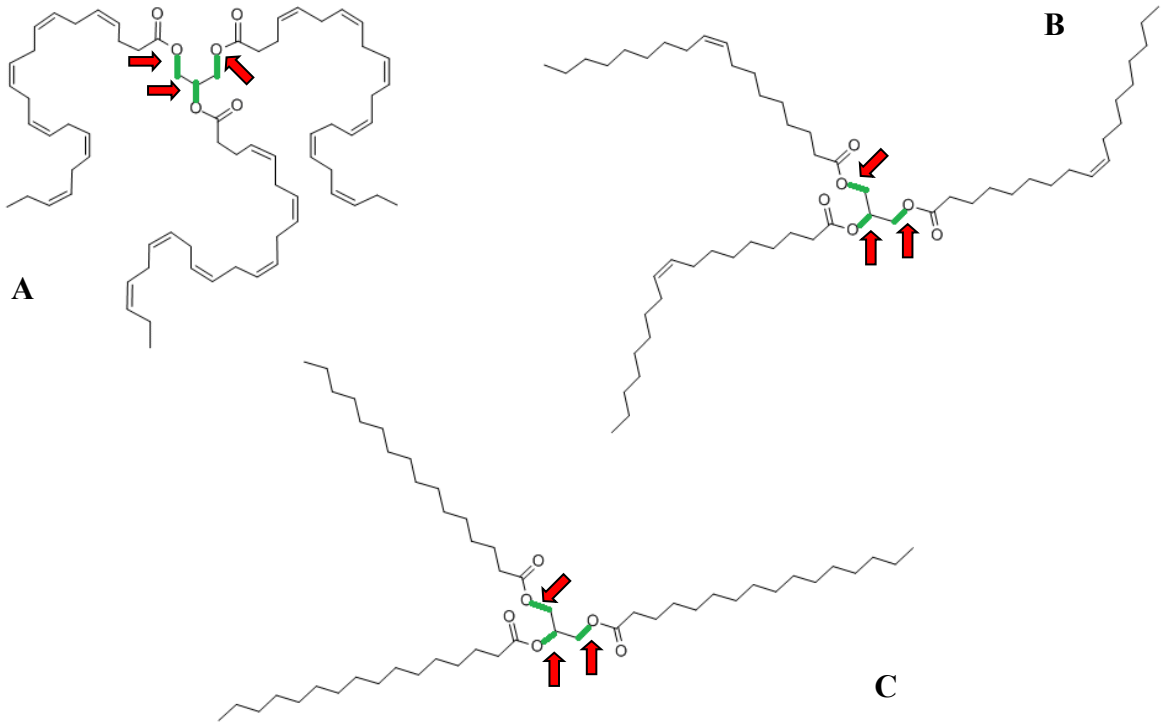


Figure 3.3: Illustration of three different triacylglycerol molecules: A - Tridocosahexaenoin – glycerol+three DHA molecules; B - Trioleoyl – glycerol+three OLA molecules; C - Tripalmitin – glycerol+three PLA molecules. Ester bonds linking the fatty acid to the glycerol molecule are marked in green; red arrows illustrate the access 'point' of the lipases (chemical structures adapted from www.chemicalbook.com).

However, different lipases show distinct levels of selectivity. For instance, the lipase from *Candida rugosa* has demonstrated high discrimination against DHA, while *Pseudomonas* lipases have shown high activity in releasing saturated and monounsaturated fatty acids in fish oil, and higher discrimination towards EPA [11, 94]. It can then be said that those lipases exhibit greater hydrolytic resistance towards ester bonds of omega-3 PUFAs as compared to

those of other fatty acids. These properties have been used for a selective release of saturated and monounsaturated fatty acids for enrichment of DHA and EPA in fish and vegetable oils [11, 14, 30, 95, 96].

3.2.3. Kinetics and challenges related to lipases in general and microbial cell mass

In general, the reaction rates of an enzymatic reaction depend on the enzyme and the substrate concentration. Normally, enzymatic reactions will be carried out at concentrations where the substrate is not limiting, and the rate is dependent only of the enzyme concentration. However, in hydrolysis of triacylglycerols, where intermediates are formed and further converted, the system is much more complex, since the concentration of the intermediates will be 'temporarily' limiting. A model describing this reaction is treated in Chapter 4.

Another challenge for lipid hydrolysis is the contact between the enzyme and the substrate. Since enzymes are water soluble, and the substrate for the reaction is a lipid, it may be a challenge to get a high contact surface. A system creating a high contact surface between oil and water is of crucial importance for an efficient hydrolysis. Addition of emulsifiers and/or emulsion stabilisers has been studied [13, 97, 98]. In emulsion systems with free enzymes functioning at the oil/water interface, mass transfer can also be enhanced by high intensity mixing. Microemulsions have been considered as facilitators of enzyme reactions [99-102].

Two principal methods of conducting these enzymatic reactions are either through liquid-liquid contact with the lipase freely acting at the interface, or with the enzyme immobilised onto a solid support with solid-liquid contact between an oil/water emulsion and the solid phase [58, 98, 103]. Giorno *et al.* claimed that the presence of emulsion improved the catalytic activity and the enantioselectivity of the immobilised enzymes (namely lipase),

while testing with naproxen esters and with triacylglycerols [58]. Both of these techniques have limitations but in particular both would require a discrete separation process for the continuous removal of the reaction products in order to achieve high degrees of equilibrium conversion, and to alleviate product induced enzyme inhibition. Integration of reaction and separation is addressed in this investigation (Chapter 6).

However, the contact between enzyme and substrate is even more challenging when other compounds are present in the reaction mixture, for instance when the hydrolysis of lipids is performed directly in the microbial cell mass, as is the case of the present work. Similar challenges to the extraction of lipids from wet cell mass, as described in section 1.2.2, are faced. Mechanical or chemical pre-treatment of the microbial cell mass may be required. These aspect is explored later in this chapter (section 3.4.2.4).

3.2.4. Analytical methods for quantification of acylglycerols and free fatty acids

Acylglycerols are commonly quantified by HP-TLC [76]. However, HP-TLC methods do not give any information about the fatty acid composition of each individual acylglycerol. Publications including detailed data regarding triacylglycerols, diacylglycerols, and monoacylglycerols formed and consumed throughout enzymatic hydrolysis of natural/native oils were not found so far. Previous studies of lipid hydrolysis have been carried out using model systems consisting of triacylglycerols containing the same fatty acid in all three positions, e.g. triolein (Hermansyah *et al.* [104, 105]), and tributyrin (Jurado *et al.* [106]). In this way, it is not possible to access information on how a lipase would behave when triacylglycerols containing different fatty acids are present in the same reaction mixture.

For the quantification of released fatty acids, GC methods are well established, but the complicated derivatisation steps required prior analysis are very time consuming, and potential loss and transformation of fatty acids may occur [107]. Furthermore, the remaining acylglycerol fraction would also react during derivatisation, and so it would not be possible to obtain information on how the composition of tri-, di- and monoacylglycerols varies throughout the enzymatic hydrolysis tests. Liquid chromatography (LC) does not require fatty acids derivatisation and also benefits from simple, mild sample-processing conditions, short running time and high selectivity and sensitivity, hence it has become more attractive for the analysis of fatty acids [108] and acylglycerols.

A novel method for quantification of acylglycerols and free fatty acids, using liquid chromatography, electrospray mass spectrometry (ESI-MS), and chemometrics, has been developed by Eide & Kolbjørn for analyses of oil and other petroleum compounds [109], and biodiesel [110]. In ESI-MS, positive and negative ionisation can be used for identification of, respectively, positive charged molecules, such as acylglycerols and FAMEs, and negative charged, namely free fatty acids. By preparation of a series of diluted samples, with known concentrations of the compounds of interest, calibration curves may be established for further quantification of such compounds in solution. A variation of this method was used for qualitative and quantitative analyses of acylglycerols and free fatty acids in this chapter.

3.2.5. Objectives and process hypotheses

Published work cited refers to research carried out using isolated oil from different sources. Reference to direct enzymatic hydrolysis of lipids as part of a microbial cell mass for the separation of specific fatty acids was not found in the literature. From an industrial point of view, when the raw material is a wet microbial cell mass, it would be advantageous to omit

the drying and extraction steps, carrying out the lipid hydrolysis directly on the cell mass suspension. Therefore, it was intended to develop a method for the enzymatic hydrolysis of the microbial cell mass lipid content without previous extraction, i.e. the hydrolysis of lipids was conducted directly in the wet cell mass.

The main goal of the work presented in this chapter was to evaluate the performance of a range of enzymes for the hydrolysis of triacylglycerols, in terms of release rates and selectivity obtained for the main fatty acids present in the cell mass, namely palmitic acid (PLA, C16:0), oleic acid (OLA, C18:1), and docosahexaenoic acid (DHA, C22:6). The specific objectives included:

- Determine the total fatty acid composition of the microbial cell mass as free fatty acids after performing chemical hydrolysis of the cell mass lipid content;
- Study the influence of cell mass concentration, enzyme concentration, stirring rate, temperature and pH on the release rates and final yields of free fatty acids for each lipase;
- Characterise the kinetics for formation and further conversion of the intermediate and final products (di- and monoacylglycerols, and the main fatty acids);
- Evaluate lipase selectivity based on composition profiles of tri-, di- and monoacylglycerols, and the main fatty acids released throughout the reaction;
- Investigate the influence of cell mass pre-treatment by hydrolysis of the protein and phospholipid content of the cell mass on the enzymatic hydrolysis of triacylglycerols.

The ultimate objective was to find a combination of enzymes that would be suitable for the desired sequential release of the targeted fatty acids, as a part of a process for extraction and fractionation of LC-PUFA from a wet microbial cell mass, as described in section 1.3.

3.3. Materials and Methods

3.3.1. Cell mass and enzymes

Freeze-dried cell mass of strain T29, produced as described in section 2.3.1, was used in all experiments. The freeze-dried cell mass was suspended in deionised water or buffer solution to recreate the desired cell mass concentration in each particular case.

For the study of enzymatic hydrolysis, four commercially available lipases were selected (Table 3.1). Three of them are non-specific and one is specific for sn-1,3 positions. These lipases are commonly applied as hydrolytic enzymes for DHA enrichment and/or saturated fatty acids removal. Lipozyme TL 100L was provided by Novozymes Corp (Denmark), and the remaining lipases were purchased from Sigma Aldrich (UK). For cell mass pre-treatment evaluation, the protease Alcalase 2.4 L from *Bacillus licheniformis,* provided by Novozymes Corp (Denmark), was used for the protein hydrolysis, and Phospholipase A1 from *Thermomyces lanuginosos* for the phospholipids hydrolysis was purchased from Sigma Aldrich (UK).

Table 3.1: Enzymes applied in the study of hydrolysis, their activity and specificity according to the supplier. One unit (1U) will hydrolyse 1 micromole of fatty acid from a triacylglycerol molecule in one hour at the optimum operating conditions of each lipase.

Enzymes	Abbreviation	Activity (U mg^{-1})	Specificity
Candida rugosa	CR	500	Triacylglycerol lipase Non-specific
Pseudomonas sp	PS	2700	Triacylglycerol lipase Non-specific
Lipozyme TL 100 L	LPZ	10	Oil based specialities Non-specific
Mucor javanicus	MJ	10	Triacylglycerol lipase Specific for 1- and 3-positions

3.3.2. Chemical hydrolysis of lipids as part of the microbial cell mass suspension

Water (4, 2 and 1.33 mL) was added to screw cap tubes containing 200-220 mg freeze-dried cell mass in order to give cell mass concentrations of 50, 100 and 150 g L^{-1} dry weight. 5 mL of 0.5 M KOH solution in ethanol were added (giving concentrations of 0.28, 0.36 and 0.39 M) and the solution was blended at 9500 rpm for 30 seconds using an Ultra-turrax T25 homogeniser (IKA Labortechnik). All tubes were flushed with nitrogen, properly sealed, and then incubated at 60ºC (1, 2 and 3 hours) and 70ºC (1 hour) in a water bath. 2 mL of deionised water were added in each tube after the incubation period and the resulting solution acidified to pH 1, using a 1 M H_2SO_4 solution. Free fatty acids were extracted by washing the hydrolysed solution with three aliquots of 2 mL hexane. Between extractions, tubes were centrifuged (3,200 × g, 5 min, 4ºC) and the upper phase (hexane containing the extracted fatty acids) transferred to a new test tube. An exact volume (2 mL) of the combined hexane phase containing the free fatty acids was withdrawn to a pre-weighed tube and the hexane further evaporated under nitrogen. Free fatty acids were then dissolved in ethanol for further analysis by LC-ESI-MS.

3.3.3. Enzymatic hydrolysis of triacylglycerols as part of the microbial cell mass suspension

Screening of lipases and selection of operating conditions

250, 500 and 750 mg of freeze-dried cell mass was suspended in 5 mL potassium phosphate buffer (0.1 M, pH 7 at 37 ºC), for preparation of cell mass suspensions with concentrations of 50, 100 and 150 g L^{-1} dry weight, respectively. Screw cap tubes containing the cell mass suspension were then heated in a water bath at 98 ºC for 10 min, and immediately cooled to room temperature, before adding the corresponding amount of lipase (as specified in the

results and discussion section). Individual tubes were prepared for each time point. A magnetic stirrer bar (PTFE round stirrer, 20 mm length, 5 mm diameter, without pivot ring) was added to each tube. All tubes were then flushed with nitrogen and properly sealed before being placed in a multipoint stirring plate (Cimarec^{TM} Telesystem Multipoint Stirrer, from Thermo Scientific^{TM}) in an incubator at 37 ºC, for the desired reaction period. After removal of the test tubes from the incubator, 2 mL of deionised water and 2 mL of ethanol were added, and the resulting hydrolysed solution washed five times with aliquots of 2 mL hexane. An exact volume of the hexane phase containing the free fatty acids was then withdrawn to a pre-weighed tube and the solvent further evaporated under nitrogen. The fatty acids were then dissolved in ethanol for later analysis by LC-ESI-MS.

Continuous evaluation of the enzymatic hydrolysis of triacylglycerols

Freeze-dried cell mass (2.5 g) was suspended in 50 mL potassium phosphate buffer (0.1 M, pH 7 at 37ºC), giving a cell mass concentration of 50 g L^{-1}. All flasks containing cell mass suspensions were then heated in a water bath at 98ºC for 10 min, and immediately cooled to room temperature, before adding the corresponding amount of lipase (as specified in results and discussion section). A magnetic stirrer bar (PTFE round stirrer, 30 mm length, 5 mm diameter, without pivot ring) was added to each flask. All flasks were flushed with nitrogen, properly sealed, and then placed on a multipoint stirring plate (Cimarec^{TM} Telesystem Multipoint Stirrer, from Thermo Scientific^{TM}), at a stirring rate of 500 rpm, into an incubator at 37ºC. The reaction was performed for a period of 28 hours. Samples (0.5 mL) were withdrawn at intervals throughout the reaction period. Fatty acids released and remaining acylglycerols were extracted from the samples by addition of 1 mL deionised water, 1 mL ethanol, followed by three times extraction with aliquots of 1 mL hexane. 1 mL of the combined hexane phase was then transferred to two separate vials. Hexane was evaporated

under nitrogen, and the remaining acylglycerols and free fatty acids re-dissolved in ethanol for further quantification by LC-ESI-MS.

3.3.4. Pre-treatment of the microbial cell mass before triacylglycerol hydrolysis

In some cases, pre-treatment of the microbial cell mass to hydrolyse its protein and phospholipid content was performed before lipase addition. For protein hydrolysis, 20 mg of Alcalase per mL solution was added to flasks containing the cell mass suspension (50 g L^{-1} dry weight) in potassium phosphate buffer (0.1 M, pH 7 at 37 ºC), which were further placed in a water bath at 60ºC for 30 min. For the phospholipid hydrolysis, cell mass was first suspended (50 g L^{-1}) in a potassium phosphate buffer of pH 5, and then 10 mg of phospholipase A1 was added per mL solution, and further incubated for 1 hour at 50 ºC. In both cases, cell mass suspension was cooled to room temperature and the pH adjusted when necessary before proceeding with the enzymatic hydrolysis of triacylglycerols present in the cell mass suspensions, as described above.

3.3.5. Analytical methods – LC-ESI-MS

Samples were analysed by full scan spectrometry on an Agilent 1100 Series LC/MSD system (Agilent Technologies Inc., Canada). The system consisted of a G1322A mobile phase degassing unit, a G1311A quaternary pump with gradient mixer for up to four mobile phase constituents, a G1367A autosampler, and a G1946D single quadrupole mass spectrometer. Samples of 2 μL were injected by the autosampler and fed into the mass spectrometer by a 70 cm PEEK tubing (i.d. 0.18 mm), without separation on a chromatographic column. The mobile phase consisted of methanol and ammonium acetate (50 mM) at a ratio of 90:10, and the mobile phase flow was 0.2 mL min^{-1}. Negative electrospray ionisation (ESI) was used to detect the free fatty acids, and positive ESI for the acylglycerols. The instrument was operated

in full scan mode in the m/z range from 65 to 1300, at a scan rate of approximately 1 scan s^{-1}. Amounts of free fatty acids and acylglycerols were calculated based on individual calibration curves obtained for each compound, which were prepared from analyses carried out with standard solutions at ten different concentration levels. Tridocosahexaenoin, didocosahexaenoin and monodocosahexaenoin standards were purchased from Larodan Fine Chemicals (Sweden). Glyceryl trioleate, tripalmitate, 1,3-dioleoyl-2-palmitoyl, 1,3-dipalmitoyl-2-oleoyl, mixed isomers of dioleoylglycerol and dipalmitin, 1-oleoyl and DL-α-palmitin were bought from Sigma Aldrich (UK). Individual standards of fatty acids, namely docosahexaenoic acid, oleic acid, and palmitic acid, were also purchased from Sigma Aldrich (UK).

3.4. Results and Discussion

3.4.1. Chemical hydrolysis of lipids as part of the microbial cell mass

Methods for performing chemical hydrolysis of lipids in a wet thraustochytrid cell mass were not found in the literature, and the optimum conditions for the hydrolysis reaction and recovery of the free fatty acids released had to be determined.

Alkaline hydrolysis was carried out by saponification with KOH, followed by extraction with hexane. In order to ensure a complete extraction of the released fatty acids, acidification is required to dissolve the K-salts and obtain the undissociated fatty acids. The recoveries of the main fatty acids as a function of pH were determined, and showed that pH 1-2 gave the highest recovery (Figure 3.4). At pH 6, the recovery was only 61% of the yield at pH 1.

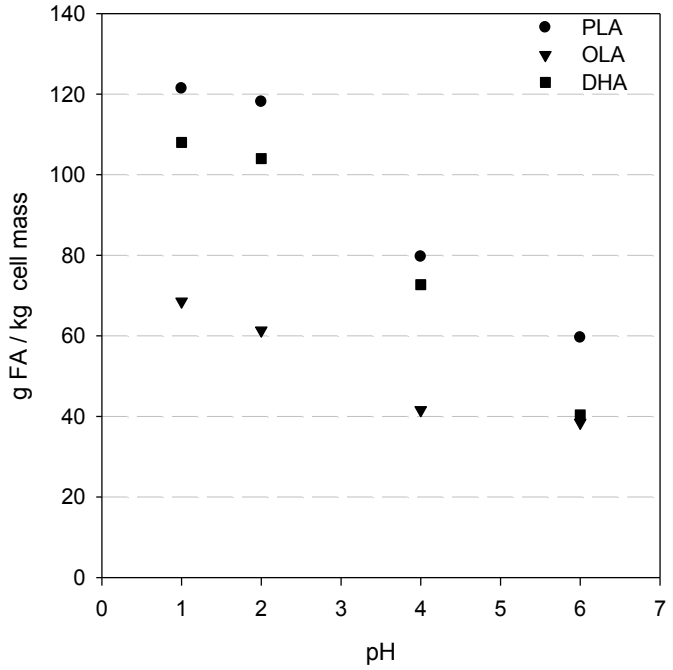


Figure 3.4: Amounts of main fatty acids extracted at different pH-values, after chemical hydrolysis of microbial cell mass lipid content (150 g L^{-1}, 1 hour, 60°C; PLA-palmitic acid; OLA-oleic acid; DHA docosahexaenoic acid).

In order to ensure a complete hydrolysis different cell mass concentrations, reaction times and temperatures were also tested, based on conditions normally applied for alkaline hydrolysis of oils [24]. It was evident that the hydrolysis was most effective at the highest cell mass and KOH-concentrations, i.e. when the cell mass suspension water content was lower. 150 g L^{-1} cell mass gave higher yields than 50 g L^{-1}, three times more fatty acids were released for the higher cell mass content. The KOH solution added was the same in all trials (0.5 M KOH in ethanol), so in such cases with less water, the strength of the hydrolysing agent was higher and hence more fatty acids were released. It can also be concluded that the hydrolysis might be complete around 2 hours, since no significant increase was observed after 3 hours, possibly also a decrease, which might be due to degradation of the free fatty acids. Incubation at 70ºC for 1 hour gave the same yields as 2 hours reaction at 60ºC (data not shown).

The maximum yields of total fatty acids obtained by chemical hydrolysis were 98 wt% of the values previously determined by direct transesterification (Table 3.2). Amounts of PLA and OLA obtained by chemical hydrolysis were higher than those obtained by direct transesterification, and the opposite was observed for DHA. This might be due to an incomplete transesterification, and partial degradation of DHA during chemical hydrolysis.

Table 3.2: Content of the main fatty acids (FFA) of the cell mass, determined by chemical hydrolysis (150 g L^{-1} cell mass, 0.39 M KOH, 2 hours at 60°C), and direct transesterification (FAME), see section 2.4.1.3.

Category	Compound	Composition (g kg^{-1} cell mass)	Fraction (wt%)
FAME	PLA	118.4 ± 2.7	29.0
	OLA	76.0 ± 2.2	18.6
	DHA	174.9 ± 4.8	42.8
	Others	38.9 ± 1.8	8.6
	Total	408.2 ± 11.5	100
FFA	PLA	153.0 ± 5.2	38.4
	OLA	84.8 ± 3.4	21.3
	DHA	137.4 ± 6.4	34.4
	Others	23.6 ± 2.5	5.9
	Total	398.8 ± 17.5	100

The highest amount determined for each of the targeted fatty acids were used as reference values (RV) for the calculation of hydrolysis yields in the further work. Thus, RV for PLA was 153 g kg^{-1} of cell mass, 85 g kg^{-1} for OLA, and finally 175 g kg^{-1} for DHA. As pointed out above, these values correspond to the total fatty acids present in the triacylglycerol and phospholipid fractions, not only the triacylglycerol fraction.

3.4.2. Enzymatic hydrolysis of triacylglycerols as part of the microbial cell mass suspension

3.4.2.1. Evaluation of operating conditions affecting enzymatic hydrolysis rates

Selectivity with respect to specific fatty acids and the release rates of the individual fatty acids were the criteria for the selection of the most suitable lipases. Reference to lipases with a proven specificity for the release of DHA was not found in the literature. The group of lipases tested was selected from those typically used for enrichment of DHA in fish oils [11, 14, 30, 38, 94, 111].

Initially, the performance of the four commercial lipases for the hydrolysis of triacylglycerols was investigated at different stirring rates, temperatures, and pH values. The influence of lipase concentration and substrate concentration was also studied. It was evaluated how those operating conditions affect the initial release rates and the final hydrolysis yields.

The screening of stirring rate, reaction temperature and pH was conducted with the same cell concentration (50 g L^{-1}) and, enzyme concentration (50 kU per litre of cell mass suspension). Three pH-values (6.5, 7 and 7.5), three temperatures (30°C, 37°C and 40°C), and two stirring rates (350 and 500 rpm) were tested. The trials were run in triplicate and for a total of 24 hours. The optimum temperature (37°C) and pH 7, as indicated by the supplier for each enzyme gave the best performance. The stirring rate considerably influenced the degree of hydrolysis. Overall, after 24 hours at a stirring rate of 350 rpm, the amounts of free fatty acids in solution were just 25% of what was released when a stirring rate of 500 rpm was used. However, this difference was most likely due to the low volume of cell mass suspension used in these trials (5 mL), and the dimensions of the magnetic stirrer bar were not the most appropriate for the test tube used (ratio between tube diameter and magnetic bar diameter was

1.5), which may have resulted in a poor mixing of the reaction mixture, as the difference in stirring speeds is not considerable.

Two higher enzyme concentrations were tested in experiments with the same cell mass concentration (50 g L^{-1}). The results obtained for two of the enzymes tested, namely Lipozyme TL 100L (LPZ) and *Candida rugosa* (CR) are presented in Figure 3.5. In both cases it can be observed that the volumetric release rates of fatty acids increased almost proportionally to the increase in enzyme concentration, confirming that the enzyme concentration was rate limiting. The initial release rates of total fatty acids could be calculated to approximately 10, 20 and 30 g kg^{-1} cell mass per hour, or 0.5, 1.0 and 1.5 g L^{-1} of cell mass suspension per hour, corresponding to 0.2 g FFA per kU per kg of cell mass per hour. Although no significant difference was observed between lipases initially, LPZ maintained a higher rate for a longer period than CR, resulting in higher yields after 24 hours (60-67 % for LPZ, 45-57 % for CR, relative to the reference values, as defined above. These differences can be explained by the differences in the enzyme specificities. As mentioned earlier, CR lipase has shown high discrimination towards DHA [11, 94], therefore the amount of DHA released by this lipase was certainly lower than what has been released by LPZ, hence the difference observed in the total fatty acids released. Later, detailed analyses of the individual fatty acids released throughout the hydrolysis of the triacylglycerol fraction confirmed this hypothesis.

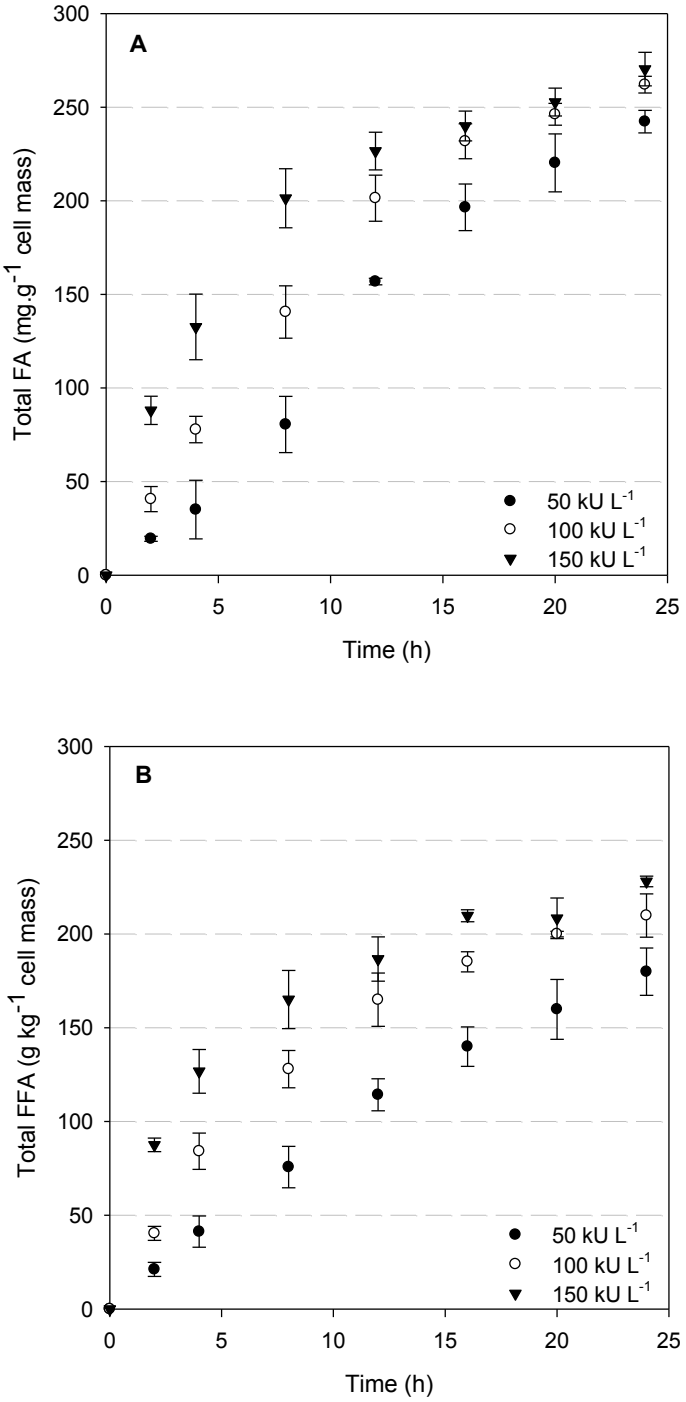


Figure 3.5: Total fatty acids released by enzymatic hydrolysis of the microbial cell mass lipid fraction for different reaction times and three different enzyme concentrations, for two of the four enzymes under study: A – Lipozyme TL 100L (LPZ); B – *Candida rugosa* (CR).

In order to study if, and how, the cell concentration affects the enzymatic reaction, experiments with cell mass suspensions of 100 and 150 g L^{-1} dry weight were also conducted, simulating high-cell density fermentations. The enzyme concentration was increased proportionally to the cell concentration. The initial hydrolysis rates were similar to those achieved with 50 g L^{-1} cell mass and an enzyme concentration of 50 kU L^{-1}. However, after 5-10 hours the reaction rate decreased significantly and almost ceased for the two higher cell mass concentrations, first for the highest concentration. The yields of FFA obtained for a cell mass concentration of 150 g L^{-1} after 24 hours reaction were less than a half of what was achieved with a cell mass concentration of 50 g L^{-1}. A possible explanation may be that the higher cell mass concentration affected the mixing and reduced the contact between enzyme and substrate, e.g. by generating larger cell mass aggregates, limiting the hydrolysis reaction. Further experiments were therefore carried out with 50 g L^{-1} cell mass. For a future scale-up, reactor design and mixing need to be optimised. It was then confirmed that a low water content affects considerably the release rates and the degree of hydrolysis. For this reason, concentration of the fermentation broth using cross flow microfiltration would seem to be not advantageous.

3.4.2.2. Evaluation of lipases selectivity

The selectivity of the four lipases was further investigated with a cell mass concentration of 50 g L^{-1}, an enzyme concentration of 100 kU L^{-1} of cell mass suspension, and a stirring rate of 500 rpm. The yields of the targeted fatty acids achieved after 24 hours reaction at the selected operating conditions for each enzyme are presented in Figure 3.6.

Although LPZ and PS were more effective for the release of the fatty acids considered, CR and MJ were more selective, i.e. they preferentially released PLA and OLA, with a complete recovery of PLA while using MJ. Those results were in accordance with what has been

previously reported by Lyberg *et al.* and Haraldson *et al.* for fish oils [11, 94]. Therefore, it appeared that the selectivity of the lipases was not compromised by the fact that in the present investigation enzymatic hydrolysis of triacylglycerols was carried out directly in the wet cell mass.

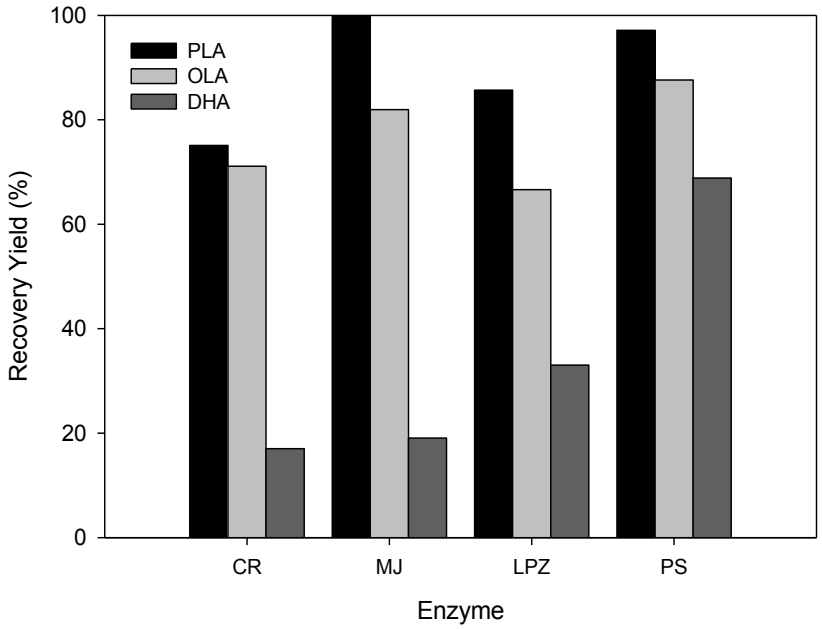


Figure 3.6: Yields of the main fatty acids obtained after enzymatic hydrolysis of the triacylglycerol fraction of the wet cell mass after 24 hours reaction for the four enzymes in this study (CR – *Candida rugosa*; MJ – *Mucor javanicus*; LPZ – Lipozyme TL 100L; PS - *Pseudomonas sp*). Cell mass concentration of 50 g L^{-1}; enzyme concentration of 100 kU L^{-1} of cell mass suspension.

3.4.2.3. Quantification of mono, di and triacylglycerols throughout enzymatic hydrolysis

For a better understanding of the reaction kinetics and selectivity of each lipase, more information about the time courses for conversion of the triacylglycerols (TAG) and formation of diacylglycerols (DAG) and monoacylglycerols (MAG) was required.

Using liquid chromatography coupled with electro spray mass spectrometry (LC-ESI-MS), it

was possible to identify and follow the composition of the individual TAGs, DAGs and MAGs during the reaction. All acylglycerols present in the reaction mixture could be detected, and their relative increase or decrease accompanied throughout the reaction. However, exact quantification was only possible for those compounds where standards were available. In this investigation, tri-, di- and monoacylglycerols containing DHA, PLA and OLA were quantified by this method. The acylglycerols considered, respective distributions of fatty acids and their molecular weights are listed in Table 3.3.

Table 3.3: Acylglycerols selected for quantification throughout the enzymatic hydrolysis reaction, corresponding molecular weight and position of the fatty acids in the acylglycerol molecule.

Compound	Molecular weight ($g\ mol^{-1}$)	Regiospecific distribution (sn1,3-sn2-sn1,3)
Triacylglycerols (TAGs)		
Tridocosahexaenoin	1024	DHA-DHA-DHA
Trioleate	885	OLA-OLA-OLA
Tripalmitate	807	PLA-PLA-PLA
1,3-dioleoyl-2-palmitoyl	859	OLA-PLA-OLA
1,3-dipalmitoyl-2-oleoyl	833	PLA-OLA-PLA
Diacylglycerols (DAGs)		
Didocosahexaenoin	712	DHA-DHA-OH
Dioleoyl	621	OLA-OLA-OH
Dipalmitin	568	PLA-PLA-OH
Monoacylglycerols (MAGs)		
Monodocosahexaenoin	402	OH-DHA-OH
1-Oleoyl	356	OH-OLA-OH
DL-α-palmitin	330	OH-PLA-OH

The content of tripalmitin, trioleate, 1,3-dioleoyl-2-palmitoyl and 1,3-dipalmitoyl-2-oleoyl in the cell mass suspension decreased considerably in the first hours, proving that all three

lipases preferentially hydrolysed PLA and OLA (Figures 3.7a and 3.7b). As expected, the lipases were less susceptible to react with the tridocosahexaenoin, hence its composition in the cell mass suspension increased initially, indicating that tridocosahexaenoin was released from the cell mass, but barely hydrolysed. This proved the initial hypothesis that the configuration of the tridocosahexaenoin affects the access of the lipase to the ester bond linking the DHA to the glycerol molecule. However, in the trials with LPZ lipase, the concentration of tridocosahexaenoin decreased when most of the triacylglycerols composed of PLA and OLA had reacted, and a similar performance was observed in the case of MJ lipase. CR lipase showed the highest discrimination towards DHA.

According to the MS spectrums obtained (supplementary information, Appendix A), tridocosahexaenoin, tripalmitin and trioleoin account for less than 5% of the whole TAG fraction of the thraustochytrid cell mass (357 g kg^{-1} cell mass). TAGs comprising combinations of OLA and PLA, namely 1,3-dioleoyl-2-palmitoyl and 1,3-dipalmitoyl-2-oleoyl, correspond to around 20% of the total TAG fraction. TAGs comprising at least one DHA and combinations of PLA and OLA corresponded to the largest fraction, more than 50% of the total triacylglycerols. The predominant TAGs identified were composed by one DHA, one PLA and one OLA, followed by TAGs comprising two PLA and one DHA, and TAGs with two DHA and one PLA. It is expected that PLA and OLA from such TAGs are easily hydrolysed. Consequently, DAGs comprising two DHA (didocosahexaenoin) and one DHA and one PLA must correspond to the larger fraction of DAGs formed. From the same MS spectrums (supplementary information – Appendix A), it can also be seen that diacylglycerols containing one DHA and one PLA were predominant, accounting to more than 50% of the whole DAG fraction, followed by didocosahexaenoin.

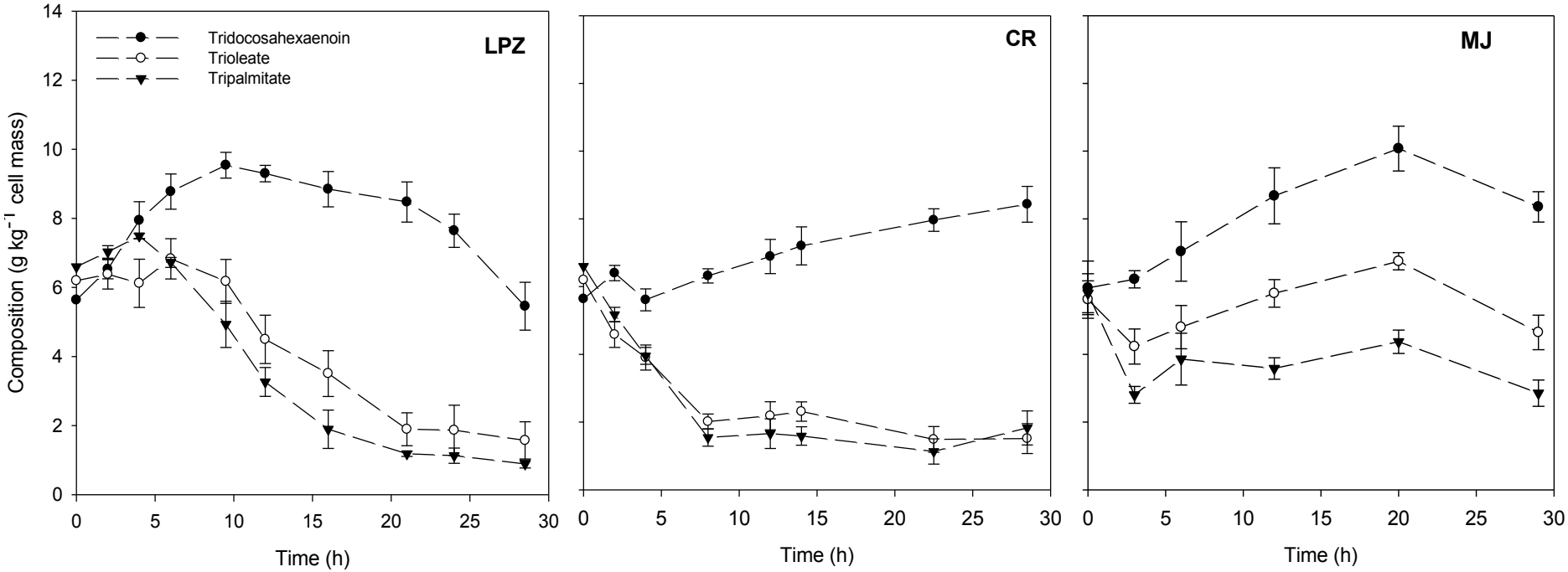


Fig 3.7a: Composition profile of selected TAGs during enzymatic hydrolysis of the lipid fraction of the microbial cell mass suspension for each of the enzymes considered in this study, namely Lipozyme TL 100L (LPZ), *Candida rugosa* (CR), and *Mucor javanicus* (MJ). (Tests carried out with a cell mass concentration of 50 g L^{-1}, and an enzyme concentration of 100 kU L^{-1}).

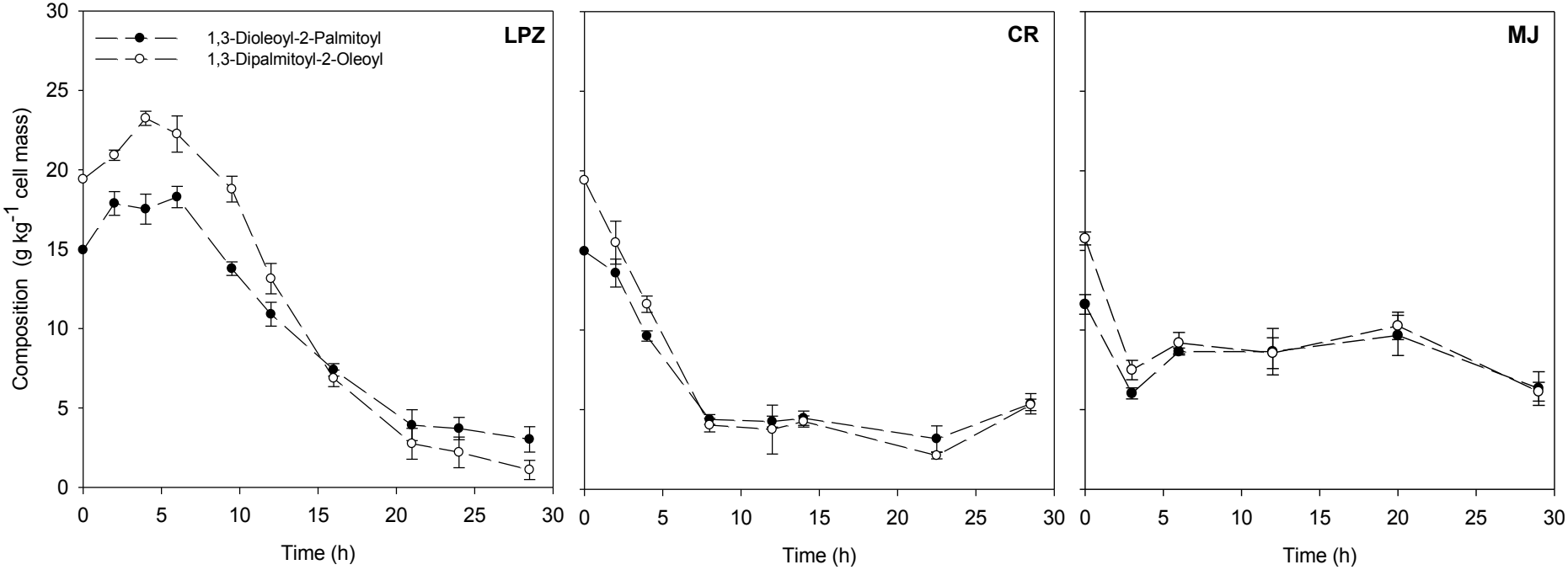


Fig 3.7b: Composition profile of selected TAGs during enzymatic hydrolysis of the lipid fraction of the microbial cell mass suspension for each of the enzymes considered in this study, namely Lipozyme TL 100L (LPZ), *Candida rugosa* (CR), and *Mucor javanicus* (MJ). (Tests carried out with a cell mass concentration of 50 g L^{-1}, and an enzyme concentration of 100 kU L^{-1}).

In Figure 3.8, the composition profiles of didocosahexaenoin, dioleoyl, and dipalmitin in the cell mass suspension throughout the reaction for each of the lipases considered in this study are presented. Overall, there was no relevant difference in the full DAG profile obtained for each of the three lipase trials. As expected, didocosahexaenoin content in the cell mass suspension throughout the reaction was higher than the other two DAGs quantified, showing once again that lipases preferably catalysed PLA and OLA. This observation was more evident for tests carried out with the CR and MJ lipases. In the case of LPZ lipase, concentration of didocosahexaenoin decreased considerably more or less at the same stage of the reaction as observed for the tridocosahexaenoin (between 22 and 24 h).

Strangely, the content of dioleoyl in the MJ trials during the reaction course was clearly higher than in the other two cases, which may indicate that MJ lipase discriminates against OLA, mainly when two OLA molecules are present in consecutive positions in the acylglycerol molecule.

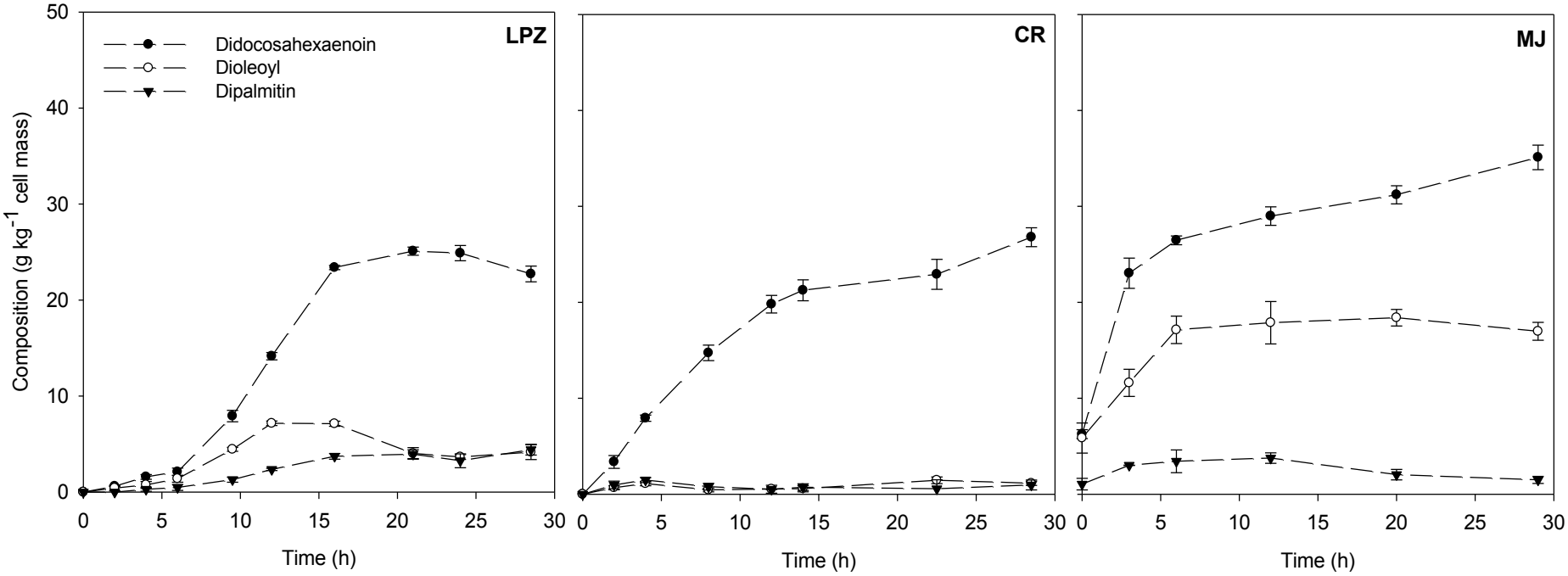


Figure 3.8: Composition profile of selected DAGs during enzymatic hydrolysis of the lipid fraction of the microbial cell mass suspension for each of the enzymes considered in this study, namely Lipozyme TL 100L (LPZ), *Candida rugosa* (CR), and *Mucor javanicus* (MJ). (Tests carried out with a cell mass concentration of 50 g L^{-1}, and an enzyme concentration of 100 kU L^{-1}).

MAG composition profiles presented in Figure 3.9 provided a better understanding of the action of the sn-1,3 position specific lipase (MJ), and it also allowed more information to be obtained on the positional distribution of the three main fatty acids.

As expected, the highest composition of MAGs containing DHA (monodocosahexaenoin) in the cell mass suspension was obtained with the MJ lipase. Monodocosahexaenoin content also increased in the CR trials. However, the lower values in this case may be due to the high amounts of tridocosahexaenoin and didocosahexaenoin which were still in suspension. It confirms that lipases are not only position specific, but also that the fatty acid structure prevents access to release the DHA in the sn-1,3 positions, limiting the hydrolysis performance (as previously illustrated in Figure 3.3A).

DL-α-palmitin appeared to be completely hydrolysed after 28 hours by the LPZ lipase, but the same was not observed for CR and MJ lipases. Apparently, the amount of 1-oleoyl formed was too low to be detected in any case, which might indicate that 1-oleoyl resultant from the DAG fraction was immediately hydrolysed. In the case of MJ, it was expected to obtain an increasing composition in MAGs for each individual fatty acid, once as a sn-1,3 position specific lipase, sn-2 position of the acylglycerol molecule should not be hydrolysed. However, the fact that 1-oleoyl was not detected in the MJ trials, suggested that more than PLA, OLA is mostly present in sn-1,3 positions, and acylglycerols with OLA in sn-2 were still in the dioleoyl form. The fact that the amounts of DL-α-palmitin obtained were considerably higher also supports this observation.

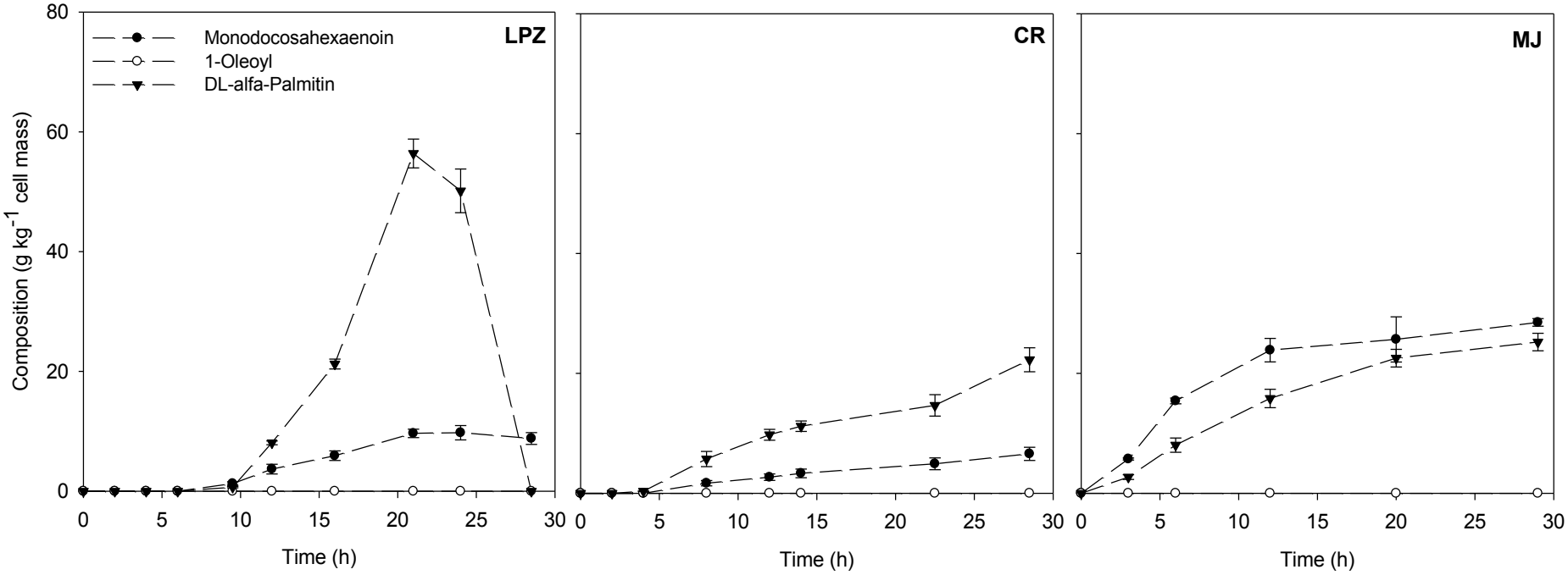


Figure 3.9: Composition profile of selected MAGs during enzymatic hydrolysis of the lipid fraction of the microbial cell mass suspension for each of the enzymes in study, namely Lipozyme TL 100L (LPZ), *Candida rugosa* (CR), and *Mucor javanicus* (MJ). (Tests carried out with a cell mass concentration of 50 g L^{-1}, and an enzyme concentration of 100 kU L^{-1}).

Composition profiles of the main free fatty acids (DHA, PLA and OLA) in the reaction mixture are depicted in Figure 3.10. This information supports what has been discussed previously in analysing the acylglycerols composition.

The main differences observed between the performances of the three lipases were the amount of DHA released during the enzymatic reaction, and the initial release rates of PLA and OLA. Lower amounts of free DHA in suspension in the cases of CR and MJ are due to the selectivity of these lipases; both were less efficient for the release of DHA. Despite the final amounts of PLA and OLA released being quite similar, the initial release rates were remarkably different between lipases. Previously, the sn-1,3 position specific lipase, i.e. MJ, seemed to be the most effective in the release of PLA and OLA (Figure 3.6). However, the reason for the high initial release rates observed for PLA and OLA in the trials with MJ lipase is that they may not correspond only to the PLA and OLA from the acylglycerols fraction. It has been reported that lipase from *Mucor javanicus* exhibits phospholipase A1 activity, which means that, besides sn-1,3 positions of triacylglycerols, it may also hydrolyse the fatty acid at the sn-1 position of phospholipids [112]. Therefore, it is assumed that part of the released PLA and OLA in the trials with MJ lipase may also come from the phospholipid fraction of the cell mass, hence the higher release rates and yields.

In the concentration profiles obtained with the LPZ lipase an initial lag-phase can be observed (see plots for LPZ in Figures 3.7a,b-3.10), which indicates that the reaction was very slow at the beginning. However, it did not compromise the overall performance of the lipase. In fact this lipase was the most efficient for the release of DHA among the lipases considered in this investigation, and may be considered in a multi-stage enzymatic hydrolysis, when recovery of the DHA fraction is desired.

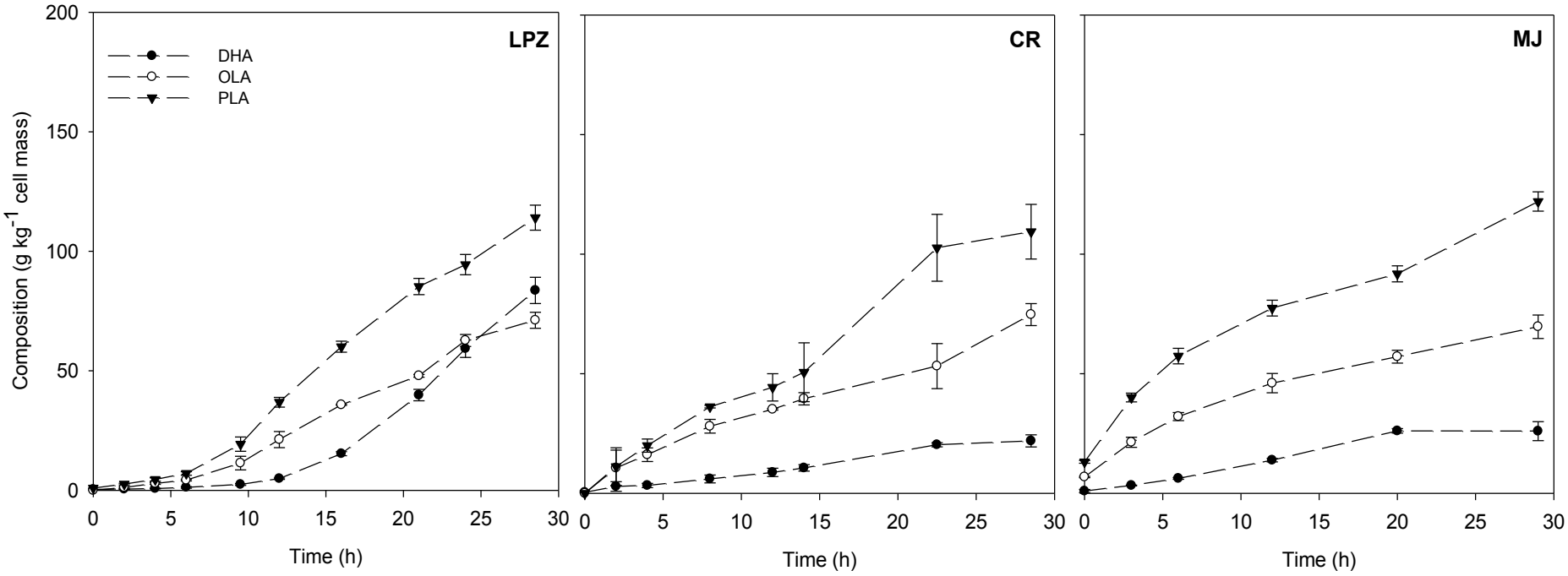


Figure 3.10: Composition profile of the main fatty acids released during enzymatic hydrolysis of the lipid fraction of the microbial cell mass suspension for each of the enzymes under study, namely Lipozyme TL 100L (LPZ), *Candida rugosa* (CR), and *Mucor javanicus* (MJ). (Tests carried out with a cell mass concentration of 50 g L^{-1}, and an enzyme concentration of 100 kU L^{-1}).

3.4.2.4. Influence of pre-treatment of the cell mass in the hydrolysis of triacylglycerols

It is general knowledge that a large contact surface between water and oil is desired for efficient enzymatic reactions of oil-soluble substrates, since the enzymes are normally water soluble. The triacylglycerol fraction of the microbial cell mass is mainly stored in lipid bodies inside the microbial cells, as has been reported [19, 74, 91]. Pre-treatment with protease increased the extraction yields while evaluating total lipid composition of the microbial cell mass, as verified previously (section 2.4.1.1). The disruption of the lipid bodies made the intracellular lipids more available for solvent extraction. As the membrane of the microbial cells is mainly composed of phospholipids, the same would be expected if the hydrolysis of the phospholipids of the cell membrane was performed. Therefore, the influence that the pre-treatment of the cell mass with protease or phospholipase would have on the reaction rates of triacylglycerol hydrolysis, and on the maximum amount of fatty acids released was investigated, in order to find out if the substrate availability would favour contact between enzyme and substrate, and improve the hydrolysis of triacylglycerols performance. Protein and phospholipid hydrolyses were then performed individually as pre-treatment of the aqueous cell mass prior to triacylglycerol hydrolysis. After the respective pre-treatment, the hydrolysis of the triacylglycerol fraction was performed with the sn-1,3 position specific lipase MJ. As previously, the enzyme concentration was equivalent to 100 kU L^{-1} of the cell mass suspension, with a cell mass content of 50 g L^{-1} dry weight.

The initial amounts of triacylglycerols in suspension after protease treatment were much higher than previously obtained (Figure 3.11), as can be verified by comparison with the profiles obtained for hydrolysis of TAG with MJ without pre-treatment (see Figure 3.7a, and Table 3.4). It confirmed that the protease pre-treatment enhanced the release of triacylglycerols from the cell mass lipid fraction. However, the hydrolysis of triacylglycerols

was much slower, hence the high amounts detected during the reaction course. Amounts of DAG and MAG formed were minimal in comparison to those obtained earlier, and the same is true for the FFA (compare to Figures 3.8-3.10). Therefore, despite the protease pre-treatment facilitating the release of the cell mass lipid fraction, it seriously compromised the triacylglycerol hydrolysis.

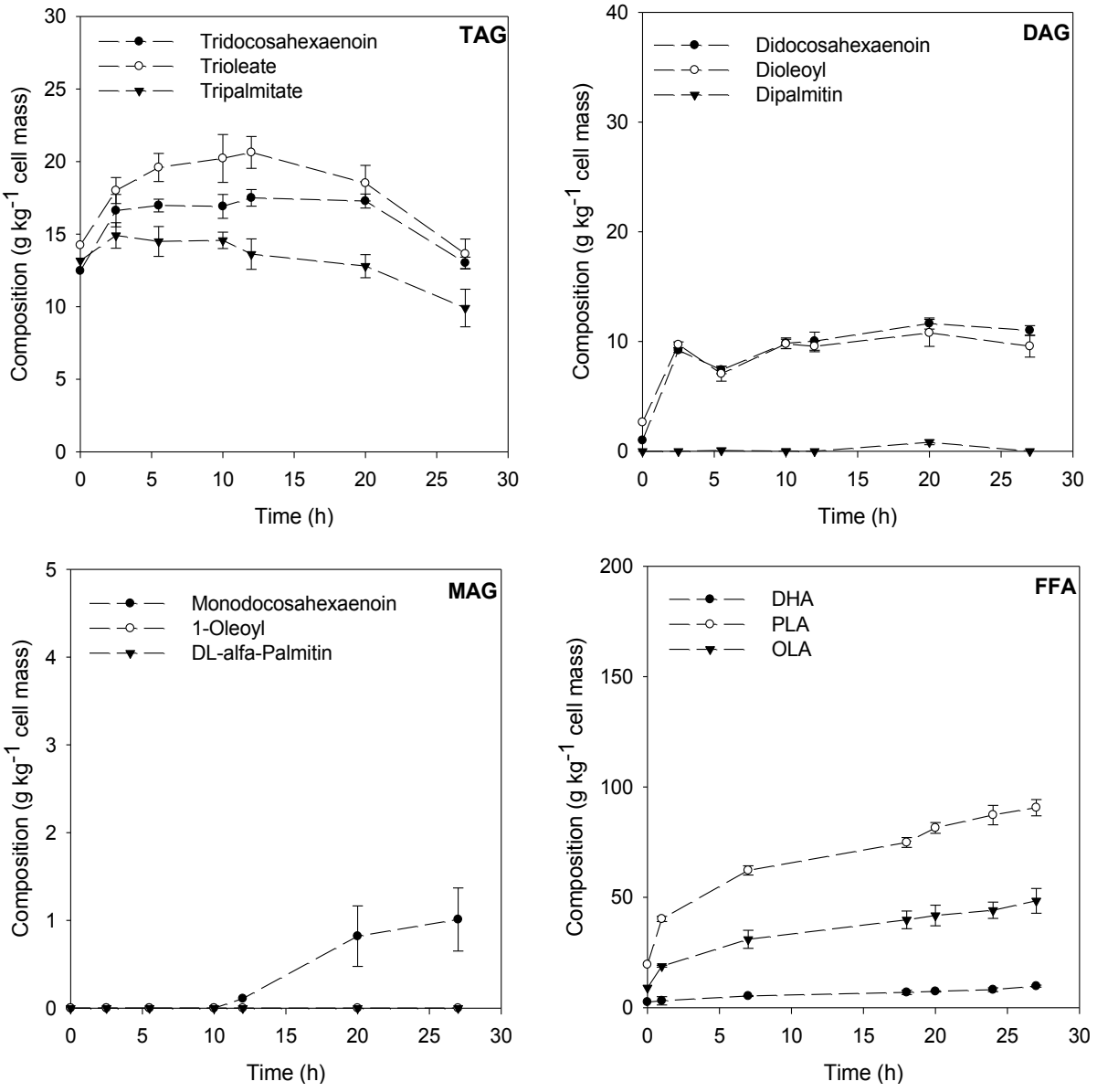


Figure 3.11: Composition of selected acylglycerols and free fatty acids in the reaction mixture during enzymatic hydrolysis of the lipid fraction of the microbial cell mass suspension after protease pre-treatment. (TAG-triacylglycerols; DAG-diacylglycerols; MAG-monoacylglycerols; FFA-free fatty acids).

Hydrolysis of phospholipids present in the cell mass suspension results in cell lysis, and may also help in the disruption of lipid bodies, hypothetically facilitating further contact between lipases and triacylglycerols for triacylglycerol hydrolysis. Phospholipase A1 hydrolyses the fatty acid in sn-1 position of the phospholipid molecule; consequently the molecule becomes more hydrophilic, and is preferably dissolved in the aqueous phase.

Analysing the profiles obtained for PLA and OLA presented in Figure 3.12, it can be concluded that the phospholipase pre-treatment had no significant influence on the initial release rates, and, besides the higher amounts of DHA released, the total amount of the other fatty acids released was not affected. However, it must be pointed out that in this case, the fatty acids released correspond not only to the acylglycerols fraction, but also arise from the hydrolysis of phospholipids, which explains the higher composition of PLA and OLA at the beginning of the triacylglycerol hydrolysis (Table 3.4). Consequently, the final amount of fatty acids released do not correspond solely to the acylglycerol hydrolysis. Furthermore, part of the DHA in the phospholipid fraction may also have been released, contributing to the higher amount of DHA released.

Composition profiles of TAG and DAG throughout the reaction were comparable to what has been observed previously in experiments with MJ lipase without pre-treatment (Figure 3.7a, 3.8). However, the phospholipase seems to have somehow influenced the lipase performance or was still active, because fatty acids from monoacylglycerols were also hydrolysed. This observation is supported by the fact that the amount of monoacylglycerols (MAG) decreased throughout the reaction (see Figure 3.12-MAG). It is very unlikely that the phospholipase changed the specificity of the lipase; therefore, it was concluded that sn-2 position of

acylglycerols was cleaved by the phospholipase, despite the optimum operating conditions having changed. It also resulted in higher amounts of DHA being released, which means that the desired selective release would be compromised by the phospholipase pre-treatment.

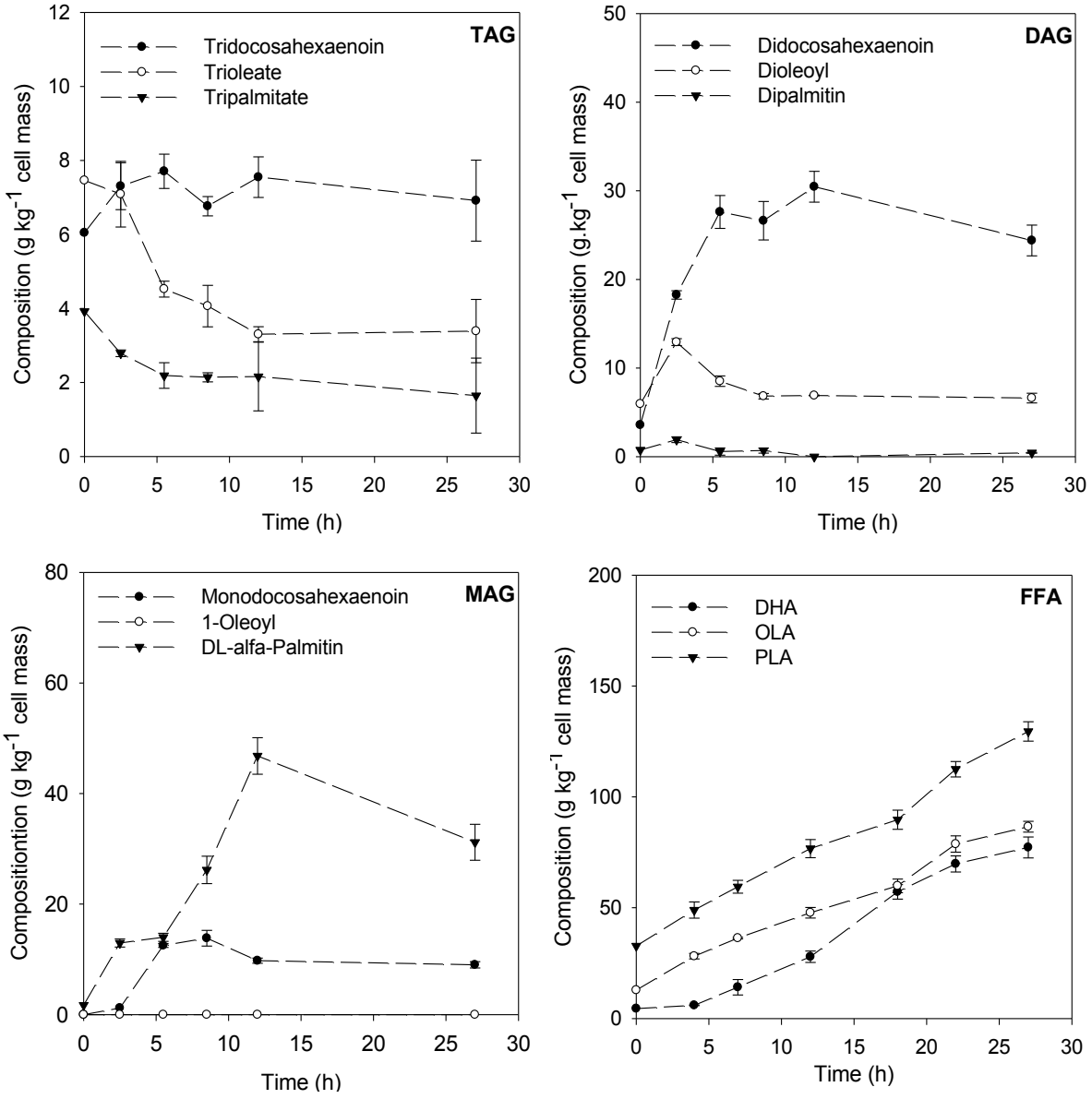


Figure 3.12: Composition of selected acylglycerols and free fatty acids in the reaction mixture during enzymatic hydrolysis of the lipid fraction of the microbial cell mass suspension after phospholipase pre-treatment. (TAG-triacylglycerols; DAG-diacylglycerols; MAG-monoacylglycerols; FFA-free fatty acids).

Amounts of triacylglycerols and free fatty acids readily available in the cell mass suspension prior to addition of the lipase for the triacylglycerol hydrolysis, when pre-treatment was not performed and after protein and phospholipid hydrolyses, are listed in Table 3.4.

Table 3.4: Triacylglycerols and free fatty acids composition in the cell mass before lipase addition, as determined with and without pre-treatment of the cell mass.

Compound	Composition (g kg^{-1} cell mass)		
	No pre treatment	Protease treatment	Phospholipase treatment
Triacylglycerols (TAG)			
Tridocosahexaenoin	5.9 ± 0.8	12.5 ± 1.1	6.0 ± 0.6
Trioleate	5.6 ± 0.5	14.2 ± 0.9	7.5 ± 0.9
Tripalmitate	5.8 ± 0.6	13.2 ± 0.9	3.9 ± 0.6
Free Fatty Acids (FFA)			
PLA	13.2 ± 0.6	19.5 ± 1.2	32.7 ± 3.6
OLA	6.8 ± 0.3	9.0 ± 0.4	12.8 ± 1.2
DHA	0.9 ± 0.2	2.6 ± 0.9	4.5 ± 0.1

These results were important to understand to which extent the cell mass protein and phospholipid content affected the triacylglycerol hydrolysis. It was evident that the enzymatic hydrolysis of the microbial cell mass triacylglycerol fraction was more successful when pre-treatment was not performed. The availability of the substrate in suspension did not justify the use of pre-treatment, as the hydrolysis performance did not benefit from it in any case, both in terms of selectivity and final hydrolysis yields.

A likely explanation for this is that proteins and phospholipids function as emulsion stabilisers, and their presence is crucial for a successful hydrolysis of triacylglycerols in this specific case. Proteins have interfacial properties which allow them to form a protective membrane around the oil droplets/lipid bodies, preventing them from coalescing, and so

creating a stable emulsion. It has been reported that hydrolysis of proteins results in the loss of their emulsifying properties [113]. The small peptides resulting from protein hydrolysis diffuse rapidly and adsorb at the interface between oil and water, and so they are less efficient at stabilising emulsions. Then, the oil droplets/lipid bodies tend to form larger agglomerates, as illustrated in Figure 3.13, and the interfacial area between oil and water decreases, explaining the results obtained. It has then indicated that the protein content of the cell mass played an important role in the lipid hydrolysis by enzymes in the present case.

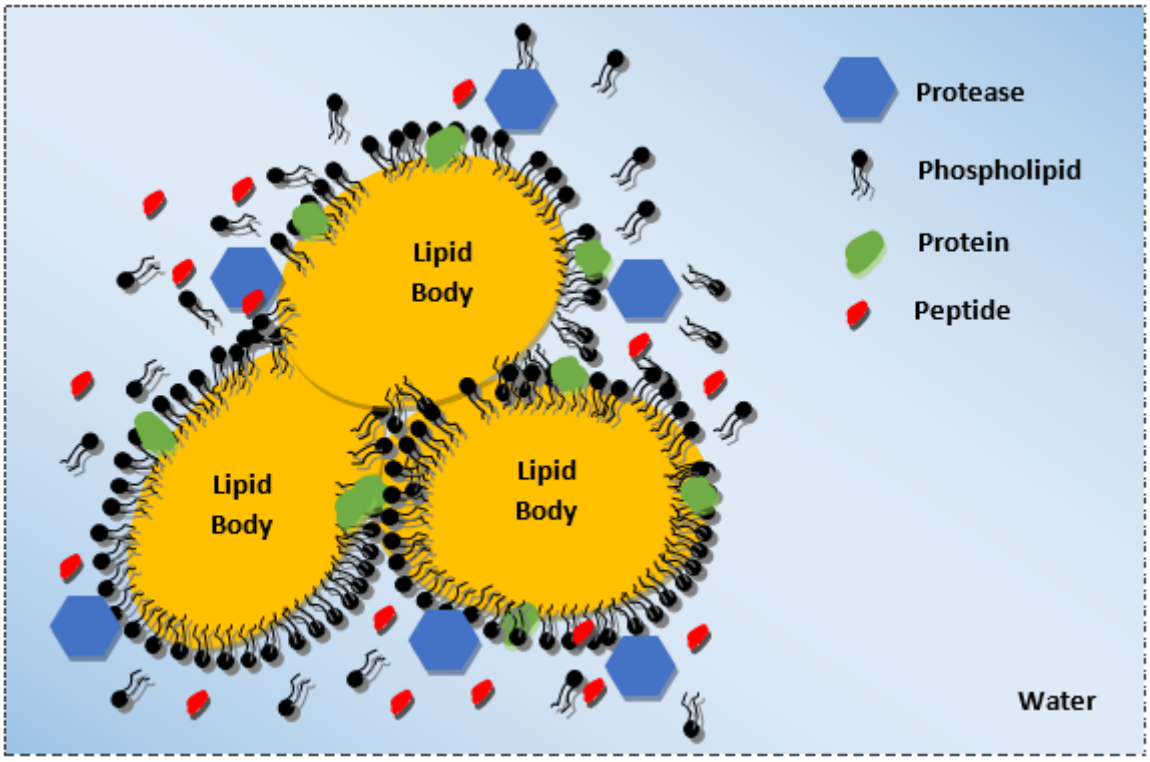


Figure 3.13: Illustrative diagram of lipid bodies agglomeration formed as a consequence of hydrolysis of proteins present in the microbial cell mass suspension.

Despite the known emulsifying properties of phospholipids, the phospholipase pre-treatment did not seem to disturb the emulsion stability in this specific case, since the protein fraction was not hydrolysed, as illustrated in Figure 3.14. The hydrolysis rates and yields were similar to what was achieved without the cell mass pre-treatment. The drawback was the effect on the

hydrolysis selectivity. Furthermore, from an industrial point of view, and depending on the desired final product and the value of the phospholipid fraction, it would preferably be kept intact in suspension to be recovered separately.

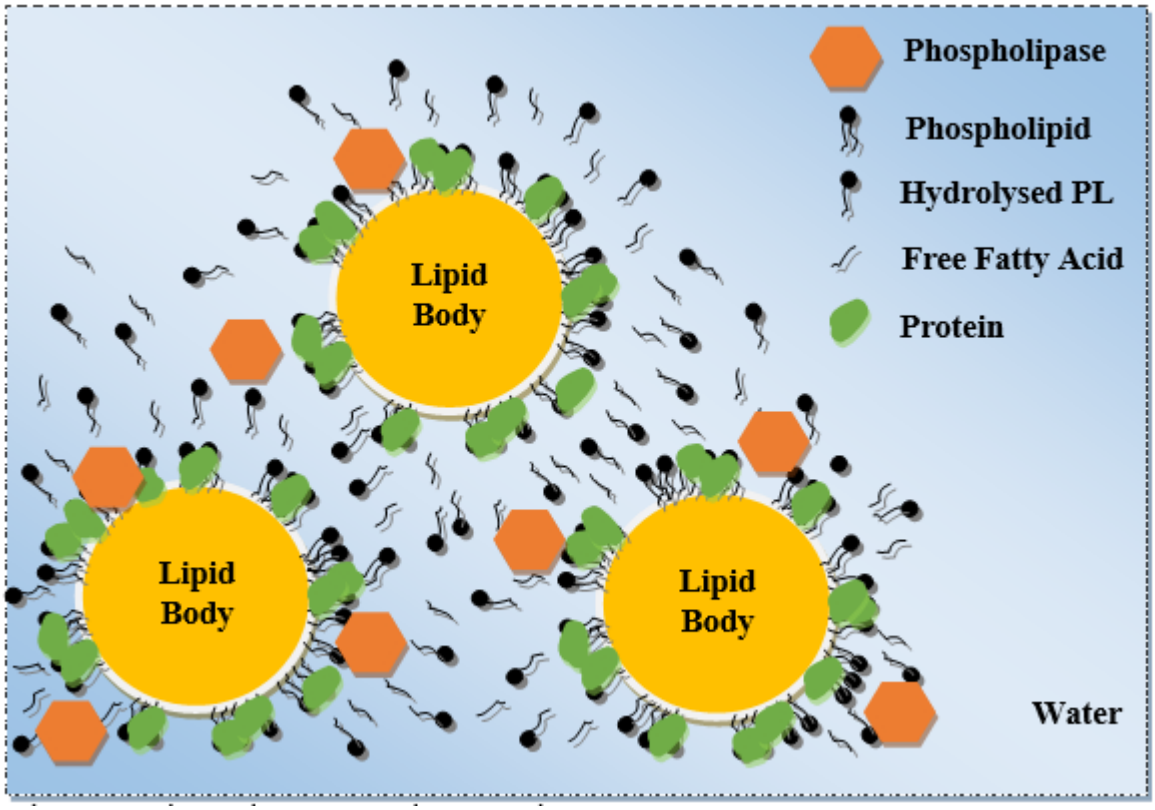


Figure 3.14: Illustrative diagram of distribution of lipid bodies in the wet cell mass suspension after hydrolysis of the phospholipid fraction of the microbial cell mass.

These results indicated that the presence of protein and phospholipid fractions of the cell mass while carrying enzymatic hydrolysis of triacylglycerols directly in the cell mass suspension, did not compromise the hydrolysis performance, and probably had a positive effect compared to an oil-water system where addition of emulsifiers is required in order to obtain a stable emulsion and maximize the interfacial area between enzyme and substrate.

Microscopic images of the thraustochytrid cells in the fermentation broth (A), and the cell

mass suspension during lipid hydrolysis without pre-treatment (B) are presented in Figure 3.15. In the fermentation broth, the single thraustochytrid cells (10-20 μm) are intact, and tend to form agglomerates in the aqueous medium (A). During lipid hydrolysis, cells are disrupted and the internal lipids released, the cell mass suspension is then composed of released lipids/free fatty acids, intact single cells and cell debris in the water/aqueous medium containing the enzyme (B). The presence of protein from the cell debris and good mixing allow the formation of a stable cell mass suspension.

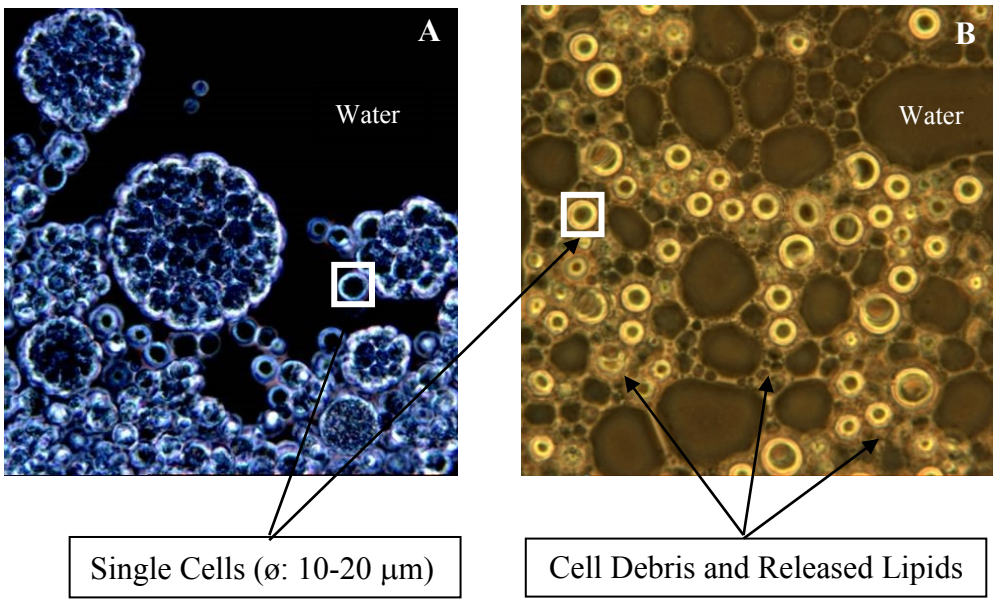


Figure 3.15: Microscopic images of the fermentation broth (A), and the cell mass suspension during lipid hydrolysis without pre-treatment (B).

Therefore, it was demonstrated that when working with the whole cell mass, the addition of emulsifiers is avoided and still it is possible to perform the desired selective hydrolysis of triacylglycerols. It may also have helped in preventing oxidation of the released DHA; they were not that susceptible to oxidation as in oil-in-water emulsions, as will be shown in Chapter 4.

3.4.2.5. Strategy and selection of enzymes for stepwise enzymatic hydrolysis of triacylglycerols and simultaneous separation of released fatty acids

As mentioned in section 1.3, one of the main objectives of the present work was to find suitable enzymes for the stepwise enzymatic hydrolysis of triacylglycerols. Previous results suggested that the use of a sn-1,3 position specific lipase would release most of the PLA and OLA, since over 80% of the SFA and MUFA are distributed among these two positions. Additionally, lipases tested have shown different levels of discrimination towards DHA. Combining enzymatic hydrolysis of triacylglycerols with membrane separation, the released fatty acids could be continuously removed. Therefore, when using the appropriate enzymes, different fractions of PLA/OLA and DHA could be obtained at different stages of the reaction.

The stepwise enzymatic hydrolysis for the three main TAG configurations found in the microbial cell mass used in this investigation, as well as the intermediate substrates (di- and monoacylglycerols) and products (free fatty acids) formed throughout the reaction in each case, can be illustrated as presented in Figure 3.16. Based on results presented in sections 3.4.2.2 and 3.4.2.3, it is expected that by adding the position specific lipase MJ in the first stage, PLA and OLA would be preferably released; when most of these two fatty acids have been separated, the least selective lipase, namely lipase LPZ, would then be added to the cell mass suspension, and the remaining acylglycerols containing mainly DHA would be hydrolysed; consequently, a solution enriched in DHA would be obtained at the end of the process.

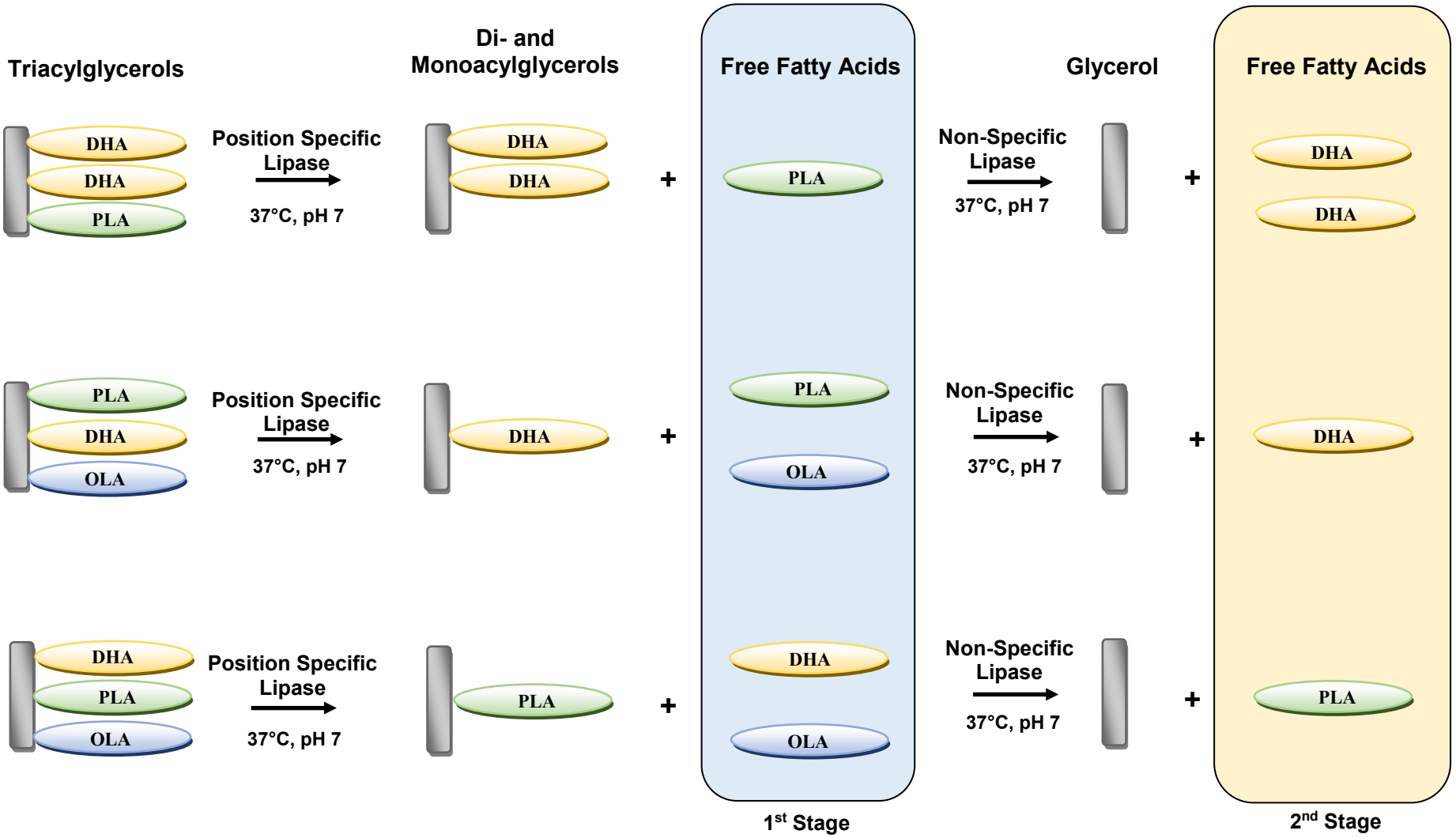


Figure 3.16: Schematic representation of the stepwise enzymatic hydrolysis of triacylglycerols.

3.5. Conclusions

Chemical hydrolysis was shown to be a quick and effective method for the release of fatty acids from a lipid containing microbial cell mass suspension. However, as expected, it proved to be harmful in the hydrolysis of polyunsaturated fatty acids, as the lower yields of DHA obtained in this specific case showed.

It was demonstrated that enzymatic hydrolysis of triacylglycerols can be performed directly on the microbial cell mass suspension. Pre-treatment of the cell mass is not necessary; although it facilitated lipid extraction, it had a negative influence on the hydrolysis of triacylglycerols, probably because the presence of other cell mass compounds (such as proteins and phospholipids) is advantageous for the hydrolysis reaction, by stabilising the emulsion and preventing oxidation of the released fatty acids.

LC-ESI-MS analytical methods developed for the analysis of acylglycerols enabled determination of the concentration profiles of individual tri-, di-, and monoacylglycerols throughout the reaction. This information allowed a better evaluation of the performance of each lipase, which was important for the understanding of the reaction kinetics and selectivity. Previously published works have based their investigations only on the determination of total tri-, di- and monoacylglycerol fractions containing a single kind of fatty acid. Furthermore, in particular for the analysis of free fatty acids by LC-ESI-MS, the sample preparation was simplified, there was no need for methylation, which would be required if using gas chromatography, and only 10 min were required for a complete characterisation of each sample.

Overall, all lipases tested preferably hydrolysed the ester bonds between saturated and monounsaturated fatty acids and the glycerol molecule, due to their configuration. As a result of the easier access of the lipase, the acylglycerols comprising oleic (OLA) and palmitic (PLA) acids reacted first, hence the high yields observed for those fatty acids. As the acylglycerols containing PLA and OLA decreased nearly to zero, a decrease in the acylglycerols containing DHA was observed for LPZ and MJ. This was not the case for CR, which presented a higher selectivity towards DHA. It confirmed that the fatty acid structure prevented access to PUFA even in the sn-1,3 positions. Therefore, the hydrolysis performance for each lipase seemed to be more dependent on the fatty acid structure than on the position specificity.

The aim of this work was to develop a sequential release of the targeted fatty acids directly from the wet cell mass, which was accomplished. It can then be concluded that selective hydrolysis can be attained by employing specific and non-specific lipases in the enzymatic hydrolysis of lipids present in the cell mass suspension. These results form the basis for design of the process involving stepwise hydrolysis of the cell mass lipid content with lipases MJ and LPZ, and simultaneous separation of the released fatty acids in the biphasic membrane contactor system, as will be presented in Chapter 6.

Chapter 4

Kinetic Model for the Stepwise Enzymatic Hydrolysis of Triacylglycerols in O/W Emulsions – Multiple Substrates and Products

4.1. Summary

In this chapter a mathematical model for the evaluation of the reaction kinetics in the hydrolysis of triacylglycerols, involving multiple substrates and products is presented. Most of the published works consider the kinetics study of one single substrate and/or product. It is known that in marine or vegetable oils, triacylglycerols with numerous combinations of fatty acids can be found, and so, such models do not represent a real system. In the present study, the kinetic model developed by Hermansyah *et al.* [105] was adapted for the stepwise hydrolysis of multiple substrates and products. Fatty acids were divided in two groups, saturated+monounsaturated (S) and polyunsaturated fatty acids (P). Three of the most common configurations of triacylglycerol molecules found in marine oils were considered, which are hydrolysed according to three different mechanisms. The model is then solved using the Runge-Kutta method in MatLab.

4.2. Background and Literature Review

4.2.1. Existing models for the evaluation of enzyme kinetics

The hydrolysis of triacylglycerols in biphasic or emulsion systems (oil:water or oil:water:solvent) using lipases has been widely studied [64, 104-106, 114-120]. Several mathematical models have been proposed for the characterisation of the kinetics of hydrolysis of triacylglycerols. Parameters such as enzyme and substrate concentrations, operating conditions (e.g. temperature, pH), oil:water ratios, interfacial area, have been considered for the evaluation of release rates given by the models developed, e.g. by Kawano et al. [120].

Kawano *et al.* studied the hydrolysis kinetics of olive oil dissolved in i-octane with lipase in water in a biphasic system under various conditions using a Lewis-type transfer cell [120]. The formation rates of fatty acids were found to be affected by the volume of the aqueous solution and the concentrations of lipase and olive oil. The rates followed a reaction scheme in which either the decomposition of a complex at the interface or the desorption of fatty acids formed on the interface into the organic solution was postulated as the rate-determining step. Parameters for the interfacial reaction rate and adsorption equilibrium of lipase were determined so as to satisfy the experimental result.

Hermansyah H. *et al.* proposed a mathematical model for the stepwise hydrolysis of triolein using *Candida rugosa* lipase in a biphasic O/W system, assuming a Ping Pong Bi mechanism with competitive inhibition by the fatty acid at the three stages of the reaction [104, 105]. The model developed was very effective for predicting the appropriate conditions for an efficient production of the desired diolein.

Pilarek *et al.* developed a kinetic model for sn-1,3 specific triacylglycerol alcoholysis catalysed by lipases [118]. They assumed irreversibility of the acyl bonds cleavage in glycerides, a reversible monoacylglycerols isomerisation, and an irreversible enzyme deactivation. The Ping Pong Bi Bi mechanism with competitive inhibition by alcohol was applied to describe rates of acyl bonds cleavage. The enzymatic propanolysis and iso-propanolysis of triacetin and tricaprylin catalyzed by immobilised lipase B from *Candida antarctica* (Novozym 435((R))) was investigated to verify the model. Good agreement between experimental data and calculations was obtained. They showed that the rate of tricaprylin alcoholysis is higher than the triacetin alcoholysis and that the rate of iso-propanolysis reactions are higher than propanolysis. The irreversible enzyme deactivation affects the conversion of glycerides whereas competitive alcohol inhibition may be neglected. Empirical correlations of rates for monoacylglycerols isomerisation and enzyme deactivation were proposed.

Jurado E. *et al.* developed a kinetic model for the study of initial release rates and the reaction time course for the enzymatic hydrolysis of tributyrin in O/W emulsions at several temperatures, lipase concentrations and volume fractions of tributyrin. This model successfully predicted the initial release rates and the reaction progress curves [116].

4.2.2. New challenges in the enzyme kinetic studies – multiple substrates and products

However, in most of the works published the kinetics study was simplified by considering one single substrate and/or product, i.e. triacylglycerols used contained three molecules of the same fatty acid or when different fatty acids are present only the total amount of fatty acids released at a certain stage of the reaction is considered. Furthermore, most of the kinetic studies on the hydrolysis published so far consider only the initial reaction rates. The

prediction of the reaction time course would be of much higher importance in simulating the performance of enzymatic bioreactors and also for the study of the mechanism of enzyme action throughout the reaction.

It is known that in marine or vegetable oil, triacylglycerols with numerous combinations of fatty acids can be found, and so, it is also important to know how lipases react with the different fatty acids present in the triacylglycerol molecule. For reactions with two or more substrates and/or products, the rate equations are much more complex and cannot be expressed in terms only of maximum velocities and simple Michaelis-Menten constants. Existing models do not give information about the release rates of different fatty acids, and comparison of different enzymes performance is not well explored.

Kinetic data obtained experimentally can be modelled for scale-up purposes and also for the evaluation of the influence of different reaction parameters on the enzymatic hydrolysis reaction. Moreover, it can also be used to maximise an objective, for example the yield or purity of the fatty acid of interest in the extract obtained.

4.2.3. Objectives and model hypotheses

In the present chapter, the kinetic model developed by Hermansyah H. *et al.* [104, 105] is adapted to the stepwise enzymatic hydrolysis of triacylglycerols, considering multiple substrates and products. Three of the most common configurations of triacylglycerol molecules found in microbial oils were considered which are hydrolysed according to three different mechanisms. Fatty acids were divided in two groups, saturated and monounsaturated and polyunsaturated fatty acids. The aim was to create a model which would help to predict

the reaction time required and which enzymes should be used to release a certain group of fatty acids. If successful, this model might be used for optimising yield and purity of DHA.

4.3. Materials and Methods

4.3.1. Oil, chemicals and enzymes

Oil used in the present experiments was extracted from freeze-dried thraustochytrids biomass as previously described (Chapter 2). Lipases *Mucor javanicus*, *Pseudomonas sp* and *Candida rugosa* were purchased from Sigma Aldrich (UK). Lipozyme TL 100L was kindly donated by Novozymes (Denmark). Emulsifiers bovine serum albumin and Triton X100 were purchased from Sigma Aldrich (UK). Guar gum was provided by Nofima AS (Norway). All reagents used were of analytical grade.

4.3.2. Preparation of the O/W emulsions

For the preparation of stable emulsions, initially, three different aqueous solutions containing an emulsification agent were tested, namely: 0.5% (w/v) bovine serum albumin (BSA), 1.0% (w/v) Triton X100 (TT), and 0.5% (w/v) guar gum (GG). Emulsions at three different oil:water ratios were prepared, namely 0.013, 0.026 and 0.053 (w/v). After mixing, oil-water mixtures were homogenised for 30 seconds at different stirring rates (as indicated in the results and discussion section) in an Ultra-turrax T25 homogeniser (IKA Labortechnik).

4.3.3. Determination of interfacial area of O/W emulsions

Droplet size distribution was determined by laser diffraction using a Coulter® L230 instrument. Interfacial area was calculated based on the Sauter diameter (D(3,2) = ratio between the average volume and the surface area), as given by the Coulter software. Droplet size measurements were repeated at the end of the reaction period (24 hours later).

4.3.4. Enzymatic hydrolysis of microbial oil in an O/W emulsion

Oil-in-water (O/W) emulsions were prepared with an oil:water ratio equivalent to the oil composition of a fermentation broth with a cell mass concentration of 50 g L^{-1} dry weight. 1.4-1.5 g of microbial oil was suspended in 50 mL potassium phosphate buffer (0.1 M, pH 7 at 37ºC), containing 0.5% (w/v) bovine albumin for emulsion stabilisation. These tests were carried out for the four lipases under study (Table 3.1). This suspension was then blended for 30 seconds at 20,000 rpm, in order to obtain uniform droplet size distribution. Flasks containing the reaction mixture were flushed with nitrogen and properly sealed, and then placed in a multi-position stirring plate, into an incubator kept at 37ºC. Stirring speed was 500 rpm. The experiment was performed for a total of 24 hours. 1 mL of deionised water and 1 mL of ethanol were added to 0.5 mL sample withdrawn at different reaction times. Free fatty acids and remaining acylglycerols were then extracted by washing the hydrolysed solution with three aliquots of 1 mL hexane. An exact volume of the hexane phase (1 mL) was then transferred to two separate vials and further evaporated under nitrogen. Released fatty acids and remaining acylglycerols were then re-dissolved in ethanol for further quantification by LC-ESI-MS.

4.3.5. Analytical methods

For the present study, quantification of acylglycerols and free fatty acids throughout the experiments was carried out by LC-ESI-MS, as previously described (section 3.3.5). In order to simplify the mechanism of the reaction and consequently the treatment of the analytical data, three main fatty acids were considered, namely palmitic acid (C16:0, PLA), oleic acid (C18:1, OLA), and docosahexaenoic acid (C22:6, DHA) and all possible combinations as mono-, di- and triacylglycerols were conjugated and the corresponding molecular masses calculated as shown in Table 4.1. All compounds were divided in groups according to the

composition of the molecule, which also represents the different groups of substrates and products that are considered later in the description of the mechanism of the stepwise hydrolysis reaction.

Table 4.1: List of most common monoacylglycerols (MAG), diacylglycerols (DAG) and triacylglycerols (TAG) by combinations of main fatty acids present in the oil (DHA, PLA and OLA), and respective molecular weight. (G – glycerol, S – saturated and monounsaturated fatty acis, P – polyunsaturated fatty acids).

Group	Fatty Acid/Glyceride	Molecular Weight ($g\ mol^{-1}$)
S	PLA	256
	OLA	282
P	DHA	328
MAG2	G + PLA	330
	G + OLA	356
MAG1	G + DHA	402
DAG3	G + PLA + PLA	568
	G + PLA + OLA	595
	G + OLA + OLA	621
DAG1	G + PLA + DHA	640
	G + OLA + DHA	667
DAG2	G + DHA + DHA	712
TAG3	G + PLA + PLA + PLA	807
	G + PLA + PLA + OLA	833
	G + PLA + OLA + OLA	859
	G + OLA + OLA + OLA	885
TAG1	G + PLA + PLA + DHA	879
	G + PLA + OLA + DHA	905
	G + OLA + OLA + DHA	931
TAG2	G + DHA + DHA + PLA	951
	G + DHA + DHA + OLA	977

4.4. Mathematical Model and Simulation

4.4.1. Mechanism of the process

In the present study, three of the most common configurations of triacylglycerol molecules found in marine oils were considered (TAG1, TAG2 and TAG3 in Figure 4.1), which are hydrolysed sequentially according to three different sub-mechanisms (Figure 4.1, Figure 4.2, Figure 4.3 and Figure 4.4). Diacylglycerols (DAG1, DAG2 and DAG3) and monoacylglycerols (MAG1 and MAG2) are intermediary substrates. Products, i.e. released fatty acids, were divided in two groups, saturated and monounsaturated (S) and polyunsaturated (P) fatty acids. Enzyme is designated by E, and G represents glycerol.

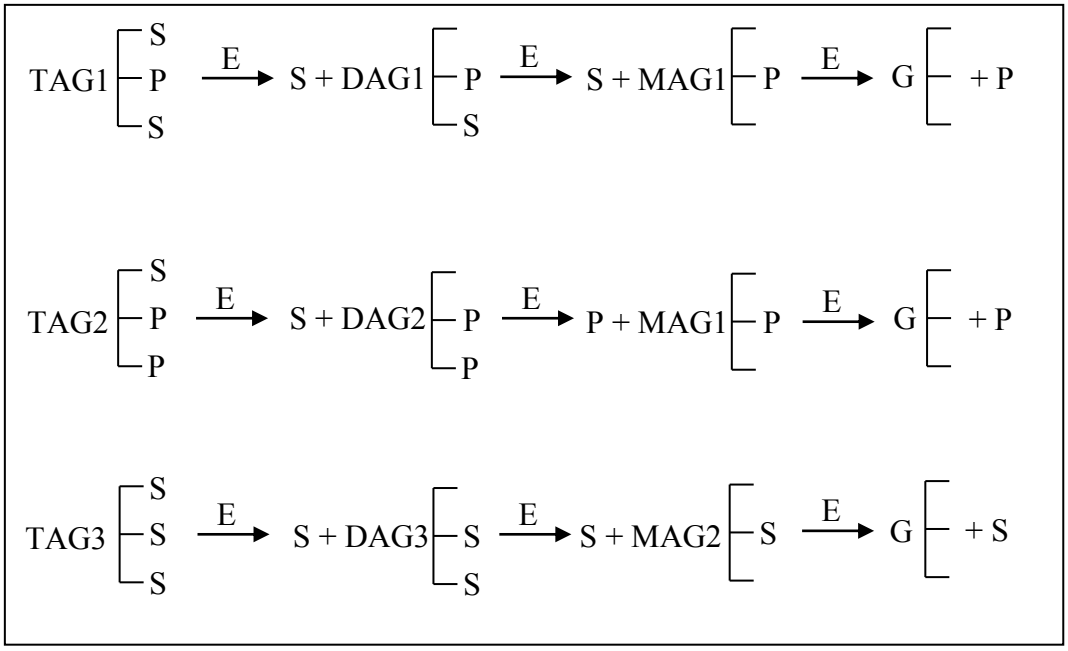


Figure 4.1: Schematic representation of the stepwise reactions for the three parallel mechanisms considered (triacylglycerols – TAG1, TAG2, TAG3; diacylglycerols – DAG1, DGA2, DAG3; monoacylglycerols – MAG1, MAG2; saturated and monounsaturated fatty acids – S; polyunsaturated fatty acids – P; glycerol – G; enzyme – E).

In the case of a non-specific lipase, all the three positions of the triacylglycerol molecule may be cleaved; therefore, there are 3 reaction steps, and consequently there will be competition between three substrates, namely triacylglycerols, diacylglycerols and monoacylglycerols, for the same enzyme molecule. Furthermore, when different triacylglycerols molecules are present, different substrates will be in competition too.

As illustrated in Figures 4.2-4.4, the mechanism of these reactions starts by the adsorption of the enzyme in the water-oil interface, involving the formation of the activated enzyme (E). When the activated enzyme gets access to an ester bond of the substrate, the complex enzyme-substrate is formed (ETAG). Finally, the product (S or P) is separated from the complex formed, liberating the enzyme and originating an intermediary substrate (DAG and MAG) which will be subsequently hydrolysed.

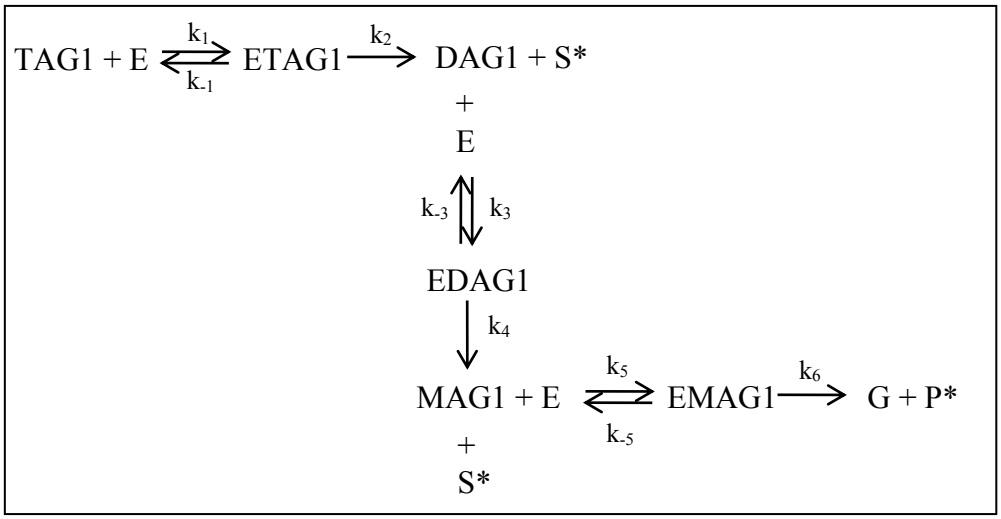


Figure 4.2: Sub-mechanism TAG1.

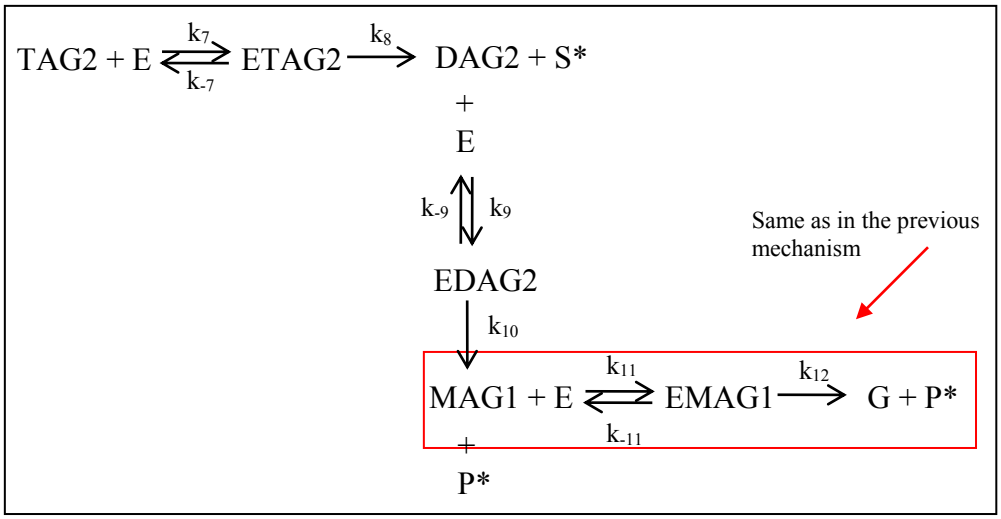


Figure 4. 3: Sub-mechanism TAG2.

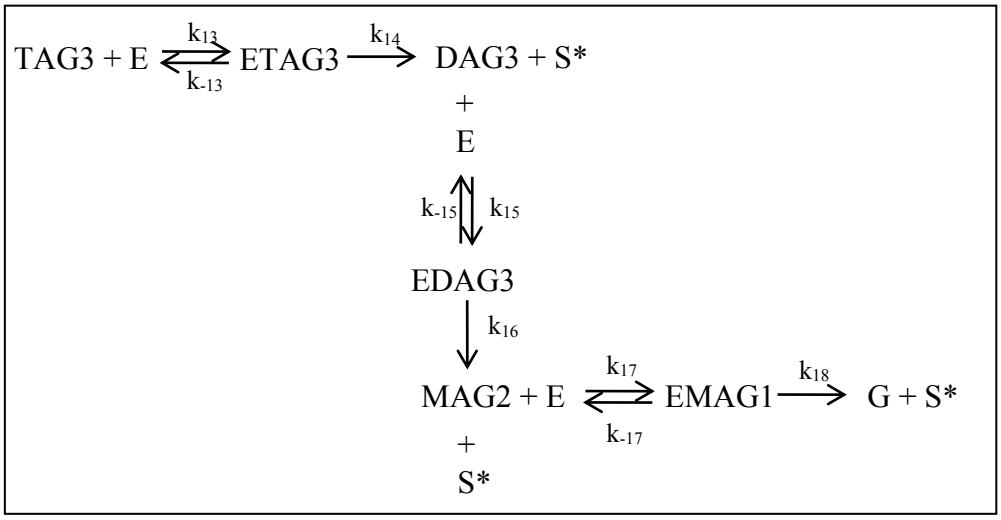


Figure 4.4: Sub-mechanism TAG3.

The model developed by Pilarek et al. [118] did not take into account the fact that the various substrates within the reaction compete for the same enzyme. Mitchell et al. [121] proposed a model for the sequential hydrolysis of triolein by lipases, which also allowed predicting the specificity of each lipase to the different substrates present in the reaction mixture, but they have not taken into account the product inhibition either.

Fatty acids released are not dissolved in the aqueous phase. Therefore, competitive inhibition is observed when released fatty acids react with the enzyme dissolved in the aqueous phase. In this way, less enzyme will be available to hydrolyse the ester bonds of acylglycerol molecules and, consequently, the reaction rates will be affected; hence it is important to account for this effect when developing a kinetic model. The competitive inhibition by released fatty acids can be expressed as:

$$S^* + W \xrightarrow{k_{19}} S + E \underset{k_{-20}}{\overset{k_{20}}{\rightleftharpoons}} ES$$

$$P^* + W \xrightarrow{k_{21}} P + E \underset{k_{-22}}{\overset{k_{22}}{\rightleftharpoons}} EP$$

4.4.2. Development of the reaction rate equations

For the development of the present kinetic model, the following assumptions were made for each mechanism:

- Product inhibition follows the competitive inhibition mechanism (if product concentration is low, product inhibition may be considered negligible, but this is not the case)
- Total concentration of the free enzyme and enzyme complex at the interface is expressed by Langmuir adsorption isotherm:

$$q_{E,total} = \frac{K_E C_E q_{E,\max}}{1 + K_E C_E} \qquad \text{(Eq. 4.1)}$$

- the molecular sizes of the substrates and products are much smaller than that of the enzyme, so that, the interfacial concentrations do not reach saturation and the linear adsorption isotherm provides the relationship for the interfacial and bulk concentrations as:

$$q_i = K_i C_i \quad \text{(Eq. 4.2)}$$

The reaction rates of all components are described by:

$$r_{TAG1} = -k_1 q_E q_{TAG1} + k_{-1} q_{ETAG1} \quad \text{(Eq. 4.3)}$$

$$r_{TAG2} = -k_7 q_E q_{TAG2} + k_{-7} q_{ETAG2} \quad \text{(Eq. 4.4)}$$

$$r_{TAG3} = -k_{13} q_E q_{TAG3} + k_{-13} q_{ETAG3} \quad \text{(Eq. 4.5)}$$

$$r_{DAG1} = k_2 q_{ETAG1} - k_3 q_E q_{DAG1} + k_{-3} q_{EDAG1} \quad \text{(Eq. 4.6)}$$

$$r_{DAG2} = k_8 q_{ETAG2} - k_9 q_E q_{DAG2} + k_{-9} q_{EDAG2} \quad \text{(Eq. 4.7)}$$

$$r_{DAG3} = k_{14} q_{ETAG3} - k_{15} q_E q_{DAG3} + k_{-15} q_{EDAG3} \quad \text{(Eq. 4.8)}$$

$$r_{MAG1} = k_4 q_{EDAG1} - k_5 q_E q_{MAG1} + k_{-5} q_{EMAG1} + k_{10} q_{EDAG2} \quad \text{(Eq. 4.9)}$$

$$r_{MAG2} = k_{16} q_{EDAG3} - k_{17} q_E q_{MAG2} + k_{-17} q_{EMAG2} \quad \text{(Eq. 4.10)}$$

$$r_S = k_{19} q_{S*} - k_{20} q_E q_S + k_{-20} q_{ES} \quad \text{(Eq. 4.11)}$$

$$r_P = k_{21} q_{P*} - k_{22} q_E q_P + k_{-22} q_{EP} \quad \text{(Eq. 4.12)}$$

Briggs-Haldane approach [122] considers that the change of the enzyme complex concentration with respect to time is assumed to be negligible, which is also known as the pseudo-steady-state assumption in chemical kinetics. Therefore, assuming a pseudo-steady-state for the respective concentrations of the enzyme complex:

$$\frac{dq_{ETAG1}}{dt} = k_1 q_E q_{TAG1} - k_{-1} q_{ETAG1} - k_2 q_{ETAG1} = 0 \quad \text{(Eq. 4.13)}$$

$$\frac{dq_{ETAG2}}{dt} = k_7 q_E q_{TAG2} - k_{-7} q_{ETAG2} - k_8 q_{ETAG2} = 0 \quad \text{(Eq. 4.14)}$$

$$\frac{dq_{ETAG3}}{dt} = k_{13} q_E q_{TAG3} - k_{-13} q_{ETAG3} - k_{14} q_{ETAG3} = 0 \quad \text{(Eq. 4.15)}$$

$$\frac{dq_{EDAG1}}{dt} = k_3 q_E q_{DAG1} - k_{-3} q_{EDAG1} - k_4 q_{EDAG1} = 0 \quad \text{(Eq. 4.16)}$$

$$\frac{dq_{EDAG2}}{dt} = k_9 q_E q_{DAG2} - k_{-9} q_{EDAG2} - k_{10} q_{EDAG2} = 0 \quad \text{(Eq. 4.17)}$$

$$\frac{dq_{EDAG3}}{dt} = k_{15} q_E q_{DAG3} - k_{-15} q_{EDAG3} - k_{16} q_{EDAG3} = 0 \quad \text{(Eq. 4.18)}$$

$$\frac{dq_{EMAG1}}{dt} = k_5 q_E q_{MAG1} - k_{-5} q_{EMAG1} - k_6 q_{EMAG1} = 0 \quad \text{(Eq. 4.19)}$$

$$\frac{dq_{EMAG2}}{dt} = k_{17} q_E q_{MAG2} - k_{-17} q_{EMAG2} - k_{18} q_{EMAG2} = 0 \quad \text{(Eq. 4.20)}$$

$$\frac{dq_{S^*}}{dt} = k_2 q_{ETAG1} + k_4 q_{EDAG1} + k_8 q_{ETAG2} + k_{14} q_{ETAG3} + k_{16} q_{EDAG3} + k_{18} q_{EMAG2} - k_{19} q_{S^*} = 0 \quad \text{(Eq. 4.21)}$$

$$\frac{dq_{P^*}}{dt} = k_6 q_{EMAG1} + k_{10} q_{EDAG2} - k_{21} q_{P^*} = 0 \quad \text{(Eq. 4.22)}$$

$$\frac{dq_{ES}}{dt} = k_{20} q_E q_S - k_{-20} q_{ES} = 0 \qquad \text{(Eq. 4.23)}$$

$$\frac{dq_{EP}}{dt} = k_{22} q_E q_P - k_{-22} q_{EP} = 0 \qquad \text{(Eq. 4.24)}$$

The total concentration of the free enzyme and the enzyme complex adsorbed at the interface stays constant during the reaction and is given as:

$$q_{E,total} = q_E + q_{ETAG1} + q_{ETAG2} + q_{ETAG3} + q_{EDAG1} + q_{EDAG2} + q_{EDAG3} + q_{EMAG1} + q_{EMAG2} + q_{S*} + q_{P*} + q_{ES} + q_{EP}$$

(Eq. 4.25)

Rearranging equations (13)-(25) and substituting them into equations (3)-(12), the following equations for the reaction rates are obtained:

$$r_{TAG1} = \frac{-K_1 q_{TAG1} q_{E,total}}{Y} \qquad \text{(Eq. 4.26)}$$

$$r_{TAG2} = \frac{-K_3 q_{TAG2} q_{E,total}}{Y} \qquad \text{(Eq. 4.27)}$$

$$r_{TAG3} = \frac{-K_4 q_{TAG3} q_{E,total}}{Y} \qquad \text{(Eq. 4.28)}$$

$$r_{DAG1} = \frac{q_{E,total}\left(K_1 q_{TAG1} - K_2 q_{DAG1}\right)}{Y} \qquad \text{(Eq. 4.29)}$$

$$r_{DAG2} = \frac{q_{E,total}\left(K_3 q_{TAG2} - K_8 q_{DAG2}\right)}{Y} \qquad \text{(Eq. 4.30)}$$

$$r_{DAG3} = \frac{q_{E,total}\left(K_4 q_{TAG3} - K_5 q_{DAG3}\right)}{Y} \qquad \text{(Eq. 4.31)}$$

$$r_{MAG1} = \frac{q_{E,total}\left(K_2 q_{DAG1} + K_8 q_{DAG2} - K_7 q_{MAG1}\right)}{Y} \quad \text{(Eq. 4.32)}$$

$$r_{MAG2} = \frac{q_{E,total}\left(K_5 q_{DAG3} - K_6 q_{MAG2}\right)}{Y} \quad \text{(Eq. 4.33)}$$

$$r_S = \frac{q_{E,total}\left(K_1 q_{TAG1} + K_2 q_{DAG1} + K_3 q_{TAG2} + K_4 q_{TAG3} + K_5 q_{DAG3} + K_6 q_{MAG2}\right)}{Y} \quad \text{(Eq. 4.34)}$$

$$r_P = \frac{q_{E,total}\left(K_7 q_{MAG1} + K_8 q_{DAG2}\right)}{Y} \quad \text{(Eq. 4.35)}$$

Where:

$$Y = 1 + K_1 K_9 q_{TAG1} + K_3 K_{10} q_{TAG2} + K_4 K_{11} q_{TAG3} + K_2 K_{12} q_{DAG1} + K_8 K_{13} q_{DAG2} + K_5 K_{14} q_{DAG3} + \\ + K_7 K_{15} q_{MAG1} + K_6 K_{16} q_{MAG2} + K_I q_S + K_J q_P \quad \text{(Eq. 4.36)}$$

and

$$K_1 = \frac{k_1 k_2}{k_{-1} + k_2} \quad \text{(Eq. 4.37)}$$

$$K_2 = \frac{k_3 k_4}{k_{-3} + k_4} \quad \text{(Eq. 4.38)}$$

$$K_3 = \frac{k_7 k_8}{k_{-7} + k_8} \quad \text{(Eq. 4.39)}$$

$$K_4 = \frac{k_{13} k_{14}}{k_{-13} + k_{14}} \quad \text{(Eq. 4.40)}$$

$$K_5 = \frac{k_{15} k_{16}}{k_{-15} + k_{16}} \quad \text{(Eq. 4.41)}$$

$$K_6 = \frac{k_{17} k_{18}}{k_{-17} + k_{18}} \quad \text{(Eq. 4.42)}$$

$$K_7 = \frac{k_5 k_6}{k_{-5} + k_6} \quad \text{(Eq. 4.43)}$$

$$K_8 = \frac{k_9 k_{10}}{k_{-9} + k_{10}} \quad \text{(Eq. 4.44)}$$

$$K_I = \frac{k_{20}}{k_{-20}} \quad \text{(Eq. 4.45)}$$

$$K_9 = \frac{k_2 + k_{19}}{k_2 k_{19}} \quad \text{(Eq. 4.46)}$$

$$K_{10} = \frac{k_8 + k_{19}}{k_8 k_{19}} \quad \text{(Eq. 4.47)}$$

$$K_{11} = \frac{k_{14} + k_{19}}{k_{14} k_{19}} \quad \text{(Eq. 4.48)}$$

$$K_{12} = \frac{k_4 + k_{19}}{k_4 k_{19}} \quad \text{(Eq. 4.49)}$$

$$K_{13} = \frac{k_{10} + k_{21}}{k_{10} k_{21}} \quad \text{(Eq. 4.50)}$$

$$K_{14} = \frac{k_{16} + k_{19}}{k_{16} k_{19}} \quad \text{(Eq. 4.51)}$$

$$K_{15} = \frac{k_6 + k_{21}}{k_6 k_{21}} \quad \text{(Eq. 4.52)}$$

$$K_{16} = \frac{k_{18} + k_{19}}{k_{18} k_{19}} \quad \text{(Eq. 4.53)}$$

$$K_J = \frac{k_{22}}{k_{-22}} \quad \text{(Eq. 4.54)}$$

The total enzyme concentration in previous equations is determined from the mass balance for the enzyme in the system, given as follows:

$$q_{E,total} = \frac{V}{A}\left(C_{E,0} - C_E\right) \qquad \text{(Eq. 4.55)}$$

Substituting Eq. 4.1 into Eq. 4.55, and rearranging terms:

$$q_{E,total} = \frac{b - \sqrt{b^2 - 4(A/V)\left(C_{E,0} q_{E,\max}\right)}}{2(A/V)} \qquad \text{(Eq. 4.56a)}$$

Where b is:

$$b = \frac{A}{V} q_{E,\max} + C_{E,0} + \frac{1}{K_E} \qquad \text{(Eq. 4.56b)}$$

The mass balance for each component (i) in the system is given by:

$$V \frac{dC_i}{dt} + A \frac{dq_i}{dt} = A r_i \qquad \text{(Eq. 4.57)}$$

The initial conditions (t=0) are:

$$\begin{array}{llll} C_{TAG1} = C_{TAG1,0} & C_{DAG1} = 0 & C_{MAG1} = 0 & C_S = 0 \\ C_{TAG2} = C_{TAG2,0} & C_{DAG2} = 0 & C_{MAG2} = 0 & C_P = 0 \\ C_{TAG3} = C_{TAG3,0} & C_{DAG3} = 0 & & \end{array} \qquad \text{(Eq. 4.58)}$$

Rearranging the mass balance equation for each component:

$$\frac{dC_i}{dt} = \frac{(A/V)r_i}{1+(A/V)(dq_i/dC_i)} \quad \text{(Eq. 4.59)}$$

Substituting Eq. 4.2, reaction rates, constants and total enzyme equations in the mass balance equation (Eq.4.59) for each component, the following model equations are obtained:

$$\frac{dC_{TAG1}}{dt} = \frac{-(A/V)K_1K_{TAG1}C_{TAG1}q_{E,total}}{(1+(A/V)K_{TAG1})Z} \quad \text{(Eq. 4.60)}$$

$$\frac{dC_{TAG2}}{dt} = \frac{-(A/V)K_3K_{TAG2}C_{TAG2}q_{E,total}}{(1+(A/V)K_{TAG2})Z} \quad \text{(Eq. 4.61)}$$

$$\frac{dC_{TAG3}}{dt} = \frac{-(A/V)K_4K_{TAG3}C_{TAG3}q_{E,total}}{(1+(A/V)K_{TAG3})Z} \quad \text{(Eq. 4.62)}$$

$$\frac{dC_{DAG1}}{dt} = \frac{(A/V)(K_1K_{TAG1}C_{TAG1}-K_2K_{DAG1}C_{DAG1})q_{E,total}}{(1+(A/V)K_{DAG1})Z} \quad \text{(Eq. 4.63)}$$

$$\frac{dC_{DAG2}}{dt} = \frac{(A/V)(K_3K_{TAG2}C_{TAG2}-K_8K_{DAG2}C_{DAG2})q_{E,total}}{(1+(A/V)K_{DAG2})Z} \quad \text{(Eq. 4.64)}$$

$$\frac{dC_{DAG3}}{dt} = \frac{(A/V)(K_4K_{TAG3}C_{TAG3}-K_5K_{DAG3}C_{DAG3})q_{E,total}}{(1+(A/V)K_{DAG3})Z} \quad \text{(Eq. 4.65)}$$

$$\frac{dC_{MAG1}}{dt} = \frac{(A/V)(K_2 K_{DAG1} C_{DAG1} + K_8 K_{DAG2} C_{DAG2} - K_7 K_{MAG1} C_{MAG1}) q_{E,total}}{(1 + (A/V) K_{MAG1}) Z} \quad \text{(Eq. 4.66)}$$

$$\frac{dC_{MAG2}}{dt} = \frac{(A/V)(K_5 K_{DAG3} C_{DAG3} - K_6 K_{MAG2} C_{MAG2}) q_{E,total}}{(1 + (A/V) K_{MAG2}) Z} \quad \text{(Eq. 4.67)}$$

$$\frac{dC_S}{dt} = \frac{(A/V)(K_1 K_{TAG1} C_{TAG1} + K_2 K_{DAG1} C_{DAG1} + K_3 K_{TAG2} C_{TAG2} + K_4 K_{TAG3} C_{TAG3} + K_5 K_{DAG3} C_{DAG3} + K_6 K_{MAG2} C_{MAG2}) q_{E,total}}{(1 + (A/V) K_S) Z} \quad \text{(Eq. 4.68)}$$

$$\frac{dC_P}{dt} = \frac{(A/V)(K_7 K_{MAG1} C_{MAG1} + K_8 K_{DAG2} C_{DAG2}) q_{E,total}}{(1 + (A/V) K_P) Z} \quad \text{(Eq. 4.69)}$$

Where,

$$Z = 1 + K_1 K_9 K_{TAG1} C_{TAG1} + K_3 K_{10} K_{TAG2} C_{TAG2} + K_4 K_{11} K_{TAG3} C_{TAG3} + K_2 K_{12} K_{DAG1} C_{DAG1} + K_8 K_{13} K_{DAG2} C_{DAG2} + \\ + K_5 K_{14} K_{DAG3} C_{DAG3} + K_7 K_{15} K_{MAG1} C_{MAG1} + K_6 K_{16} K_{MAG2} C_{MAG2} + K_I K_S C_S + K_J K_P C_P \quad \text{(Eq. 4.70)}$$

The model is then composed by 10 ODEs and 29 unknown constants. These constants must be determined by fitting experimental data with the model equations. Initially, arbitrary values were given to the constants for the numerical resolution of the differential equations. The model was solved using the Runge-Kutta method in MatLab. The best fitted values for the constants must be determined using the simplex method by minimizing the squared-sum of the relative errors between the calculated values and the experimental data for the concentration of each component.

Equation for the calculation of the squared-sum of the relative errors between the calculated values and the experimental data for the concentration of each component:

$$S = \sum_{i=1}^{n}\left(\frac{TAG1_{ei} - TAG1_{mi}}{TAG1_{ei}}\right)^2 + \sum_{i=1}^{n}\left(\frac{TAG2_{ei} - TAG2_{mi}}{TAG2_{ei}}\right)^2 + \sum_{i=1}^{n}\left(\frac{TAG3_{ei} - TAG3_{mi}}{TAG3_{ei}}\right)^2 +$$
$$\sum_{i=1}^{n}\left(\frac{DAG1_{ei} - DAG1_{mi}}{DAG1_{ei}}\right)^2 + \sum_{i=1}^{n}\left(\frac{DAG2_{ei} - DAG2_{mi}}{DAG2_{ei}}\right)^2 + \sum_{i=1}^{n}\left(\frac{DAG3_{ei} - DAG3_{mi}}{DAG3_{ei}}\right)^2 +$$
$$\sum_{i=1}^{n}\left(\frac{MAG1_{ei} - MAG1_{mi}}{MAG1_{ei}}\right)^2 + \sum_{i=1}^{n}\left(\frac{MAG2_{ei} - MAG2_{mi}}{MAG2_{ei}}\right)^2 + \sum_{i=1}^{n}\left(\frac{S_{ei} - S_{mi}}{S_{ei}}\right)^2 + \sum_{i=1}^{n}\left(\frac{P_{ei} - P_{mi}}{P_{ei}}\right)^2$$

(Eq. 4.71)

4.5. Results and Discussion

4.5.1. Evaluation of emulsion stability and calculation of the interfacial area

Sauter diameter (D (3,2)) as given by Coulter software, and total interfacial area calculated for each emulsion are presented in Table 4.2 for the two measurements carried out (at the moment of emulsion preparation and 24 hours later). A first group of samples were prepared in order to select the emulsifier which would give the more stable emulsion. The same oil:water ratio was used. Further, emulsions with different oil:water ratios and homogenised at different rates were prepared with the selected emulsifier (BSA), droplet size measurements are also indicated in Table 4.2.

Results presented in Table 4.2 show that emulsifier and homogenisation rate were very important in determining the droplet size and the emulsion stability. BSA was selected to be used as an emulsifier in further experiments; in the case of GG and TT a significant change in the droplet size was observed. It was also evident that the droplet size did not change significantly with the oil:water fraction in the emulsion. It can also be concluded that the smaller the droplet size is, the more stable is the emulsion.

Table 4.2: Sauter diameter (D (3,2)) and total interfacial area calculated for the emulsions tested.

Sample	Run	Oil:Water ($cm^3\ L^{-1}$)	D (3,2) (μm)	At ($m^2\ L^{-1}$)
Preliminary tests – different emulsifiers				
BSA_0.5%	1h	52.6	1.00 ± 0.02	314.4 ± 5.5
	24h	52.6	1.54 ± 0.00	205.4 ± 0.3
GG_0.5%	1h	52.6	2.70 ± 0.07	117.1 ± 2.9
	24h	52.6	4.16 ± 0.36	76.2 ± 6.6
TT_1%	1h	52.6	5.98 ± 0.15	52.9 ± 1.3
	24h	52.6	4.42 ± 0.07	71.4 ± 1.2
BSA_0.5% - different homogenisation rates				
13500 rpm				
A_50	1h	13.2	1.22 ± 0.02	64.6 ± 0.8
	24h	13.2	1.50 ± 0.02	52.8 ± 0.7
A_100	1h	26.3	-	-
	24h	26.3	1.29 ± 0.03	122.8 ± 2.6
A_150	1h	52.6	1.22 ± 0.09	260.1 ± 19.8
	24h	52.6	1.59 ± 0.01	198.3 ± 1.3
20500 rpm				
B_50	1h	13.2	1.12 ± 0.01	70.6 ± 0.3
	24h	13.2	1.11 ± 0.00	71.4 ± 0.0
B_100	1h	26.3	1.07 ± 0.08	147.8 ± 11.1
	24h	26.3	1.15 ± 0.04	137.6 ± 4.9
B_150	1h	52.6	1.17 ± 0.02	270.5 ± 4.4
	24h	52.6	1.22 ± 0.01	259.0 ± 2.6
8000 rpm				
C_50	1h	13.2	4.73 ± 0.67	17.5 ± 2.5
	24h	13.2	4.68 ± 0.52	16.7 ± 2.2
24000 rpm				
D_50	1h	13.2	1.011 ± 0.004	81.2 ± 0.3
	24h	13.2	1.030 ± 0.004	79.7 ± 0.3

4.5.2. Application of the model

Experiments were carried out with the four enzymes as previously mentioned, and also for various interfacial areas and enzymes concentrations with lipase LPZ. However, unfortunately it was not possible to verify the model utilising the experimental data collected. It turned out to be extremely challenging to gather experimental data according to the model proposed. Certain fatty acids and acylglycerols present in the oil:water emulsion could not be quantified, only the ones where standards were available, as specified in sections 3.3.5 and 3.4.2.3, and as a result the mass balances could not be closed. It was attempted to solve the problem by considering peak area ratios based on the MS spectrums obtained instead of concentrations, but still unsuccessful.

However, in order to test if the system of differential equations was possible to solve and if the results output was given as expected and somehow coincident with experimental results, two subroutines were created in MatLab for the resolution of the proposed kinetic model. A system composed by 1 m^3 of emulsion, with oil:water ratio of 0.0137 (w/v, equivalent to oil fraction in the fermentation broth with a biomass concentration of 50 g L^{-1}). Initial concentrations were calculated based on the oil fraction in the emulsion. A droplet size of 4.7 μm was considered and the corresponding interfacial area taken into account. Amount of enzyme added was also in accordance with previous work. Arbitrary values were given to the kinetics and adsorption constants (model parameters), these values were adjusted in a way that the desired shape of concentration profiles of all components throughout the experiment was obtained. Part of the MatLab algorithm used to solve the model is transcript in Appendix B, including the arbitrary values given to the constants, initial concentrations and system characteristics (interfacial area and volume). Running the subroutines created, the plots

including the concentration profiles of TAGs, DAGs, MAGs, S and P throughout the reaction presented in Figure 4.5 were obtained.

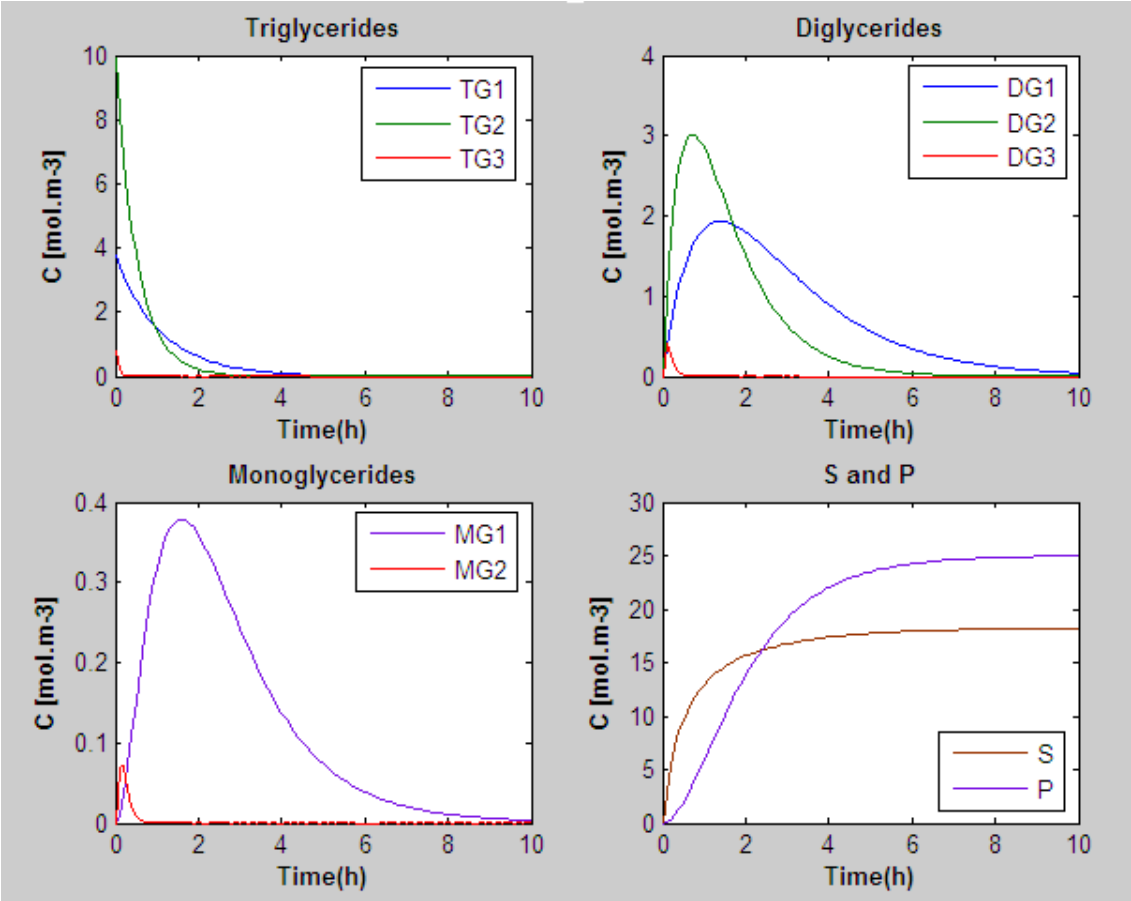


Figure 4.5: Concentration profiles of TAG, DAG, and MAG, S and P throughout enzymatic hydrolysis of triacylglycerols in a stable oil:water emulsion as given by the kinetic model developed.

For comparison, the experimental results obtained for the trials carried out with the sn-1,3 specific lipase MJ are presented in Figure 4.6.

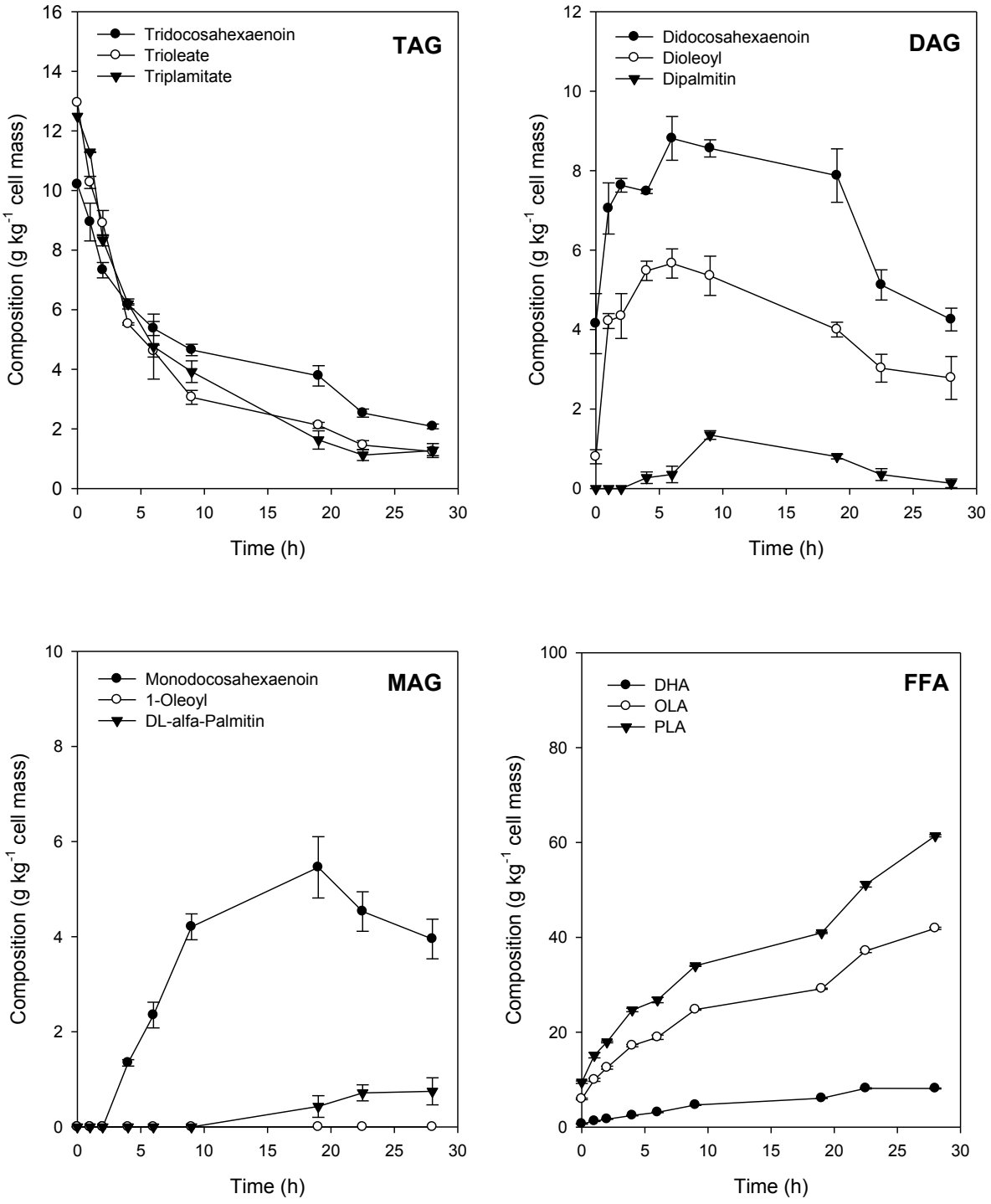


Figure 4.6: Profile of triacylglycerols (TAG), diacylglycerols (DAG), monoacylglycerols (MAG) and fatty acids (FFA) composition during enzymatic hydrolysis of microbial oil in an oil-in-water emulsion with lipase *Mucor javanicus* (o/w ratio: 0.0137; enzyme concentration: 100 kU enzyme mL^{-1} emulsion).

As depicted by the composition profiles, the hydrolysis rates of TAG and DAG in the oil-in-water emulsion were greater than previously observed in the trials carried out with the cell mass suspension (Figures 3.7a and 3.8, MJ plots). But surprisingly, composition of MAG and free fatty acids in suspension throughout the reaction was lower than expected, which may indicate that the stability of those compounds was compromised.

4.6. Conclusions

Unfortunately, it was not possible to fit the experimental data to the model proposed, due to the complexity of the reaction mixture, and so its applicability could not be verified. However, the shape of theoretical concentration profiles given by the model, solved using arbitrary values for the kinetic constants, are coincident to what has been observed experimentally.

Chapter 5

Transport of Fatty Acids through Asymmetric Polyimide Membranes in a Biphasic Membrane Contactor System

5.1. Summary

Four asymmetric polyimide membranes, namely the commercially available nanofiltration membrane, Starmem™ 240, and three laboratory fabricated ultrafiltration membranes made from P84 and Matrimid® 5218 polyimide polymers, were tested for the separation of fatty acids from a fatty acid rich solution (aqueous phase) to an organic phase (hexane) in a biphasic membrane contactor system. Initially, the mass transfer rates of the targeted fatty acids, namely docosahexaenoic acid (DHA) and palmitic acid (PLA), were determined for evaluation of mass transfer performance of the four membranes. Aqueous/organic volume ratios were adjusted in order to improve the volumetric productivities. The best mass transfer rates were obtained with ultrafiltration membranes prepared from Matrimid polyimide. In the best scenario, 95-98 wt% of total DHA and PLA in the aqueous phase was recovered in the organic phase, and overall mass transfer coefficients estimated for DHA and PLA were, respectively, 1.7×10^{-6} and 1.6×10^{-6} m s^{-1}, tenfold greater than in other published works reporting extraction of fatty acids from an edible oil in a membrane contactor system [21].

To gain insight into the solute transport phenomena in a biphasic system comprising an asymmetric porous membrane, a model for solvent extraction in a system with immobilised interfaces involving a microporous hydrophobic membrane as presented by Kiani *et al.* [123] was used. Individual liquid-film mass transfer coefficients in the aqueous and organic boundary layers were determined based on the flow characteristics. The membrane mass transfer coefficient of the desired solute through the membrane was calculated as a function of the membrane thickness and porosity. The model presented by Bowen and Welfoot [124] was applied for estimation of porosity of the membranes considered in this investigation, based on the measured membrane flux and solute rejections/molecular weight cut-off curve (MWCO). The objective was to find out how closely the theoretical membrane mass transfer coefficient estimated according to these two models, would describe experimental observations.

5.2. Background and Literature Review

5.2.1. Biphasic membrane contactor systems in the extraction of solutes from complex mixtures

The use of solvent extraction to selectively transport a chemical species from one phase to a second immiscible phase is a common industrial practice [125]. It is a process widely used throughout the chemical process industries to separate or purify chemical species. To perform an extraction, the two liquid phases are contacted together and mixed thoroughly to generate interfacial area for mass transport of the extracted species to take place. During mixing, one of the phases, usually the one present at a lower volumetric fraction, forms discrete droplets within the second phase to generate a dispersion that provides high interfacial area for rapid mass transport. The key operating parameters for solvent extraction processes include the choice of solvent, extraction temperature, the flow or volume ratio of the two phases when they are contacted, in some cases the extraction pressure, the extractor type used, and the

mixing intensity in the extractor [126]. These parameters must be optimised to obtain the target yield and/or purity of the extracted species. However, a very important factor is how readily the two phases separate from each other once the extraction is complete. In many applications, this can be a problematic aspect of the process, mainly in applications where surface-active species are present that have the potential to stabilise the interface between the two phases, such us surfactants, proteins, biological polymers, etc. Hence, the difficulty of the phase separation may prevent the use of solvent extraction due to the formation of stable emulsions.

A number of approaches have been investigated and developed to try and overcome the limitations due to formation of stable emulsions, for example the installation of a secondary unit operation, to break the emulsion after it is formed [28], or the direct use of surfactants to break the emulsion or dispersion [127]. However, an alternative approach is to prevent or minimise the formation of the emulsion or dispersion in the first place. One way of achieving this is through the addition of a further chemical compound to the system that disrupts the system's inherent ability to form emulsions [128].

A further approach to prevent or minimise the formation of the emulsion or dispersions is to provide a fixed interfacial area for mass transfer, rather than generate the area through mixing of the fluids. In this approach, the fluid boundary of one liquid phase is located in or at the surface of a porous medium, which provides a fixed interface. The second liquid phase is then contacted with the porous medium containing the first liquid phase and the species to be extracted transports from the second liquid phase into the first liquid phase. As the two liquid phases do not mix together, consequently emulsions do not form. The porous medium for this type of process is typically a synthetic membrane material, such as a microfiltration or

ultrafiltration membrane, and this approach is commonly referred to as membrane solvent extraction or membrane phase contacting [129].

Despite the inherent advantages of the membrane phase contactor, one critical problem in their application is the elimination of phase breakthrough [130, 131]. This phenomenon occurs when the breakthrough pressure of the membrane, which is the pressure that must be applied to the membrane to force the non-impregnating liquid phase through the pores of the membrane, reduces. The breakthrough pressure is a function of both the pore size and the interfacial tension. According to the Laplace-Young equation, breakthrough pressure can be described by the following equation:

$$P_b = 2\sigma Cos\theta/r$$

Where Pb = breakthrough pressure, σ = interfacial tension at the liquid-liquid interface, θ = contact angle between the wetting liquid and the membrane, and r = pore radius.

From this equation it is clear that the breakthrough pressure decreases as the pore radius increases, but importantly it also decreases as the interfacial tension decreases. Materials that can reduce surface tension include chemicals such as surfactants and proteins, and other materials such as dust. In nearly all industrial environments, there are materials present that can reduce the surface tension and thus decrease the breakthrough pressure. As reported by Vaidya *et al.*, this is particularly problematic where membrane phase contactors are used with biological solutions, as biological polymers such as proteins are very potent surfactants that readily reduce the breakthrough pressure [127]. Membranes with smaller pores are often used to counteract the reduction in surface tension, but nanofiltration and tight ultrafiltration

membranes have low porosity and consequently their mass transfer rates are low compared to loose ultrafiltration and microfiltration membranes.

Work by Valadez-Blanco *et al*. has shown that organic solvent nanofiltration membranes prepared using P84 polyimide polymer are suitable for use in a membrane phase contactor in applications involving whole cell biocatalysis [132]. It their work they found out that these membranes did not suffer from the phase breakthrough that occurs with looser membranes, however the measured mass transfer rates of the solute per unit membrane area were not found to be high enough to offer volumetric productivities higher than a direct-contact two-phase system and thus provide a viable industrial solution.

5.2.2. Transport phenomena through membranes

Two models are widely applied for the description of transport through membranes, namely, the pore flow model and the solution diffusion model [133, 134]. The pore flow model postulates that the permeate travels down the pores of the membrane, due to the pressure driven convective flow and separation is achieved by size exclusion. The solution-diffusion model claims that the permeate dissolves in the membrane material and then diffuses through the membrane due to the concentration gradient created. Separation is achieved through differences in the amounts which partition into the membrane, and the rate at which the permeate diffuses through the membrane.

The solution-diffusion model is now almost universally accepted and well-supported by experimental evidence for reverse osmosis, gas permeation and pervaporation [135]. However, the solution-diffusion model has been less successful at providing a link between the nature of the membrane material and the membrane permeation properties. The theory of

permeation through porous membranes in ultrafiltration and nanofiltration is less developed. Permeation through these membranes is a function of membrane structure and composition. The membrane geometry influences the rate of extraction through its properties of porosity, tortuosity and thickness.

Silva *et al*. studied solvent transport in organic solvent nanofiltration membranes in a lab-scale cross-flow unit over extended periods using common solvents, namely methanol, toluene, ethyl acetate and their mixtures [136]. Geens *et al*. presented a new approach for the modelling of solute transport of small organic components in nanofiltration of organic solvents. For them, solute transport rejection in a non-aqueous system depended on a number of membrane-solvent-solute interactions, which should be incorporated in a generalised transport model [137, 138]. Han *et al*. studied the diffusion mechanisms for mass transfer of solutes through three different membranes, a microporous membrane, a nanofiltration membrane, and a non-porous silicone rubber membrane [45].

However, the membrane in a biphasic process does not function as a species selective transport medium in the traditional sense; it just prevents the dispersion of one phase into another [133]. Only one interface is considered important in this case as opposed to two in a traditional filtration. Kiani *et al*. has explored the role played by the boundary layer resistances, and interpreted the intrinsic mass transfer rate through the porous membrane or the membrane resistance using the notion of simple unhindered diffusion of a solute through a liquid filled tortuous porous medium of uniform pore size [123].

Doig *et al.* evaluated the mass transfer of hydrophobic solutes in non-porous, solvent swollen silicone rubber membranes, contacting an aqueous and an organic phase, using a resistances

in series model for the description of the mass transfer characteristics of a range of solutes [139]. However, the diffusion mechanism for the solute mass transport through integrally skinned OSN membranes in non-pressure-driven systems has not been much explored. Valadez-Blanco *et al.* presented a new approach for the structure of polyimide asymmetric membranes [140], based on previously published works [141], and studied the effect of membrane formation parameters, such us casting thickness and evaporation time, on the diffusive mass transport of organic solutes through an OSN membrane in a dialysis system.

5.2.3. Objectives and process hypotheses

In this chapter, the main goal was to evaluate the mass transfer rates and the solute transport mechanism for a given solute being transferred from a complex aqueous mixture to an organic solvent through distinct asymmetric polyimide membranes in a biphasic system. It is intended to find a suitable membrane for the separation of fatty acids from a fatty acid rich solution (aqueous phase) to hexane (organic phase).

Thus, the following objectives were appointed:

- Prepare asymmetric polyimide membranes with molecular weight cut-offs in the ultrafiltration range;
- Characterise membranes in terms of solvent flux and molecular weight cut-off;
- Evaluate the performance of the selected membranes for the separation of fatty acids from the complex aqueous phase (fatty acid rich solution) to the organic phase (hexane) in the membrane biphasic system; and identify which parameters affect the mass transfer rates across the membrane;
- Understand the solute transport mechanism in a biphasic system comprising an asymmetric polyimide porous membrane;

- Estimate porosity and thickness of the distinct membrane layers by the modified pore flow model;
- Predict the membrane mass transfer rates based on the membrane characteristics, and verify how closely they can describe what is observed experimentally.

5.3. Materials and Methods

5.3.1. Cell mass and chemicals

Thraustochytrid cell mass (strain T29) used for the preparation of the fatty acid rich solution was produced by fermentation as described in section 2.3.1.

Hexane (GPR Rectapur), 96% ethanol (v/v, GPR grade) and 37% chloridric acid (HCl, Normapur grade) were purchased from VWR. Potassium hydroxide, KOH, was purchased from Fisher. Dimethylformamide (DMF) was purchased from Rathburn Chemicals, UK (HPLC grade). P84 polyimide polymer was purchased from HP Polymer GmbH (Austria), and Matrimid® 5218 from Huntsman (US). 99% maleic acid, used as additive in membrane preparation, was purchased from Fluka. Styrene oligomers used for membrane characterisation tests were purchased from Polymer Laboratories, UK, and polyethylene glycol compounds from Fluka-Biochemika, Switzerland.

5.3.2. Preparation of fatty acid rich solution – chemical hydrolysis

The solution rich in fatty acids was prepared by direct chemical hydrolysis of the oil content of the microbial cell mass. 5 g of freeze-dried cell mass were dissolved in 150 mL of 0.5 M KOH in ethanol, homogenised and left overnight with continuous stirring at room temperature. The flask was then incubated in a water bath at 60ºC for 2 hours. After cooling,

75 mL of deionised water were added. The aqueous solution containing the salts of fatty acids was then acidified to pH 1 using a solution of 6 M HCL, in order to obtain the free fatty acids.

5.3.3. Asymmetric membranes preparation

Four membranes were considered for this study, one commercial nanofiltration membrane Starmem^{TM} 240 (W. R. Grace and Co.), and three lab prepared ultrafiltration membranes – see Table 5.1. The lab made integrally skinned asymmetric polyimide membranes were prepared by phase inversion, according to method described in WO Patent Application No. 2010/142979 [142]. Two different polyimides were used, namely P84 and Matrimid® 5218. In order to obtain membranes in the UF range, co-solvent was not added to the dope solution in any case. 2 wt% maleic acid was added to the dope solution in every case.

Table 5.1 Composition of the ultrafiltration membranes prepared for the study of transport of fatty acids in a biphasic system.

Membrane	Polymer	Polymer Concentration (wt%)	Dope Solvent	Backing
M1	P84	22	DMF	PP
M2	Matrimid® 5218	26	NMP	PP
M3	Matrimid® 5218	22	DMF	PP

PP - Polypropylene (Viledon, Germany), non-woven backing

5.3.4. Asymmetric membranes characterisation

Membranes were characterised under pressure filtration in relation to the membrane flux and the MWCO. Experiments carried out for this purpose were conducted in a dead-end MET Cell (from Evonik - MET Ltd, London). A constant pressure of 5 bar was used for membranes

M1, M2 and M3, and 30 bar for Starmem^{TM} 240. Flux measurements were carried out with toluene, and the rejection tests with a polystyrene solution (PS, 1 g L^{-1}, 200-1100 Da) in toluene. The same PS solution was used in the rejection tests of Starmem^{TM} 240, and individual solutions comprising polyethylene glycol molecules (PEG, 1 g L^{-1}, 3-35 kDa) in toluene for M1, M2 and M3. MWCO curves were obtained plotting the calculated rejections against the molecular weight of the tested compounds. The procedure followed to obtain the MWCO curves was as described by See-Toh *et al*. [143].

5.3.5. Measurement of organic/aqueous partition coefficients

Partition coefficients of DHA and PLA in an organic/aqueous system, composed of hexane:water:ethanol (1:0.5:0.5, v/v/v) were determined. Known amounts of DHA and PLA standards were added to screw cap tubes containing the solvent mixture, and then stirred until complete dissolution. After flushing with nitrogen, the tubes were placed in an incubator at 25°C for 24h. After this period, mixtures were centrifuged for complete separation of organic and aqueous phases, and an aliquot of each phase was withdrawn. DHA and PLA dissolved in the organic and aqueous phases were then recovered. Samples were further analysed by LC-ESI-MS for quantification of DHA and PLA dissolved in each phase. These tests were run in triplicate.

5.3.6. Mass transfer experiments – Membrane contactor design

A schematic representation of the membrane biphasic system used is presented in Figure 5.1. The fatty acid rich solution is circulated from a feed container (T1), to the aqueous compartment (1) of the membrane contactor module (M1) and back to the feed container (T1). The organic solvent (hexane) is circulated from a product recovery container (T2) to the organic compartment (3) of the membrane contactor module (M1) and back to the product

recovery container (T2), while the free fatty acids are extracted across the asymmetric polyimide membrane (2) to the organic compartment (3) where the product of interest accumulates. Both liquid flow rates were adjusted in order to maintain the transmembrane pressures that prevent phase breakthrough. Fatty acids are extracted from the aqueous phase into the bulk of the organic phase through the organic solvent wetting the hydrophobic membrane (in Figure 5.1, arrow in the membrane module indicates the direction of solute transport). Polyimide membranes were selected, due to their highly hydrophobic characteristics, preventing water breakthrough through the membrane, and consequently the contamination of the organic phase receiving the solute.

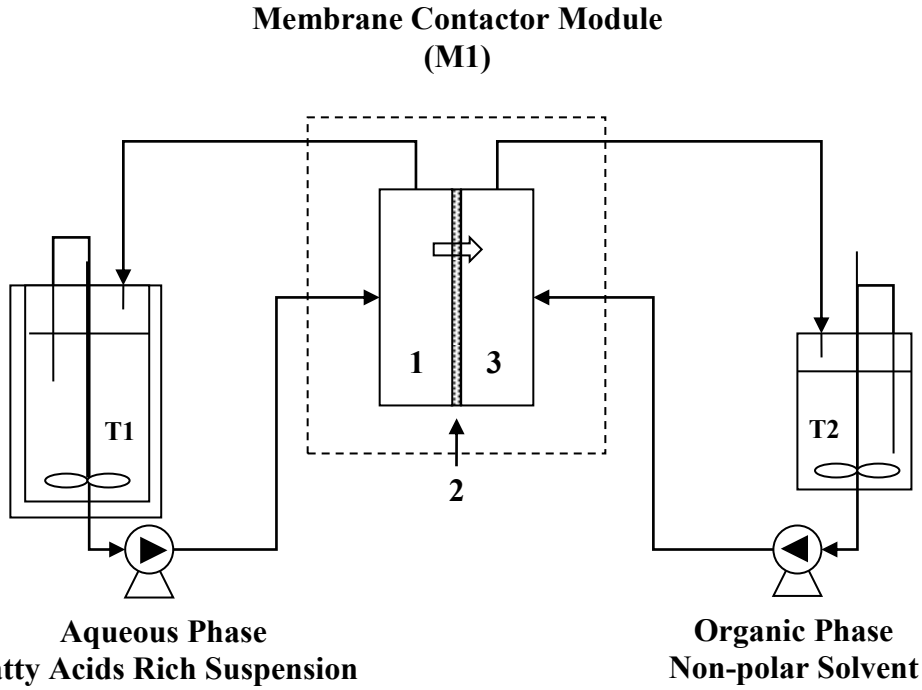


Figure 5.1: Schematic of biphasic membrane contactor used for extraction of fatty acids. The arrow indicates the direction of solute transport. (T1-bioreactor containing the fatty acid rich suspension; T2-reservoir containing the organic solvent; M1-Membrane Contactor Module; (1) aqueous compartment of the membrane contactor module; (2) asymmetric polyimide membrane; (3) organic compartment of the membrane contactor module).

The system comprised two liquid circuits, the fatty acid rich phase (pH 1-1.5) and the organic phase (hexane). The organic phase contained 0.1% BHT (Butylated hydroxytoluene) to avoid oxidation of fatty acids. The two phases were in continuous circulation via gear pumps on each side of the membrane contactor cell (M1).

5.3.7. Analytical methods

The free fatty acid fraction of the samples withdrawn during the experiments was methylated according to the method described by Metcalfe *et al*. [89]. The fatty acid methyl esters were further quantified by gas chromatography. Analysis of the methyl esters of fatty acids was carried out using an Agilent 6850 series gas chromatograph equipped with an autoinjector (injection volume of 1 μL, split ratio of 25:1) operated at 250°C and a flame ionization detector operated at 280°C. A DB-FFAP fused silica capillary column, 30 m x 0.25 mm inner diameter and 0.25 mm film thickness (J&W Scientific catalogue no. 122-3232) was used. The column oven was operated at 100ºC to 150ºC at 20ºC/min, then to 240ºC at 3ºC/min and finally holding at 240ºC until complete at 39 min. Helium was used as the carrier gas. The signals were identified by comparison with known standards (mixture ME 81; Larodan Fine Chemicals, Sweden) and quantified according to the response factor of the internal fatty acid standard C21:0 (Larodan Fine Chemicals, Sweden). Calibration curves for each fatty acid were defined based on four different concentrations of the same standard mixture.

5.4. Mathematical Analysis

For the evaluation of the solute transport mechanism in the biphasic membrane contactor system in casu, a model for solvent extraction in a system with immobilised interfaces involving a microporous hydrophobic membrane as presented by Kiani *et al.* was used [123].

5.4.1. Solute transport through porous membranes in a biphasic system

Figure 5.2 shows a flat porous hydrophobic asymmetric membrane in a biphasic system with the pores filled with an organic solvent flowing on the right-hand side of the contactor module. To avoid phase breakthrough, the pressure in the non-wetting phase should be higher than that of the wetting phase. Therefore, on the left-hand side of the membrane, the aqueous solution (non-wetting phase) flows at a pressure greater than that of the organic phase (wetting phase). The steady state concentration profiles in the hydrodynamic boundary layer in the aqueous phase, through the asymmetric membrane, and in the solvent phase boundary layer are also illustrated in Figure 5.2. Solute is extracted from the aqueous phase into the bulk of the organic solvent phase through the solvent wetting the membrane (arrow in the illustration indicates the direction of the solute transport).

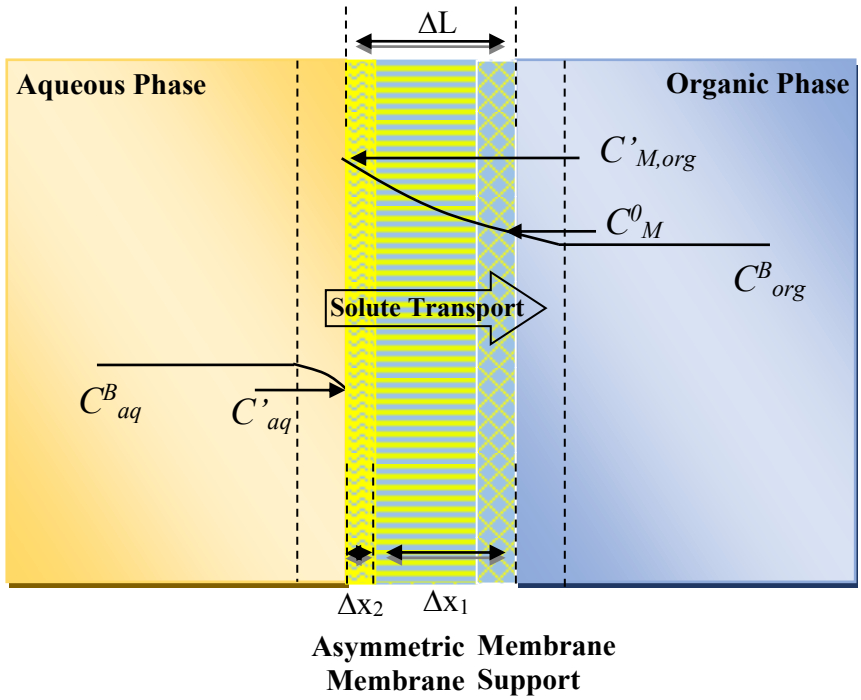


Figure 5.2. Schematic of solute concentrations with interfaces immobilised in a porous hydrophobic asymmetric membrane in a biphasic membrane contactor system.

The schematic representation of the asymmetric membrane presented in Figure 5.2, was constructed based on SEM pictures and comments by See-Toh *et al.* [141] and Valadez-Blanco *et al*. [140]. The asymmetric membrane with an overall thickness ΔL, can be divided in two main layers, with thickness: Δx_1, which comprises the non-woven backing material where the dope solution is cast (membrane support, as indicated in Figure 5.2) and the transition layer; and Δx_2, which corresponds to the top layer thickness.

The distribution coefficient, $m_{org/aq}$, defines the ratio between the solute concentration in the extraction solvent phase, C_{org}, and the solute concentration in the aqueous phase, C_{aq}, at equilibrium:

$$m_{org/aq} = \frac{C^*_{org}}{C^*_{aq}} \qquad \text{(Eq. 5.1)}$$

The partition coefficient of solute at the interface membrane-aqueous is given by:

$$m_{M/aq} = \frac{C^*_{M}}{C^*_{aq}} \qquad \text{(Eq. 5.2)}$$

Assuming the following:

a) Steady state mass transfer process through interfaces at equilibrium with no immiscible displacement taking place through the membrane;

b) Uniform wetting characteristics throughout the membrane;

d) Negligible influence of pore mouth interface curvature on rate of transfer or distribution coefficient.

e) Unhindered diffusion of solute through organic-solvent-filled porous membrane of thickness ΔL such that the effective diffusivity, $D_{i,eff}$, is given by $(D_{i,o}\varepsilon_M/\tau_M)$, where ε_M is the membrane porosity, τ_M is an estimate of the tortuosity of the pores, and D_i, is the free diffusion coefficient of species i in the organic liquid.

f) Solute transport in the aqueous boundary layer and in the organic boundary layer can be characterised by simple film-type mass transfer coefficients without bulk flow correction.

g) The distribution coefficient in the concentration range of C^B_{aq} to C'_{aq} is constant at the value $m_{org/aq}$.

At steady state, with immobilised interfaces, the transfer rate of solute from the aqueous phase bulk to the organic phase bulk could be described in terms of individual and overall mass transfer coefficients as follows:

$$N = k_{aq}\left(C^B_{aq} - C'_{aq}\right) = k_M\left(C'_{M,org} - C^0{}_{M,org}\right) = k_{org}\left(C^0_{M,org} - C^B_{org}\right) \quad \text{(Eq. 5.3)}$$

$$N = K_{aq}\left(C^B_{aq} - C^*_{aq}\right) \quad \text{(Eq. 5.4)}$$

or

$$N = K_{org}\left(C^*_{org} - C^B_{org}\right) \quad \text{(Eq. 5.5)}$$

Where C^*_{aq} and C^*_{org} are hypothetical aqueous and organic phase concentrations, in equilibrium with the bulk concentrations, C^B_{org} *and* C^B_{aq}, of the solute in the organic and aqueous phases, respectively. k_{aq}, k_M, k_{org} are the individual mass transfer coefficients for the aqueous phase, the membrane and the organic phase, respectively. K_{aq} and K_{org} are, respectively, an aqueous phase based overall mass transfer coefficient, and an organic phase

based overall mass transfer coefficient of solute considered. Using now standard techniques and definitions (Eq. 5.1) and (Eq. 5.2), the following resistances-in-series mass transfer models for the mass transfer of solute from the aqueous phase to the organic through the membrane are obtained:

$$\frac{1}{K_{aq}} = \frac{1}{k_{aq}} + \frac{1}{m_{M/aq}} \frac{1}{k_M} + \frac{1}{m_{org/aq}} \frac{1}{k_{org}} \qquad \text{(Eq. 5.6)}$$

or

$$\frac{1}{K_{org}} = \frac{m_{org/aq}}{k_{aq}} + \frac{1}{k_M} + \frac{1}{k_{org}} \qquad \text{(Eq. 5.7)}$$

It is important to note that although both k_M, and k_{org}, deal with solute diffusion through the organic solvent, it is necessary to separate the membrane diffusional resistance, ($1/k_M$), from the combined organic boundary layer and screen resistance, ($1/k_{org}$,), because of their different nature. ($1/k_{org}$) decreases with increasing Reynolds number of the bulk organic phase, but the intrinsic membrane resistance, ($1/k_M$), is not in general influenced by bulk velocities of either phase.

The membrane resistance to solute diffusion in an asymmetric porous membrane with two distinct layers as illustrated in Figure 5.2 may be simply expressed through the flux expression:

$$N = k_M \left(C'_M - C^0_M \right) = \left(\frac{D_{i,org}}{\Delta x_1} + \frac{D_{i,org} \varepsilon_M}{\tau_M \Delta x_2} \right) \left(C'_M - C^0_M \right) \qquad \text{(Eq. 5.8)}$$

When experimental data is available, it is possible to verify how closely $\left(\frac{D_{i,org}}{\Delta x_1}+\frac{D_{i,org}\varepsilon_M}{\tau_M \Delta x_2}\right)$ describes the observed membrane mass transfer coefficient k_M.

As illustrated in Figure 5.2, the layer comprising the backing material and the transition of the asymmetric membrane (Δx_1) is highly porous (see cross section of Matrimid membrane prepared in Figure 5.12), and the pores completely filled with the organic solvent. Therefore, this was considered as a stagnant phase, with ε and τ equal 1.

Porosity of the top layer, ε_M, of thickness Δx_2, can be estimated based on the experimental rejections and permeation fluxes measured for each membrane, as will be demonstrated later (section 5.5.4).

5.4.2. Calculation of the experimental overall mass transfer coefficient, OMTC – Kaq

In order to evaluate the performance of the four polyimide membranes in the biphasic membrane contactor system for the transport of fatty acids, and since the exact configuration/structure of the membranes is unknown, initially the overall mass transfer coefficient (OMTC), Kaq, is estimated using a solution-diffusion model. In this case, the membrane is considered as an additional distinct phase, comprising both the membrane material and the wetting liquid (organic solvent).

It was then assumed:

a) Steady state mass transfer through interfaces at equilibrium with no immiscible displacement taking place through the membrane;

b) Uniform wetting characteristics through the membrane;

c) Solute transport in the aqueous boundary layer and in the organic boundary layer can be characterised by simple film-type mass transfer coefficients without bulk flow correction;

d) The distribution coefficient in the concentration range of C^{B}_{aq} to C'_{aq} is constant at the value $m_{org/aq}$.

The flux of solute from the aqueous phase to the organic phase through the membrane is then given by:

$$N = \frac{V_{org}}{A}\frac{dC_{org}}{dt} = -\frac{V_{aq}}{A}\frac{dC_{aq}}{dt} \qquad \text{(Eq. 5.9)}$$

And so, overall mass transfer definition in terms of organic phase concentrations is described by Eq. 5.10:

$$N = \frac{V_{org}}{A}\frac{dC_{org}}{dt} = K_{aq}\left(C_{aq} - C^{*}_{aq}\right) \qquad \text{(Eq. 5.10)}$$

Using the definition of solute distribution coefficient in equilibrium (Eq. 5.1), $m_{org/aq}$, the following equation is obtained:

$$N = \frac{V_{org}}{A}\frac{dC_{org}}{dt} = K_{aq}\left(C_{aq} - \frac{C_{org}}{m_{org/aq}}\right) \qquad \text{(Eq. 5.11)}$$

The solute mass balance is expressed as follows:

$$C_{aq,i} = C_{aq,0} - \frac{V_{org}}{V_{aq}} C_{org,i} \qquad \text{(Eq. 5.12)}$$

Rearranging the equation, and integrating results:

$$\frac{1}{\phi + \frac{1}{m_{org/aq}}} \ln\left(\frac{C_{aq,0}}{C_{aq,0} - C_{org}\left(\phi + \frac{1}{m_{org/aq}}\right)} \right) = \left(\frac{K_{aq} A}{V_{org}} \right) t \qquad \text{(Eq. 5.13)}$$

Where ϕ represents V_{org}/V_{aq}. Plotting the left hand side of Eq. 5.13 against time Kaq can be estimated, i. e. the aqueous based OMTC for the different experiments carried out.

5.4.3. Estimation of individual liquid-film mass transfer coefficients – k_{aq} and k_{org}

For estimating the individual liquid-film mass transfer coefficients, k_{aq} and k_{org}, three different correlations can be used: (1) an exact correlation for fully developed flow (Eq. 5.14); (2) Leveque solution for rectangular ducts (Eq. 5.15), and (3) an empirical correlation for rectangular ducts (Eq. 5.15), as previously described by Valadez-Blanco *et al.* [132]:

$$Sh = \mathrm{Re}^{1/3}\, Sc^{1/3} \left(\frac{de}{L} \right)^{0.43} \qquad \text{(Eq. 5.14)}$$

$$Sh = a \left(\frac{\mathrm{Re}\, Sc\, de}{L} \right)^{1/3} \qquad \text{(Eq. 5.15)}$$

Where,

a= 2.33 Empirical correlation

a= 1.85 Leveque correlation

and $Sh=k_{liq}d_e/D_{i,liq}$, $Re=\rho\upsilon d_e/\mu$ and $Sc= \mu/\rho D_{i,liq}$.

The diffusion coefficent, $D_{i,liq}$, for the solute (i) in solvent (liq), are estimated using the Wilke-Chang correlation, as will be described later.

5.5. Results and Discussion

5.5.1. Organic/aqueous partition coefficients – $m_{org/aq}$

In a membrane biphasic system, the mass transfer rates depend on the partitioning of the compounds between phases. When higher partition coefficients are observed, higher mass transfer rates are likely to be achieved. Thus, the partition coefficient, $m_{org/aq}$, needed for calculation of the mass transfer rates of DHA and PLA, was measured in a system containing hexane, ethanol and water (Table 5.2). The organic phase consisted of hexane, and the aqueous phase of water and ethanol (1:1, (v/v)). Ethanol was added to the microbial cell mass suspension, forming the aqueous fatty acid rich phase. The addition of ethanol was crucial for obtaining satisfactory mass transfer rates when enzymatic hydrolysis was used, as will be discussed later.

Table 5.2: Partition coefficients (morg/aq) of docosahexaenoic acid (DHA) and palmitic acid (PLA) between hexane (org) and water:ethanol (aq).

Fatty Acid	Partition Coefficient
DHA – C22:6	729 ± 102
PLA – C16:0	18 383 ± 5772

The solubility of fatty acids in water:ethanol is very low, hence measurements of fatty acid concentrations in the aqueous phase were inaccurate, as the concentrations were close to the detection limit for the analysis. However, differences observed experimentally were not significant for the calculation of the overall mass transfer coefficients. As expected, the partition coefficients varied with the alkyl chain length, being higher for shorter fatty acids.

5.5.2. Membranes flux, rejection and MWCO curves

Experiments for measurement of fluxes and determination of the MWCO curves of the membranes considered in this investigation (as listed in Table 5.1) were conducted under pressure filtration in a dead-end MET Cell. Flux measurements were carried out with toluene and also with a polystyrene solution (PS, 200-1200 Da, 1 g L^{-1}) in toluene. Values determined are presented in Table 5.3.

Solute rejections were calculated according to the following equation:

$$R_i(\%) = \left(1 - \frac{C_{p,i}}{C_{r,i}}\right) \times 100 \qquad \text{(Eq. 5.16)}$$

Where $C_{p,i}$ corresponds to the concentration of the solute i in the permeate phase, and $C_{r,i}$ to the solute concentration in the retentate phase.

Table 5.3: Flux values for the four membranes tested with toluene and polystyrene oligomers (PS, 200-1200 Da, 1 g L^{-1}) solution in toluene.

Membrane	Pressure (bar)	Flux (L m^{-2} h^{-1})	
		Toluene	PS in Toluene
M1	5	870 ± 2	865 ± 5
M2	5	55 ± 5	38 ± 1
M3	5	255 ± 3	255 ± 1
Starmem™ 240	30	97 ± 8	73 ± 5

Membrane Area = 1.3×10^{-3} m^2

MWCO curve obtained for Starmem™ 240 is presented in Figure 5.3, according to measured rejections for the PS solution. It was then concluded that the MWCO of Starmem™ 240 is around 500 Da.

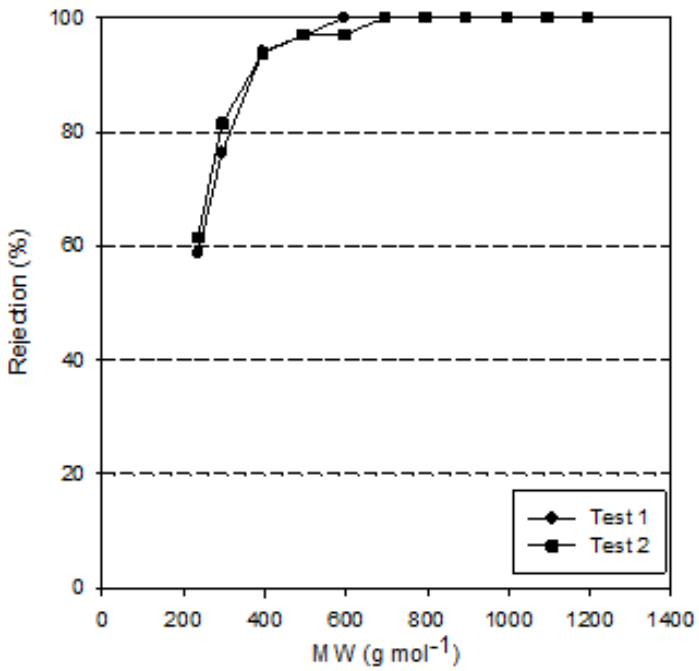


Figure 5.3: Molecular weight cut off curve, MWCO, for Starmem™ 240 membrane (filtration carried out at a constant pressure of 30 bar and with polystyrene oligomers solution (PS, 200-1200 Da, 1 g L^{-1}) in toluene.

However, the rejection values obtained for membranes M1, M2 and M3 were below 10%, which means that those membranes presented no rejection to the PS solution used. Experiments for determination of the MWCO curves of M1, M2 and M3 were then conducted using polyethylene glycol (PEG). Individual PEG solutions (1 g L^{-1}) of 3 kDa, 6 kDa, 10 kDa, 12 kDa, 20 kDa and 35 kDa were prepared in toluene (dissolved after heating up to 50ºC) and tested individually. Figure 5.4 illustrates the MWCO curves obtained for M1, M2 and M3, based on rejections calculated for each PEG solution.

M1 presented very low rejections, therefore it was not possible to obtain a good estimate of the MWCO. Rejection tests showed that molecular weight cut-off of Matrimid membranes M2 and M3 are approximately 5 and 35 kDa, respectively, i.e. in the lower UF range.

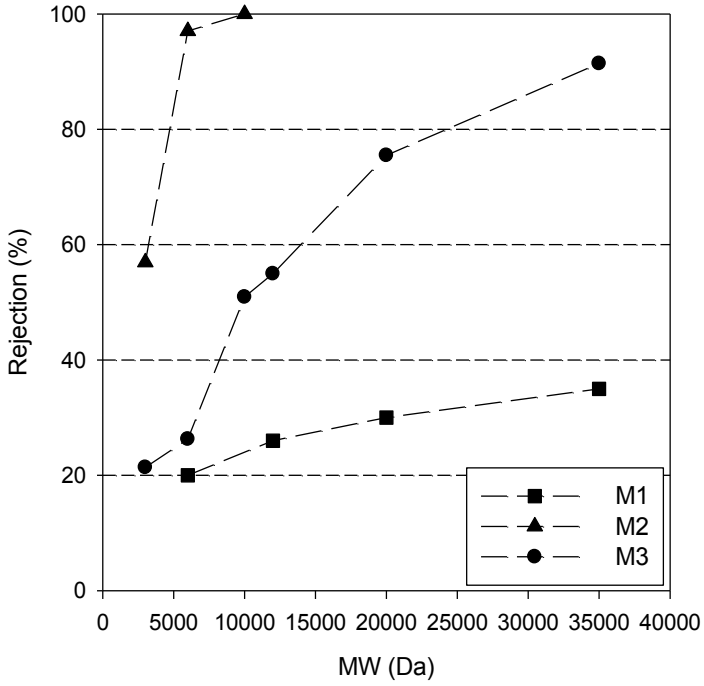


Figure 5.4: Molecular weight cut off curves, MWCO, for M1, M2 and M3 (filtrations carried out at a constant pressure of 5 bar and with individual polyethylene glycol solutions (1 g L^{-1}, of 3 kDa, 6 kDa, 10 kDa, 12 kDa, 20 kDa and 35 kDa PEG) in toluene.

5.5.3. Evaluation of the performance of different polyimide membranes for the separation of fatty acids in the biphasic system

The membrane evaluation was carried out using an aqueous solution rich in fatty acids obtained by chemical hydrolysis of the microbial cell mass lipid content. Polyimide membranes were chosen, since they are highly hydrophobic, which will prevent water breakthrough through the membrane. Nanofiltration membranes prepared from P84 polyimide have been tested previously in a biphasic system, and showed to avoid phase breakthrough [132]. However the mass transfer rates did not overcome what would be achieved in a direct liquid-liquid extraction. Here P84 membranes with higher MWCO were prepared, in order to improve the mass transfer rates. It is expected that by increasing the pore size, the mass transfer would be favoured and consequently better mass transfer rates would be achieved.

A series of experiments were carried out with the three membranes prepared as listed earlier (Table 5.1) and Starmem^{TM} 240, at different operating conditions. The main parameters changed, and the membrane tested in each experiment, are indicated in Table 5.4. For membrane M3, two series of experiments were performed, in which volumes of aqueous and organic solution were changed, in order to evaluate how the phase volume ratios would affect extraction yields and mass transfer rates. Samples were collected periodically from both phases. Collected samples were immediately methylated and analysed by GC for fatty acids quantification.

Initially, two different membranes prepared with each of the two polyimides were tested: M1 prepared from P84 polyimide (Exp. A), and M2 prepared from Matrimid polyimide (Exp. B). In these experiments, the volumes of the aqueous fatty acids rich phase and the organic phase were 550 mL and 100 mL, respectively.

Table 5.4: Membrane, initial concentration of DHA in the aqueous phase ($C_{DHA,i}$), flow rates of aqueous and organic streams, and initial volumes of aqueous ($V_{i,aq}$) and organic ($V_{i,org}$) phases for each of the experiments carried out.

Exp.	Membrane[a]	$C_{DHA,i}$ (g L^{-1})	Flow Rate (L h^{-1})		$V_{i,aq}$ (L)	$V_{i,org}$ (L)
			AQ	ORG		
A	M1	3.7	90	20	0.55	0.10
B	M2	3.7	90	20	0.55	0.10
C	M3	3.8	90	20	0.55	0.20
D	M3	3.8	90	20	0.27	0.20
E	Starmem^{TM} 240	3.8	90	20	0.27	0.20

[a] Description of M1, M2 and M3 in Table 5.1

Composition of DHA and PLA in the aqueous and organic phases were monitored throughout each experiment. After the same running period, DHA and PLA content in the organic phase was about threefold higher in the experiments with membrane M2 (Exp. B) than with membrane M1 (Exp. A), as indicated by the concentration profiles of each solute in the organic phase shown in Figure 5.7. It would be expected that the fatty acids transport would be higher for M1, as the membrane molecular weight cut off is larger (>>35 kDa for M1, and 5 kDa for M2). Surprisingly, this was not observed experimentally. It is thought that the effect of increasing hydrophobicity of the polyimide contributes to the advantageous performance that the Matrimid membrane presented.

The P84 polyimide contains approximately 20% of polyimide of structure A (BTDA, 3,3',4,4'-benzophenone tetracarboxylic acid dianhydride - MDI, 4,4'-methylene-bis(phenylisocyanate)) and 80% of structure B (BTDA-TDI, toluene diisocyanate), as presented in Figure 5.5. Matrimid 5218 polyimide is prepared from a polyimide copolymer based on 3,3',4,4'-benzophenone tetracarboxylic acid dianhydride (BTDA) and diamino-phenylindane (DAPI), as shown in Figure 5.6.

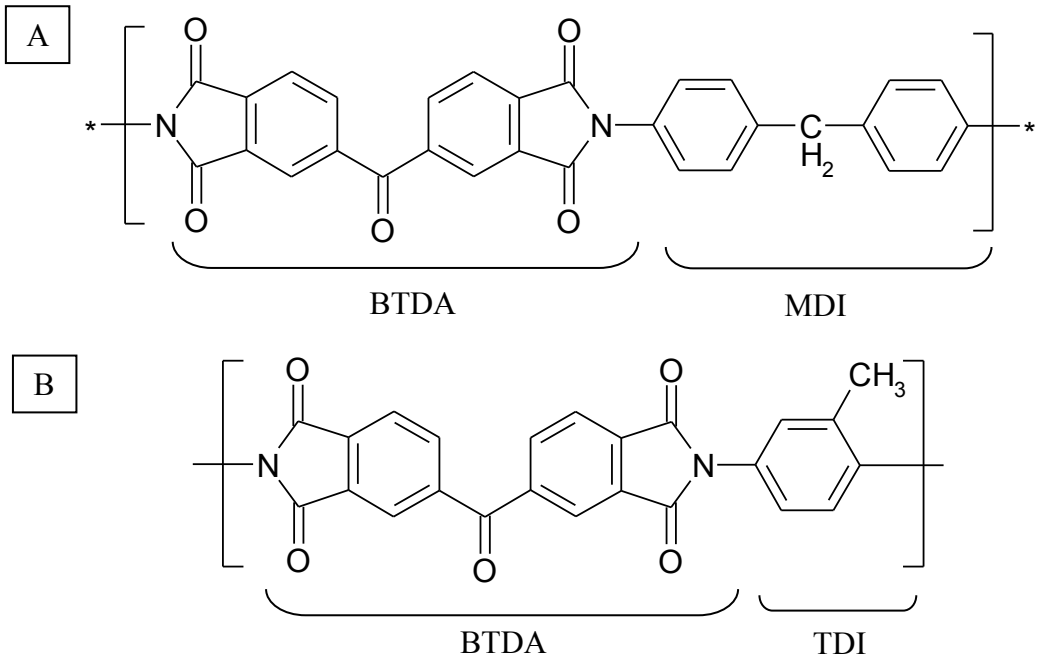


Figure 5.5: Chemical structure of P84 polyimide polymer (BTDA - benzophenone tetracarboxylic acid dianhydride; MDI - 4,4'-methylene-bis(phenylisocyanate); TDI - toluene diisocyanate).

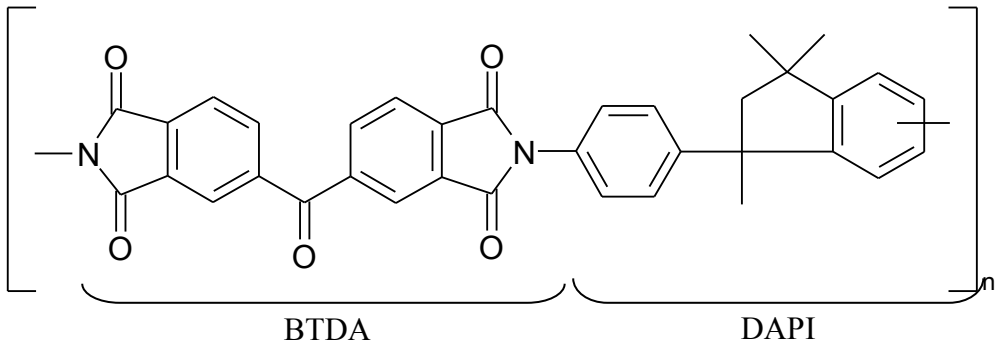


Figure 5.6: Chemical structure of Matrimid 5218 (BTDA - benzophenone tetracarboxylic acid dianhydride; DAPI - 4',6-diamidino-2-phenylindole).

The water contact angle is commonly used for evaluation of hydrophobicity of different polymers. A water contact angle of 83-87° has been reported for non crosslinked flat-sheet Matrimid membranes [165], while the measured water drop contact angle of non crosslinked P84 membranes varies between 62-67° (data not published), which confirms that Matrimid is

more hydrophobic than P84, and this characteristic contributed to the different extraction performance observed.

Matrimid was then selected as the most effective polyimide polymer for manufacturing membranes to be used for this specific separation. A new membrane was prepared from Matrimid using DMF as dope solvent (M3), in order to obtain a higher cut-off. The measured cut-off of M3 was ~35 kDa. In Exp. B., the maximum extraction yield reached after 24 hours was about 35 wt% of the total fatty acids. Extraction yields were compromised by the reduced membrane contact area available (0.004 m^2) for the high fatty acids content of the aqueous phase, or eventually, by the ratio between the volume of aqueous and organic phases. As a membrane contactor with larger contact area was not available, the volume of the organic phase was increased from 100 to 200 mL in further experiments.

However, the mass transfer rates obtained with this membrane in Exp. C were quite similar to what was obtained previously in Exp. B while using M2, despite the six fold larger cut-off of M3. The change of the solvent volume did not seem to have any effect on the mass transfer rates, which indicated that the limitation on the solute transfer rate was not due to saturation of the organic phase.

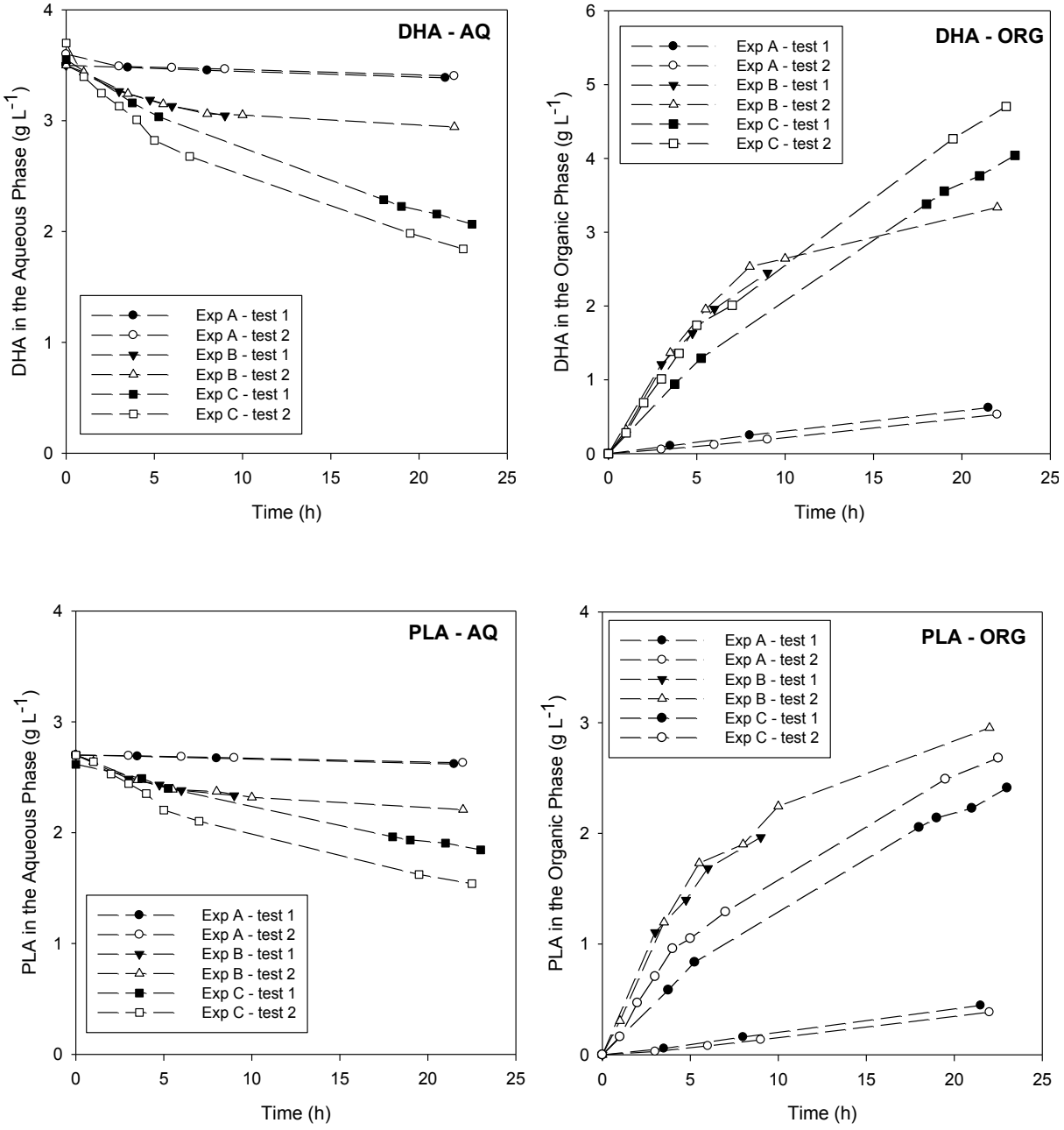


Figure 5.7: Concentration profile of docosahexaenoic acid (DHA) and palmitic acid (PLA) in the aqueous phase (AQ) and organic phase (ORG) (Exp. A: membrane M1, Vaq=550 mL, Vorg=100 mL; Exp. B: membrane M2, Vaq=550 mL, Vorg=100 mL; Exp. C: membrane M3, Vaq=550 mL, Vorg=200 mL).).

For the second series of experiments carried out with membrane M3 (Exp. D), the volume of the aqueous phase was reduced from 550 mL to 275 mL. The extraction rates were considerably enhanced. Yields reached after 28 hours were between 95-98%, i.e. about 95-98% of main fatty acids in the fatty acids rich solution were recovered. By reducing the feed phase volume, there was more membrane area available per solute unit present in the feed, consequently the solute mass transfer was enhanced.

Figure 5.8 presents the DHA and PLA concentration profiles in the aqueous and organic phases obtained throughout the experiment D for each of the trials carried out.

In Exp. E, the commercial nanofiltration membrane Starmem^{TM} 240, with a measured MWCO of 500 Da, was tested. But as expected, the mass transfer rates obtained were lower than that achieved for the loosest membranes tested, as indicated in Table 5.5.

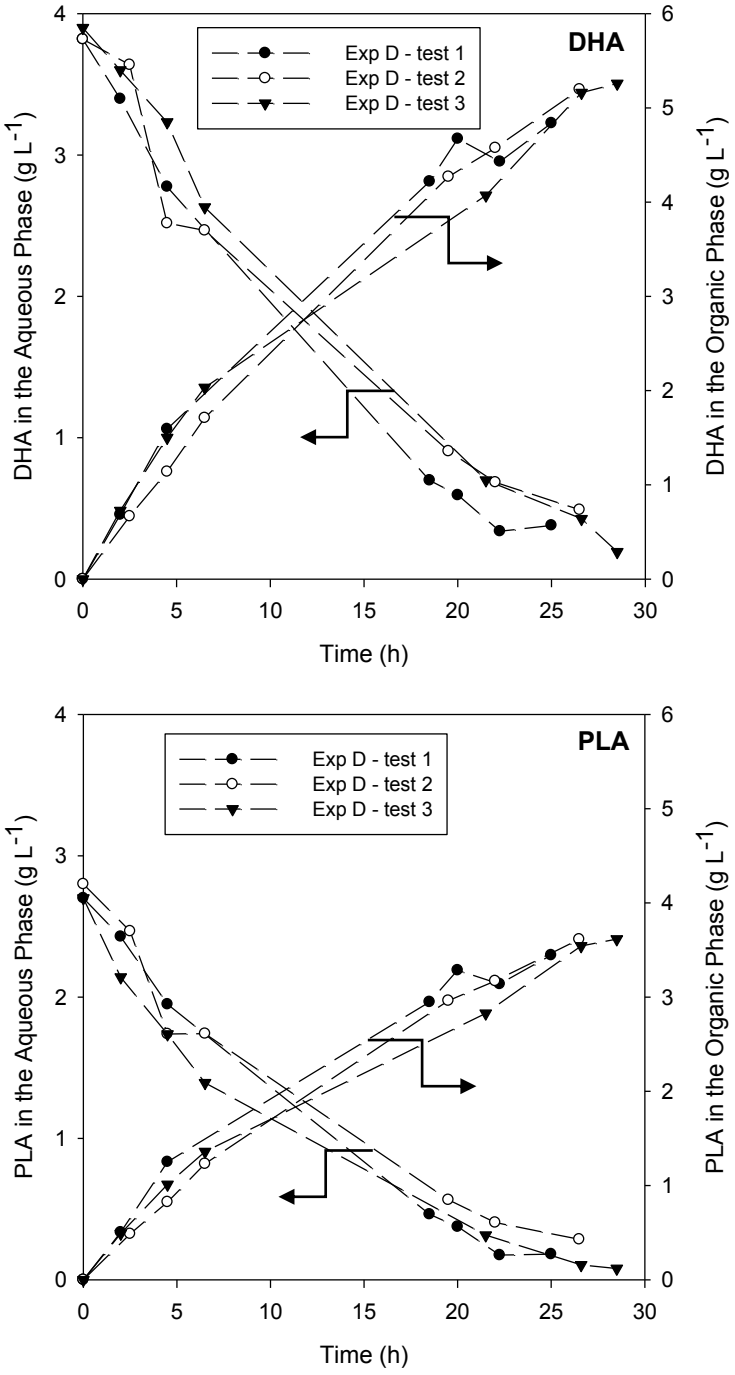


Figure 5.8: Concentration profile of docosahexaenoic acid (DHA) and palmitic acid (PLA) in the aqueous and organic phases (Exp. D: membrane M3, Vaq=275 mL, Vorg=200 mL).

Overall mass transfer coefficients – OMTC, K_{aq}

Overall mass transfer coefficients calculated based on the experimental organic concentrations for DHA and PLA transferred from the chemical hydrolysed marine cell mass (fatty acids rich solution) to the organic solvent through the different polyimide membranes in the membrane contactor system are presented in Table 5.5. These values are estimated by plotting the right hand side of Eq. 5.13 against time. This plot yields a linear curve with the slope $K_{aq}A/V_{org}$ from which K_{aq} is estimated. An example based on the experimental data obtained in Exp. C is shown in Figure 5.9. The linear cumulative mass transfer over time (R^2=0.98) suggests that membrane fouling did not compromise the mass transfer rates in this specific case, as would be expected due to the solid content of the aqueous phase (cell debris, ~2% w/v).

Table 5.5: Overall mass transfer coefficients - OMTC, Kaq, of docosahexaenoic acid (DHA) and palmitic acid (PLA) from the aqueous fatty acids rich phase (water:ethanol) to the organic phase (hexane) for the four asymmetric polyimide membranes tested in the membrane contactor system.

Exp.	Membrane	OMTC, Kaq $\times 10^7$ (m s^{-1})	
		DHA	PLA
A	M1	0.54 ; 0.42	0.52 ; 0.42
B	M2	6.46 ; 6.48	7.98 ; 8.64
C	M3	7.22 ; 8.30	6.09 ; 7.56
D	M3	16.85 ; 17.54	17.44 ; 16.06
E	Starmem^{TM} 240	3.57 ; 2.99	3.67 ; 3.26

Membrane Area = 0.004 m^2

In all cases, the overall mass transfer coefficients, K_{aq}, obtained were considerably higher when compared with other published works which report values that are one tenth of those

shown here. In 1992, Keurentjes *et al.* tested a membrane based liquid-liquid extraction for removal of fatty acids from oil employing cellulose based ultrafiltration membranes [21]. Erucic acid (C22:1) was the longest fatty acid included in their study and the OMTC observed was below 0.07×10^{-7} m s^{-1}. The shortest fatty acid studied was caproic acid (C6:0), which gave an OMTC of 5.0×10^{-7} m s^{-1}. In their case it was evident that the OMTC was dependent on the fatty acid chain length, being better for short chain fatty acids. However, this difference seems not to be so obvious when the discrepancy between fatty acids molecular weight is not considerable, which is the case of PLA (C16:0) and DHA (C22:6), despite the significantly different partition coefficients measured. It can then be concluded that the developed polyimide asymmetric membranes performed much better than the cellulose based membranes tested by Keurentjes *et al.* [21].

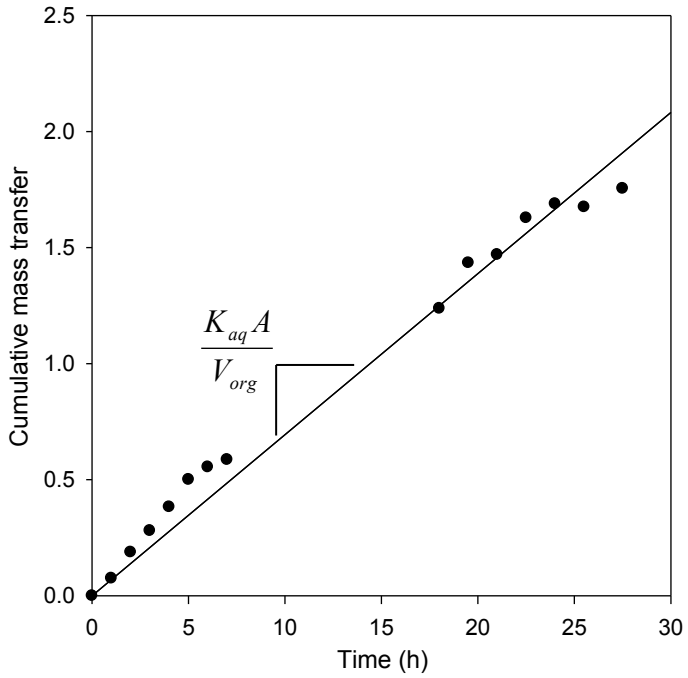


Figure 5.9: Cumulative mass transfer (right hand side of Eq. 5.13) against time for the calculation of the overall mass transfer coefficient (OMTC, K_{aq}) of DHA from the fatty acids rich solution (aqueous phase) to hexane (organic phase) (Exp. C: membrane M3).

Influence of volume ratio and membrane cut-off in the OMTC, volumetric productivity and final yields

In the following, the performance of the three Matrimid membranes tested in terms of mass transfer coefficients (Kaq), volumetric productivity and final recovery of DHA in the organic phase is compared. Based on the mass transfer coefficients obtained for the Matrimid membranes, it can be said that the best performance was achieved with the loosest membrane (M3), suggesting that, as could be antecipated, tighter membranes gave lower mass transfer rates (Figure 5.10).

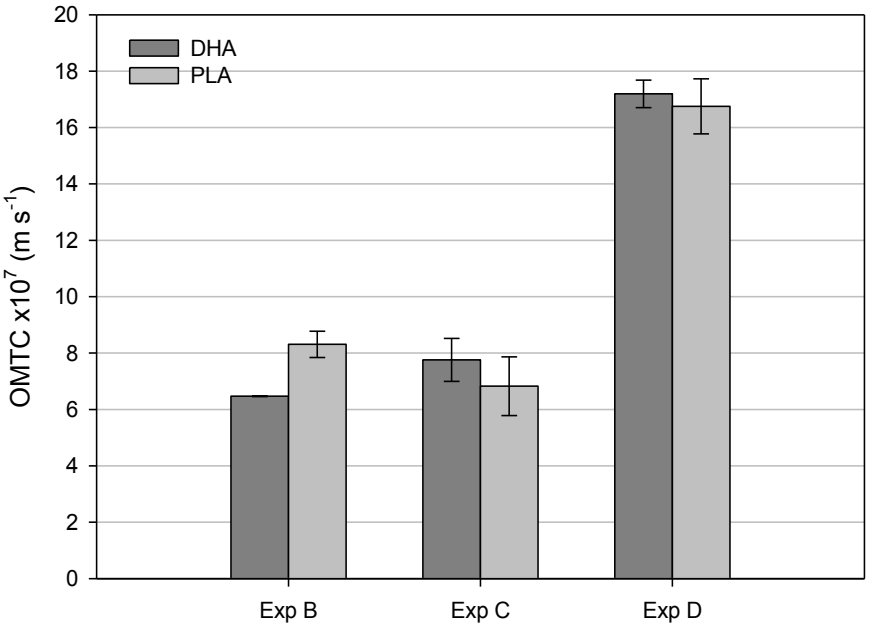


Figure 5.10: Overall mass transfer coefficients (OMTC) obtained for DHA and PLA at different aqueous/organic volume ratios. (Exp B: M2, Vaq/Vorg= 5.5; Exp C: M3, Vaq/Vorg= 2.75; Exp D: M3, Vaq/Vorg= 1.325).

However, in terms of volumetric productivities, differences observed in Exp. B, C and D were not very significant, despite the different membrane cut-off and aqueous/organic phase ratios (Figure 5.11). These results suggest that the higher OMTC observed in Exp. D was due to the lower ratio, Vaq/Vorg, and Vaq/A, and consequently lower solute (DHA and PLA) per unit

area, and not to the higher cut-off, which also contributed to the higher yields. However, in Exp. E the volumetric productivity observed was much lower, as well as the recovery, and this was determined by the nanoscale cut-off of the membrane. Nominal cut-off of Starmem^{TM} 240 is around 500 Da, which is just above the molecular size of DHA (328 g mol^{-1}).

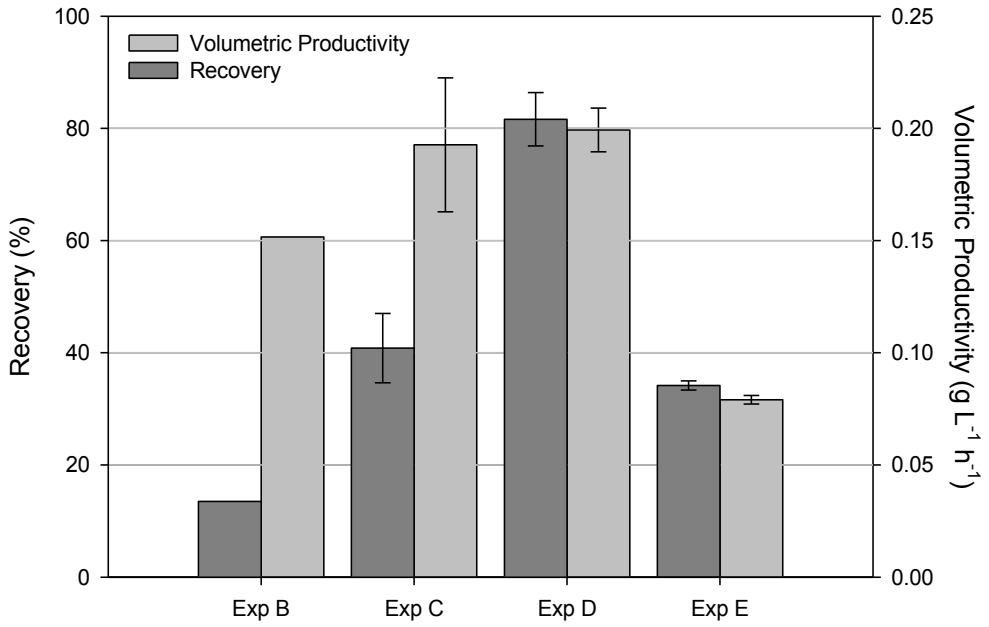


Figure 5.11: Volumetric productivities and yields of DHA obtained after 22 hours in experiments with Matrimid based membranes. (Exp B: M2, Vaq/Vorg= 5.5; Exp C: M3, Vaq/Vorg= 2.75; Exp D: M3, Vaq/Vorg= 1.325; Exp E: Starmem^{TM} 240, Vaq/Vorg=1.325).

Overall, it was expected that tighter membranes would give lower mass transfer rates, and it was true whilst comparing the case of M3 and Starmem^{TM} 240, but surprisingly, the loosest membrane (M1 prepared from P84 polyimide) presented the worst performance with a Kaq of 0.05×10^{-6} m s^{-1}. It was then concluded that not only the membrane cut-off, but also the polyimide used affects the mass transfer rates. It was also demonstrated that aqueous/organic volume ratios and solute/membrane area play an important role in the mass transfer rates.

5.5.4. Characterisation of solute transport through porous membranes in the biphasic system

Previously, whilst evaluating the performance of the different membranes for the extraction of a given solute from the aqueous phase to the organic phase through the membrane, the resistance created by the membrane to the mass transfer was not taken into account, since the membrane porosity is unknown. It is general knowledge that the mass transfer behaviour is mainly determined by the membrane characteristics, such as porosity, tortuosity and thickness, thus they need to be determined to estimate the solute transport rates through the membrane.

See-Toh *et al.* [144] used two models for the interpretation of the experimental data in order to determine the pore size distribution in asymmetric polyimide membranes. The first was based on empirical fitting of experimental rejection data to a log-normal distribution to obtain estimates of $\overline{d}_p$ (average pore diameter) and σ_p (standard deviation). The second method utilises a hydrodynamic model of hindered solute transport in pores, as described by Bowen and Welfoot [124], for the estimation of the same parameters, and so has a physical basis, and is the one chosen for the present study.

Resistances to the mass transfer in the aqueous and organic phases, 1/*kaq* and 1/*korg*, depend only on the flow characteristics, and the individual liquid-film mass transfer coefficients can be easily estimated (see section 5.4.3). k_M experimental can then be calculated using the overall resistance to mass transfer definitions (Eq. 5.6 and 5.7) and experimental values of K_{aq} and K_{org}. For calculating the theoretical membrane mass transfer coefficient, k_M, according to Eq. 5.8, the membrane porosity ε_M, tortuosity τ_M, and thickness of the different layers of the asymmetric membrane (as illustrated in Figure 5.2), need to be estimated.

5.5.4.1. Estimation of membrane porosity based on solute rejection using the Bowen and Welfoot model

In the present investigation the hydrodynamic model of hindered solute transport in pores, as described by Bowen and Welfoot [124], was considered for the estimation of the pore radius, r_p.

The starting point for this model is the Nernst Planck equation for the transport of charged solutes, which is simplified to the following equation after elimination of the terms related to the electric field gradient, the activity gradient in the pore, and the effect of pressure on chemical potential within the pore.

$$j_i = -K_{i,d} D_{i,\infty} \frac{dc_i}{dx} + K_{i,c} c_i V \qquad \text{(Eq. 5.17)}$$

Neglecting the effects of concentration polarisation ($c_{i,m}=c_{i,f}$) and integrating the previous equation across the thickness of the membrane ($0 < x < \Delta x$) with the boundary conditions where $c_{i,x=0}=\phi_i C_{i,f}$ and $c_{i,x=\Delta x}=\phi_i C_{i,p}$ allows the derivation of an explicit expression for rejection as a function of the pore size:

$$R_i = 1 - \frac{\phi_i K_{i,c}}{1 - \left[1 - \phi_i K_{i,c}\right] \exp\left(-P_{i,e}\right)} = 1 - \frac{C_{i,p}}{C_{i,f}} \qquad \text{(Eq. 5.18)}$$

Where

$$P_{i,e} = \frac{K_{i,c} V \Delta x}{D_{i,p}} = \frac{K_{i,c}}{K_{i,d} D_{i,\infty}} \left(\frac{r_p^2 \Delta P}{8\mu} \right) \qquad \text{(Eq. 5.19)}$$

$$\phi_i = (1-\lambda_i)^2 \quad \text{(Eq. 5.20)}$$

$$K_{i,d} = 1.0 - 2.30\lambda_i + 1.154\lambda_i^2 + 0.224\lambda_i^3 \quad \text{(Eq. 5.21)}$$

$$K_{i,c} = (2-\phi_i)(1.0 + 0.054\lambda_i - 0.988\lambda_i^2 + 0.441\lambda_i^3) \quad \text{(Eq. 5.22)}$$

When the pore radius are significantly small ($r_p \sim r_{solv}$), pore viscosities need to be calculated, they might be significantly higher than the bulk values, therefore it requires a correction factor, which is given by the following equation:

$$\frac{\mu}{\mu_0} = 1 + 18\left(\frac{r_{solv}}{r_p}\right) - 9\left(\frac{r_{solv}}{r_p}\right)^2 \quad \text{(Eq. 5.23)}$$

In this single parameter model, the solute rejection is only dependent on r_p. Solving the equation for rejection (Eq. 5.18) in order to get a function such that $R(r_p)=0$, using the experimental rejections corresponding to each solute and giving values to r_p, this multiple equation system can be solved and a value for r_p estimated.

Radius of different solutes used in the rejection tests were determined using the Stokes Einstein equation:

$$r_{i,s} = \frac{k.T}{6.\pi.\mu_o.D_{i,\infty}} \quad \text{(Eq. 5.24)}$$

For the polystyrene oligomers, the diffusion coefficient of the solute in the bulk solvent ($D_{i,\infty}$) was determined by the Wilke-Chang method [145], where the solute molar volume (V_{Sol}) at the boiling point is obtained using a group contribution method as presented by Geankoplis [146].

$$D_{i,\infty} = 7.4\times10^{-8}\left(\varphi.M_{Solv}\right)^{0.5}\frac{T}{\mu.V_{Sol}^{0.6}} \qquad \text{(Eq. 5.25)}$$

Values obtained for the different polystyrene oligomers in solution are presented in Table 5.6.

Table 5.6: Calculated solute radius used determining the MWCO of Starmem™ 240.

Polystyrene Oligomers MW (g mol^{-1})	Solute radius (nm)
236	0.34
295	0.39
395	0.46
495	0.53
595	0.59
695	0.65
795	0.70
895	0.75
995	0.80
1095	0.85
1195	0.89

However, according to literature [146], the previous equation cannot be applied to solutes with a molecular weight much larger than 1000 Da or when V_{Sol} is above 0.500 m^3 kg^{-1} mol^{-1}.

Therefore for the different polyethylene glycol (PEG) solutes used in the rejection tests the following equation was applied:

$$D_{i,\infty} = 9.96 \times 10^{-16} \frac{T}{\mu . V_{Sol}^{1/3}} \qquad \text{(Eq. 5.26)}$$

Values obtained for the PEGs radius are presented in Table 5.7.

Table 5.7: Calculated solute radius determining MWCO of M1 and M3.

Polyethylene Glycol MW (kDa)	Solute Radius (nm)
3	1.12
6	1.41
10	1.67
12	1.78
20	2.11
35	2.54

Knowing the experimental rejections and the solute radius, the membrane pore size was estimated using the hydrodynamic model proposed by Bowen and Welfoot. Tables 5.8 and 5.9 present the values of r_p estimated for each membrane, based on the experimental rejection data obtained and the solute radius calculated. Only the solutes that presented a rejection greater than 60% were considered (not the case of M1).

Table 5.8: Estimated pore radius of Starmem™ 240 membrane based on the rejection and solute radius of polystyrene oligomers which presented rejections above 60%.

MW (g mol^{-1})	Pore radius (nm)
395	0.63
495	0.59
595	0.66

Table 5.9: Estimated pore radius of M1 and M3 membranes based on the rejection and solute radius of polyethylene glycol solutions which presented rejections above 60%.

Polyethylene Glycol MW (kDa)	Pore Radius (nm)	
	M1	M3
20	7.09	3.41
35	7.76	3.62

Assuming a value for the pores length (top layer thickness, Δx_2) and the pore as being a cylinder (radius equal to the pore radius and length equal to the pores length), the flux per pore, *J*, is calculated using the Hagen Poiseuille equation,

$$J = \frac{r_p^2 . \Delta P . A_k}{8 \mu . \Delta x_2} \qquad \text{(Eq. 5.27)}$$

Number of pores was determined dividing the total flux (measured experimentally, see Table 5.3) by the flux per pore, *J*. The surface area occupied by pores corresponds to the area of the pores mouth multiplied by the number of pores. Membrane porosity, ε_M, is calculated dividing the total area corresponding to the pores mouth by the total membrane surface area.

Values obtained for each of the membranes in casu are presented in Tables 5.10, 5.11 and 5.12.

Table 5.10: Calculated membrane porosities, ε, for Starmem™ 240 membrane as a function of membrane thickness, flux per pore, number of pores and surface area occupied by pores.

Δx_2 (μm)	*J*, flux per pore ($m^3\ h^{-1}$)	No. pores	Surface area occupied by pores (m^2)	Membrane porosity ε (%)
0.10	3.028×10^{-18}	3.052×10^{13}	6.052×10^{-5}	4.6
0.15	2.018×10^{-18}	4.578×10^{13}	9.078×10^{-5}	6.9
0.20	1.514×10^{-18}	6.104×10^{13}	1.210×10^{-4}	9.2
0.50	6.055×10^{-19}	1.526×10^{14}	3.026×10^{-4}	22.9
1.00	3.03×10^{-19}	3.05×10^{14}	6.05×10^{-4}	45.9

Table 5.11: Calculated membrane porosities, ε, for M1 membrane as a function of membrane thickness, flux per pore, number of pores and surface area occupied by pores.

Δx_2 (μm)	*J*, flux per Pore ($m^3\ h^{-1}$)	No. pores	Surface area occupied by pores (m^2)	Membrane porosity ε (%)
0.1	9.340×10^{-15}	7.066×10^{10}	1.340×10^{-5}	1.0
1.0	1.87×10^{-15}	3.53×10^{11}	6.70×10^{-5}	5.1
2.0	9.34×10^{-16}	7.07×10^{11}	1.34×10^{-4}	10.2
5.0	3.74×10^{-16}	1.77×10^{12}	3.35×10^{-4}	25.4
10	1.87×10^{-16}	3.53×10^{12}	6.70×10^{-4}	50.8

Table 5.12: Calculated membrane porosities, ε, for M3 membrane as a function of membrane thickness, flux per pore, number of pores and surface area occupied by pores.

Δx_2 (μm)	*J*, flux per Pore ($m^3\ h^{-1}$)	No. pores	Surface area occupied by pores (m^2)	Membrane porosity ε (%)
1	4.20×10^{-17}	3.14×10^{11}	1.15×10^{-5}	0.9
2	2.10×10^{-17}	6.25×10^{11}	2.30×10^{-5}	1.7
10	4.20×10^{-18}	3.14×10^{12}	1.15×10^{-4}	8.7
15	2.80×10^{-18}	4.71×10^{12}	1.73×10^{-4}	13.1
20	2.10×10^{-18}	6.28×10^{12}	2.30×10^{-4}	17.5
25	1.68×10^{-18}	7.85×10^{12}	2.88×10^{-4}	21.8
50	8.40×10^{-19}	1.57×10^{13}	5.76×10^{-4}	43.6

Curiously, for the same porosity value (~40%), the pore length of Starmem™ 240 membrane is much shorter (1 μm) than the estimated pore length for the Matrimid membrane M3 (50 μm), which confirms the expected distinct morphology of these membranes. SEM pictures of cross sections of each membrane depict the differences between the membrane layer structure for each of these two membranes – see Figures 5.11 and 5.12.

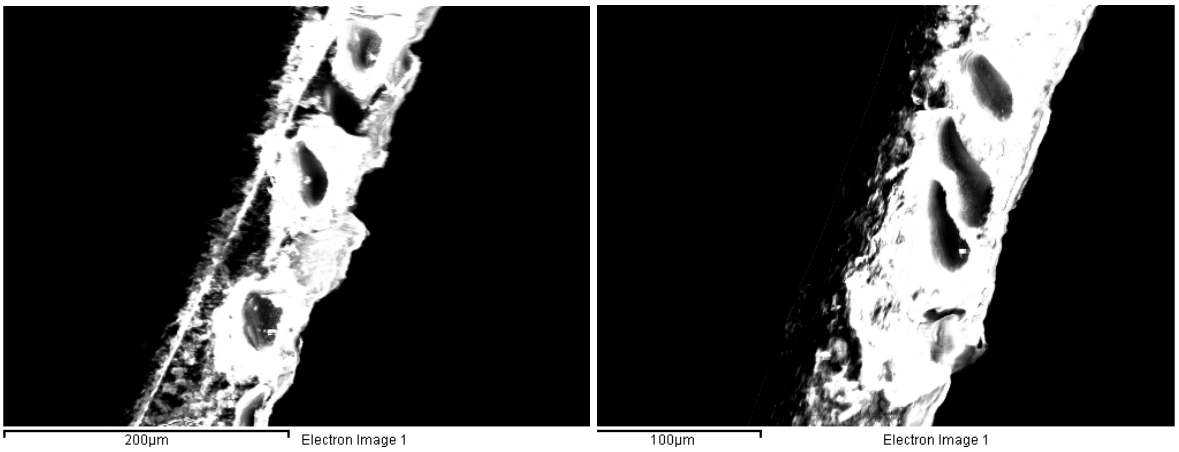


Figure 5.11: Starmem™ 240.

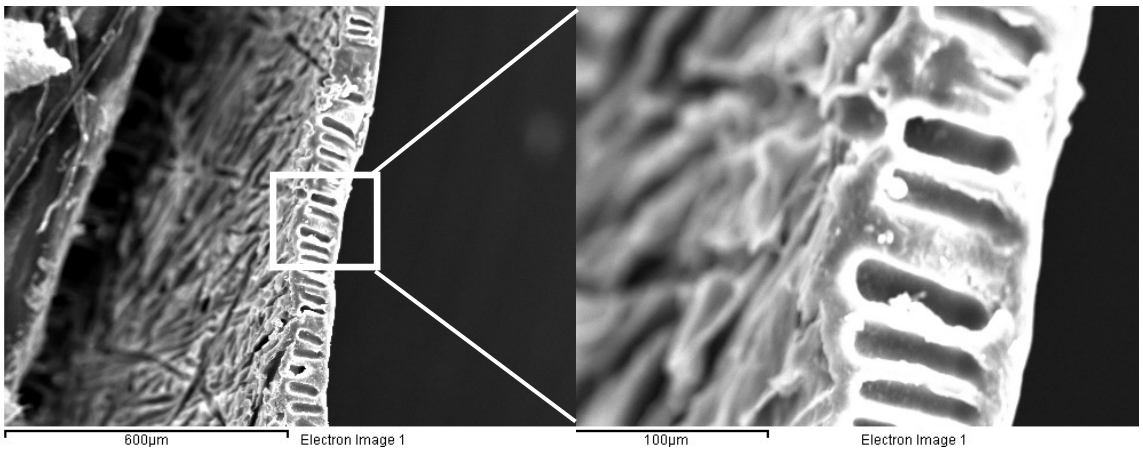


Figure 5.12: Membrane M3 – Matrimid in DMF.

5.5.4.2. Estimation of individual mass transfer coefficients

Individual liquid-film mass transfer coefficients, k_{aq} and k_{org}, were estimated using the three correlations as mentioned previously (section 5.4.3). Using the experimental overall mass transfer coefficients, K_{aq} and K_{org}, and definitions of the resistances in series model (Eqs. 5.6 and 5.7), the experimental membrane mass transfer coefficient, $k_{M,exp}$, could then be determined.

Given the diffusivity coefficient as defined in Eq. 5.28, the theoretical mass transfer coefficient $k_{M,}$ for the specific solute, can now be calculated using the estimated membrane porosity, tortuosity and thickness for each layer considered, in order to verify how closely it describes the observed membrane mass transfer coefficient $k_{M,exp}$.

$$k_M = \left(\frac{D_{i,org}}{\Delta x_1} + \frac{D_{i,org}\varepsilon_M}{\tau_M \Delta x_2} \right) \qquad \text{(Eq. 5.28)}$$

The diffusion coefficient of chosen solute DHA in hexane ($D_{i,org}$) at 20ºC was determined by the Wilke-Chang method as previously. τ_M was estimated using the definition τ=1-ln(ε)

[147]. Values estimated for the liquid-film mass transfer coefficients, k_{aq} and k_{org}, experimental and theoretical membrane mass transfer coefficients, $k_{M,exp}$ and k_M, are shown in Table 5.13. The theoretical membrane mass transfer coefficients k_M, calculated based on the solute transport model proposed, did not translate what was observed experimentally.

Table 5.13: Estimated individual mass transfer coefficients.

Membrane	k_{org} (m s^{-1})	k_{aq} (m s^{-1})	$k_{M\ exp}$ (m s^{-1})	k_M (m s^{-1})
				$\Delta x_1 + \Delta x_2$
M1			8.1×10^{-11}	7.3×10^{-6}
M3	6.2×10^{-6}	2.8×10^{-6}	6.1×10^{-9}	8.8×10^{-6}
Starmem^{TM} 240			6.4×10^{-10}	7.0×10^{-6}

Δx_1 - transition + backing material
Δx_2 - top layer
Re_{aq}= 556.2
Re_{org}= 30.9

The experimental values determined for the membrane mass transfer coefficient indicated that the membrane offers the greater resistance to the mass transfer in the biphasic membrane contactor system. As mentioned previously (section 5.5.3), membrane fouling does not seem to affect the mass transfer through the membrane, hence the resistance to mass transfer is due to the membrane itself, suggesting that it may not be the most appropriate for this particular application.

5.6. Conclusions

The asymmetric polyimide porous membranes tested proved to be suitable for separation of fatty acids from the fatty acids rich solution to the organic solvent in the biphasic membrane contactor system. Phase breakthrough was not observed in any case. However, as expected,

different mass transfer performances were observed for each membrane. It was found that, more than the cut-off, the hydrophobicity of the polyimide used in the preparation of the membranes had a great influence on the mass transfer rates. The overall mass transfer data indicates that when used as a phase contacting membrane, the Matrimid polyimide membranes have an overall mass transfer coefficient ten times higher than the P84 membrane tested. This was an unexpected result, as the P84 membrane presented a much higher flux and MWCO than the Matrimid membranes when tested in a conventional pressure driven filtration system. Aqueous/organic volume ratios, and solute concentration per unit membrane area available were also found to play an important role in the mass transfer performance.

These results demonstrated that, from the membranes tested, Matrimid membranes offer significantly superior and enhanced performance for the application desired. A suitable membrane was identified and overall mass transfer coefficients obtained were tenfold greater than in other published works [21]. A recovery of 95 wt% of DHA of the initial aqueous phase composition was achieved.

The solute transport mechanism through asymmetric polyimide porous membranes in the biphasic membrane contactor system was explored. The experimental membrane mass transfer coefficients estimated ($k_{M,exp}$) confirmed that the membrane offers the higher resistance to the mass transfer in the biphasic membrane contactor system. Membrane fouling did not seem to be an issue in this particular case, as the linear cumulative mass transfer over time demonstrated. Thus, in order to improve the mass transfer performance, other hydrophobic membranes fabricated from different polymers (e.g. polyfluorene based membranes) should be considered.

The theoretical membrane mass transfer coefficients calculated (k_M) based on the solute transport model proposed, did not translate what was observed experimentally. For the calculation of the theoretical k_M, membrane characteristics were estimated based on the measured membrane flux and molecular weight cut-off curve (MWCO). The asymmetric membrane was divided in two main layers, and only the top layer considered as causing resistance to the mass transfer. Obviously, this approach did not seem to be correct, suggesting that the mass transfer resistance is applied throughout the whole membrane thickness, and not only the top-layer thickness.

Chapter 6

Fractionation of Fatty Acids in a Biphasic Membrane Contactor System using Asymmetric Polyimide Membranes

6.1. Summary

In this chapter, a new approach for the fractionation of polyenoic medium and long chain fatty acids, from high-density microbial cultures, in a biphasic membrane contactor system, utilising an asymmetric polyimide porous membrane is presented. The process, as described in section 1.3, combines: (i) selective enzymatic hydrolysis of the cell mass lipid content, and (ii) simultaneous extraction of the released fatty acids from the reaction mixture to the organic solvent through the membrane in the biphasic system. Previously in Chapter 3, suitable lipases for the stepwise enzymatic hydrolysis of the lipid fraction of the aqueous biomass were selected. In Chapter 5, several membranes were evaluated in terms of mass transfer performance using an aqueous fatty acids rich solution obtained by chemical hydrolysis of the lipid content of microbial cell mass. The Matrimid polyimide membrane with a molecular weight cut-off of ~35 kDa provided the best mass transfer rates for the targeted fatty acids, and is used in the experiments described in the present chapter.

The strong emulsion formed in the aqueous phase when using the whole cell mass suspension and enzymatic hydrolysis, seriously compromised the performance of the biphasic system for the fractionation of fatty acids, and initially, mass transfer was non-existent. This initial problem was overcome by adding ethanol to the cell mass suspension and conducting a partial hydrolysis of the cell mass phospholipid fraction. Despite the low mass transfer rates observed, it was possible to observe the desired selective separation between PLA and DHA. 61 wt% of total PLA was removed from the aqueous to the organic phase against 24 wt% of total DHA, which resulted in an increase of the DHA fraction in the fatty acids rich phase from 42 to 60 wt% of the total fatty acids. This novel process may be an alternative to conventional fractionation techniques currently applied at industrial scale, or used in complementary way to simplify further purification.

6.2. Background and Literature Review

6.2.1. Membrane bioreactors for simultaneous production and separation of a desired product

Methods conventionally used for fractionation and purification of fatty acids or fatty acid derived esters are chromatography [40, 41, 148], molecular distillation [149-151], urea complexation [16], and supercritical extraction [47, 152]. However, the fatty acids are subjected to extensive processing, and elevated temperatures throughout these processes. This can be detrimental to the fatty acid quality, particularly the unstable polyunsaturated fatty acids. Furthermore, as discussed previously, a single method may not be enough to achieve high degrees of purity in most of the cases. Depending on the complexity of the raw material and the desired purity of the final product, more than one fractionation technique, or even the combination of reaction and separation methods may be required.

There is an increasing interest in using membranes for constructing combined reaction and separation systems. Paiva and co-workers have reviewed how integration of sequential reaction and separation units influences the recovery of a desired product [153-156]. In general, the continuous removal of products enhances the reaction rates. When enzymes are involved, product inhibition effects are also reduced, and the enzyme activity is preserved. Therefore, the combination of membrane processes with enzymatic reactions has received much attention.

Several authors have studied different configurations of membrane processes, combining simultaneous enzymatic reaction and separation [28, 29, 31, 58, 59]. Giorno *et al.* has presented an approach to improve the performance of a two-phase enzyme membrane reactor by immobilising lipase in presence of emulsion [58]. Molinari *et al.* presented one of the first membrane reactors for fatty acid production [29]. In their work an UF membrane reactor was used, the enzyme was partly immobilised on the pressurised side of the UF membrane and in solution. However, the enzyme tends to accumulate on the pressurised surface as a result of concentration polarisation, consequently the ultrafiltration flux decreased by 90% in the first 2 hours. Simultaneous reaction and separation in enzymatic hydrolysis of high oleate sunflower oil using membrane filtration technology was also explored by Gan *et al.* [28, 31]. An ultrafiltration membrane was applied in their case as well, and a de-emulsifier unit was required in order to enhance the removal of glycerol released. The lower fluxes and recoveries obtained were the main limitations of such systems.

As discussed earlier, emulsions may be advantageous in extraction processes, since the contact between the aqueous phase containing the solute and water immiscible extraction solvent is promoted [58, 60, 157]. In an emulsion, the superficial contact area is larger, which

may allow an increment of extraction yields. A large contact surface between water and oil phases is also desired for enzymatic reactions on oil-soluble substrates, since the enzymes are normally water soluble.

However, when the solute is already dissolved in the extractant, the emulsion has to be destabilised to separate the aqueous and solvent phases. The standard method for the treatment of emulsions is chemical demulsification followed by gravity settling [158], but it often makes the further purification even more demanding.

Other methods have been published presenting distinct solutions to destabilise emulsions in these cases. Martek has patented in 2000 (Hoeksema, US Patent No. 6166231) a process for two phase extraction of edible oil from aqueous biomass using a packed column, operating in counter current [22]. In their work, for an efficient result either multiple columns were needed, or the solvent and slurry must be recycled through the same column several times. Another process for extraction of triacylglycerols from wet biomass of oil producer microorganisms, namely of thraustochytrids, was patented in 2001 by John M. Liddell (US Patent No. 6180376 B1). They have experienced that, while increasing the solvent ratio in order to form a water-in-solvent dispersion (e.g. 1:3), the emulsion was easily destabilised in the absence of a demulsifier using gravity settling or centrifugation. However, these methods may involve large volumes of solvents and large equipment, increasing considerably the costs of extraction.

Several studies have reported that cross-flow micro and ultrafiltration are effective processes in breaking oil-in-water emulsions [60, 159, 160], as well as water-in-oil emulsions [158, 161-163]. Hydrophobic membranes have been considered to function as a coalescer [164],

increasing the size of oil droplets in the permeate. Nevertheless, the application of hydrophobic membranes in cross flow micro/ultrafiltration for demulsification of aqueous-solvent emulsions containing oil from microbial biomass has not been reported.

6.2.2. Biphasic membrane contactor systems for fractionation of fatty acids

Membrane contactors have been reported as efficient systems for in situ separation of chemical and biochemical reaction products from a feed solution to an extraction phase, separated by a membrane, overcoming emulsion problems [21, 123, 132]. Porous membrane modules have been effectively used in such biphasic bioreactors as an alternative to direct two-liquid contact systems, as long as phase breakthrough was avoided. The use of ultrafiltration membranes is advised, as compared to microfiltration membranes, since the smaller pores of UF membranes led to higher breakthrough pressures. Work involving a membrane contactor for removal of free fatty acids from an edible oil was presented by Keurentjes *et al.* [21]. Cellulose hollow fibre ultrafiltration membranes were considered in their study for the separation of erucic acid (C22:1) from an edible oil in a membrane contactor, which gave an overall mass transfer coefficient of 7×10^{-9} m s^{-1}. The fact that the mass transfer coefficients vary with the fatty acid chain length was used in this case for fractionation of the fatty acid mixture [21]. However, the process productivities were not sufficient for industrial application. Mass transfer rates are often the overall rate-limiting step. More research is needed in order to overcome such limitations, developing new process configurations and membranes.

Reference to the combination of selective enzymatic hydrolysis of microbial cell mass lipid content, and simultaneous separation of the released fatty acids in a biphasic membrane contactor system has not been found in literature.

6.2.3. Objectives and process hypotheses

The main goal of the present investigation was to develop an innovative process for fractionation of fatty acids as part of a microbial cell mass suspension, by combining stepwise enzymatic hydrolysis of triacylglycerols, and simultaneous separation of the released fatty acids in a biphasic membrane contactor system, as illustrated in Figure 6.1.

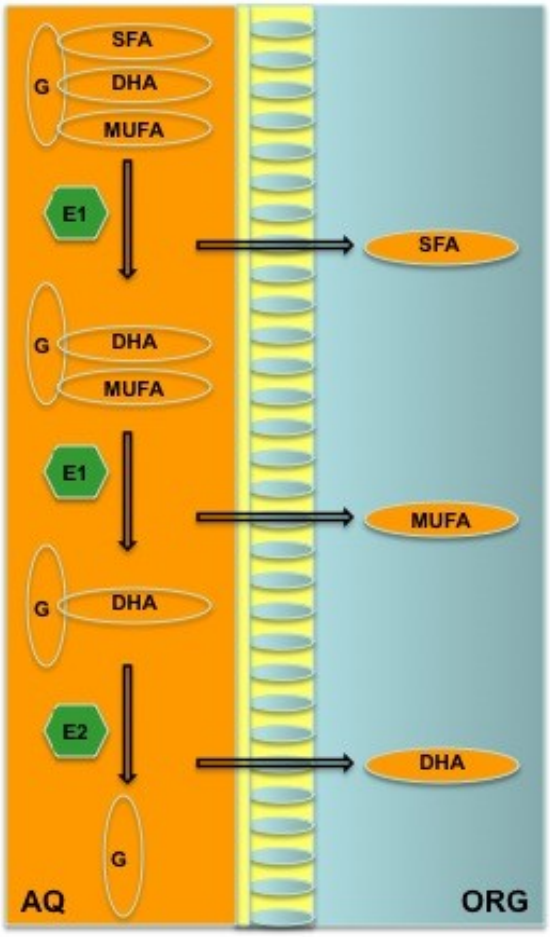


Figure 6.1. Schematic representation of the stepwise enzymatic hydrolysis of triacylglycerols and simultaneous extraction of released fatty acids in a membrane contactor system, comprising an asymmetric polyimide ultrafiltration membrane. (G – Glycerol; SFA – Saturated Fatty Acids: MUFA – Monounsaturated Fatty Acids; DHA – Docosahexaenoic Acid; AQ – Aqueous Phase; ORG – Organic Phase; E1 and E2 – Enzymes).

Previously, appropriate lipases for the selective hydrolysis of triacylglycerols (Chapter 3), and a suitable membrane for the extraction of fatty acids in the biphasic system (Chapter 5) were found. The experiments described in this chapter were conducted in order to prove that fractionation between saturated and polyunsaturated fatty acids, namely PLA and DHA, can be achieved in this novel integrated process. In order to accomplish that, the following specific objectives were defined:

- Investigate limitations to the mass transfer through the membrane created by the presence of emulsion in the aqueous side of the membrane contactor system;
- Find apposite operating conditions for performing simultaneous reaction and separation;
- Determine mass transfer coefficients for the targeted fatty acids at each stage of the process, and fractionation achieved between them;
- Evaluate the feasibility of this innovative process for implementation at industrial scale as an alternative to more conventional processes.

6.3. Materials and Methods

6.3.1. Cell mass, chemicals and membranes

Thraustochytrid cell mass (strain T29) was produced by fermentation as described in section 2.3.1. 100 g of freeze-dried cell mass of this specific microbial contains approximately 40 g oil, of which 16 g is DHA and 10 g is PLA. A detailed characterisation of this raw material, regarding lipid classes and fatty acids composition, was presented in Chapter 2.

Hexane (GPR Rectapur) and 96% ethanol (v/v, GPR grade) were purchased from VWR (UK). Dimethylformamide (DMF) was purchased from Rathburn Chemicals, UK (HPLC grade). Matrimid® 5218 was purchased from Huntsman, Belgium.

Two different lipases were used in the stepwise enzymatic hydrolysis. Lipozyme TL 100L (LPZ) was provided by Novozymes Ltd (Denmark), and the sn-1,3 position specific *Mucor javanicus* (MJ) was purchased from Sigma Aldrich (UK). Phospholipase A1 for cell mass pre-treatment was also purchased from Sigma Aldrich (UK).

6.3.2. Preparation of the fatty acid rich solution – enzymatic hydrolysis

Enzymatic hydrolysis

5 g of freeze-dried cell mass were suspended in 100 mL of 0.1 M potassium phosphate buffer (pH 7 at 37 ºC), and heated to 98 ºC in a water bath for 10 minutes, in order to deactivate natural enzymes and help opening up the cells membrane. Afterwards, 100 mL of ethanol were added to the cell mass suspension and the flask was incubated in a water bath at 37 ºC. The first lipase was added when the optimum temperature was reached. Recirculation of the cell mass suspension to the aqueous compartment of the membrane contactor was initiated 2 hours after the beginning of the triacylglycerols hydrolysis. The second lipase was added to the cell mass suspension when saturated fatty acids, such as PLA, were satisfactorily removed.

Phospholipase pre-treatment

5 g of freeze-dried cell mass were suspended in 100 mL of 0.1 M potassium phosphate buffer (pH 5 at 50 ºC), and heated to 98 ºC in a water bath for 10 minutes. For pre-treatment, 1 g of phospholipase was added to the cell mass suspension which was further placed in a water bath at 50 ºC for 2 hours with continuous stirring. After finishing the pre-treatment, the flask containing the cell mass suspension was withdrawn from the water bath and cooled to below 30 ºC. pH was then adjusted to 7 by addition of 1 M KH_2PO_4 and 1M K_2HPO_4. Afterwards,

100 mL of ethanol were added to the cell mass suspension and the flask was incubated in a water bath at 37 ºC. The first lipase was added when the optimum temperature was reached. The same procedure as for the enzymatic hydrolysis was followed from this point.

6.3.3. Mass transfer experiments – Membrane contactor design

The experimental set up was the same as in previous experiments (Chapter 5, Figure 5.1), as well as the operating conditions, e.g. flow rates. Initial volumes of fatty acid rich phase and organic phase (hexane) were 250 mL and 200 mL, respectively. Hexane circulating in the organic compartment contained 0.1% BHT (Butylated hydroxytoluene) in order to prevent fatty acid oxidation. Samples were collected periodically and immediately methylated to be further analysed by GC.

In Figure 6.2, a simplified schematic of the fractionation process, comprising stepwise enzymatic hydrolysis of triacylglycerols and simultaneous separation of the released fatty acids is presented.

In the first stage of the integrated process, the sn-1,3 position specific lipase (MJ) was added to the microbial cell mass suspension in the bioreactor T1. As DHA is mainly in sn-2 position of triacylglycerol molecules for this specific cell mass, other fatty acids, e.g. PLA, would be preferentially released at this stage, and rapidly transferred from the aqueous phase through the membrane to the organic phase circulating on the right side of the membrane contactor module (arrow in the membrane contactor module indicates the direction of solute transport). Free fatty acids transferred to the organic phase accumulate in the solvent vessel T2. When a satisfactory fraction of PLA is removed (desirably not less than 50%, with a DHA loss of no more than 10%), the second lipase would be added to the bioreactor, and the organic phase

replaced by clean solvent, marking the beginning of the second stage. The non-specific lipase (LPZ) is added at this point, as it will react with the remaining mono and diacylglycerols, liberating the polyunsaturated fatty acids, namely DHA, which are subsequently transferred to the organic phase. A solution rich in DHA (>60% of total fatty acids) is the desirable product to be obtained at the end of the process.

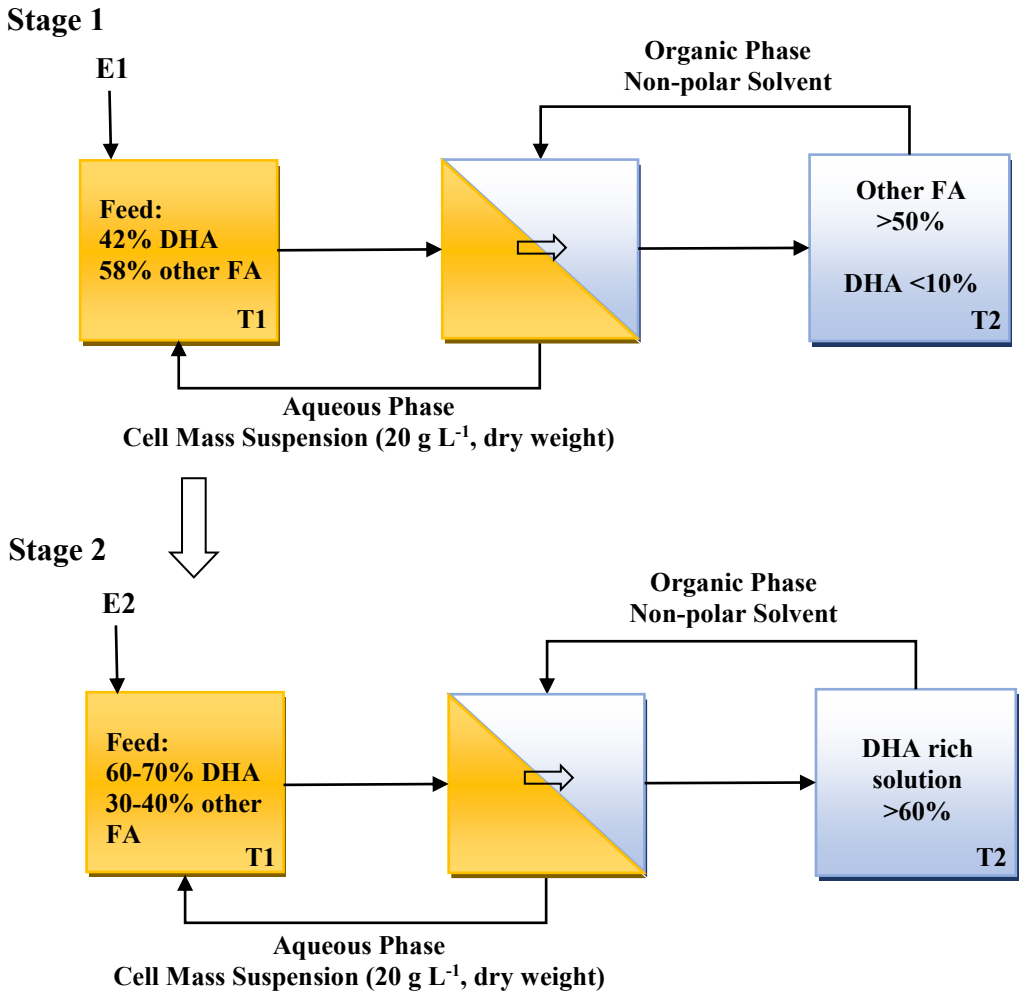


Figure 6.2: Simplified schematic of the stepwise enzymatic hydrolysis and simultaneous membrane separation for fractionation of fatty acids.

6.3.4. Analytical methods

The free fatty acid fraction of the samples withdrawn was methylated according to the method described by Metcalfe *et al*. [89] in order to obtain the fatty acid methyl esters to be further quantified based on gas chromatography analysis. Analysis of the methyl esters of fatty acids was carried out using an Agilent 6850 series gas chromatograph equipped with an autoinjector (injection volume of 1 μL, split ratio of 25:1) operated at 250°C and a flame ionization detector operated at 280°C. A DB-FFAP fused silica capillary column, 30 m x 0.25 mm inner diameter and 0.25mm film thickness (J&W Scientific catalogue no. 122-3232) was used. Oven was operated at 100ºC to 150ºC at 20ºC/min, then to 240ºC at 3ºC/min and finally holding at 240ºC until complete 39 min. Helium was used as the carrier gas. The signals were identified by comparison with known standards (mixture ME 81; Larodan Fine Chemicals, Sweden) and quantified according to the response factor of the internal fatty acid standard C21:0 (Larodan Fine Chemicals, Sweden). The calibration curve for each fatty acid was defined based on four different concentrations of the same standard mixture.

6.4. Results and Discussion

In theory, the fact that the mass transfer coefficients vary with the fatty acid chain length can be used for fractionation of a fatty acids mixture [21]. However, this difference is not so obvious when the discrepancy between fatty acids molecular weight is not considerable, which is the case of PLA and DHA. Thus, other complementary mechanisms should be used in order to obtain fractionation between such fatty acids in a membrane contactor system, such as controlled release of fatty acids by selective enzymatic hydrolysis.

The experiments described below were conducted in order to prove that fractionation between saturated and polyunsaturated fatty acids, in this specific case PLA and DHA, respectively,

may be achieved by performing simultaneous enzymatic hydrolysis and separation of sequentially released fatty acids from an aqueous cell mass rich in lipids to an organic phase in a membrane contactor system.

Experiments comprising enzymatic hydrolysis on the aqueous side of the membrane were therefore conducted. Membrane M3 (Matrimid cast from DMF) was used, with operating conditions as indicated above. Initial volumes of fatty acids rich phase and organic phase were 250 mL and 200 mL, respectively. The selection of enzymes and study of the reaction performance have been described elsewhere (Chapter 3).

6.4.1. Influence of the presence of emulsion in the simultaneous enzymatic hydrolysis and separation of fatty acids

Enzymatic hydrolysis of the cell mass lipids of the aqueous side of the membrane contactor system was carried out by use of the lipase MJ (see Chapter 3) as the first stage. The circulation caused foaming, and formation of a strong emulsion. As discussed in Chapter 3, emulsion formation was advantageous for the hydrolysis rates. However, in this case, fatty acids were not detected in the organic phase after several hours, which indicated that the released fatty acids were trapped in the emulsion (mass transfer was non-existent).

Ethanol was added to the aqueous phase, as the presence of polar solvents such as low chain alcohols and water helps breaking existing hydrogen bonds of membrane associated polar lipids, such as phospholipids, which could help reducing the emulsion formation. A considerable improvement of the fatty acid mass transfer was observed, but the rates were far lower than for chemically hydrolysed cell mass (Chapter 5). However, a significant disparity between the amounts of PLA and DHA transferred across the membrane was observed

(Figure 6.3), in contrast to what was obtained for chemically hydrolysed cell mass (Chapter 5, Figure 5.8). The higher concentrations of PLA indicate that this fatty acid was preferably released and transferred to the hexane phase. This was the first evidence that the desired sequential separation could be achieved.

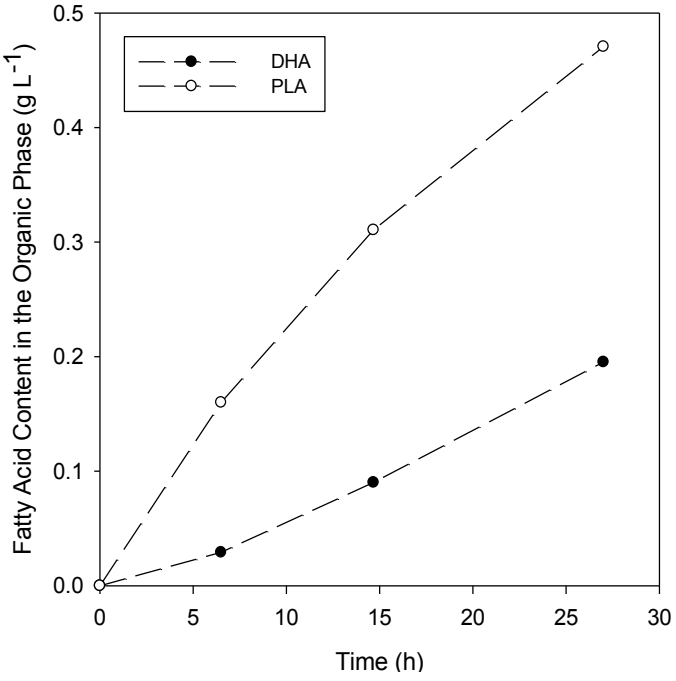


Figure 6.3. Concentration profiles of DHA and PLA in the organic phase (hexane) during mass transfer experiments while using enzymatic hydrolysis (UF membrane - M3, lipase MJ).

However, the mass transfer rates through the membrane were still low. Overall mass transfer coefficient obtained for DHA in this case was 0.28×10^{-7} m s^{-1}, and for PLA was 0.75×10^{-7} m s^{-1}. The emulsion in the feed phase needed to be minimised in order to improve the performance of this biphasic system for the fractionation of fatty acids. The experimental set up was adjusted to decrease the foam formed because of the high recirculation rates, but this was not suficient, the emulsion is mainly due to the presence of proteins and phospholipids from the microbial cell mass, which are not hydrolysed by the lipase.

Hydrolysis of the protein and phospholipid content of the cell mass prior to triacylglycerols hydrolysis has been evaluated previously (Chapter 3). The protease pre-treatment was found to break the emulsion, but it seriously compromised the performance of the subsequent hydrolysis of the acylglycerol fraction. The phospholipase pre-treatment did not affect the initial release rates of the main fatty acids from the acylglycerol fraction, which means the emulsion reduction after hydrolysis of the phospholipid fraction did not compromise the hydrolysis rates, but it affected the desired sequential release of fatty acids (as previously discussed in section 3.4.2.4).

However, a compromise between hydrolysis performance and minimisation of the emulsion formed had to be made. From the options available, the phospholipid hydrolysis was the more reasonable choice, as the extra release of DHA happens later in the reaction (see section 3.4.2.4). Therefore, it was decided to evaluate to what extent the phospholipid hydrolysis would improve the mass transfer rates in the biphasic membrane contactor system.

6.4.2. Fractionation achieved by carrying out simultaneous hydrolysis and separation of fatty acids in the biphasic membrane contactor system

Phospholipase A1, the same phospholipase as previously evaluated for pre-treatment of the cell mass, was therefore added to the cell mass suspension in order to hydrolyse the phospholipids before addition of the lipase MJ. Phospholipase A1 hydrolyses the fatty acid bond in sn-1 position of the phospholipid molecule, consequently the molecule becomes more hydrophilic and is dissolved preferably in the aqueous phase (as illustrated in Figure 3.14).

The concentration profiles of DHA and PLA in the organic phase and average recovery yields obtained in the course of the experiments including phospholipase pre-treatment of the cell mass are presented in Figure 6.4.

In stage 1, the higher concentration of PLA in the organic phase confirmed that saturated fatty acids were preferably extracted, while polyunsaturated fatty acids remained in the aqueous phase, hence the lower concentration of DHA in the organic phase. Namely, 26 wt% of total PLA was transferred from the fatty acids rich phase through the membrane to the hexane after the first stage against 8 wt% of total DHA present in the cell mass suspension. Consequently, DHA fraction in the aqueous phase increased from 42 to 52 wt% of total fatty acids, after removing saturated fatty acids. Overall mass transfer coefficient obtained for DHA in the first stage was $0.36\text{-}0.30\times10^{-7}$ m s^{-1} and for PLA was $1.63\text{-}2.37\times10^{-7}$ m s^{-1} (Table 6.1).

After 50 hours, the second lipase (LPZ) was added to the cell mass suspension, and the hexane phase replaced by clean solvent, marking the beginning of the second stage of the process. Remaining acylglycerols containing fatty acids were hydrolysed, and consequently the concentration of free polyunsaturated fatty acids, namely DHA, increased in the aqueous phase. However, the increase of free DHA in the aqueous phase did not seem to have enhanced its transfer rate through the membrane. The OMTC values calculated for DHA in the second stage were $0.29\text{-}0.36\times10^{-7}$ m s^{-1} (Table 6.1). Nevertheless, DHA concentration was still increasing linearly (constant transport rate), while the PLA transport rate decreased considerably, and as a result, lower OMTC values were obtained for PLA in the second stage (Table 6.1). By the end of this experiment, 61 wt% of PLA had been removed against 24 wt% of DHA, and DHA fraction in aqueous phase increased to 60 wt% of total fatty acids. In Figure 6.5 the average composition of DHA in relation to the total fatty acids in each phase at

different stages of the process is illustrated. Hexane containing 45-50% of DHA was obtained at the end of the experiments.

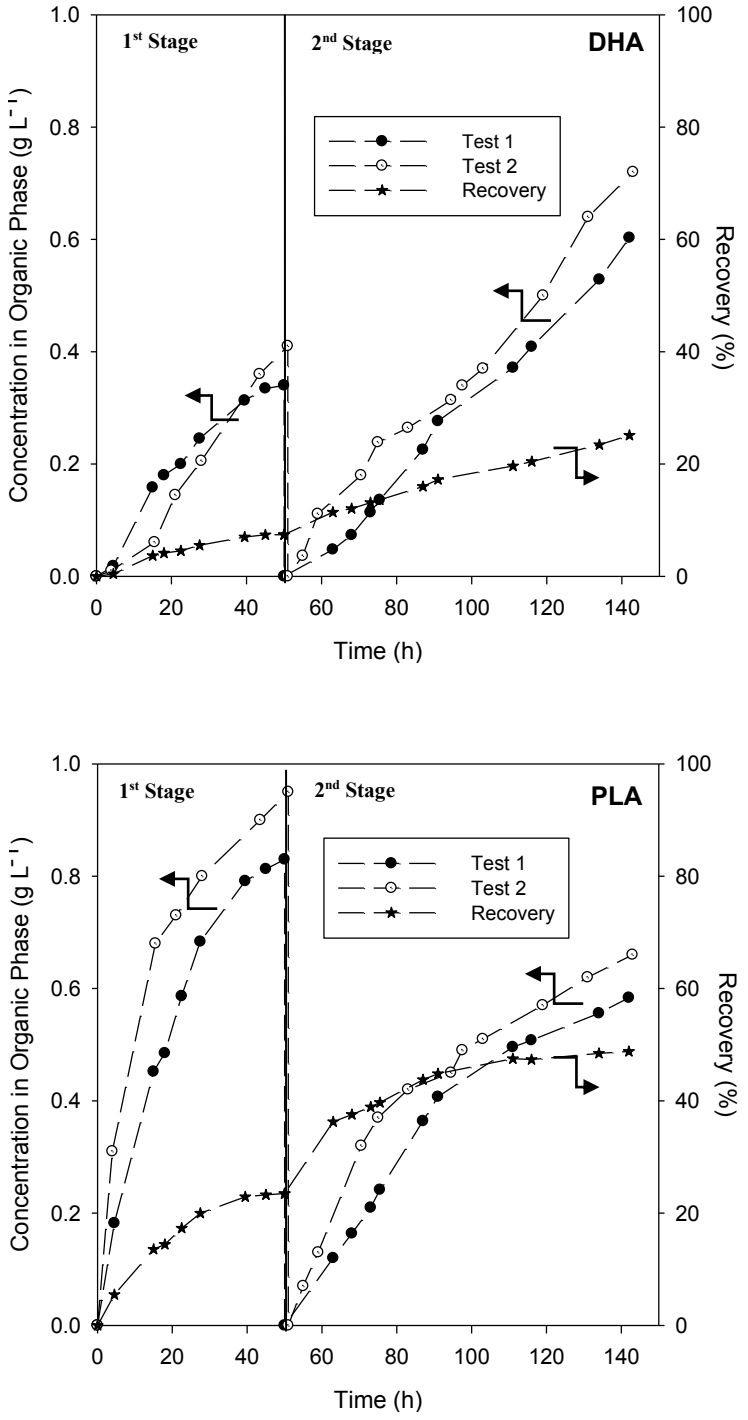


Figure 6.4: Concentration profiles of DHA and PLA in the organic phase (hexane) and recovery during simultaneous hydrolysis and separation of fatty acids in the biphasic membrane system (UF membrane - M3, 1st Stage – lipase MJ, 2nd Stage – lipase LPZ), after phospholipase pre-treatment.

Table 6.1: Overall mass transfer coefficients, OMTC/K_{aq}, of DHA and PLA from the aqueous fatty acids rich phase (water/ethanol) to the organic phase (hexane) for Matrimid membrane in DMF (M3).

Fatty Acid	OMTC, Kaq × 10^7 (m s^{-1})	
	1st Stage	2nd Stage
DHA	0.36 ; 0.30	0.29 ; 0.36
PLA	1.63 ; 2.37	0.07 ; 0.11

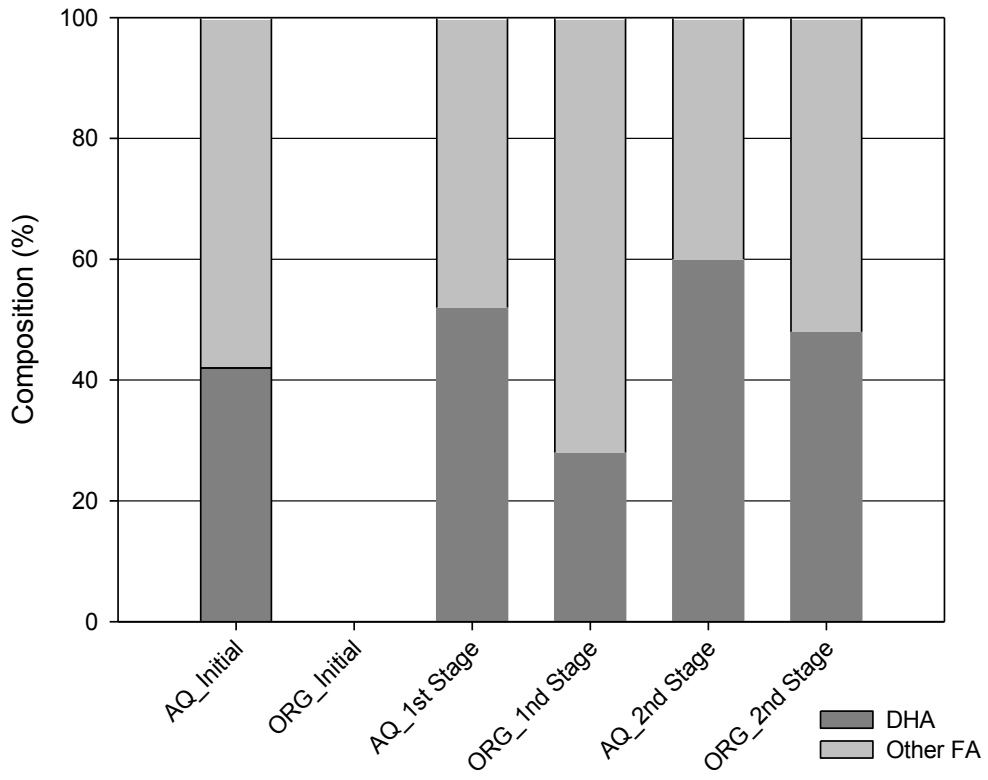
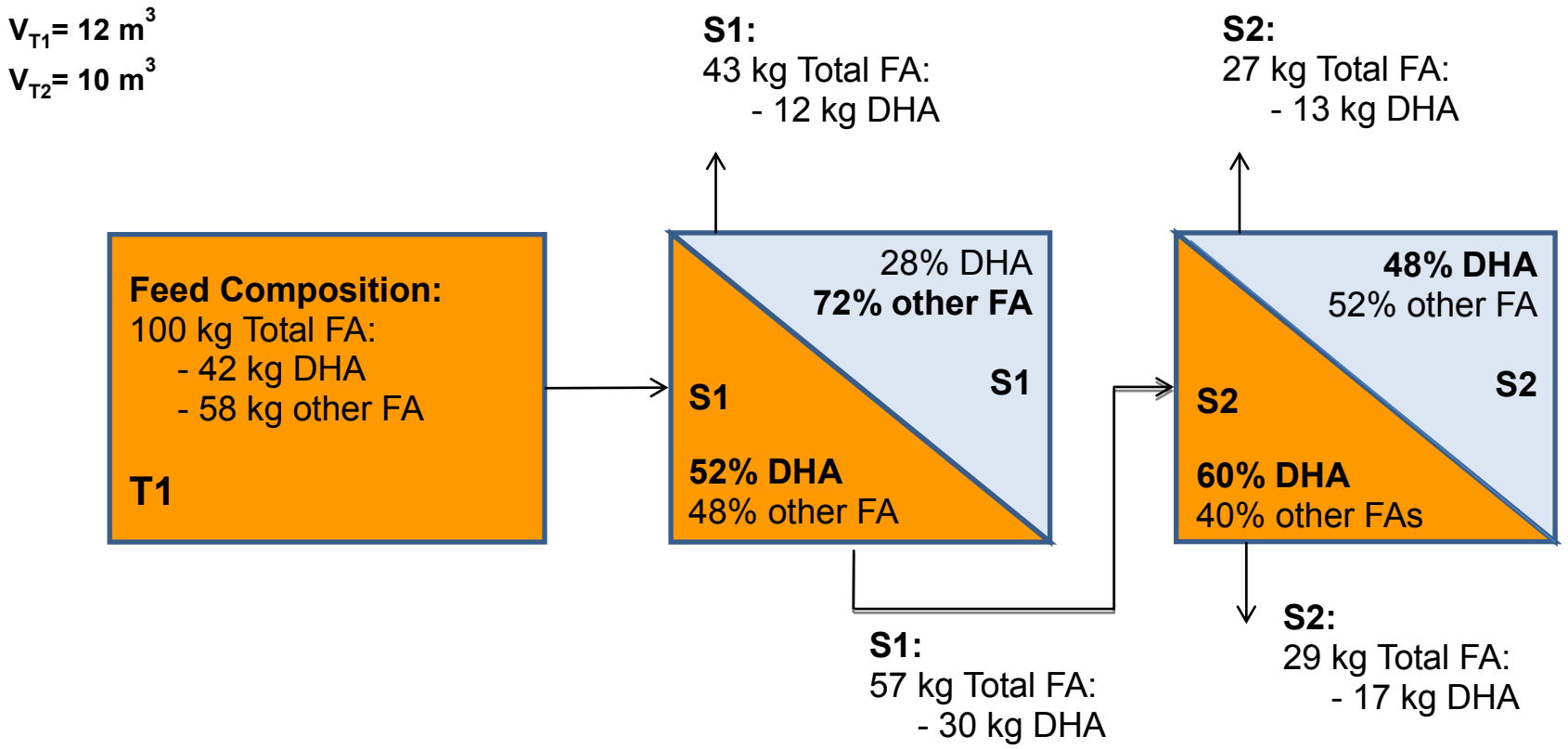


Figure 6.5: DHA fraction of the total fatty acids present in the aqueous (AQ) and organic (ORG) phases initially and at the end of each stage of the simultaneous hydrolysis and separation of fatty acids in the biphasic membrane system (UF membrane - M3), after phospholipase pre-treatment.

The aim of this investigation was to develop a process utilising enzymatic lipid hydrolysis, keeping the active enzymes in the cell mass side of the system, in order to separate the targeted fatty acids as they were released. If the first stage had been prolonged, the fraction of DHA in the aqueous phase would be higher, since saturated fatty acids would still be transferred at a higher rate. It was intended to recover most of the DHA in the organic phase, obtaining a hexane solution rich in this fatty acid. However, the emulsion characteristics of the aqueous phase affected the mass transfer rates, and consequently too long a time would be required to achieve the desired DHA recovery, which even in an inert atmosphere and addition of antioxidants would not guarantee the stability of the compounds. An adjustment of the operating conditions and increasing the membrane contact area could easily improve the extraction performance. Furthermore, as discussed in Chapter 5, the membrane itself offered the highest resistance to mass transfer, suggesting that it may not be the most indicated for this specific application, other hydrophobic membranes should be tested. Overall, more work is required for the optimisation of the integrated process, in order to make it more attractive for industrial use.



T1: Aqueous Phase (Cell mass suspension, 20 kg m^{-3}, 50% total lipids, of which ~85% TAG)

T2: Organic Phase (Hexane)

Other FAs: Mainly Palmitic and Oleic Acid (PLA and OLA, >80% for this specific microbial cell mass)

Figure 6.6: Composition of each stream of the integrated stepwise enzymatic hydrolysis of triacylglycerols directly on the cell mass suspension, and simultaneous separation of released fatty acids based on experimental results (S1-1st stage; S2-2nd stage).

6.5. Feasibility and applicability of the developed process at industrial scale

In the present investigation it was successfully demonstrated that it is possible to obtain fractionation of DHA and saturated/monounsaturated fatty acids from a microbial wet cell mass by combining selective enzymatic hydrolysis and membrane separation. The process is patented, and already granted in the United States, Norway and EP (US 8,455,669, NO 329,999, EP 2,440,670-allowed).

As mentioned before, this process is based on aqueous biomass, not on extracted oils as the current industrial technologies. The idea is to reduce costs by omitting drying and oil extraction. But, although developed for microbial biomass, it may also be applicable for e.g. fish by-products, upgrading of low-quality marine oils, and so contribute to a better utilisation of this limited resource and reduce the pressure on the fish-stocks.

Enzymatic processes for synthesis of triacylglycerol oils enriched with omega-3 PUFA, namely EPA and DHA, are already established in the lipid industry. However, enzyme costs have been a major hurdle for industry. The enzyme costs constitute 10-15 €/kg of DHA produced (based on prices given by Novozymes, Denmark). Hence, re-use of the enzymes is crucial. This will require immobilisation of the enzymes on particles or a solid support.

In an integrated process as described in this thesis, by performing simultaneous hydrolysis and separation of released products in a biphasic membrane contactor system, the advantages are two fold: the enzyme can be retained in the membrane module compartment where the reaction occurs, and at the same time products are continuously removed, thus increasing the reaction rates, and preserving the enzyme activity for longer.

Membrane technology has not been used in full scale in refining of marine oils. This project intended to introduce the use of membranes in the oil refining industry. Introducing use of membranes to this industry might pave the way for a new level of product quality and cost reduction. The aim was not only to improve one or two production steps, but also to introduce a new tool to the lipid purification industry.

However, the low mass transfer rates observed for the separation of fatty acids through the membrane in a system as proposed in this investigation, imply that a high membrane area will be required, thus increasing both capital and operating costs. An annual production of 100 tonnes DHA with continuous operation will require a membrane area of 500 m^2, based on the highest mass transfer rates obtained in this work (OMTC=$1.7x10^{-6}$ m s^{-1}, corresponding to a mass transport of 0.03 kg m^{-2} h^{-1}).

Overall, a "proof of principle" has been obtained. This process represents an innovative combination of enzyme and membrane technology for production of concentrated omega-3 polyunsaturated fatty acids. More work is required for the optimisation of the integrated process proposed, in order to make it more attractive for industrial use.

6.5.1. Preliminary economic analysis of the integrated process

Based on experimental results obtained in this investigation, and before any process optimisation, a preliminary evaluation of the integrated process feasibility and profitability in terms of estimated investment and operating costs was done, considering an annual production of 100 ton of 80% DHA.

For the production of 100 ton of DHA per year, about 5000 m^3 of fermentate are required, corresponding to 500 ton of dry cell mass in total, containing 300 ton of total lipids, of which approximately 100 ton are DHA, assuming a recovery of 80%.

Considering a production line working 24h per day and 312 days per year, a volume flow of 16 m^3 would be treated per day, which would correspond to a daily production of 320 kg of DHA. Operating costs for the production of raw material are estimated at 0.9 M€/year, and an investment of around 4 M€ would be required for raw material production (fermentation plant).

In terms of hydrolysis costs, a reaction time of 15-20 hours is estimated, using a 10 m^3 reactor, with temperature and pH control, and at an inert atmosphere. Considering use of free enzymes, 1 kg of enzyme per m^3 of cell mass to be treated would be required, with an app. cost of 20 €/kg, it would translate to a cost of 10-15 € per kg of DHA produced. Costs can be reduced about ten times if using immobilised enzymes. Operating costs for this stage of the process are then estimated to be around 0.1 M€/year, and an initial investment of 0.5 M€ in bioreactors if not available.

For the membrane separation plant, a membrane area of 500 m^2 would be required for a daily production of 320 kg of 80% DHA, based on the best mass transfer rates obtained previously (DHA transport of 0.03 kg m^{-2} h^{-1}). A solvent recovery system (OSN plant) would ideally be coupled to the membrane contactor module, for concentration of the product stream and recycling of solvent used in the process (~98% reclaim). An investment of app. 1-1.5 M€ is estimated for acquisition of the membrane plant with an overall membrane area of 1000-1500 m^2. Considering a 10 year depreciation and the annual production of 100 ton of 80% DHA,

these with translate to a cost of 1-2 €/kg of DHA produced. Operating costs including membrane plant maintenance and solvent used would be around 0.3-0.5 M€/year.

Thus, it results in a variable total investment cost of 5-6 M€, and annual operating costs of 2-3 M€. Process by-products are estimated to generate from 10-12 €/kg (mainly product stream obtained at the first stage of the process, containing ~10% DHA). Cost per kg of 80% DHA produced, would be 15-20 €, and its estimated market value is expected to be not lower than 50 €/kg and likely to reach 100 €/kg, depending on the degree of purity. It would give a minimum net margin of 30 €/kg of DHA produced. Overall, an investment payback time of 1-2 years is estimated.

6.6. Conclusions

Integrating simultaneous enzymatic hydrolysis of the cell mass lipid content with separation of released fatty acids in the membrane contactor module was challenging. The strong emulsion formed in the aqueous side limited the mass transfer rates. A compromise between hydrolysis performance and minimisation of the emulsion had to be made. Addition of ethanol to the aqueous phase and partial hydrolysis of the phospholipid cell mass fraction, helped breaking existing hydrogen-bonds of membrane associated lipids, and thus reducing the emulsion formation, without compromising the selective hydrolysis of triacylglycerols.

The desired sequential release was then observed. Overall mass transfer coefficient obtained for DHA in the first stage was $0.36\text{-}0.30\times10^{-7}$ m s^{-1} and for PLA was $1.63\text{-}2.37\times10^{-7}$ m s^{-1}. In total, 61 wt% of PLA was removed to the organic phase against 24 wt% of DHA. As a result, the DHA fraction in aqueous phase increased from 42 to 60 wt% of total fatty acids. A clean solvent phase containing 45-50 wt% DHA was obtained at the end of the process.

One can then conclude that the objective of the present work was accomplished as it was possible to obtain a partial fractionation of the main fatty acids. The process principle has been proved, however, more optimisation work is required to make this a more effective process, and hence more attractive to the marine/microbial oil refining industry.

A preliminary economical evaluation of implementation and operation of the proposed integrated process was carried out, based on an annual production of 100 ton of 80% DHA. Capital and annual running costs are estimated to be between 5-6 M€ and 2-3 M€, respectively. Assuming a market value of 50-100 €/kg for 80% DHA, an investment payback time of 1-2 years is estimated.

Chapter 7

Final Conclusions and Future Perspectives

In this thesis, new ways for extraction and fractionation of LC-PUFA (namely DHA) from a microbial cell mass, combining enzymatic lipid hydrolysis and membrane filtration were investigated. The main objectives were to characterise relevant enzymes with respect to selectivity and kinetics, and to prepare and characterise suitable membranes to be used in a biphasic membrane contactor system for fatty acids separation. It was intended to carry out the hydrolysis of the cell mass triacylglycerol content directly in the cell mass suspension in a sequential manner, and continuously separate released fatty acids in the contactor system. Using this novel process, some traditional techniques, such as drying and mechanical homogenisation, would be replaced by more innovative technologies, based mainly on enzyme and membrane filtration technology. To reach the overall goal of this project, a large number of process parameters were investigated. The following objectives were achieved:

Characterisation of the cultivated thraustochytrids cell mass:

The total lipid content of the cell mass was 42 wt%, determined after protease treatment. The protease treatment increased the lipid extraction yield considerably. This observation was taken into consideration in the enzymatic hydrolysis experiments. As expected,

triacylglycerols were the largest fraction (~85 wt%) of the total lipids, followed by the phospholipids (~14 wt%).

The fatty acid content of the microbial cell mass was determined as fatty acid methyl esters (FAMEs). DHA, palmitic and oleic acids represent 90.4 wt% of total fatty acids. The remaining 9.6 wt% are mainly composed by stearic acid (C18:0), arachidonic acid (C20:4), and docosapentaenoic acid (DPA - C22:5).

Approximately 60% of total DHA was in sn-2 position, and 80% of SFA/MUFA were distributed among sn-1,3 positions of the triacylglycerol molecules, as determined by NMR analysis. The remaining DHA was distributed between positions sn-1,3.

Concentration of the cell mass by cross-flow microfiltration:

As proposed, evaluation of the applicability of a cross-flow microfiltration system and a preliminary selection of the operation conditions for an efficient dewatering was performed. High filtration permeances (~200 L m^{-2} h^{-1} bar^{-1}) were obtained, whilst using low transmembrane pressure (TMP = 0.7 bar), which avoided the cell damage. Concentration factors of three and four fold were obtained. The water flux recovery was possible, despite some loss observed after the first experiment.

Pre-treatment of the cell mass and operating conditions for enzymatic hydrolysis:

Several parameters were studied in order to evaluate their influence on the enzymatic hydrolysis performance, including: operating conditions, enzyme concentration, cell mass concentration, and cell mass pre-treatment. It was confirmed that the ratio between water, cell mass and enzyme plays an important role in the hydrolysis rates.

The cell mass pre-treatment turned out to be not only unnecessary, but also a disadvantage for the lipid hydrolysis performance. Protein content functioned as an emulsion stabiliser, which was found to be a benefit to the triacylglycerol hydrolysis rates. Extensive hydrolysis of proteins resulted in a drastic loss of their emulsifying properties. The small peptides formed diffuse rapidly and adsorb at the interface between oil and water, therefore they are less efficient in stabilising emulsions, because they cannot unfold or reorient at the surface to the same extent as proteins.

Characterization of enzyme selectivity and kinetics:

The new analytical methods developed for the analyses of acylglycerols and fatty acids by LC-ESI-MS brought considerable advantages for the present investigation. The access to the concentration profiles of tri-, di-, and monoacylglycerols being formed throughout the reaction allowed a better evaluation of the performance of each enzyme. New information on the enzyme kinetics and selectivity enabled a 'well-founded'' selection of enzymes for selective enrichment of DHA. From a practical point of view, the sample preparation was simplified and there was no need for methylation, which would be required when using gas chromatography, and only 10 min were required for a complete characterisation of each sample.

The study of TAG, DAG and MAG profiles gave a precious insight into the understanding of the lipase selectivity. All lipases tested preferably hydrolysed the ester bonds between saturated and monounsaturated fatty acids and the glycerol molecule, due to their configuration. As a result of the easier access of the lipase, the acylglycerols composed by oleic (OLA) and palmitic (PLA) acids reacted first, hence the high release yields observed for

those fatty acids. As the acylglycerols containing PLA and OLA went nearly to zero, a decrease in the acylglycerols containing DHA was observed for LPZ and MJ, but it was not the case of CR, which presented the higher discrimination against DHA. It confirmed that the fatty acids structure prevents access to PUFA in the sn-1,3 positions, and different lipases present distinct behaviour. The hydrolysis performance seemed to be more dependent on the fatty acid structure than on the position specificity.

It was shown that the hydrolysis of cell mass lipids to free fatty acids can be performed effectively directly in the cell concentrate, without previous isolation of the lipid fraction. It was intended to develop a sequential extraction of the targeted fatty acids directly from the wet cell mass, which was accomplished. Fractionation between saturated (e.g. PLA), monounsaturated (e.g. OLA), and long chain polyunsaturated fatty acids (e.g. DHA) can then be achieved combining the stepwise hydrolysis with continuous removal of the released fatty acids in a biphasic membrane contactor system.

Selected membrane and process conditions for efficient separation of fatty acids from a fatty acids rich solution in a membrane biphasic system comprising an asymmetric polyimide membrane:

Asymmetric polyimide nano and ultrafiltration membranes were tested for the separation of fatty acids in the biphasic membrane contactor system. Promising results have been obtained, mass transfer rates of fatty acids through the membrane in the biphasic system were satisfactory. Overall mass transfer coefficients obtained were tenfold greater than in other published works [21]. In the best experiment, 95 wt% of DHA in the aqueous phase was transferred to the organic phase.

The solute transport mechanism through asymmetric polyimide porous membranes in the biphasic membrane contactor system was explored. However, the membrane mass transfer coefficients k_M, calculated based on the solute transport model proposed, did not explain experimental observations. For the calculation of the theoretical k_M, membrane characteristics were estimated based on the measured membrane flux and molecular weight cut-off curve (MWCO). The asymmetric membrane was divided in two main layers, and only the top layer considered as causing resistance to the mass transfer. Obviously, this approach did not seem to be correct, suggesting that the mass transfer resistance is applied throughout the whole membrane thickness, and not only the top-layer thickness.

Demonstrated the feasibility of the proposed integrated process for sequential hydrolysis of triacylglycerols and simultaneous separation of the released fatty acids while still present in the cell mass suspension:

Integrating simultaneous hydrolysis of lipid containing cell mass and separation of released fatty acids, 61 wt% of PLA was removed to the organic phase against 24 wt% of DHA. As a result, DHA fraction in aqueous phase increased from 42 to 60 wt% of total fatty acids. As expected, the presence of emulsion in the aqueous phase limited the mass transfer through the membrane in the biphasic membrane contactor system. However, promising results have been obtained, mass transfer rates of fatty acids through the membrane in the biphasic system may be improved by further optimisation of the operating conditions. It can then be concluded that the objective of the present work was accomplished as a partial fractionation of the main fatty acids was obtained. This process is then a promising alternative to the more conventional methods used for fatty acids fractionation.

Future Perspectives

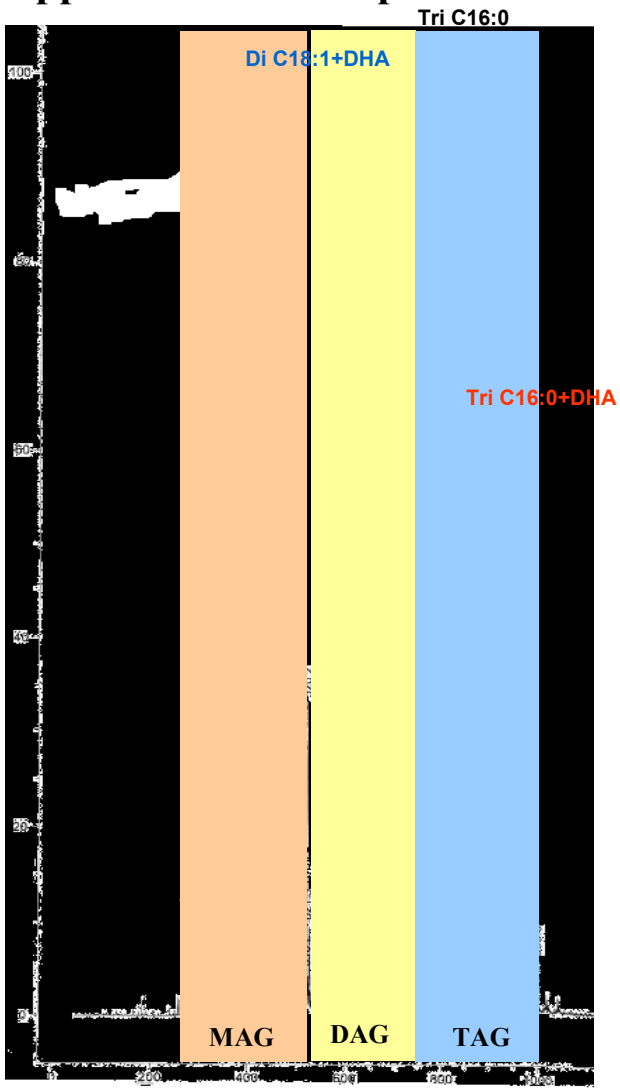
In the present work commercial non-immobilised enzymes were utilised. However, in order to reduce enzyme costs in future applications, the utilisation of immobilised enzymes should be considered. Enzyme immobilisation techniques have been widely studied both at academic and industrial level. Adsorption into a solid support (such as resin, biopolymer, silica, zeolite, ion-exchange matrix) is probably the most routinely used for analytical purposes, but it often leads to a substantial loss of enzyme activity, and the solid matrix is sometimes more expensive than the enzyme itself. Entrapment and encapsulation involve inclusion of the enzyme in a polymer network, such as a membrane, which may be attractive to a process like the one presented in this thesis. However, large molecules may have difficulty in approaching the catalytic sites of entrapped enzymes. Lately, cross-linked enzyme aggregates (CLEAs) have drawn increasing attention for the use in biotransformation. These aggregates are formed by precipitation of the enzyme from an aqueous solution, by the addition of salts, or water miscible organic solvents or non-ionic polymers, and subsequently cross-linked, becoming permanently insoluble while maintaining their catalytic activity. CLEAs may be combined with membrane filtration, making possible simultaneous reaction and separation.

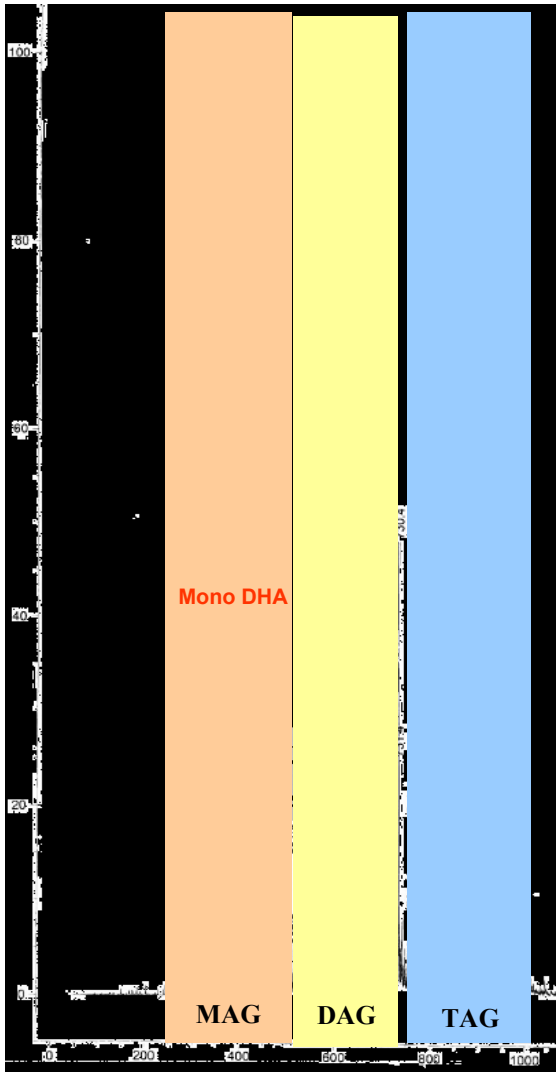
Unfortunately, in the course of this project it was not possible to verify the applicability of the kinetic model proposed in Chapter 4, for the reasons mentioned before. However, it would be worth to try making some amendments in order to simplify the system. The primary objective was to use an o/w emulsion using the microbial oil, since it was intended to create a 'real' system, but it turn out to be extremely challenging. Therefore, despite expensive, the more reasonable way (if not the only) to obtain the experimental data needed for the model fitting would be by starting with a reaction mixture containing known amounts of standards of

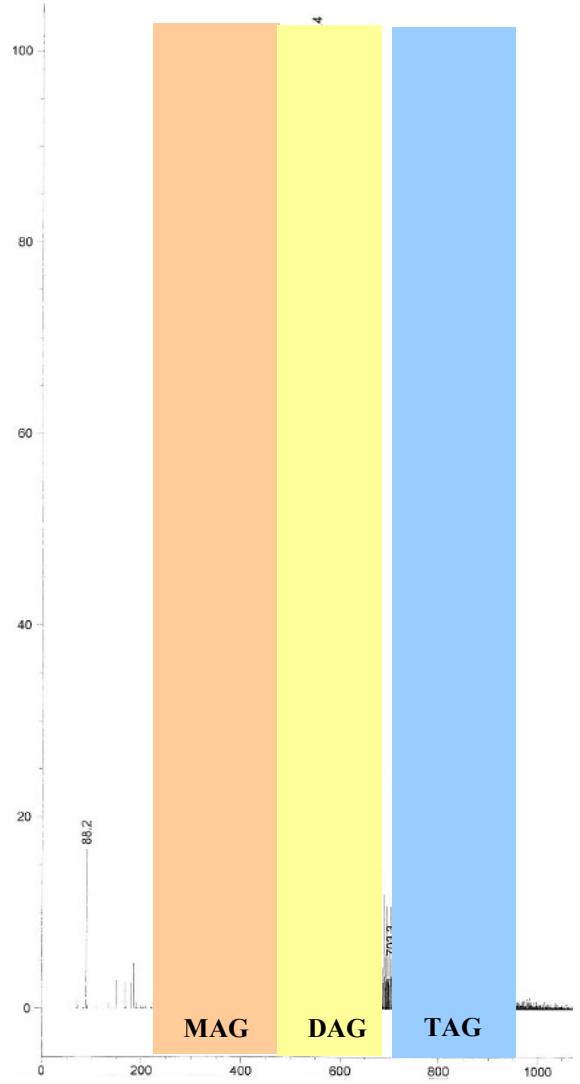
triacylglycerols comprising different fatty acids, in order to have full control of every single compound that is formed throughout the hydrolysis reaction.

The low mass transfer rates observed with the asymmetric membranes tested should also be addressed. It is crucial to improve the separation performance to make this process more efficient for fractionation of fatty acids, and hence more attractive to industry. Membrane fouling was not evaluated in detail during this investigation, but the linear cumulative mass transfer over time suggested that fouling was not the reason for the high resistance to mass transfer observed through the membrane, but the membrane itself, as further confirmed by the estimated membrane mass transfer coefficients. Therefore, research for membranes giving better mass transfer performance is needed.

Appendix A - Mass spectrums







Appendix B - Transcript of the MatLab algorithm

```
% Kinetic Model for the Enzymatic Hydrolysis of Triacylglycerols - Multiple Substrates and
Products
tspan=(0:0.1:10);                          % start time
Cini=[3.78 9.93 0.8 0 0 0 0 0 0 0]';       % initial values for C (t=0)
% arbitrary values of model parameters
K1=0.777e6; K2=2.77e6; K3=0.883e6; K4=3.54e6; K5=4.55e6; K6=2.25e6; K7=1.11e5;
K8=1.5e5;                                  % m4.mol-1.kg-1
K9=1.09e-8; K10=2.19e-8; K11=4.37e-8; K12=2.27e-4; K13=4.55e-4; K14=9.09e-4;
K15=2.73e-4; K16=5.47e-4;                  % kg.m-2
KI=2.58e-2; KJ=0.5e-2;                     % mol.m-2
KE=1;                                      % m3.kg-1
KTG1=0.598e-5; KTG2=1.2e-5; KTG3=2.58e-5;  % m
KDG1=0.9e-6; KDG2=5.79e-5; KDG3=11.6e-6;   % m
KMG1=0.537e-3; KMG2=1.07e-4;               % m
KS=1.78e-5; KP=7.13e-6;                    % m
qEmax=3e-5;                                % kg.m-2
% input values
A=17e3;      % m2     input('Interfacial Area?');
V=1;         % m3     input('Volume of Emulsion?');
CEo=1;       % kg/m3  input('Initial Enzyme Concentration?');
% Runge Kutta method and .'derv2' function where the differential equations are written
[t,C]=ode45(@derv2,tspan,Cini);
```

References

1. Ward, O.P. and A. Singh, *Omega-3/6 fatty acids: Alternative sources of production.* Process Biochemistry, 2005. **40**(12): p. 3627-3652.

2. Takahata, K., K. Monobe, M. Tada, and P. C. Weber, *The benefits and risks of n-3 polyunsaturated fatty acids.* Bioscience Biotechnology and Biochemistry, 1998. **62**(11): p. 2079-2085.

3. Kinsella, J.E., *Effects of polyunsaturated fatty-acids on factors related to cardiovascular-disease.* American Journal of Cardiology, 1987. **60**(12): p. G23-G32.

4. Lewis, T.E., P.D. Nichols, and T.A. McMeekin, *The biotechnological potential of thraustochytrids.* Marine Biotechnology, 1999. **1**(6): p. 580-587.

5. Ratledge, C., *Fatty acid biosynthesis in microorganisms being used for Single Cell Oil production.* Biochimie, 2004. **86**(11): p. 807-815.

6. Wanasundara, U.N., *Novel separation techniques for isolation and purification of fatty acids and oil by-products*. Sixth Edition ed. 2005: Bailey's Industrial Oil and Fat Products.

7. Wynn J.P., and C. Ratledge, *Oil from Microorganisms*. Sixth Edition ed. Vol. Six Volume Set. 2005: Bailey's Industrial Oil and Fat Products. Chapter 5.

8. Sijtsma, L. and M.E. de Swaaf, *Biotechnological production and applications of the omega-3 polyunsaturated fatty acid docosahexaenoic acid.* Applied Microbiology and Biotechnology, 2004. **64**(2): p. 146-153.

9. Medina, A.R., E. M. Grima, A. G. Gimenez, and M. J. I. Gonzalez, *Downstream processing of algal polyunsaturated fatty acids.* Biotechnology Advances, 1998. **16**(3): p. 517-580.

10. Muffler, K. and R. Ulber, *Downstream processing in marine biotechnology*, in *Marine Biotechnology Ii*. 2005. p. 63-103.

11. Haraldsson, G.G., B. Kristinsson, R. Sigurdardottir, G. G. Gudmundsson, and H. Breivik, *The preparation of concentrates of eicosapentaenoic acid and docosahexaenoic acid by lipase-catalyzed transesterification of fish oil with ethanol.* Journal of the American Oil Chemists Society, 1997. **74**(11): p. 1419-1424.

12. Lyberg, A.-M. and P. Adlercreutz, *Lipase-catalysed enrichment of DHA and EPA in acylglycerols resulting from squid oil ethanolysis.* European Journal of Lipid Science and Technology, 2008. **110**(4): p. 317-324.

13. Chakraborty, K. and R. Paulraj, *Enrichment of eicosapentaenoic acid from sardine oil with Delta 5-Olefinic bond specific lipase from bacillus licheniformis MTCC 6824.* Journal of Agricultural and Food Chemistry, 2008. **56**(4): p. 1428-1433.

14. Breivik, H., G.G. Haraldsson, and B. Kristinsson, *Preparation of highly purified concentrates of eicosapentaenoic acid and docosahexaenoic acid.* Journal of the American Oil Chemists Society, 1997. **74**(11): p. 1425-1429.

15. Miranda A.M.M., I. M. Aasen, and Livingston A.G., *Enzymatic hydrolysis of triacylglycerols in a lipid containing marine biomass for production of fatty acids.* Enzyme and Microbial Technology, 2014..

16. Mendes, A., T.L. da Silva, and A. Reis, *DHA concentration and purification from the marine heterotrophic microalga Crypthecodinium cohnii CCMP 316 by winterization and urea complexation.* Food Technology and Biotechnology, 2007. **45**(1): p. 38-44.

17. Darley, W.M., D. Porter, and M.S. Fuller, *Cell-wall composition and synthesis via golgi-directed scale formation in marine eucaryote, Schizochytrium-aggregatum, with a note on Thraustochytrium sp.* Archiv Fur Mikrobiologie, 1973. **90**(2): p. 89-106.

18. Burja, A.M., R. E. Armenta, H. Radianingtyas, and C. J. Barrow, *Evaluation of fatty acid extraction methods for Thraustochytrium sp ONC-T18.* Journal of Agricultural and Food Chemistry, 2007. **55**(12): p. 4795-4801.

19. Jakobsen, A.N., I. M. Aasen, K. D. Josefsen, and A. R. Strom, *Accumulation of docosahexaenoic acid-rich lipid in thraustochytrid Aurantiochytrium sp strain T66: effects of N and P starvation and O-2 limitation.* Applied Microbiology and Biotechnology, 2008. **80**(2): p. 297-306.

20. Hara, A. and N.S. Radin, *Lipid extraction of tissues with a low-toxicity solvent.* Analytical Biochemistry, 1978. **90**(1): p. 420-426.

21. Keurentjes, J.T.F., J. T. M. Sluijs, R. J. H. Franssen, and K. Vantriet, *Extraction and fractionation of fatty acids from oil using an ultrafiltration membrane.* Industrial & Engineering Chemistry Research, 1992. **31**(2): p. 581-587.

22. Hoeksema, S.D., *Two phase extraction of oil from biomass*. US Patent No. 6166231, 2000, Martek Biosciences Corporation.

23. Liddell, *Extraction of triglycerides from microorganisms*. US Patent No. 6180376 B1, 2001 Zeneca Limited.

24. Grima, E.M., A. R. Medina, A. G. Gimenez, J. A. S. Perez, F. G. Camacho, and J. L. G. Sanchez, *Comparison between extraction of lipids and fatty-acids from microalgal biomass.* Journal of the American Oil Chemists Society, 1994. **71**(9): p. 955-959.

25. Lewis, T., P.D. Nichols, and T.A. McMeekin, *Evaluation of extraction methods for recovery of fatty acids from lipid-producing microheterotrophs.* Journal of Microbiological Methods, 2000. **43**(2): p. 107-116.

26. Basheer, S., K. Mogi, and M. Nakajima, *Development of a novel hollow-fiber membrane reactor for the interesterification of triglycerides and fatty-acids using modified lipase.* Process Biochemistry, 1995. **30**(6): p. 531-536.

27. Gimenez, A.G., M. J. I. Gonzalez, A. R. Medina, E. M. Grima, S. G. Salas, and L. E. Cerdan, *Downstream processing and purification of eicosapentaenoic (20 : 5n-3) and arachidonic acids (20 : 4n-6) from the microalga Porphyridium cruentum.* Bioseparation, 1998. **7**(2): p. 89-99.

28. Gan, Q., H. Rahmat, and L.R. Weatherley, *Simultaneous reaction and separation in enzymatic hydrolysis of high oleate sunflower oil - evaluation of ultrafiltration performance and process synergy.* Chemical Engineering Journal, 1998. **71**(2): p. 87-96.

29. Molinari, R., E. Drioli, and G. Barbieri, *Membrane Reactor in Fatty-Acid Production.* Journal of Membrane Science, 1988. **36**: p. 525-534.

30. Okada, T. and M.T. Morrissey, *Production of n-3 polyunsaturated fatty acid concentrate from sardine oil by lipase-catalyzed hydrolysis.* Food Chemistry, 2007. **103**(4): p. 1411-1419.

31. Gan, Q., F. Baykara, H. Rahmat, and L. R. Weatherley, *Analysis of a direct contact membrane reactor for lipase catalysed oil hydrolysis in a dynamic emulsion system.* Catalysis Today, 2000. **56**(1-3): p. 179-190.

32. Morita, T., H.J. Lim, and I. Karube, *Enzymatic-hydrolysis of polysaccharides in water-immiscible organic-solvent, biphasic systems.* Journal of Biotechnology, 1995. **38**(3): p. 253-261.

33. Arora, S., S. Manjula, A. G. G. Krishna, and R. Subramanian, *Membrane processing of crude palm oil.* Desalination, 2006. **191**(1-3): p. 454-466.

34. Manjula, S. and R. Subramanian, *Membrane technology in degumming, dewaxing, deacidifying, and decolorizing edible oils.* Critical Reviews in Food Science and Nutrition, 2006. **46**(7): p. 569-592.

35. Bhosle, B.M. and R. Subramanian, *New approaches in deacidification of edible oils - a review.* Journal of Food Engineering, 2005. **69**(4): p. 481-494.

36. Bhosle, B.M., R. Subramanian, and K. Ebert, *Deacidification of model vegetable oils using polymeric membranes.* European Journal of Lipid Science and Technology, 2005. **107**(10): p. 746-753.

37. Hafidi, A., D. Pioch, and H. Ajana, *Membrane-based simultaneous degumming and deacidification of vegetable oils.* Innovative Food Science & Emerging Technologies, 2005. **6**(2): p. 203-212.

38. Freitas, L., T. Bueno, V. H. Perez, J. C. Santos, and H. F. de Castro, *Enzymatic hydrolysis of soybean oil using lipase from different sources to yield concentrated of polyunsaturated fatty acids.* World Journal of Microbiology & Biotechnology, 2007. **23**: p. 1725-1731.

39. Lee, J.E., Y. H. Chang, P. Ganesan, and H. S. Kwak, *Concentration of n-3 polyunsaturated fatty acids in cholesterol-reduced cod-liver oil by lipases.* International Journal of Food Science and Technology, 2011. **46**(7): p. 1462-1468.

40. Bousquet, O. and F. Legoffic, *Countercurrent chromatographic-separation of polyunsaturated fatty-acids.* Journal of Chromatography A, 1995. **704**(1): p. 211-216.

41. Bousquet, O., N. Sellier, and F. Legoffic, *Characterization and purification of polyunsaturated fatty-acids from microalgae by gas-chromatography mass-spectrometry and countercurrent chromatography.* Chromatographia, 1994. **39**(1-2): p. 40-44.

42. Teshima, S.I., A. Kanazawa, and S. Tokiwa, *Separation of poly-unsaturated fatty-acids by column chromatography on a silver nitrate-impregnated silica-gel.* Bulletin of the Japanese Society of Scientific Fisheries, 1978. **44**(8): p. 927-927.

43. Dejarlais, W.J., R.O. Adlof, and E.A. Emken, *Acetonitrile as eluente in silver resin column chromatography.* Journal of the American Oil Chemists Society, 1983. **60**(5): p. 975-978.

44. Vali, S.R., H.Y. Sheng, and Y.H. Ju, *An efficient method for the purification of arachidonic acid from fungal single-cell oil (ARASCO).* Journal of the American Oil Chemists Society, 2003. **80**(7): p. 725-730.

45. Han, S.J., S. S. Luthra, L. Peeva, X. J. Yang, and A. G. Livingston, *Insights into the transport of toluene and phenol through organic solvent nanofiltration membranes.* Separation Science and Technology, 2003. **38**(9): p. 1899-1923.

46. Perretti, G., A. Motori, E. Bravi, F. Favati, L. Montanari, and P. Fantozzi, *Supercritical carbon dioxide fractionation of fish oil fatty acid ethyl esters.* Journal of Supercritical Fluids, 2007. **40**(3): p. 349-353.

47. Bocquet, S., J. Romero, J. Sanchez, and G. M. Rios, *Membrane contactors for the extraction process with subcritical carbon dioxide or propane: Simulation of the influence of operating parameters.* Journal of Supercritical Fluids, 2007. **41**(2): p. 246-256.

48. Zinnai, A., U. Nesti, F. Venturi, G. Andrich, and R. Fiorentini, *Supercritical fluid extraction of oil from Schizochytrium sp.* Rivista Italiana Delle Sostanze Grasse, 2006. **83**(1): p. 1-5.

49. Canela, A., P. T. V. Rosa, M. O. M. Marques, and M. A. A. Meireles, *Supercritical fluid extraction of fatty acids and carotenoids from the microalgae Spirulina maxima.* Industrial & Engineering Chemistry Research, 2002. **41**(12): p. 3012-3018.

50. Boam, A. and A. Nozari, *Fine chemical: OSN - a lower energy alternative.* Filtration & Separation, 2006. **43**(3): p. 46-48.

51. White, L.S., *Development of large-scale applications in organic solvent nanofiltration and pervaporation for chemical and refining processes.* Journal of Membrane Science, 2006. **286**(1-2): p. 26-35.

52. Livingston, A., L. Peeva, S. J. Han, D. Nair, S. S. Luthra, L. S. White, and L. M. F. dos Santos, *Membrane separation in green chemical processing - Solvent nanofiltration in liquid phase organic synthesis reactions.* Advanced Membrane Technology, 2003. **984**: p. 123-141.

53. Razdan, U. and V.J. Shah, *Nanofiltration membranes as a suitable alternative to reverse osmosis/ultrafiltration membranes in separation processes.* Journal of Scientific & Industrial Research, 2001. **60**(7): p. 560-563.

54. Toh, Y.H.S., F.W. Lim, and A.G. Livingston, *Polymeric membranes for nanofiltration in polar aprotic solvents.* Journal of Membrane Science, 2007. **301**(1-2): p. 3-10.

55. Yang, X.J., A.G. Livingston, and L.F. dos Santos, *Experimental observations of nanofiltration with organic solvents.* Journal of Membrane Science, 2001. **190**(1): p. 45-55.

56. Razdan, U., S.V. Joshi, and V.J. Shah, *Novel membrane processes for separation of organics.* Current Science, 2003. **85**(6): p. 761-771.

57. Berge, J., C. Delannoy, D. Dhaler, H. Rader, B. Gilbu Tilset, E. Torp, H. Raeder, and B. G. Tilset, *Process of purifying oils, useful as an ingredient in medicine, food, feed and/or surfactant, comprises bringing the oil in contact with adsorbing or absorbing agents, and membrane filtration*. US Patent No. 129518 A1, 2010, Due Miljo As.

58. Giorno, L., and E. Drioli, *An innovative approach to improve the performance of a two separate phase enzyme membrane reactor by immobilizing lipase in presence of emulsion.* Journal of Membrane Science, 2007. **295**(1-2): p. 95-101.

59. Drioli, E., M. Mendia, and R. Molinari, *Membrane Processes Combined with Enzymatic-Reactions - Experimental-Study.* Desalination, 1978. **24**(1-3): p. 193-209.

60. Rose et al., *Solvent extraction*. US Patent No. 5378369, 1994, Sasol Chemical Industries (Proprietary) Limited.

61. Cosgrove, J.P., D.F. Church, and W.A. Pryor, *The kinetics of the autoxidation of polyunsaturated fatty-acids.* Lipids, 1987. **22**(5): p. 299-304.

62. Guil-Guerrero, J.L., et al., *Hexane reduces peroxidation of fatty acids during storage.* European Journal of Lipid Science and Technology, 2001. **103**(5): p. 271-278.

63. Orset, S., G. C. Leach, R. Morais, and A. J. Young, *Spray-drying of the microalga Dunaliella salina: Effects on beta-carotene content and isomer composition.* Journal of Agricultural and Food Chemistry, 1999. **47**(11): p. 4782-4790.

64. Certik, M. and S. Shimizu, *Kinetic analysis of oil biosynthesis by an arachidonic acid-producing fungus, Mortierella alpina 1S-4.* Applied Microbiology and Biotechnology, 2000. **54**(2): p. 224-230.

65. Iida, I., T. Nakahara, T. Yokochi, Y. Kamisaka, H. Yagi, M. Yamaoka, and O. Suzuki, *Improvement of docosahexaenoic acid production in a culture of Thraustochytrium aureum by medium optimization.* Journal of Fermentation and Bioengineering, 1996. **81**(1): p. 76-78.

66. Yokochi, T., D. Honda, T. Higashihara, and T. Nakahara, *Optimization of docosahexaenoic acid production by Schizochytrium limacinum SR21.* Applied Microbiology and Biotechnology, 1998. **49**(1): p. 72-76.

67. Yaguchi, T., S. Tanaka, T. Yokochi, T. Nakahara, and T. Higashihara, *Production of high yields of docosahexaenoic acid by Schizochytrium sp. strain SR21.* Journal of the American Oil Chemists Society, 1997. **74**(11): p. 1431-1434.

68. Gupta, A., C.J. Barrow, and M. Puri, *Omega-3 biotechnology: Thraustochytrids as a novel source of omega-3 oils.* Biotechnology Advances, 2012. **30**(6): p. 1733-1745.

69. Carvalho, A.P., L.A. Meireles, and F.X. Malcata, *Microalgal reactors: A review of enclosed system designs and performances.* Biotechnology Progress, 2006. **22**(6): p. 1490-1506.

70. Carvalho, A.P. and F.X. Malcata, *Optimization of omega-3 fatty acid production by microalgae: Crossover effects of CO2 and light intensity under batch and continuous cultivation modes.* Marine Biotechnology, 2005. **7**(4): p. 381-388.

71. Carvalho, A.P. and F.X. Malcata, *Transfer of carbon dioxide within cultures of microalgae: Plain bubbling versus hollow-fiber modules.* Biotechnology Progress, 2001. **17**(2): p. 265-272.

72. Barclay, W.R., *Schizochytrium and thraustochytrium strains for producing high concentrations of omega-3 highly unsaturated fatty acids*. US Patent No. 07022512, 2006, Martek Biosciences Corporation.

73. Barclay, W.R., *Method of producing lipids by growing microorganisms of the order thraustochyriales*. US Patent No. 07011962, 2006, Martek Biosciences Corporation.

74. Jakobsen, A.N., I.M. Aasen, and A.R. Strom, *Endogenously synthesized (-)-proto-quercitol and glycine betaine are principal compatible solutes of Schizochytrium sp strain S8 (ATCC 20889) and three new isolates of phylogenetically related thraustochytrids.* Applied and Environmental Microbiology, 2007. **73**(18): p. 5848-5856.

75. Pinkart, H.C., R. Devereux, and P.J. Chapman, *Rapid separation of microbial lipids using solid phase extraction columns.* Journal of Microbiological Methods, 1998. **34**(1): p. 9-15.

76. Fuchs, B., R. Sub, K. Teuber, M. Eibisch, and J. Schiller, *Lipid analysis by thin-layer chromatography—A review of the current state.* Journal of Chromatography A, 2011. **1218**(19): p. 2754-2774.

77. Perrut et al., *Processes for chromatographic fractionation of fatty acids and their derivatives*. US Patent No. 5719302, 1996, Pronova AS.

78. Harscoat, C., M. Y. Jaffrin, P. Paullier, B. Courtois, and J. Courtois, *Recovery of microbial polysaccharides from fermentation broths by microfiltration on ceramic membranes.* Journal of Chemical Technology and Biotechnology, 1999. **74**(6): p. 571-579.

79. Zokaee, F., T. Kaghazchi, and A. Zare, *Cell harvesting by microfiltration in a deadend system.* Process Biochemistry, 1999. **34**(8): p. 803-810.

80. Rossignol, N., L. Vandanjon, P. Jaouen, and F. Quemeneur, *Membrane technology for the continuous separation microalgae/culture medium: compared performances of cross-flow microfiltration and ultra-filtration.* Aquacultural Engineering, 1999. **20**(3): p. 191-208.

81. McGregor, W.C., J.F. Weaver, and S.P. Tansey, *Antifoam effects on ultrafiltration.* Biotechnology and Bioengineering, 1988. **31**(4): p. 385-389.

82. Yamagiwa, K., K. Ikarashi, and A. Ohkawa, *Effects of antifoam with inverted cloud point on permeation and solute rejection in membrane filtration process.* Journal of Chemical Engineering of Japan, 1989. **22**(6): p. 693-695.

83. Bocquet, S., A. Torres, J. Sanchez, G. M. Rios, and J. Romero, *Modeling the mass transfer in solvent-extraction processes with hollow-fiber membranes.* Aiche Journal, 2005. **51**(4): p. 1067-1079.

84. Rossi, N., I. Petit, P. Jaouen, P. Legentilhomme, and M. Derouiniot, *Harvesting of cyanobacterium Arthrospira platensis using inorganic filtration membranes.* Separation Science and Technology, 2005. **40**(15): p. 3033-3050.

85. Jaouen, P., L. Vandanjon, and F. Quemeneur, *The shear stress of microalgal cell suspensions (Tetraselmis suecica) in tangential flow filtration systems: the role of pumps.* Bioresource Technology, 1999. **68**(2): p. 149-154.

86. Vandanjon, L., N. Rossignol, P. Jaouen, J. M. Robert, and F. Quemeneur, *Effects of shear on two microalgae species. Contribution of pumps and valves in tangential flow filtration systems.* Biotechnology and Bioengineering, 1999. **63**(1): p. 1-9.

87. Russotti, G., K.E. Goklen, and J.J. Wilson, *Development of a pilot-scale microfiltration harvest for the isolation of physostigmine from Streptomyces-griseofuscus broth.* Journal of Chemical Technology and Biotechnology, 1995. **63**(1): p. 37-47.

88. Goklen, K.E., et al., *Development of cross-flow filtration processes for the commercial-scale isolation of a bacterial lipase.* Bioprocess Engineering, 1994. **11**(2): p. 49-56.

89. Metcalfe, L.D., A.A. Schmitz, and J.R. Pelka, *Rapid preparation of fatty acid esters from lipids for gas chromatographic analysis.* Analytical Chemistry, 1966. **38**: p. 514-515.

90. Standal, I.B., D.E. Axelson, and M. Aursand, *Differentiation of Fish Oils According to Species by (13)C-NMR Regiospecific Analyses of Triacyglycerols.* Journal of the American Oil Chemists Society, 2009. **86**(5): p. 401-407.

91. Morita, E., Y. Kumon, T. Nakahara, S. Kagiwada, and T. Noguchi, *Docosahexaenoic acid production and lipid-body formation in Schizochytrium limacinum SR21.* Marine Biotechnology, 2006. **8**(3): p. 319-327.

92. Aursand, M., L. Jorgensen, and H. Grasdalen, *Positional distribution of omega-3-fatty-acids in marine lipid triacylglycerols by high-resolution C-13 nuclear-magnetic-resonance spectroscopy.* Journal of the American Oil Chemists Society, 1995. **72**(3): p. 293-297.

93. Ackman, R.G., W.M.N. Ratnayake, and E.J. Macpherson, *EPA and DHA contents of encapsulated fish oil products.* Journal of the American Oil Chemists Society, 1989. **66**(8): p. 1162-1164.

94. Lyberg, A.-M. and P. Adlercreutz, *Lipase specificity towards eicosapentaenoic acid and docosahexaenoic acid depends on substrate structure.* Biochimica Et Biophysica Acta-Proteins and Proteomics, 2008. **1784**(2): p. 343-350.

95. Devos, M., L. Poisson, F. Ergan, and G. Pencreac'h, *Enzymatic hydrolysis of phospholipids from Isochrysis galbana for docosahexaenoic acid enrichment.* Enzyme and Microbial Technology, 2006. **39**(4): p. 548-554.

96. Kahveci, D. and X.B. Xu, *Repeated hydrolysis process is effective for enrichment of omega 3 polyunsaturated fatty acids in salmon oil by Candida rugosa lipase.* Food Chemistry, 2011. **129**(4): p. 1552-1558.

97. Koike, H., M. Imai, and I. Suzuki, *Enrichment of triglyceride docosahexanoic acid by lipase used as a hydrolysis medium in lecithin-based nano-scale molecular assemblage.* Biochemical Engineering Journal, 2007. **36**(1): p. 38-42.

98. Reis, P., K. Holmberg, H. Watzke, M. E. Leser, and R. Miller, *Lipases at interfaces: A review.* Advances in Colloid and Interface Science, 2009. **147-48**: p. 237-250.

99. Orlich, B. and R. Schomaecker, *Enzymatic reduction of a less water-soluble ketone in reverse micelles with NADH regeneration.* Biotechnology and Bioengineering, 1999. **65**(3): p. 357-362.

100. Orlich, B. and R. Schomacker, *Candida Rugosa lipase reactions in nonionic w/o-microemulsion with a technical surfactant.* Enzyme and Microbial Technology, 2001. **28**(1): p. 42-48.

101. Orlich, B., H. Berger, M. Lade, and R. Schomacker, *Stability and activity of alcohol dehydrogenases in W/O-microemulsions: Enantioselective reduction including cofactor regeneration.* Biotechnology and Bioengineering, 2000. **70**(6): p. 638-646.

102. Orlich, B. and R. Schomacker, *Enzyme catalysis in reverse micelles.* History and Trends in Bioprocessing and Biotransformation, 2002. **75**: p. 185-208.

103. Fernandez-Lorente, G., L. Betancor, A. V. Carrascosa, and J. M. Guisan, *Release of Omega-3 Fatty Acids by the Hydrolysis of Fish Oil Catalyzed by Lipases Immobilized on Hydrophobic Supports.* Journal of the American Oil Chemists Society, 2011. **88**(8): p. 1173-1178.

104. Hermansyah, H., A. Wijanarko, M. Kubo, N. Shibasaki-Kitakawa, and T. Yonemoto, *Rigorous kinetic model considering positional specificity of lipase for enzymatic stepwise hydrolysis of triolein in biphasic oil-water system.* Bioprocess and Biosystems Engineering, 2010. **33**(7): p. 787-796.

105. Hermansyah, H., A. Wijanarko, M. Kubo, N. Shibasaki-Kitakawa, and T. Yonemoto, *Mathematical model for stepwise hydrolysis of triolein using Candida rugosa lipase in biphasic oil-water system.* Biochemical Engineering Journal, 2006. **31**(2): p. 125-132.

106. Jurado, E., F. Camacho, G. Luzon, M. Fernandez-Serrano, and M. Garcia-Roman, *Kinetic model for the enzymatic hydrolysis of tributyrin in O/W emulsions.* Chemical Engineering Science, 2006. **61**(15): p. 5010-5020.

107. Carvalho, A.P. and F.X. Malcata, *Preparation of fatty acid methyl esters for gas-chromatographic analysis of marine lipids: Insight studies.* Journal of Agricultural and Food Chemistry, 2005. **53**(13): p. 5049-5059.

108. Wei, G.-L. and E.Y. Zeng, *Gas chromatography-mass spectrometry and high-performance liquid chromatography-tandem mass spectrometry in quantifying fatty acids.* TrAC Trends in Analytical Chemistry, 2011. **30**(9): p. 1429-1436.

109. Zahlsen, K. and I. Eide, *Standardizing the novel method for chemical fingerprinting of oil and petroleum products based on positive electrospray mass spectrometry and chemometrics.* Energy & Fuels, 2006. **20**(1): p. 265-270.

110. Eide, I. and K. Zahlsen, *Chemical fingerprinting of biodiesel using electrospray mass spectrometry and chemometrics: Characterization, discrimination, identification, and quantification in petrodiesel.* Energy & Fuels, 2007. **21**(6): p. 3702-3708.

111. Carvalho, P.d.O., P. R. B. Campos, M. D. Noffs, P. B. L. Fregolente, and L. V. Fregolente, *Enzymatic hydrolysis of salmon oil by native lipases: optimization of process parameters.* Journal of the Brazilian Chemical Society, 2009. **20**(1): p. 117-124.

112. Ishihara, H., H. Okuyama, H. Ikezawa, and S. Tejima, *Studies on lipase from Mucor-javanicus. 1. Purification and properties.* Biochimica Et Biophysica Acta, 1975. **388**(3): p. 413-422.

113. Slizyte, R., T. Rustad, and I. Storro, *Enzymatic hydrolysis of cod (Gadus morhua) by-products - Optimization of yield and properties of lipid and protein fractions.* Process Biochemistry, 2005. **40**(12): p. 3680-3692.

114. Camacho, F., A. Robles, B. Camacho, P. A. Gonzalez, L. Esteban, and E. Molina, *Modeling of the kinetic for the acidolysis of different triacylglycerols and caprylic acid catalyzed by Lipozyme IM immobilized in packed bed reactor.* Chemical Engineering Science, 2007. **62**(12): p. 3127-3141.

115. Foresti, M.L., A. Pedemera, M. L. Ferreira, and V. Bucala, *Kinetic modeling of enzymatic ethyl oleate synthesis carried out in biphasic systems.* Applied Catalysis a-General, 2008. **334**(1-2): p. 65-72.

116. Jurado, E., F. Camacho, G. Luzon, M. Fernandez-Serrano, and M. Garcia-Roman, *Kinetics of the enzymatic hydrolysis of triglycerides in o/w emulsions - Study of the initial rates and the reaction time course.* Biochemical Engineering Journal, 2008. **40**(3): p. 473-484.

117. Paiva, A.L., V.M. Balcao, and F.X. Malcata, *Kinetics and mechanisms of reactions catalyzed by immobilized lipases.* Enzyme and Microbial Technology, 2000. **27**(3-5): p. 187-204.

118. Pilarek, M. and K.W. Szewczyk, *Kinetic model of 1,3-specific triacylglycerols alcoholysis catalyzed by lipases.* Journal of Biotechnology, 2007. **127**(4): p. 736-744.

119. Reis, P., K. Holmberg, R. Miller, M. E. Leser, T. Raab, and H. Watzke, *Lipase reaction at interfaces as self-limiting processes.* Comptes Rendus Chimie, 2009. **12**(1-2): p. 163-170.

120. Kawano, Y., M. Kawasaki, K. Shiomori, Y. Baba, and T. Hano, *Hydrolysis kinetics of olive oil with lipase in a transfer cell.* Journal of Fermentation and Bioengineering, 1994. **77**(3): p. 283-287.

121. Mitchell, D.A., J. A. Rodriguez, F. Carriere, J. Baratti, and N. Krieger, *An analytical method for determining relative specificities for sequential reactions catalyzed by the same enzyme: Application to the hydrolysis of triacylglycerols by lipases.* Journal of Biotechnology, 2008. **133**(3): p. 343-350.

122. Briggs, G.E. and J.B. Haldane, *A Note on the Kinetics of Enzyme Action.* The Biochemical journal, 1925. **19**(2): p. 338-9.

123. Kiani, A., R.R. Bhave, and K.K. Sirkar, *Solvent-Extraction with Immobilized Interfaces in a Microporous Hydrophobic Membrane.* Journal of Membrane Science, 1984. **20**(2): p. 125-145.

124. Bowen, W.R. and J.S. Welfoot, *Modelling the performance of membrane nanofiltration - critical assessment and model development.* Chemical Engineering Science, 2002. **57**(7): p. 1121-1137.

125. *Kirk-Othmer Encyclopedia of Chemical Technology*. 4th edition, 1998, Wiley Blackwell.

126. Perry, D.G., *Perry's Chemical Engineers' Handbook*. 6th edition, 1984, McGraw-Hill.

127. Vaidya, A.M., P.J. Halling, and G. Bell, *Surfactant-induced breakthrough effects during the operation of 2-phase biocatalytic membrane reactors.* Biotechnology and Bioengineering, 1994. **44**(6): p. 765-771.

128. Lennie, S., P.J. Halling, and G. Bell, *Causes of emulsion formation during solvent-extraction of fermentation broths and its reduction by surfactants.* Biotechnology and Bioengineering, 1990. **35**(9): p. 948-950.

129. Prasad, R. and K.K. Sirkar, *Hollow fiber solvent-extraction of pharmaceutical products - a case-study.* Journal of Membrane Science, 1989. **47**(3): p. 235-259.

130. Vaidya, A.M., G. Bell, and P.J. Halling, *Aqueous-organic membrane bioreactors. 1. A guide to membrane selection.* Journal of Membrane Science, 1992. **71**(1-2): p. 139-149.

131. Vaidya, A.M., G. Bell, and P.J. Halling, *Aqueous -organic membrane bioreactors. 2. Breakthrough pressure measurement.* Journal of Membrane Science, 1994. **97**: p. 13-26.

132. Valadez-Blanco, R., F. C. Ferreira, R. F. Jorge, andA. G. Livingston, *A membrane bioreactor for biotransformations of hydrophobic molecules using organic solvent nanofiltration (OSN) membranes.* Journal of Membrane Science, 2008. **317**(1-2): p. 50-64.

133. Baker, R.W., *Membrane technology and applications*. 2nd edition, 2004, Wiley.

134. Mulder, M., *Basic Principles of Membrane Technology*. 2nd edition, 1996, Kluwer Academic Publishers.

135. Wijmans, J.G. and R.W. Baker, *The Solution-Diffusion Model - a Review.* Journal of Membrane Science, 1995. **107**(1-2): p. 1-21.

136. Silva, P., S.J. Han, and A.G. Livingston, *Solvent transport in organic solvent nanofiltration membranes.* Journal of Membrane Science, 2005. **262**(1-2): p. 49-59.

137. Doig, S.D., A. T. Boam, A. G. Livingston, and D. C. Stuckey, *Epoxidation of 1,7-octadiene by Pseudomonas oleovorans in a membrane bioreactor.* Biotechnology and Bioengineering, 1999. **63**(5): p. 601-611.

138. Geens, J., et al., *Solute transport in non-aqueous nanofiltration: effect of membrane material.* Journal of Chemical Technology and Biotechnology, 2005. **80**(12): p. 1371-1377.

139. Doig, S.D., A. T. Boam, A. G. Livingston, and D. C. Stuckey, *Mass transfer of hydrophobic solutes in solvent swollen silicone rubber membranes.* Journal of Membrane Science, 1999. **154**(1): p. 127-140.

140. Valadez-Blanco, R. and A.G. Livingston, *Solute molecular transport through polyimide asymmetric organic solvent nanofiltration (OSN) membranes and the effect of membrane-formation parameters on mass transfer.* Journal of Membrane Science, 2009. **326**(2): p. 332-342.

141. See-Toh, Y.H., F.C. Ferreira, and A.G. Livingston, *The influence of membrane formation parameters on the functional performance of organic solvent nanofiltration membranes.* Journal of Membrane Science, 2007. **299**(1-2): p. 236-250.

142. Boam, A.T., A. M. M. Miranda, and A. G. Livingston, *Polyimide membrane*. WO Patent Application No. 2010/142979 (A1), Evonik-Membrane Extraction TEchnology Ltd.

143. See-Toh, Y. H., X. X. Loh, K. Li, A. Bismarck, and A. G. Livingston, *In search of a standard method for the characterisation of organic solvent nanofiltration membranes.* Journal of Membrane Science, 2007. **291**(1-2): p. 120-125.

144. See-Toh, Y.H., M. Silva, and A. Livingston, *Controlling molecular weight cut-off curves for highly solvent stable organic solvent nanofiltration (OSN) membranes.* Journal of Membrane Science, 2008. **324**(1-2): p. 220-232.

145. Wilk, C.R. and P. Chang, *Correlation of diffusion coefficients in dilute solutions.* Aiche Journal, 1955. **1**(2): p. 264-270.

146. Geankoplis, C.J., *Transport processes and unit operations*. 2 ed. 1983: Allyn and Bacon.

147. Ho, F.-g. and W. Striender, *A variational calculation of the effective surface diffusion coefficient and tortuosity.* Chemical Engineering Science, 1981. **36**(2): p. 253-258.

148. Belarbi, E.H., E. Molina, and Y. Chisti, *A process for high yield and scaleable recovery of high purity eicosapentaenoic acid esters from microalgae and fish oil.* Process Biochemistry, 2000. **35**(9): p. 951-969.

149. Bogalhos, P., L. Fregolente, G. M. F. Pinto, M. R. Wolf-Maciel, and R. Maciel, *Monoglyceride and Diglyceride Production Through Lipase-Catalyzed Glycerolysis and Molecular Distillation.* Applied Biochemistry and Biotechnology, 2010. **160**(7): p. 1879-1887.

150. Wang, Y., J. Y. Nie, M. M. Zhao, S. Ma, L. N. Kuang, X. Han, and S. Z. Tang, *Production of Biodiesel from Waste Cooking Oil via a Two-Step Catalyzed Process and Molecular Distillation.* Energy & Fuels, 2010. **24**: p. 2104-2108.

151. Shao, P., J. Z. He, P. L. Sun, and S. T. Jiang, *Process optimisation for the production of biodiesel from rapeseed soapstock by a novel method of short path distillation.* Biosystems Engineering, 2009. **102**(3): p. 285-290.

152. Mishra, V.K., F. Temelli, and B. Ooraikul, *Extraction and purification of omega-3-fatty-acids with an emphasis on supercritical-fluid extraction - a review.* Food Research International, 1993. **26**(3): p. 217-226.

153. Paiva, A.L. and F.X. Malcata, *Comparison of the performance of integrated and sequential reaction and separation units in terms of recovery of a desired product.* Chemical Engineering Science, 2000. **55**(3): p. 589-599.

154. Paiva, A.L. and F.X. Malcata, *Integration of reaction and separation with lipases: An overview.* Journal of Molecular Catalysis B-Enzymatic, 1997. **3**(1-4): p. 99-109.

155. Paiva, A.L., D. van Rossum, and F.X. Malcata, *Integrated vs. sequential reaction and separation: contributions for a global analysis.* Chemical Engineering Science, 1999. **54**(12): p. 1825-1836.

156. Paiva, A.L. and F.X. Malcata, *How performance of integrated systems of reaction and separation relates to that of parallel and sequential configurations.* Bioprocess Engineering, 2000. **22**(2): p. 149-158.

157. Rabe, S., U. Krings, and R.G. Berger, *Influence of oil-in-water emulsion characteristics on initial dynamic flavour release.* Journal of the Science of Food and Agriculture, 2003. **83**(11): p. 1124-1133.

158. Scott, K., R.J. Jachuck, and D. Hall, *Crossflow microfiltration of water-in-oil emulsions using corrugated membranes.* Separation and Purification Technology, 2001. **22-3**(1-3): p. 431-441.

159. Konishi, M., M. Kishimoto, N. Tamesui, I. Omasa, S. Shioya, and H. Ohtake, *The separation of oil from an oil-water-bacteria mixture using a hydrophobic tubular membrane.* Biochemical Engineering Journal, 2005. **24**(1): p. 49-54.

160. Daiminger, U., W. Nitsch, P. Plucinski, and S. Hoffmann, *Novel techniques for oil-water separation.* Journal of Membrane Science, 1995. **99**(2): p. 197-203.

161. Ezzati, A., E. Gorouhi, and T. Mohammadi, *Separation of water in oil emulsions using microfiltration.* Desalination, 2005. **185**(1-3): p. 371-382.

162. Kocherginsky, N.M. and A.B. Grishchenko, *Mass transfer of long chain fatty acids through liquid-liquid interface stabilized by porous membrane.* Separation and Purification Technology, 2000. **20**(2-3): p. 197-208.

163. Kocherginsky, N.M., C.L. Tan, and W.F. Lu, *Demulsification of water-in-oil emulsions via filtration through a hydrophilic polymer membrane.* Journal of Membrane Science, 2003. **220**(1-2): p. 117-128.

164. Hlavacek, M., *Break-up of oil-in-water emulsions induced by permeation through a microfiltration membrane.* Journal of Membrane Science, 1995. **102**: p. 1-7.

165. Francis, L., H. Maab, A. AlSaadi, S. Nunes, N. Ghaffour and G. L. Amy, *Fabrication of electrospun nanofibrous membranes for membrane distillation application*. Desalination and Water Treatment, 2013. **51**(7-9): p. 1337-1343.